

Durham E-Theses

Stoichiometric and catalytic reactivity of half-sandwich imido complexes of the group 5 metals

Chan, Michael, C.W.

How to cite:

Chan, Michael, C.W. (1995) *Stoichiometric and catalytic reactivity of half-sandwich imido complexes of the group 5 metals*, Durham theses, Durham University. Available at Durham E-Theses Online:
<http://etheses.dur.ac.uk/5209/>

Use policy

The full-text may be used and/or reproduced, and given to third parties in any format or medium, without prior permission or charge, for personal research or study, educational, or not-for-profit purposes provided that:

- a full bibliographic reference is made to the original source
- a [link](#) is made to the metadata record in Durham E-Theses
- the full-text is not changed in any way

The full-text must not be sold in any format or medium without the formal permission of the copyright holders.

Please consult the [full Durham E-Theses policy](#) for further details.

Stoichiometric and Catalytic Reactivity of Half-Sandwich Imido Complexes of the Group 5 Metals

by

Michael C.W. Chan B.Sc.(Dunelm)

Collingwood College

A thesis submitted for the degree of Doctor of Philosophy
at the University of Durham.

November 1995

The copyright of this thesis rests with the author.
No quotation from it should be published without
his prior written consent and information derived
from it should be acknowledged.



Statement of Copyright

The copyright of this thesis rests solely with the author. No quotation from it should be published without the written consent of the author and information derived from it should be acknowledged.

Declaration

The work described in this thesis was carried out in the Department of Chemistry at the University of Durham between October 1992 and September 1995. The entire body of work is my own unless stated to the contrary and has not been submitted previously for a degree at this or any other University.

To my family

Acknowledgements

The compilation of this thesis would have been impossible without the assistance of a number of people. First and foremost, I would like to express my sincere gratitude to my supervisor Prof. Vernon C. Gibson for his support and guidance over the past three years. His amazing enthusiasm for the subject was truly inspirational.

I am grateful to Prof. Judith A.K. Howard and the Durham University Crystallography Group, in particular Miss Jacqueline M. Cole, for structural determinations described herein. To this end, Prof. W. Clegg and Dr. M.R.J. Elsegood of the University of Newcastle are also thanked. The efforts of the following at Durham are also much appreciated: Alan, Julia, Jarka, Lara, and of course Ray and Gordon.

I am also indebted to Dr. Ian Little (BP Chemicals, Sunbury) for his advice and encouragement and to Prof. Ken Wade for the interest he has shown in recent months. Financial Support from EPSRC and BP Chemicals Ltd. are acknowledged.

To my aisle-, lab- and group members: Matt J., Phil, Brenda, Gaz, Raz, Rich, Carl, Chris, Ulrich, Brian, Matt G., Lynn; thanks for three unforgettable years. To my fellow vertically-challenged colleagues Leela and Martyn: I reckon we stuck together pretty well! A special mention for Dr. Eddie Marshall for his obliging proof-reading, not forgetting his unrivalled mastery in the art of suba distribution and storytelling. Iain May deserves praise for his saintly cooperation and finally to Penny Herbertson: thanks for the Mac, the banoffee pie and finding Nuff!

Finally, I am eternally grateful to my mother and father for their love and care, to Sim and Jen for trusting and sharing, and last but not least to Jan for her patience and affection.

Abstract : Stoichiometric and Catalytic Reactivity of Half-Sandwich Imido Complexes of the Group 5 Metals

This thesis describes investigations into the chemistry of half-sandwich imido complexes of the Group 5 metals, with particular emphasis on the development of complexes which can be applied to catalytic processes.

Chapter 1 provides an introduction to the imido ligand and highlights aspects of the reactivity of half-sandwich transition metal imido and related complexes. The isolobal analogy between Group 4 bent metallocene, Group 5 half-sandwich imido and Group 6 bis(imido) metal fragments is outlined.

In Chapter 2, reactions of $\text{CpV}(\text{NR})\text{Cl}_2$ ($\text{R}=2,6\text{-}^i\text{Pr}_2\text{C}_6\text{H}_3$, $2,6\text{-Me}_2\text{C}_6\text{H}_3$) with alkylating agents are described, yielding a number of highly unusual products. The novel structures of $[\text{CpV}(\text{N-}2,6\text{-}^i\text{Pr}_2\text{C}_6\text{H}_3)(\mu\text{-Me})_2]_2(\mu\text{-Mg})$ and $[\text{CpV}(\mu\text{-N-}2,6\text{-}^i\text{Pr}_2\text{C}_6\text{H}_3)]_2(\mu\text{-Me})$, featuring bridging methyl and imido substituents, have been determined. The former also possesses the first crystallographically characterised V-Mg bond and multiple agostic interactions.

The aim of Chapter 3 was to evaluate the steric and electronic influence of the imido substituent in half-sandwich imido complexes of niobium. For the $[\text{CpNb}(\text{N-}2\text{-}^t\text{BuC}_6\text{H}_4)]$ system, the successful isolation of a number of previously unstable species has been reported. The orientations of the diphenylacetylene and the ethylene ligands in $\text{CpNb}(\text{N-}2\text{-}^t\text{BuC}_6\text{H}_4)(\text{PhC}\equiv\text{CPh})(\text{PMe}_3)$ and $\text{CpNb}(\text{N-}2,6\text{-Cl}_2\text{C}_6\text{H}_3)(\text{C}_2\text{H}_4)(\text{PMe}_3)$ respectively have been established through crystal structures and lend support to the isolobal relationship between the $[\text{Cp}_2\text{Zr}]$ and $[\text{CpNb}(\text{NR})]$ fragments.

In Chapter 4, the tantalum dialkyl complexes $\text{Cp}^*\text{Ta}(\text{N}^t\text{Bu})(\text{CH}_2\text{R})_2$ [$\text{R}=\text{Ph}$, CMe_2Ph , CMe_3] are described and the molecular structure of $\text{Cp}^*\text{Ta}(\text{N}^t\text{Bu})(\text{CH}_2\text{CMe}_3)$ reveals multiple agostic interactions. Reactions of $\text{Cp}^*\text{Ta}(\text{N}^t\text{Bu})(\text{CH}_2\text{R})_2$ with excess $\text{C}_6\text{F}_5\text{OH}$ yield a number of crystallographically characterised pentafluorophenoxide and oxo-bridged products, namely $[\text{Cp}^*\text{Ta}(\text{CH}_2\text{Ph})(\text{OC}_6\text{F}_5)(\mu\text{-O})]_2$, $\text{Cp}^*\text{Ta}(\text{OC}_6\text{F}_5)_4$ and $[\text{Cp}^*\text{Ta}(\text{OC}_6\text{F}_5)_2(\mu\text{-O})]_2$.

Chapter 5 discusses attempts to develop and explore the oxidative coupling chemistry at the half-sandwich tantalum imido fragment. Hence, a number of new tantalacyclopentane complexes and related species have been prepared, including $\text{Cp}^*\text{Ta}(\text{N-}2,6\text{-}^i\text{Pr}_2\text{C}_6\text{H}_3)(\sigma\text{-}1,4\text{-}(2\text{-Et})\text{C}_4\text{H}_7)$ and $\text{Cp}^*\text{Ta}(\text{N-}2,6\text{-}^i\text{Pr}_2\text{C}_6\text{H}_3)[\sigma\text{-}1,6\text{-C}(\text{O})(3\text{-Et})\text{C}_4\text{H}_7\text{C}(\text{O})]$.

Chapter 6 contains the experimental details for Chapter 2-5.

Michael Chi Wang Chan (November 1995)

Abbreviations and Nomenclature

L	General 2-electron donor ligand
R	General alkyl/aryl group
X	General 1-electron donor ligand
Cp	Cyclopentadienyl C ₅ H ₅
Cp*	Pentamethylcyclopentadienyl C ₅ Me ₅
Cp'	General C ₅ R ₅ ring
Me	Methyl CH ₃
Et	Ethyl C ₂ H ₅
Pr	Propyl C ₃ H ₇
Bu	Butyl C ₄ H ₉
Cy	Cyclohexyl C ₆ H ₁₁
Ph	Phenyl C ₆ H ₅
MO	Molecular Orbital
nOe	nuclear Overhauser effect
DSC	Differential Scanning Calorimetry
MAO	Methylaluminoxane
NMR	Nuclear Magnetic Resonance
THF	Tetrahydrofuran
COSY	¹ H Homonuclear Correlation
DEAC	Diethylaluminium chloride
HOMO	Highest Occupied Molecular Orbital
LUMO	Lowest Unoccupied Molecular Orbital
ROMP	Ring-Opening Metathesis Polymerisation
HETCOR	Heteronuclear Correlation
Neophyl	CH ₂ CMe ₂ Ph
Neopentyl	CH ₂ CMe ₃

Contents

	<u>Page</u>
Chapter 1 :	
An Overview of Half-Sandwich Imido and Related Complexes of the Transition Metals: Bonding, Reactivity and Applications in Catalysis	1
1.1. Introduction	2
1.2. Relationship between Metal-Imido and Metal-(η -cyclopentadienyl) Bonding Interactions	2
1.2.1. Imido Bonding Modes	2
1.2.2. Bonding Patterns in Tetrahedral Transition Metal Imido Complexes	5
1.2.3. Bonding Patterns for the Group 4 Metallocene, Group 5 Half-Sandwich Imido and Group 6 Bis(imido) Fragments : An Isolobal Relationship	8
1.3. Highlights of Transition Metal Complexes Bearing the Cyclopentadienyl and Imido Ligands	10
1.3.1. Group 4	11
1.3.2. Group 5	13
1.3.3. Group 6 to Group 9	16
1.4. Reactivity of Group 4 Metallocenes	19
1.4.1. Olefin Polymerisation Catalysts	19
1.4.2. Reagents in Organic Synthesis	22
1.4.3. Alkylidene Complexes	24
1.5. Reactivity of Group 6 Bis(imido) Complexes	25
1.5.1. Olefin Polymerisation Catalysts	25
1.5.2. Precursors to Alkylidene Complexes as ROMP Initiators	25
1.6. Summary and Objectives	27
1.7. References	28

Chapter 2 : Synthesis of Half-Sandwich Vanadium Arylimido Dichlorides and their Reactivity towards Alkylating Agents	33
2.1. Introduction	34
2.2. A Convenient Synthesis of CpV(NR)Cl ₂ Derivatives: Imido Ligand Exchange using a Tert-Butylimido Precursor	35
2.2.1. Reaction of CpV(N ^t Bu)Cl ₂ with 2,6-Dimethylaniline: Preparation and Molecular Structure of CpV(N-2,6-Me ₂ C ₆ H ₃)Cl ₂ (1)	36
2.2.2. Reaction of CpV(N ^t Bu)Cl ₂ with 2,6-Diisopropylaniline: Preparation of CpV(N-2,6- ⁱ Pr ₂ C ₆ H ₃)Cl ₂ (2)	39
2.3. Alkylation Studies on CpV(NR)Cl ₂ Complexes	39
2.3.1. Reaction of CpV(N ^t Bu)Cl ₂ with Zn(CH ₂ Ph) ₂ : Preparation of [CpV(N ^t Bu)(μ-Cl)] ₂ (3)	40
2.3.2. Reaction of CpV(N ^t Bu)Cl ₂ with PhCH ₂ MgCl: Preparation of [CpV(CH ₂ Ph)(μ-N ^t Bu)] ₂ (4)	42
2.3.2.1. Molecular Structure of [CpV(CH ₂ Ph)(μ-N ^t Bu)] ₂ (4)	43
2.3.3. Reaction of CpV(N-2,6- ⁱ Pr ₂ C ₆ H ₃)Cl ₂ with MeMgBr in Et ₂ O : Preparation of [CpV(N-2,6- ⁱ Pr ₂ C ₆ H ₃)(μ-Me) ₂] ₂ (μ-Mg) (5)	47
2.3.3.1. Molecular Structure of [CpV(N-2,6- ⁱ Pr ₂ C ₆ H ₃)(μ-Me) ₂] ₂ (μ-Mg) (5)	48
2.3.4. Reaction of CpV(N-2,6- ⁱ Pr ₂ C ₆ H ₃)Cl ₂ with MeMgCl in THF/Et ₂ O : Preparation of [CpV(μ-N-2,6- ⁱ Pr ₂ C ₆ H ₃)] ₂ (μ-Me) (6)	52
2.3.4.1. Molecular Structure of [CpV(μ-N-2,6- ⁱ Pr ₂ C ₆ H ₃)] ₂ (μ-Me) (6)	53
2.3.5. Other Reactions of CpV(NR)Cl ₂ towards Grignard Reagents	57
2.4. Studies on Half-Sandwich Vanadium Imido Complexes as Catalyst Precursors for Ethylene Polymerization	59

2.5. Implications and Solutions	61
2.6. Summary	63
2.7. References	64

Chapter 3 :

Investigation into the Steric and Electronic Effects of the Imido Substituent in the Half-Sandwich Niobium Arylimido System	66
3.1. Introduction	67
3.1.1. Steric Influence of the Imido Moiety: Synthesis and Reactivity of $\text{CpNb}(\text{N}-2\text{-}^t\text{BuC}_6\text{H}_4)\text{Cl}_2$	67
3.1.2. Reaction of CpNbCl_4 with $\text{Me}_3\text{SiNH}(2\text{-}^t\text{BuC}_6\text{H}_4)$ and 2,6-Lutidine: Preparation of $\text{CpNb}(\text{N}-2\text{-}^t\text{BuC}_6\text{H}_4)\text{Cl}_2$ (8)	67
3.1.2.1. Molecular Structure of $\text{CpNb}(\text{N}-2\text{-}^t\text{BuC}_6\text{H}_4)\text{Cl}_2$ (8)	69
3.1.3. Reaction of $\text{CpNb}(\text{N}-2\text{-}^t\text{BuC}_6\text{H}_4)\text{Cl}_2$ with PMe_3 : Preparation of $\text{CpNb}(\text{N}-2\text{-}^t\text{BuC}_6\text{H}_4)(\text{PMe}_3)\text{Cl}_2$ (9)	71
3.1.4. Formation of Phosphine-Stabilised Half-Sandwich Niobium Imido Olefin Complexes	74
3.1.4.1. Reaction of $\text{CpNb}(\text{N}-2\text{-}^t\text{BuC}_6\text{H}_4)\text{Cl}_2$ with $n\text{-C}_2\text{H}_5\text{MgCl}$ in the presence of Trimethylphosphine : Preparation of $\text{CpNb}(\text{N}-2\text{-}^t\text{BuC}_6\text{H}_4)(\eta^2\text{-C}_2\text{H}_4)(\text{PMe}_3)$ (10)	74
3.1.4.2. Reaction of $\text{CpNb}(\text{N}-2\text{-}^t\text{BuC}_6\text{H}_4)(\text{PMe}_3)\text{Cl}_2$ with $n\text{-C}_3\text{H}_7\text{MgCl}$: Preparation of $\text{CpNb}(\text{N}-2\text{-}^t\text{BuC}_6\text{H}_4)(\eta^2\text{-C}_3\text{H}_6)(\text{PMe}_3)$ (11)	75
3.1.5. Reduction of $\text{CpNb}(\text{N}-2\text{-}^t\text{BuC}_6\text{H}_4)\text{Cl}_2$ with Magnesium in the Presence of Trimethylphosphine : Preparation of $\text{CpNb}(\text{N}-2\text{-}^t\text{BuC}_6\text{H}_4)(\text{PMe}_3)_2$ (12)	76
3.1.6. Reaction of $\text{CpNb}(\text{N}-2\text{-}^t\text{BuC}_6\text{H}_4)(\text{PMe}_3)_2$ (12) with Alkynes	79

3.1.6.1.	Preparation of CpNb(N-2- ^t BuC ₆ H ₄)(PhC≡CH)(PMe ₃) (13)	79
3.1.6.2.	Preparation and Molecular Structure of CpNb(N-2- ^t BuC ₆ H ₄)(PhC≡CPh)(PMe ₃) (14) ; Structural Comparisons with Isolobal Complexes	83
3.2.	Introduction	90
3.2.1.	Electronic Influence of the Imido Moiety : Synthesis and Reactivity of CpNb(N-2,6-Cl ₂ C ₆ H ₃)Cl ₂	90
3.2.2.	Reaction of CpNbCl ₄ with Me ₃ SiNH(2,6-Cl ₂ C ₆ H ₃) and 2,6- Lutidine : Preparation of CpNb(N-2,6-Cl ₂ C ₆ H ₃)Cl ₂ (15)	90
3.2.3.	Reaction of CpNb(N-2,6-Cl ₂ C ₆ H ₃)Cl ₂ with PMe ₃ : Preparation of CpNb(N-2,6-Cl ₂ C ₆ H ₃)(PMe ₃)Cl ₂ (16)	92
3.2.4.	Reaction of CpNb(N-2,6-Cl ₂ C ₆ H ₃)Cl ₂ with C ₂ H ₅ MgCl in the presence of Trimethylphosphine : Preparation of CpNb(N-2,6-Cl ₂ C ₆ H ₃)(η ² -C ₂ H ₄)(PMe ₃) (17)	93
3.2.4.1.	Molecular Structure of CpNb(N-2,6-Cl ₂ C ₆ H ₃)(η ² -C ₂ H ₄)(PMe ₃) (17)	94
3.2.4.2.	Reactivity of CpNb(N-2,6-Cl ₂ C ₆ H ₃)(η ² -C ₂ H ₄)(PMe ₃) with Alkynes	99
3.2.5.	Attempted Formation of CpNb(N-2,6-Cl ₂ C ₆ H ₃)(PMe ₃) ₂	101
3.3.	Studies on CpNb(N-2- ^t BuC ₆ H ₄)Cl ₂ and CpNb(N-2,6-Cl ₂ C ₆ H ₃)Cl ₂ as Catalyst Precursors for Ethylene Polymerization	102
3.3.1.	Introduction	102
3.3.2.	Catalysis Results	102
3.4.	Summary	104
3.5.	References	107

Chapter 4 : Synthesis and Reactivity of Tantalum(V) Alkyl Complexes	109
4.1. Introduction	110
4.2. Synthesis of $\text{Cp}^*\text{Ta}(\text{N}^t\text{Bu})(\text{CH}_2\text{R})_2$ [R = Ph (20) , CMe_2Ph (21) , CMe_3 (22)] : Evidence for Multiple Agostic Interactions	112
4.2.1. Molecular Structure of $\text{Cp}^*\text{Ta}(\text{N}^t\text{Bu})(\text{CH}_2\text{CMe}_3)_2$ (22)	115
4.3. Reactivity of $\text{Cp}^*\text{Ta}(\text{N}^t\text{Bu})(\text{CH}_2\text{Ph})_2$ (20)	120
4.3.1. Alkyl Abstraction Reactions; Generation of $[\text{Cp}^*\text{Ta}(\text{N}^t\text{Bu})(\text{CH}_2\text{Ph})]^+$ in the Presence of Ethylene	120
4.3.2. Reaction of $\text{Cp}^*\text{Ta}(\text{N}^t\text{Bu})(\text{CH}_2\text{Ph})_2$ with Alcohols	123
4.3.2.1. Reaction of $\text{Cp}^*\text{Ta}(\text{N}^t\text{Bu})(\text{CH}_2\text{Ph})_2$ with Pentafluorophenol : Preparation of $[\text{Cp}^*\text{Ta}(\text{CH}_2\text{Ph})(\text{OC}_6\text{F}_5)(\mu\text{-O})]_2$ (24)	123
4.3.2.2. Molecular Structure of $[\text{Cp}^*\text{Ta}(\text{CH}_2\text{Ph})(\text{OC}_6\text{F}_5)(\mu\text{-O})]_2$ (24)	126
4.3.3. Attempted Reaction of $\text{Cp}^*\text{Ta}(\text{N}^t\text{Bu})(\text{CH}_2\text{Ph})_2$ with Trimethylphosphine	130
4.4. Reactivity of $\text{Cp}^*\text{Ta}(\text{N}^t\text{Bu})(\text{CH}_2\text{CMe}_2\text{Ph})_2$ (21)	130
4.4.1. Reaction of $\text{Cp}^*\text{Ta}(\text{N}^t\text{Bu})(\text{CH}_2\text{CMe}_2\text{Ph})_2$ with Pentafluorophenol : Preparation of $\text{Cp}^*\text{Ta}(\text{OC}_6\text{F}_5)_4$ (26) and $[\text{Cp}^*\text{Ta}(\text{OC}_6\text{F}_5)_2(\mu\text{-O})]_2$ (27)	130
4.4.1.1. Molecular Structure of $\text{Cp}^*\text{Ta}(\text{OC}_6\text{F}_5)_4$ (26)	132
4.4.1.2. Molecular Structure of $[\text{Cp}^*\text{Ta}(\text{OC}_6\text{F}_5)_2(\mu\text{-O})]_2$ (27)	136
4.5. Reactivity of $\text{Cp}^*\text{Ta}(\text{N}^t\text{Bu})(\text{CH}_2\text{CMe}_3)_2$ (22)	139
4.6. Summary	140
4.7. References	141

Chapter 5 : Studies Towards the C–C Coupling of Unsaturated Organic

Molecules at the Half-Sandwich Tantalum Imido Fragment	143
5.1. Introduction	144
5.2. Synthesis of Cp [*] Ta(NR)Cl ₂ and Related Complexes	146
5.2.1. Molecular Structure of [Li(OEt ₂)] [Cp [*] Ta(N-2- ^t BuC ₆ H ₄) ₂ Cl] (31)	147
5.3. Reactivity of Cp [*] Ta(NR)Cl ₂ Complexes	150
5.4. Synthesis of Cp [*] Ta(NR)(CH ₂ =CHR')(PMe ₃) Derivatives and their Reactivity with Unsaturated Hydrocarbons	151
5.4.1. Reaction of Ethylene with Cp [*] Ta(NR)(CH ₂ =CHR')(PMe ₃) Complexes	152
5.4.2. Reaction of Alkynes with Cp [*] Ta(NR)(CH ₂ =CHR')(PMe ₃)	154
5.5. New C–C Coupled Products and Related Complexes of the [Cp [*] Ta(N-2,6- ⁱ Pr ₂ C ₆ H ₃)] System	155
5.5.1. Reaction of Cp [*] Ta(N-2,6- ⁱ Pr ₂ C ₆ H ₃)Cl ₂ with 2 ⁿ BuLi in the presence of Ethylene: Preparation of Cp [*] Ta(N-2,6- ⁱ Pr ₂ C ₆ H ₃)(σ-1,4-(2-Et)C ₄ H ₇) (41)	155
5.5.2. Reactivity of Cp [*] Ta(N-2,6- ⁱ Pr ₂ C ₆ H ₃)(σ-1,4-(2-Et)C ₄ H ₇) (41)	159
5.5.2.1. Reactivity of Cp [*] Ta(N-2,6- ⁱ Pr ₂ C ₆ H ₃)(σ-1,4-(2-Et)C ₄ H ₇) with CO: Preparation of Cp [*] Ta(N-2,6- ⁱ Pr ₂ C ₆ H ₃)[σ-1,6- C(O)(3-Et)C ₄ H ₇ C(O)] (42)	159
5.5.3. Synthesis of Cp [*] Ta(N-2,6- ⁱ Pr ₂ C ₆ H ₃)(η ² -CH ₂ =CH ₂ Et)(PMe ₃) (43)	162
5.5.3.1. Reactivity of Cp [*] Ta(N-2,6- ⁱ Pr ₂ C ₆ H ₃)(η ² -CH ₂ =CH ₂ Et)(PMe ₃) (43)	163
5.6. Summary	164
5.7. References	166

Chapter 6 : Experimental Details	168
6.1. General	169
6.1.1. Experimental and Characterisation Techniques	169
6.1.2. Purification and Preparation of Solvents and Reagents	170
6.2. Experimental Details for Chapter 2	171
6.2.1. Reaction of $\text{CpV}(\text{N}^t\text{Bu})\text{Cl}_2$ with 2,6-Dimethylaniline : Preparation of $\text{CpV}(\text{N}-2,6\text{-Me}_2\text{C}_6\text{H}_3)\text{Cl}_2$ (1)	171
6.2.2. Reaction of $\text{CpV}(\text{N}^t\text{Bu})\text{Cl}_2$ with 2,6-Di(isopropyl)aniline : Preparation of $\text{CpV}(\text{N}-2,6\text{-}^i\text{Pr}_2\text{C}_6\text{H}_3)\text{Cl}_2$ (2)	172
6.2.3. Reaction of $\text{CpV}(\text{N}^t\text{Bu})\text{Cl}_2$ with $\text{Zn}(\text{CH}_2\text{Ph})_2$: Preparation of $[\text{CpV}(\text{N}^t\text{Bu})(\mu\text{-Cl})]_2$ (3)	173
6.2.4. Reaction of $\text{CpV}(\text{N}^t\text{Bu})\text{Cl}_2$ with PhCH_2MgCl : Preparation of $[\text{CpV}(\mu\text{-N}^t\text{Bu})(\text{CH}_2\text{Ph})]_2$ (4)	174
6.2.5. Reaction of $\text{CpV}(\text{N}-2,6\text{-}^i\text{Pr}_2\text{C}_6\text{H}_3)\text{Cl}_2$ with MeMgBr : Preparation of $[\text{CpV}(\text{N}-2,6\text{-}^i\text{Pr}_2\text{C}_6\text{H}_3)(\mu\text{-Me}_2)]_2(\mu\text{-Mg})$ (5)	175
6.2.6. Reaction of $\text{CpV}(\text{N}-2,6\text{-}^i\text{Pr}_2\text{C}_6\text{H}_3)\text{Cl}_2$ with MeMgCl : Preparation of $[\text{CpV}(\mu\text{-N}-2,6\text{-}^i\text{Pr}_2\text{C}_6\text{H}_3)]_2(\mu\text{-Me})$ (6)	176
6.2.7. Reaction of $\text{CpV}(\text{N}^t\text{Bu})\text{Cl}_2$ with Aniline : Preparation of $\text{CpV}(\text{NPh})\text{Cl}_2$ (7)	176
6.2.8. Preparation of Supported Catalyst	177
6.3. Experimental Details for Chapter 3	178
6.3.1. Reaction of CpNbCl_4 with $\text{Me}_3\text{SiNH}(2\text{-}^t\text{BuC}_6\text{H}_4)$: Preparation of $\text{CpNb}(\text{N}-2^t\text{BuC}_6\text{H}_4)\text{Cl}_2$ (8)	178
6.3.2. Reaction of $\text{CpNb}(\text{N}-2\text{-}^t\text{BuC}_6\text{H}_4)\text{Cl}_2$ with Trimethylphosphine : Preparation of $\text{CpNb}(\text{N}-2\text{-}^t\text{BuC}_6\text{H}_4)(\text{PMe}_3)\text{Cl}_2$ (9)	179

6.3.3.	Reaction of $\text{CpNb}(\text{N}-2\text{-}^t\text{BuC}_6\text{H}_4)\text{Cl}_2$ with $\text{C}_2\text{H}_5\text{MgCl}$ in the presence of Trimethylphosphine :	
	Preparation of $\text{CpNb}(\text{N}-2\text{-}^t\text{BuC}_6\text{H}_4)(\eta^2\text{-C}_2\text{H}_4)(\text{PMe}_3)$ (10)	180
6.3.4.	Reaction of $\text{CpNb}(\text{N}-2\text{-}^t\text{BuC}_6\text{H}_4)(\text{PMe}_3)\text{Cl}_2$ with $n\text{-C}_3\text{H}_7\text{MgCl}$:	
	Preparation of $\text{CpNb}(\text{N}-2\text{-}^t\text{BuC}_6\text{H}_4)(\eta^2\text{-C}_3\text{H}_6)(\text{PMe}_3)$ (11)	181
6.3.5.	Reduction of $\text{CpNb}(\text{N}-2\text{-}^t\text{BuC}_6\text{H}_4)\text{Cl}_2$ with Magnesium in the presence of Trimethylphosphine :	
	Preparation of $\text{CpNb}(\text{N}-2\text{-}^t\text{BuC}_6\text{H}_4)(\text{PMe}_3)_2$ (12)	184
6.3.6.	Reaction of $\text{CpNb}(\text{N}-2\text{-}^t\text{BuC}_6\text{H}_4)(\text{PMe}_3)_2$ with Phenylacetylene:	
	Preparation of $\text{CpNb}(\text{N}-2\text{-}^t\text{BuC}_6\text{H}_4)(\text{PhC}\equiv\text{CH})(\text{PMe}_3)$ (13)	185
6.3.7.	Reaction of $\text{CpNb}(\text{N}-2\text{-}^t\text{BuC}_6\text{H}_4)(\text{PMe}_3)_2$ with Diphenylacetylene:	
	Preparation of $\text{CpNb}(\text{N}-2\text{-}^t\text{BuC}_6\text{H}_4)(\text{PhC}\equiv\text{CPh})(\text{PMe}_3)$ (14)	186
6.3.8.	Reaction of CpNbCl_4 with $\text{Me}_3\text{SiNH}(2,6\text{-Cl}_2\text{C}_6\text{H}_3)$:	
	Preparation of $\text{CpNb}(\text{N}-2,6\text{-Cl}_2\text{C}_6\text{H}_3)\text{Cl}_2$ (15)	188
6.3.9.	Reaction of $\text{CpNb}(\text{N}-2,6\text{-Cl}_2\text{C}_6\text{H}_3)\text{Cl}_2$ with Trimethylphosphine :	
	Preparation of $\text{CpNb}(\text{N}-2,6\text{-Cl}_2\text{C}_6\text{H}_3)(\text{PMe}_3)\text{Cl}_2$ (16)	189
6.3.10.	Reaction of $\text{CpNb}(\text{N}-2,6\text{-Cl}_2\text{C}_6\text{H}_3)\text{Cl}_2$ with $\text{C}_2\text{H}_5\text{MgCl}$ in the presence of Trimethylphosphine :	
	Preparation of $\text{CpNb}(\text{N}-2,6\text{-Cl}_2\text{C}_6\text{H}_3)(\eta^2\text{-C}_2\text{H}_4)(\text{PMe}_3)$ (17)	190
6.4.	Experimental Details For Chapter 4	191
6.4.1.	Reaction of $\text{Cp}^*\text{Ta}(\text{N}^t\text{Bu})\text{Cl}_2$ with Benzylmagnesium chloride:	
	Preparation of $\text{Cp}^*\text{Ta}(\text{N}^t\text{Bu})(\text{CH}_2\text{Ph})_2$ (20)	191
6.4.2.	Reaction of $\text{Cp}^*\text{Ta}(\text{N}^t\text{Bu})\text{Cl}_2$ with Neophylmagnesium chloride:	
	Preparation of $\text{Cp}^*\text{Ta}(\text{N}^t\text{Bu})(\text{CH}_2\text{CMe}_2\text{Ph})_2$ (21)	192
6.4.3.	Reaction of $\text{Cp}^*\text{Ta}(\text{N}^t\text{Bu})\text{Cl}_2$ with Neopentylmagnesium chloride:	
	Preparation of $\text{Cp}^*\text{Ta}(\text{N}^t\text{Bu})(\text{CH}_2\text{CMe}_3)_2$ (22)	194
6.4.4.	Generation of $[\text{Cp}^*\text{Ta}(\text{N}^t\text{Bu})(\text{CH}_2\text{Ph})]^+[\text{B}(\text{C}_6\text{F}_5)_4]^-$ (23)	195

6.4.5.	Reaction of $\text{Cp}^*\text{Ta}(\text{N}^t\text{Bu})(\text{CH}_2\text{Ph})_2$ with Pentafluorophenol: Preparation of $[\text{Cp}^*\text{Ta}(\text{CH}_2\text{Ph})(\text{OC}_6\text{F}_5)(\mu\text{-O})]_2$ (24)	195
6.4.6.	Reaction of $\text{Cp}^*\text{Ta}(\text{N}^t\text{Bu})(\text{CH}_2\text{CMe}_2\text{Ph})_2$ with Pentafluorophenol: Preparation of $\text{Cp}^*\text{Ta}(\text{OC}_6\text{F}_5)_4$ (26) and $[\text{Cp}^*\text{Ta}(\text{OC}_6\text{F}_5)_2(\mu\text{-O})]_2$ (27)	196
6.5.	Experimental Details for Chapter 5	198
6.5.1.	Reaction of CpTaCl_4 with $\text{LiNH}(2,6\text{-Me}_2\text{C}_6\text{H}_3)$: Preparation of $\text{CpTa}(\text{N-}2,6\text{-Me}_2\text{C}_6\text{H}_3)\text{Cl}_2$ (28)	198
6.5.2.	Reaction of Cp^*TaCl_4 with $\text{LiNH}(2,6\text{-Me}_2\text{C}_6\text{H}_3)$: Preparation of $\text{Cp}^*\text{Ta}(\text{N-}2,6\text{-Me}_2\text{C}_6\text{H}_3)\text{Cl}_2$ (29)	199
6.5.3.	Reaction of Cp^*TaCl_4 with $2\text{LiNH}(2\text{-}^t\text{BuC}_6\text{H}_4)$: Preparation of $\text{Cp}^*\text{Ta}(\text{N-}2\text{-}^t\text{BuC}_6\text{H}_4)\text{Cl}_2$ (30)	200
6.5.4.	Reaction of Cp^*TaCl_4 with $4\text{LiNH}(2\text{-}^t\text{BuC}_6\text{H}_4)$ in Et_2O : Preparation of $[\text{Li}(\text{Et}_2\text{O})][\text{Cp}^*\text{Ta}(\text{N-}2\text{-}^t\text{BuC}_6\text{H}_4)_2\text{Cl}]$ (31)	201
6.5.5.	Reduction of $\text{Cp}^*\text{Ta}(\text{N-}2,6\text{-Me}_2\text{C}_6\text{H}_3)\text{Cl}_2$ with Magnesium in the presence of Trimethylphosphine : Preparation of $\text{Cp}^*\text{Ta}(\text{N-}2,6\text{-Me}_2\text{C}_6\text{H}_3)(\text{PMe}_3)_2$ (32)	202
6.5.6.	Reaction of $\text{Cp}^*\text{Ta}(\text{N}^t\text{Bu})\text{Cl}_2$ with $\text{C}_2\text{H}_5\text{MgCl}$ in the presence of Trimethylphosphine : Preparation of $\text{Cp}^*\text{Ta}(\text{N}^t\text{Bu})(\eta^2\text{-C}_2\text{H}_4)(\text{PMe}_3)$ (33)	203
6.5.7.	Reaction of $\text{Cp}^*\text{Ta}(\text{N}^t\text{Bu})\text{Cl}_2$ with $n\text{-C}_3\text{H}_7\text{MgCl}$ in the presence of Trimethylphosphine : Preparation of $\text{Cp}^*\text{Ta}(\text{N}^t\text{Bu})(\eta^2\text{-C}_3\text{H}_6)(\text{PMe}_3)$ (34)	204
6.5.8.	Reaction of $\text{Cp}^*\text{Ta}(\text{N-}2,6\text{-Me}_2\text{C}_6\text{H}_3)\text{Cl}_2$ with $\text{C}_2\text{H}_5\text{MgCl}$ in the presence of Trimethylphosphine : Preparation of $\text{Cp}^*\text{Ta}(\text{N-}2,6\text{-Me}_2\text{C}_6\text{H}_3)(\eta^2\text{-C}_2\text{H}_4)(\text{PMe}_3)$ (35)	206
6.5.9.	Reaction of $\text{Cp}^*\text{Ta}(\text{N}^t\text{Bu})(\eta^2\text{-C}_2\text{H}_4)(\text{PMe}_3)$ with Ethylene : Observation of $\text{Cp}^*\text{Ta}(\text{N}^t\text{Bu})(\sigma\text{-}1,4\text{-C}_4\text{H}_8)$ (36)	207

6.5.10. Reaction of $\text{Cp}^*\text{Ta}(\text{N}^t\text{Bu})(\text{CH}_2=\text{CHMe})(\text{PMe}_3)$ with $\text{PhC}\equiv\text{CH}$:	
Observation of $\text{Cp}^*\text{Ta}(\text{N}^t\text{Bu})(\text{PhC}\equiv\text{CH})(\text{PMe}_3)$ (37)	207
6.5.11. Reaction of $\text{Cp}^*\text{Ta}(\text{N}-2,6\text{-Me}_2\text{C}_6\text{H}_3)(\text{CH}_2=\text{CH}_2)(\text{PMe}_3)$ with $\text{PhC}\equiv\text{CPh}$:	
Observation of $\text{Cp}^*\text{Ta}(\text{N}-2,6\text{-Me}_2\text{C}_6\text{H}_3)(\text{PhC}\equiv\text{CPh})(\text{PMe}_3)$ (38)	208
6.5.12. Reaction of $\text{Cp}^*\text{Ta}(\text{N}-2,6\text{-}^i\text{Pr}_2\text{C}_6\text{H}_3)(\text{CH}_2=\text{CH}_2)(\text{PMe}_3)$ with $\text{PhC}\equiv\text{CPh}$:	
Observation of $\text{Cp}^*\text{Ta}(\text{N}-2,6\text{-}^i\text{Pr}_2\text{C}_6\text{H}_3)(\text{PhC}\equiv\text{CPh})(\text{PMe}_3)$ (39)	208
6.5.13. Reaction of $\text{Cp}^*\text{Ta}(\text{N}-2,6\text{-}^i\text{Pr}_2\text{C}_6\text{H}_3)(\text{PhC}\equiv\text{CPh})(\text{PMe}_3)$ with $\text{PhC}\equiv\text{CPh}$:	
Observation of $\text{Cp}^*\text{Ta}(\text{N}-2,6\text{-}^i\text{Pr}_2\text{C}_6\text{H}_3)(\text{PhC}\equiv\text{CPh})_2$ (40)	209
6.5.14. Reaction of $\text{Cp}^*\text{Ta}(\text{N}-2,6\text{-}^i\text{Pr}_2\text{C}_6\text{H}_3)\text{Cl}_2$ with 2^nBuLi in the presence of Ethylene : Preparation of	
$\text{Cp}^*\text{Ta}(\text{N}-2,6\text{-}^i\text{Pr}_2\text{C}_6\text{H}_3)(\sigma\text{-}1,4\text{-}(2\text{-Et})\text{C}_4\text{H}_7)$ (41)	209
6.5.15. Reaction of $\text{Cp}^*\text{Ta}(\text{N}-2,6\text{-}^i\text{Pr}_2\text{C}_6\text{H}_3)(\sigma\text{-}1,4\text{-}(2\text{-Et})\text{C}_4\text{H}_7)$ with Carbon Monoxide : Preparation of	
$\text{Cp}^*\text{Ta}(\text{N}-2,6\text{-}^i\text{Pr}_2\text{C}_6\text{H}_3)[\sigma\text{-}1,6\text{-C}(\text{O})(3\text{-Et})\text{C}_4\text{H}_7\text{C}(\text{O})]$ (42)	210
6.5.16. Reaction of $\text{Cp}^*\text{Ta}(\text{N}-2,6\text{-}^i\text{Pr}_2\text{C}_6\text{H}_3)\text{Cl}_2$ with 2^nBuLi in the presence of Trimethylphosphine :	
Preparation of $\text{Cp}^*\text{Ta}(\text{N}-2,6\text{-}^i\text{Pr}_2\text{C}_6\text{H}_3)(\eta^2\text{-C}_4\text{H}_8)(\text{PMe}_3)$ (43)	212
6.6. Polymerization Procedure	213
6.7. References	214
Appendices	215
Appendix A: X-Ray Crystallographic Data	216
Appendix B: Colloquia, Lectures and Seminars Organised by the Department of Chemistry 1992-1995	223
Appendix C: Conferences attended	228

Chapter 1

An Overview of Half-Sandwich Imido and Related Complexes of the Transition Metals: Bonding, Reactivity and Applications in Catalysis



1.1. Introduction

Imido ligation in transition metal chemistry has gained prominence in recent years as a result of the remarkable range of reactivity which has been observed in these systems. The metal-imido interaction intrinsically allows access to high metal oxidation states, and can confer unusual reactivity upon the imido moiety or the complex as a whole depending on the nature of the metal, the ancillary ligands and the steric and electronic properties of the imido substituent.

The cyclopentadienyl ligand has also found extensive use in organotransition metal chemistry and its beneficial stabilising and solubility characteristics are widely documented. This thesis is concerned with the chemistry of half-sandwich imido complexes of specifically the Group 5 metals, with a view to developing reagents which can be employed in polymerisation catalysis and/or organic synthesis.

The remainder of this chapter provides an introduction to imido ligation and highlights aspects of the reactivity of half-sandwich imido and related complexes. For a comprehensive review of organoimido chemistry, a major compilation by Nugent and Haymore and a recent survey by Wigley are available.¹

1.2. Relationship between Metal-Imido and Metal-(η -cyclopentadienyl) Bonding Interactions

1.2.1. Imido Bonding Modes

The imido ligand has the capacity to bind to a metal *via* one σ and either one or two π interactions. Four modes of imido ligation have been

characterised by X-ray crystallography (Figure 1.1). The terminal linear arrangement, which is observed in the majority of cases, consists of a sp-hybridised nitrogen with effective p_{π} to metal- d_{π} donation by the lone pair. In the closed-shell formalism, the imido dianion $[\text{NR}]^{2-}$ is a 6 electron donor and results in a metal-nitrogen bond order of 3. In reality, steric constraints upon the imido moiety by the organic substituent R and/or by other ancillary ligands in the metal coordination sphere often cause deviation from linearity.

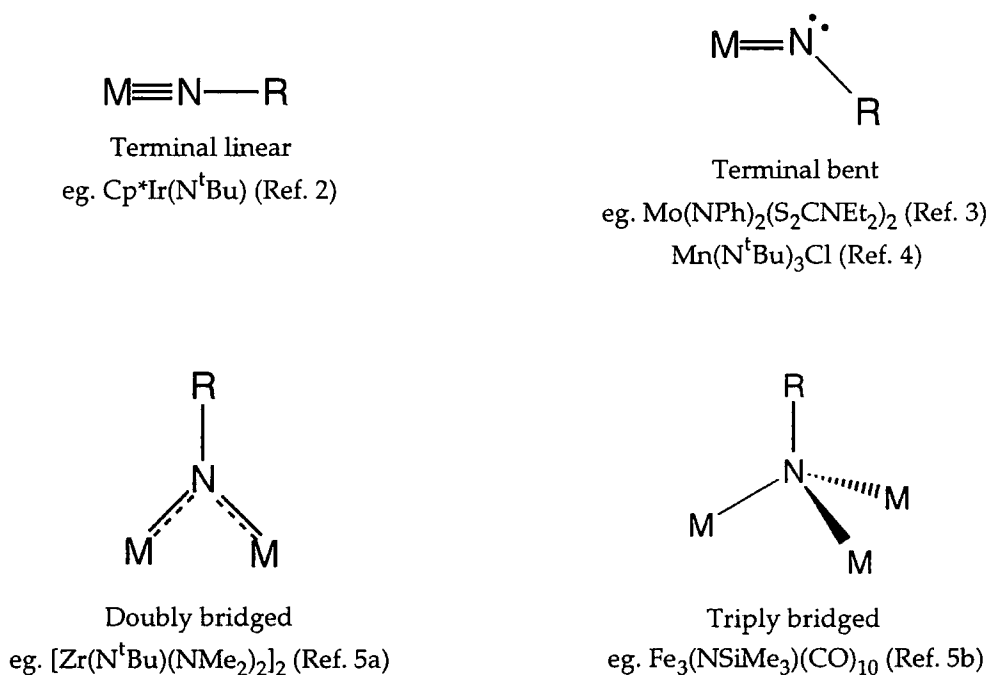


Figure 1.1.

However, the correlation between the geometry of the imido nitrogen and the metal-nitrogen bond order is tenuous. Consider the molecular structure of the trigonal planar osmium tris(imido) complex $\text{Os}(\text{N}-2,6\text{-}^i\text{Pr}_2\text{C}_6\text{H}_3)_3$, which contains linear imido ligands ($\text{Os}-\text{N}-\text{C}_{\text{ipso}}$ 178-180°).⁶ Using the above assumption, $\text{Os}(\text{N}-2,6\text{-}^i\text{Pr}_2\text{C}_6\text{H}_3)_3$ is therefore a "20-electron" complex. However, symmetry considerations of the molecular orbitals reveal that one combination of nitrogen p_{π} orbitals, which consists of the in-plane set of p orbitals, has a'_2 symmetry and consequently is incompatible with any

metal d orbital. This ligand-based orbital is occupied and hence Os(N-2,6-ⁱPr₂C₆H₃)₃ is more accurately described as an 18-electron species. In effect, the notion that a linear imido moiety corresponds to lone-pair donation to the metal and therefore a metal-nitrogen triple bond can be inappropriate, especially in examples where multiple π donor ligands are present in the molecule.

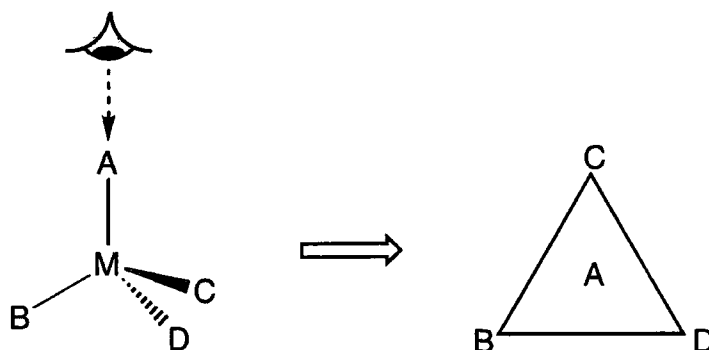
The terminal bent structure represents a sp^2 -hybridised nitrogen forming a metal-nitrogen double bond, with the lone pair residing solely on the nitrogen. This configuration is very rare and can be rationalised in terms of electron localisation at the nitrogen in order to achieve an 18-electron configuration.

Doubly bridging derivatives usually occur for the early transition metals. A pyramidal nitrogen is observed when the lone pair remains localised, but significant delocalisation of the lone pair through interaction with the adjacent metals will result in planar geometry at the nitrogen. Their respective metal-nitrogen bond orders are obviously reduced compared to a terminal bonding mode; for the pyramidal cases, metal-nitrogen single bonds are expected.

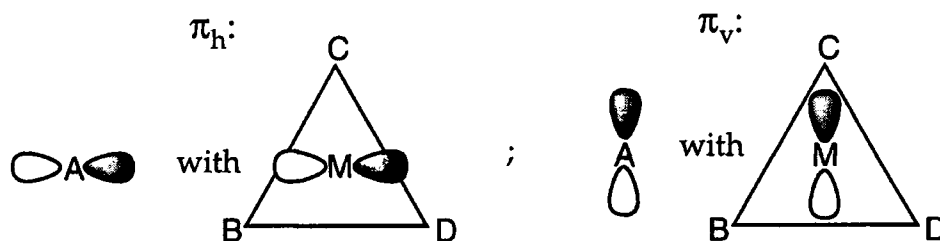
1.2.2. Bonding Patterns in Tetrahedral Transition Metal Imido Complexes

The competition between strong π -donor ligands can be studied by the qualitative MO approach adopted by Gibson and is conveniently illustrated using triad representations⁷ (Figure 1.2, see reference 7 for details) :

By viewing a tetrahedral molecule MABCD down the A–M axis, the ligands B,C and D can be placed at the corners of a triangle:



If A is capable of π bonding to the metal (eg. an imido ligand), it can interact with either (or both) of the horizontal or vertical p-symmetry orbitals (π_h or π_v respectively) in the diagram below which illustrates the MBCD pyramid as viewed from A.



π_h and π_v on the metal are represented as p-type orbitals lying parallel to the BCD plane but they are more likely to be forward-projecting lobes of hybrids of both p and d orbitals.

Figure 1.2.

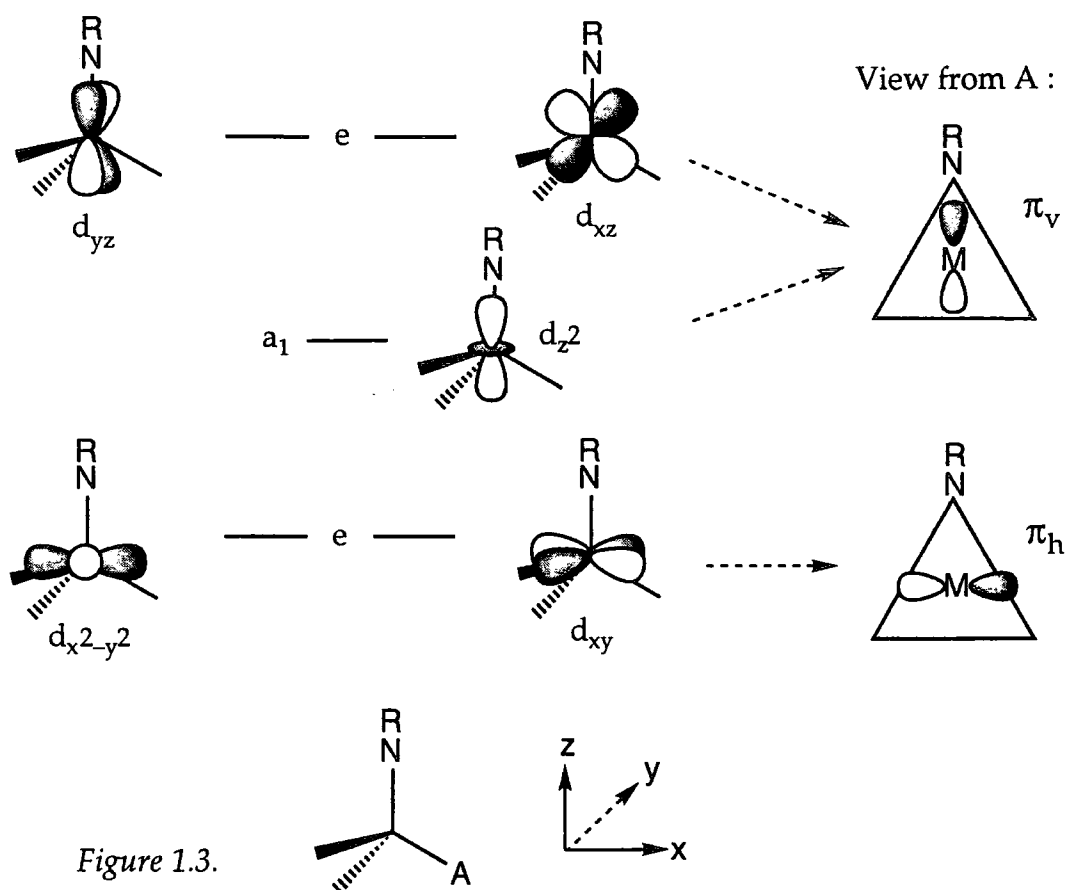


Figure 1.3.

Figure 1.3 shows the d orbital splitting diagram for a pseudo-tetrahedral complex derived (unconventionally) with the z-axis aligned along the imido-metal axis.⁸ The bonding in such species containing an imido ligand, which is a strong Π_2 donor,[§] is in general dominated by this moiety so that instead of the normal 'three over two' pattern, the degeneracy of the upper triplet is split into an e and a_1 set. It is now apparent that d_{xy} effectively corresponds to π_h while both d_{xz} and d_{z^2} can form π interactions with A in the vertical plane (π_v).

[§] Π_2 -type ligands are defined as those which possess one σ - and two π -symmetry orbitals and therefore can potentially form two equivalent π bonds and hence a triple bond with the metal. Π_2' -type ligands contain non-degenerate π orbitals. Lastly, ligands which have one π -symmetry orbital and can only form a double bond to the metal ($1\sigma, 1\pi$) are referred to as Π_1 .⁷

Next, consider the triad representation of the Schrock ROMP catalyst $\text{Mo}(\text{N-2,6-}i\text{Pr}_2\text{C}_6\text{H}_3)(\text{CH}^t\text{Bu})(\text{O}^t\text{Bu})_2$ in Figure 1.4. The orientation of the alkylidene substituent,⁹ which is depicted by the wedge-shaped lines, shows it 'pointing' to the imido group. This is rationalised by the alignment of the single frontier π orbital of the alkylidene with d_{xy}/π_h of the metal centre, in order to avoid competition for the π_v orbital of the metal which is already engaged in bonding with the strongest π donor in the triad, namely the imido ligand.

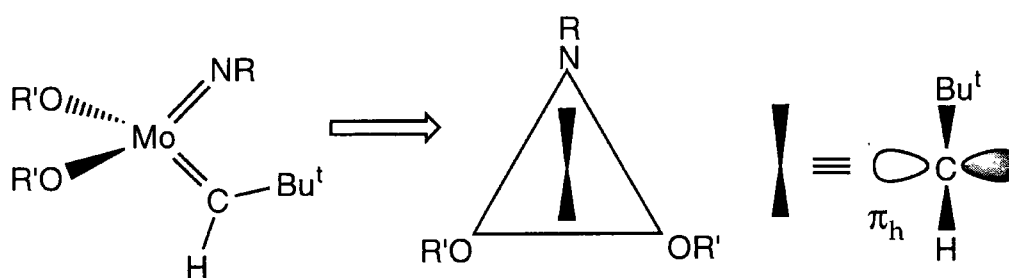


Figure 1.4.

When two Π_2 ligands are present in a molecule, as in the case of $\text{CpM}(\text{NR})\text{Cl}_2$ ($\text{M}=\text{Group 5 metal}$) complexes, a slippage of the cyclopentadienyl ring is observed where the carbon which eclipses the metal imido bond is noticeably closer to the metal, resulting in an allyl-ene distortion.¹⁰ By again assuming that the imido ligand is dominant, one can visualise that the π_h Cp-metal interaction will be greater than the perpendicular π_v interaction, since the latter is competing with the parallel metal-imido bond. Hence the filled Cp π_v orbital will remain largely ligand-based and give rise to the allyl-ene configuration (Figure 1.5).

To summarise, Gibson proposed that in complexes containing a single strong Π_2 donor, such as an imido ligand, the orientation of Π_1 ligands will reflect the competition for metal-ligand π -bonds such that this single π -interaction will occur in a plane orthogonal to the metal-imido bond.

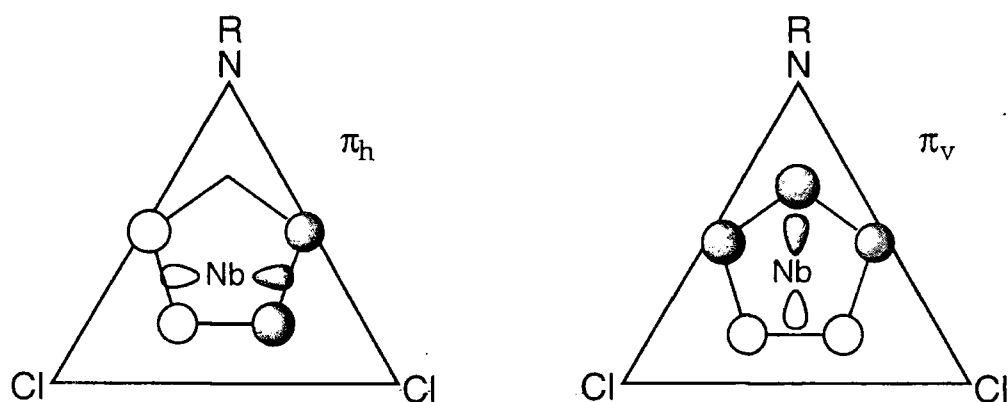


Figure 1.5.

1.2.3. Bonding Patterns for the Group 4 Metallocene, Group 5 Half-Sandwich Imido and Group 6 Bis(imido) Fragments: An Isolobal Relationship.

From a simple MO treatment, the imido and cyclopentadienyl ligands are closely related because they primarily interact with a transition metal *via* one σ and two π bonds; the Cp group also possesses empty δ -orbitals but back donation from the metal is relatively insignificant so their impact on the metal-Cp bond is minimal. Since the closed-shell imido ligand carries a formal 2- charge compared with the uni-negative Cp group, an 'isolobal' series of complexes bearing Cp and/or imido moieties with identical d electron counts is generated by crossing from Group 4 to Group 6 (Figure 1.6).

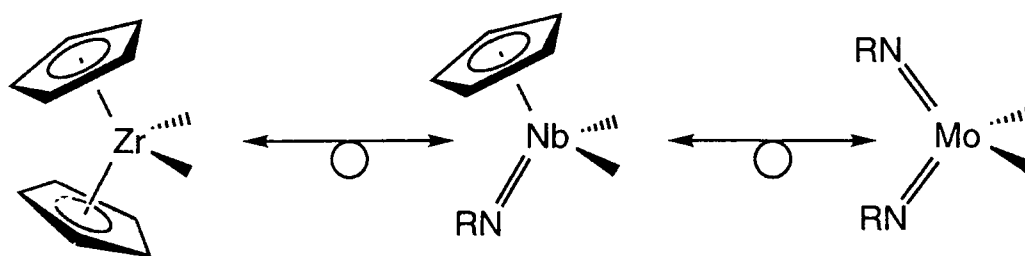


Figure 1.6.

The frontier orbitals of the Group 4 bent metallocenes have long been established to consist of three low-lying orbitals which project in the plane bisecting the Cp-metal-Cp angle.¹¹ Calculations showing metallocene-like orbitals for the [CpNb(NR)] fragment¹⁰ with similar symmetry and energies reinforce the isolobal relationship between the Group 4 metallocene, Group 5 half-sandwich imido and Group 6 bis(imido) metal fragments.¹²⁻¹⁴

Structural evidence for this correlation can be illustrated using triad representations.⁷ Gibson concluded that in complexes which contain two dominant Π_2 donor ligands, a third Π_1 ligand which can only form one π bond with the metal will align its frontier π orbital with the weakest π donor to maximise $p\pi-d\pi$ interaction and avoid competition with both dominant ligands. Hence the examples in Figure 1.7 demonstrate that for the three isolobal fragments, alkylidene substituents^{15,12b} underline the weakest π donor while alkynes^{14,16} (and similarly alkenes) point to it. Ultimately, this relationship can be utilised to identify new systems which, by comparison with the established reactivity of metallocenes, may potentially yield new catalysts or reagents for organic synthesis.

Finally, the replacement of a Cp group by other 'isolobal' ligands can afford fragments which also display metallocene-like reactivity. For example, Nakamura and co-workers have shown that the living polymerisation of ethylene is catalysed by half-sandwich η^4 -diene complexes of niobium and tantalum in the presence of methylaluminoxane.¹⁷

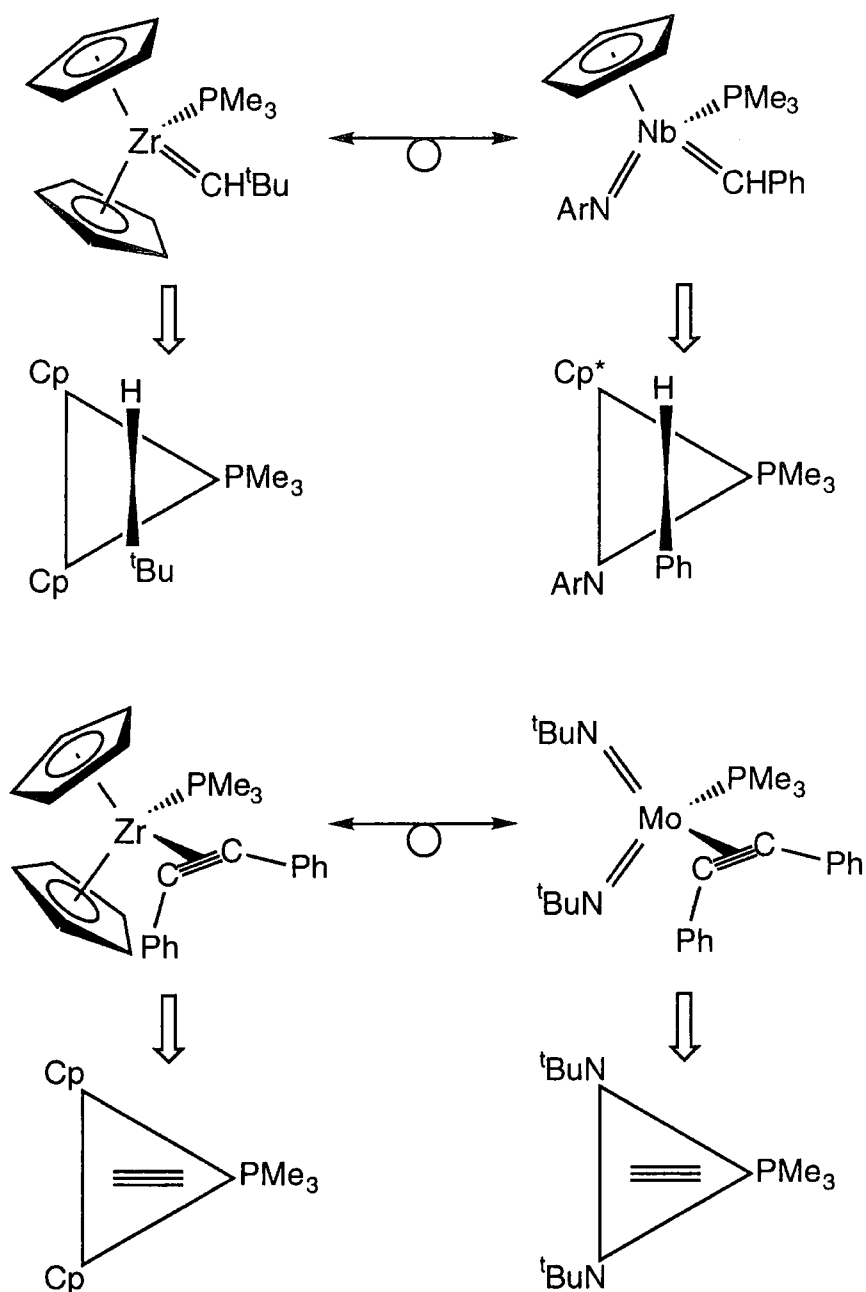


Figure 1.7.

1.3. Highlights of Transition Metal Complexes Bearing the Cyclopentadienyl and Imido Ligands

The descriptive chemistry which follows has been selected to demonstrate different preparative routes to species containing

cyclopentadienyl and imido ligands and to emphasise their wide-ranging and often novel reactivity.

1.3.1. Group 4

The generation of the transient zirconocene imido species $[\text{Cp}_2\text{Zr}(\text{NR})]$ has been reported by Bergman and co-workers^{18,19} (Figure 1.8). Thermolysis of $\text{Cp}_2\text{Zr}(\text{NHR})\text{Me}$ ($\text{R}=4\text{-}^t\text{BuC}_6\text{H}_4$, ^tBu) or $\text{Cp}_2\text{Zr}(\text{NHR})(\text{CH}_2\text{CH}_2^t\text{Bu})$ ($\text{R}=2,6\text{-Me}_2\text{C}_6\text{H}_3$, SiMe_2^tBu , CH_2Ph) releases the corresponding alkane to form $[\text{Cp}_2\text{Zr}(\text{NR})]$, which can either dimerise or be trapped by π donors and unsaturated organic substrates. Thus, when R is $4\text{-}^t\text{BuC}_6\text{H}_4$, the reaction in THF affords dimeric $[\text{Cp}_2\text{Zr}(\mu\text{-N-}4\text{-}^t\text{BuC}_6\text{H}_4)]_2$. However, for species with bulkier imido substituents, the THF-stabilised monomeric complexes $\text{Cp}_2\text{Zr}(\text{NR})(\text{thf})$ ($\text{R}=^t\text{Bu}$, $2,6\text{-Me}_2\text{C}_6\text{H}_3$, SiMe_2^tBu) are isolated.

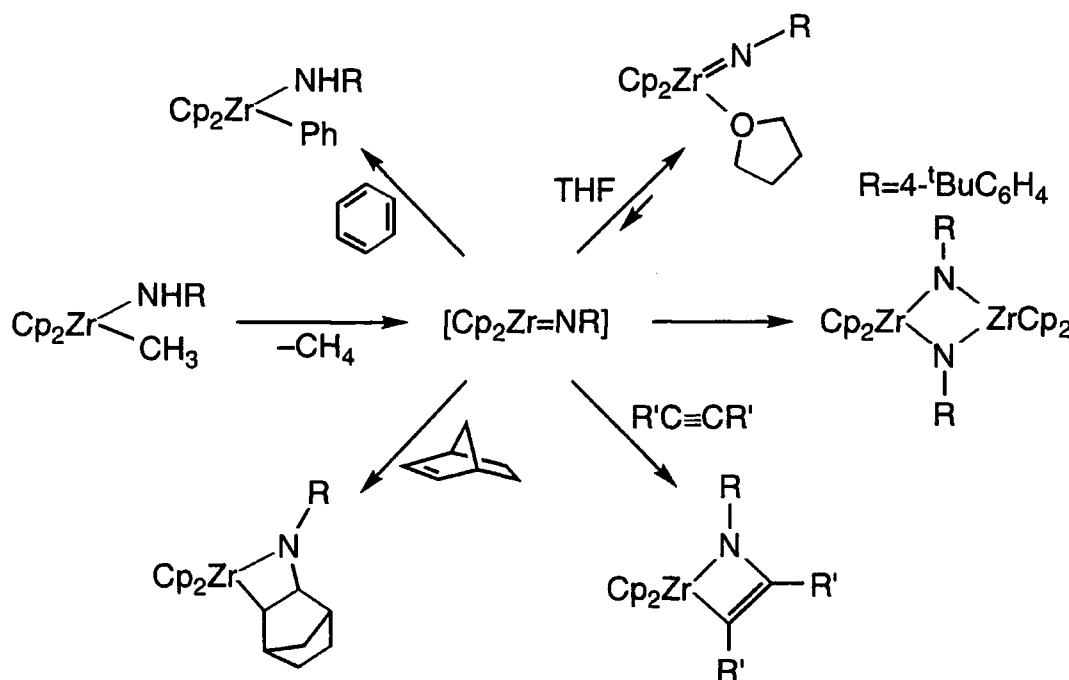


Figure 1.8.

Transient $[\text{Cp}_2\text{Zr}(\text{NR})]$ undergoes aromatic C–H bond cleavage and cycloaddition chemistry. For example, thermolysis of $\text{Cp}_2\text{Zr}(\text{NH}^t\text{Bu})\text{Me}$ in benzene results in the release of free alkane and addition of an aromatic C–H bond across the $\text{Zr}=\text{N}^t\text{Bu}$ bond to yield $\text{Cp}_2\text{Zr}(\text{NH}^t\text{Bu})\text{Ph}$. A number of metallacycles, including $\text{Cp}_2\text{Zr}[\text{N}^t\text{Bu}(\text{PhC}=\text{CPh})]$ and $\text{Cp}_2\text{Zr}[\text{N}(2,6\text{-Me}_2\text{C}_6\text{H}_3)\text{MeC}=\text{C}^t\text{Bu}]$, are formed when $[\text{Cp}_2\text{Zr}(\text{NR})]$ and alkynes react in benzene at ambient temperatures. With excess norbornene, the zircona-azacyclobutane $\text{Cp}_2\text{Zr}[\text{N}^t\text{Bu}(\text{C}_7\text{H}_{10})]$ can be isolated, although like other cycloadditions in this system, the reaction is reversible. The structures of $\text{Cp}_2\text{Zr}[\text{N}^t\text{Bu}(\text{PhC}=\text{CPh})]$ and $\text{Cp}_2\text{Zr}[\text{N}^t\text{Bu}(\text{C}_7\text{H}_{10})]$ have been determined.¹⁸

An important aspect of the $[\text{Cp}_2\text{Zr}(\text{N}^t\text{Bu})]$ fragment is the presence of multiple π donors, which evidently activates the imido ligand by destabilising strong p_π donation to the metal. This induces highly polar $\text{M}^{\delta+}-\text{N}^{\delta-}$ linkages and thus renders the imido moiety particularly susceptible to electrophilic attack. Other examples of reactive imido groups in this section can also be rationalised by the ligation of multiple π donors.

A system which also warrants discussion is the related d^0 zirconium amido complexes $(^t\text{Bu}_3\text{SiNH})_3\text{ZrR}$ ($\text{R}=\text{Me}, \text{Ph}, \text{Cy}$) synthesised by Wolczanski and co-workers.²⁰ In addition to activating aromatic C–H bonds under mild conditions, these species also engage in *methane* activation. Hence $(^t\text{Bu}_3\text{SiNH})_3\text{ZrMe}$ is generated from the thermolysis of $(^t\text{Bu}_3\text{SiNH})_3\text{ZrR}$ ($\text{R}=\text{CD}_3, \text{Cy}$) in the presence of 3 atmosphere of CH_4 in C_6D_{12} with the elimination of CD_3H and CyH respectively (Figure 1.9).

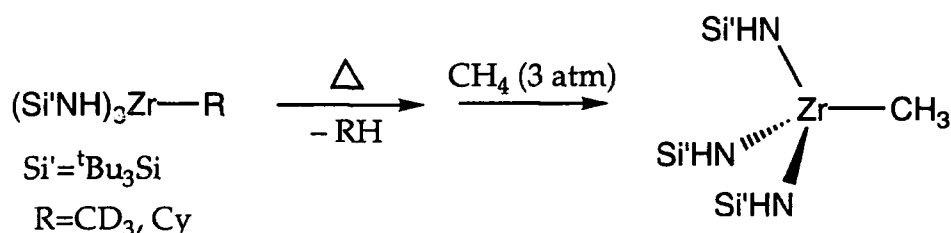


Figure 1.9.

1.3.2. Group 5

Vanadium : Maatta and co-workers described the formation of $\text{CpV}(\text{Ntol})\text{Cl}_2$ from $\text{V}(\text{Ntol})\text{Cl}_3$ and CpSiMe_3 .²¹ Preuss has also made a number of significant contributions, including the series $\text{CpV}(\text{N}^t\text{Bu})(\text{O}^t\text{Bu})_n\text{Cl}_{2-n}$ ($n=0, 1, 2$) afforded by treatment of $\text{V}(\text{N}^t\text{Bu})(\text{O}^t\text{Bu})_n\text{Cl}_{3-n}$ with LiCp .²²⁻²³

Recently, Teuben and Buijink reduced $\text{CpV}(\text{N-2,6-}i\text{Pr}_2\text{C}_6\text{H}_3)\text{Cl}_2$ with Mg in trimethylphosphine and THF to form the d^2 complex $\text{CpV}(\text{N-2,6-}i\text{Pr}_2\text{C}_6\text{H}_3)(\text{PMe}_3)_2$.²⁴ Reaction of this species with the phosphorane $\text{Ph}_3\text{P}=\text{CHPh}$ proceeds with the loss of PMe_3 to yield the first vanadium(V) alkylidene complex $\text{CpV}(\text{N-2,6-}i\text{Pr}_2\text{C}_6\text{H}_3)(=\text{CHPh})(\text{PMe}_3)$, which has been structurally characterised. However, its inactivity in the ROMP of norbornene has been attributed to coordination saturation and the lack of dissociation of the phosphine ligand from the Lewis acidic metal centre (Figure 1.10).

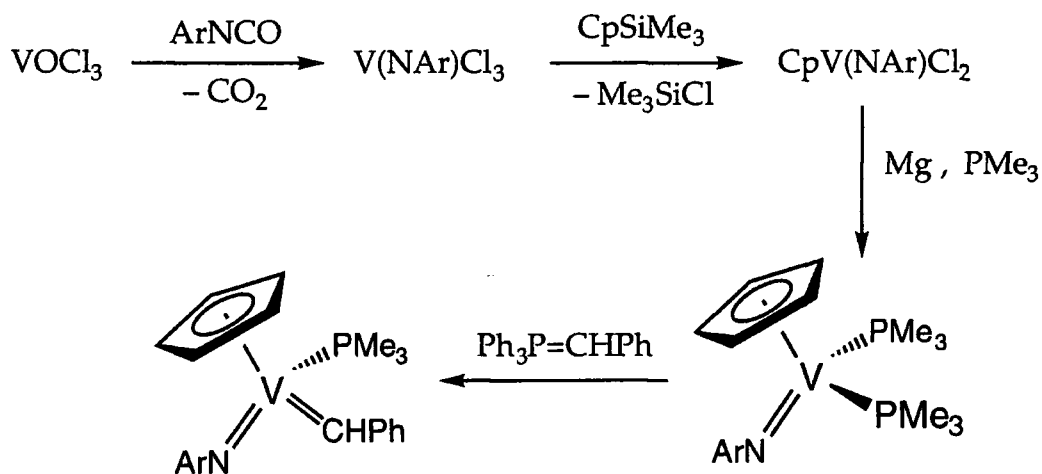


Figure 1.10. $\text{Ar} = 2,6\text{-}i\text{Pr}_2\text{C}_6\text{H}_3$.

Horton *et al* published the first structurally characterised vanadium(V) imido alkyl derivative $\text{Li}[\text{V}(\text{N}^t\text{Bu})_2\text{Me}_2]$.²⁵ The activation of C–H bonds (including methane)²⁶ and cycloaddition chemistry with alkenes and alkynes²⁷ has also been reported using the transient bis(imido) amide species

$(t\text{Bu}_3\text{SiN})_2\text{V}(\text{NHSi}^t\text{Bu}_3)$ which is generated through loss of CH_4 from the thermolysis of $(t\text{Bu}_3\text{SiN})\text{V}(\text{NHSi}^t\text{Bu}_3)_2\text{Me}$.

Niobium : Numerous half-sandwich niobium imido derivatives have been prepared by the Gibson group.^{10,12,28} Of special interest is the benzylidene complex $\text{Cp}^*\text{Nb}(\text{N-2,6-}i\text{Pr}_2\text{C}_6\text{H}_3)(=\text{CHPh})(\text{PMe}_3)$, which is generated from $\text{Cp}^*\text{Nb}(\text{N-2,6-}i\text{Pr}_2\text{C}_6\text{H}_3)(\text{CH}_2\text{Ph})_2$ via α -abstraction in the presence of the phosphine. In a related process, β -H elimination from $\text{CpNb}(\text{N-2,6-}i\text{Pr}_2\text{C}_6\text{H}_3)(\text{Ph})_2(\text{PMe}_3)$ at 60°C results in displacement of benzene and isolation of the η^2 -benzyne species $\text{CpNb}(\text{N-2,6-}i\text{Pr}_2\text{C}_6\text{H}_3)(\eta^2\text{-C}_6\text{H}_4)(\text{PMe}_3)$ (Figure 1.11). Its structure reveals a 2-electron donor, delocalised benzyne ring. The triple bond is aligned in the plane bisecting the $\text{Cp}_{\text{centroid}}\text{-Nb-N}$ angle and points at the phosphine ligand in a similar manner to the zirconocene analogue.^{12b}

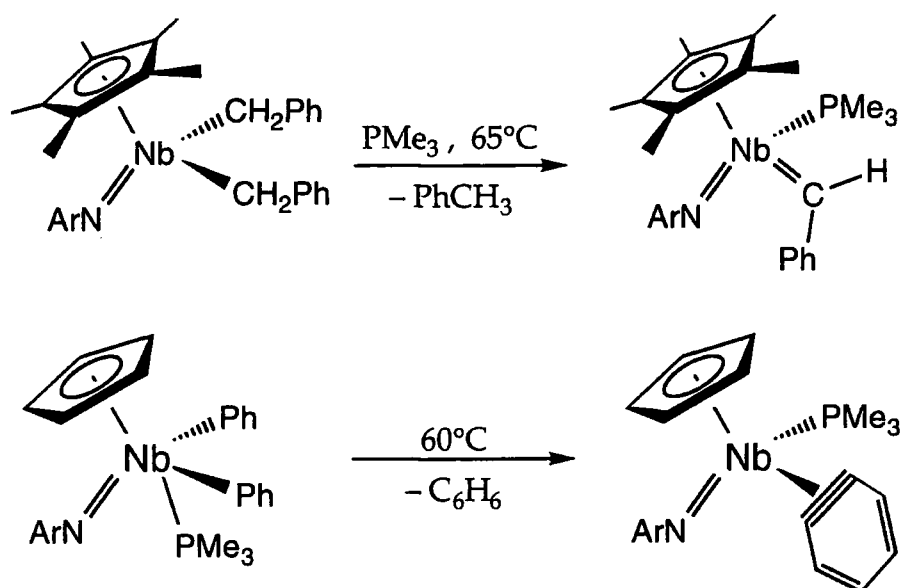


Figure 1.11. Ar=2,6-*i*Pr₂C₆H₃.

Green and co-workers have reported the one-pot reaction between NbCl_5 and $\text{C}_5\text{H}_4(\text{SiMe}_3)(\text{CH}_2)_3\text{N}(\text{SiMe}_3)_2$ to yield the intriguing product $\text{Nb}(\eta:\sigma\text{-C}_5\text{H}_4(\text{CH}_2)_3\text{N})\text{Cl}_2$.²⁹ The imido moiety here is tethered to the Cp ring

by an n-propyl unit and thus the complex is an 'isolobal' analogue to *ansa*-bridged metallocenes. The Green group also isolated $\text{Cp}_2\text{Nb}(\text{N}^t\text{Bu})(\eta^1\text{-C}_5\text{H}_5)$ by treatment of $\text{CpNb}(\text{N}^t\text{Bu})\text{Cl}_2$ with 2NaCp in THF. Variable temperature NMR studies reveal the expected Nb–C_{ipso} rotation but in addition, migration of the metal between the $\eta^1\text{-C}_5\text{H}_5$ carbon atoms in a 1,2 fashion and an $\eta^1\text{-}\eta^5$ exchange between C_5H_5 ligands were also observed.³⁰

Tantalum : $\text{Cp}'\text{Ta}(\text{N}^t\text{Bu})\text{Cl}_2$ ($\text{Cp}'=\text{Cp}, \text{Cp}^*$) (and its niobium analogues) are readily afforded upon reaction of $\text{Cp}'\text{MCl}_4$ with $^t\text{BuNH}_2$ in the presence of bases such as LiNH^tBu and $\text{LiN}^t\text{Bu}(\text{SiMe}_3)$.³¹ Treatment of the pentamethylcyclopentadienyl derivatives with 2 equivalents of methyllithium leads to the corresponding dimethyl complexes (Figure 1.12).

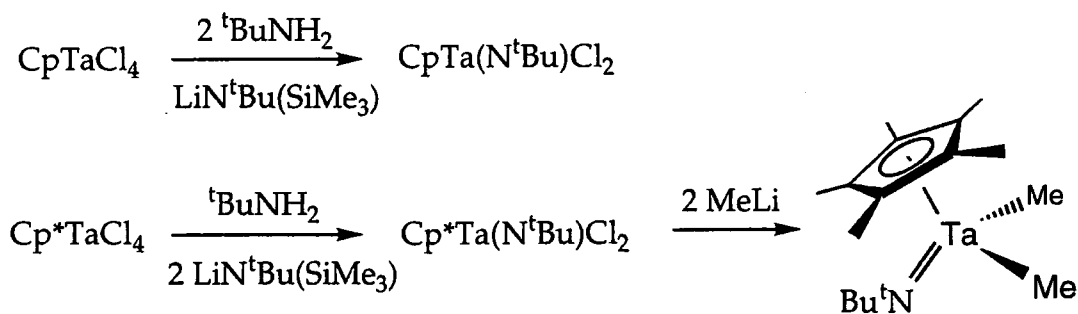


Figure 1.12.

Treatment of $\text{Cp}^*\text{TaCl}_2\text{Me}_2$ with 2 equivalents of isocyanides $\text{RN}\equiv\text{C}$ ($\text{R}=2,6\text{-Me}_2\text{C}_6\text{H}_3, 2,4,6\text{-Me}_3\text{C}_6\text{H}_2$) at ambient temperatures affords the imido derivatives $\text{Cp}^*\text{Ta}(\text{NR})\text{Cl}_2$ in almost quantitative yields, with the elimination of the imino ketene $\text{RN}=\text{C}=\text{CMe}_2$.³² The reaction is thought to proceed *via* the azatantalacyclopropane species $\text{Cp}^*\text{Ta}[\eta^2\text{-N}(\text{R})\text{CMe}_2]\text{Cl}_2$ (Figure 1.13).

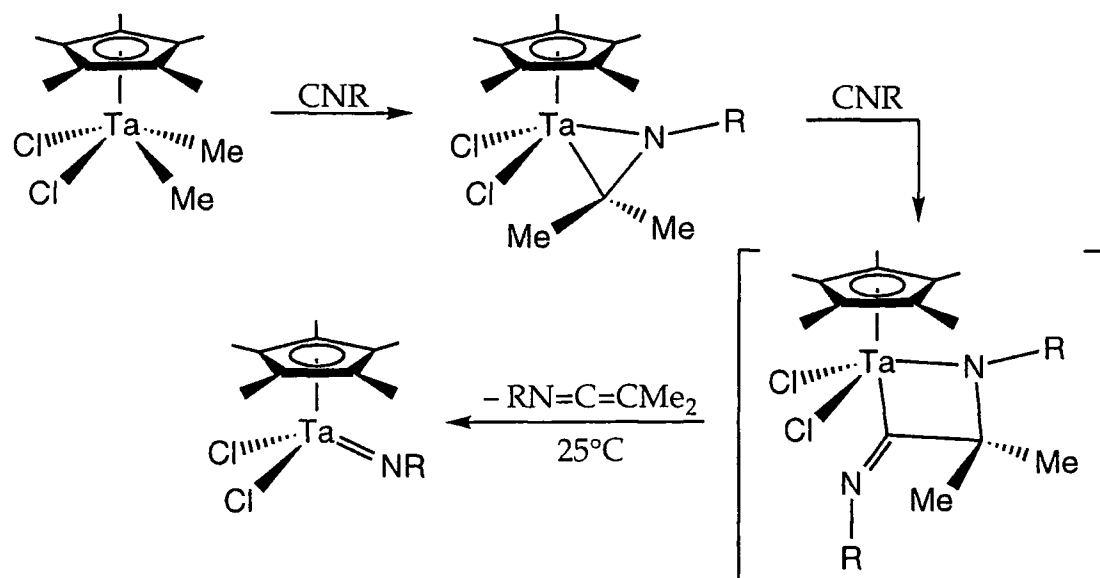


Figure 1.13.

1.3.3. Group 6 to Group 9

Molybdenum : Photolysis of a solution of $(\eta\text{-C}_5\text{H}_4^i\text{Pr})\text{Mo}(\text{N}^t\text{Bu})(\text{CH}_2=\text{CH}_2)\text{Cl}$ in the presence of 1 equivalent of NaCp gives the complex $\text{Cp}(\eta\text{-C}_5\text{H}_4^i\text{Pr})\text{Mo}(\text{N}^t\text{Bu})$ in high yield. Furthermore, the use of excess NaCp displaces the $\text{C}_5\text{H}_4^i\text{Pr}$ ligand to afford $\text{Cp}_2\text{Mo}(\text{N}^t\text{Bu})$. A structural analysis of this species revealed a pseudo-trigonal molecule in which ring distortion is evident and MO calculations and photoelectron spectroscopy studies indicate that a mainly ligand-based orbital accommodates the surplus of electrons. Accordingly, photolysing $(\eta\text{-C}_5\text{H}_4^i\text{Pr})\text{Mo}(\text{N}^t\text{Bu})(\text{CH}_2=\text{CH}_2)\text{Cl}$ with $\text{Li}(\text{C}_9\text{H}_7)$ [$(\text{C}_9\text{H}_7^-)=\text{indenyl}$] yields the slipped η^3 complex $(\eta\text{-C}_5\text{H}_4^i\text{Pr})(\eta^3\text{-C}_9\text{H}_7)\text{Mo}(\text{N}^t\text{Bu})$.³³

Tungsten : The bis(imido) complex $\text{W}(\text{N-2,6-}^i\text{Pr}_2\text{C}_6\text{H}_3)_2\text{Cl}_2(\text{thf})_2$ reacts with LiCp^* to yield burgundy $\text{Cp}^*\text{W}(\text{N-2,6-}^i\text{Pr}_2\text{C}_6\text{H}_3)_2\text{Cl}$.³⁴ Subsequent treatment with $\text{LiNH}(2,6\text{-}^i\text{Pr}_2\text{C}_6\text{H}_3)$ affords the novel 'tucked-in' complex $(\eta^5, \eta^1\text{-C}_5\text{Me}_4\text{CH}_2)\text{W}(\text{N-2,6-}^i\text{Pr}_2\text{C}_6\text{H}_3)_2$ in nearly quantitative yield (Figure 1.14).

The proposed intermediate $[\text{Cp}^*\text{W}(\text{N}-2,6\text{-}i\text{Pr}_2\text{C}_6\text{H}_3)_2(\text{NH}-2,6\text{-}i\text{Pr}_2\text{C}_6\text{H}_3)]$ is thought to contain an amido lone pair which does not interact with the metal, as a result of the extensive π bonding in the $[\text{Cp}^*\text{W}(\text{N}-2,6\text{-}i\text{Pr}_2\text{C}_6\text{H}_3)_2]$ fragment. Hence this lone pair is highly accessible for deprotonating a Cp* methyl group in $[\text{Cp}^*\text{W}(\text{N}-2,6\text{-}i\text{Pr}_2\text{C}_6\text{H}_3)_2(\text{NH}-2,6\text{-}i\text{Pr}_2\text{C}_6\text{H}_3)]$ to form 2,6- $i\text{Pr}_2\text{C}_6\text{H}_3\text{NH}_2$ and the 'tucked-in' product.

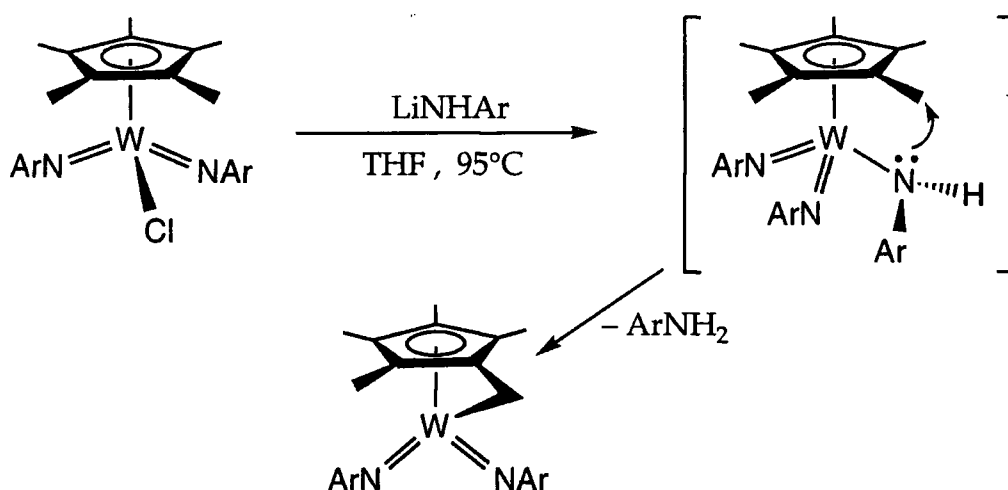


Figure 1.14. Ar=2,6- $i\text{Pr}_2\text{C}_6\text{H}_3$.

Iridium : Bergman *et al* have demonstrated that the treatment of dimeric $[\text{Cp}^*\text{IrCl}_2]_2$ with four equivalents of LiNH^tBu in THF affords yellow crystals of $\text{Cp}^*\text{Ir}(\text{N}^t\text{Bu})$ in high yield.^{2,35} $\text{Cp}^*\text{Ir}(\text{NR})$ (R=2,6-Me₂C₆H₃, 2,6- $i\text{Pr}_2\text{C}_6\text{H}_3$) can be prepared by exchange reactions between $\text{Cp}^*\text{Ir}(\text{N}^t\text{Bu})$ and RNH_2 . The structures of these 'pogo-stick' molecules reveal their monomeric nature and emphasise linearity at the Ir-N-C linkage. These complexes are nucleophilic at the imido nitrogen and display remarkable cycloaddition reactivity across the Ir-N bond with unsaturated substrates.

For example, the reaction of $\text{Cp}^*\text{Ir}(\text{N}^t\text{Bu})$ with two equivalents of $^t\text{BuNC}$ gives the carbodiimide complex $\text{Cp}^*\text{Ir}(\eta^2\text{-}^t\text{BuN}=\text{CN}^t\text{Bu})(\text{CN}^t\text{Bu})$. With excess CO the isocyanate derivative $\text{Cp}^*\text{Ir}(\eta^2\text{-}^t\text{BuN}=\text{CO})(\text{CO})$ is yielded, while in the presence of CO_2 the metallacycle $\text{Cp}^*\text{Ir}[^t\text{BuNC}(\text{O})\text{O}]$ is afforded.

In addition, treatment of $\text{Cp}^*\text{Ir}(\text{N}^t\text{Bu})$ with $\text{MeO}_2\text{CC}\equiv\text{CCO}_2\text{Me}$ results in cleavage of the Ir–N bond to form the η^4 -pyrrole product $\text{Cp}^*\text{Ir}[\eta^4\text{-C}_4(\text{CO}_2\text{Me})_4\text{N}(^t\text{Bu})]$ ³⁵ (Figure 1.15).

The isoelectronic monomeric complexes $(\eta^6\text{-arene})\text{Os}(\text{NR})$ (arene=*p*-cymene, C_6Me_6 ; $\text{R}=\text{}^t\text{Bu}$, $2,6\text{-}^i\text{Pr}_2\text{C}_6\text{H}_3$) also undergo similar cycloadditions to yield novel metallacyclic derivatives.³⁶

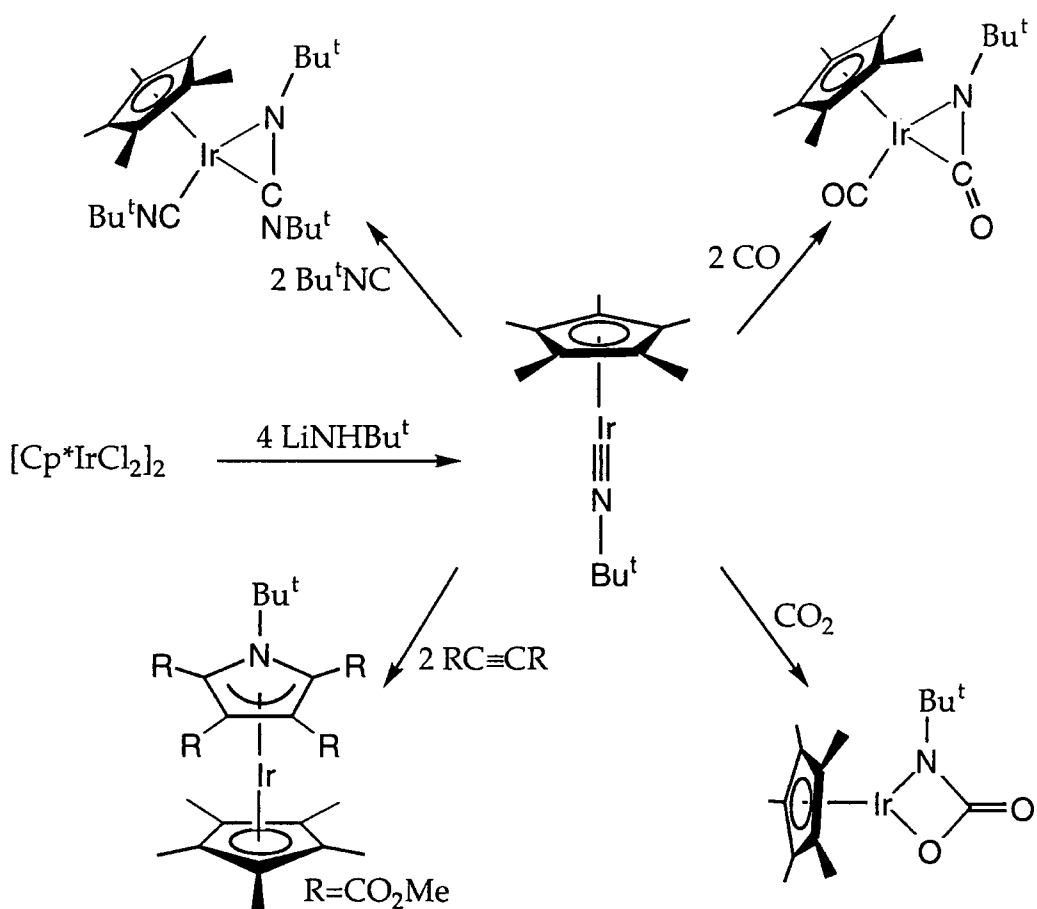


Figure 1.15.

1.4. Reactivity of Group 4 Metallocenes

1.4.1. Olefin Polymerisation Catalysts³⁷

Metallocene complexes Cp_2MCl_2 ($\text{M} = \text{Ti}, \text{Zr}$), in the presence of aluminium alkyl reagents, have long been an important class of soluble catalysts for Ziegler-Natta type olefin polymerization.³⁸⁻⁴¹ The cationic nature of the active species was proposed as early as 1961.⁴²

In recent years, the resurgence of interest in these species is partly due to the discovery by Kaminsky *et al* of the spectacular rate enhancement afforded by the use of methylaluminoxane (MAO) as co-catalyst.⁴³ In addition, this group demonstrated that the higher olefins propene and butene may be polymerised in a stereoregular manner by chiral *ansa*-bis(indenyl)-zirconium derivatives in the presence of MAO.^{44,45}

In 1985, Eisch and co-workers also suggested that the active species in these systems were cationic.⁴⁶ The following year, Jordan and co-workers isolated the tetraphenylborate salts of cationic $[\text{Cp}_2\text{ZrR}(\text{thf})]^+$ ($\text{R} = \text{CH}_3, \text{CH}_2\text{Ph}$) and demonstrated their capability to polymerise ethylene in the absence of a co-catalyst.⁴⁷ Hlatky and Turner have studied the polymerisation chemistry of the base-free zwitterionic complexes $\text{Cp}^*\text{Zr}[2\text{-Me}, 5\text{-}(\text{B}(\text{C}_5\text{H}_4\text{Me})_3)\text{Ph}]$ and $\text{Cp}^*\text{Zr}(\text{Me})(\text{C}_2\text{B}_9\text{H}_{12})$ and found both to be active catalysts for the formation of linear polyethylene (Figure 1.16).⁴⁸ However, these large weakly coordinating anions can still participate in strong interactions with the cationic alkyl species and thus polymerisation activity is reduced.

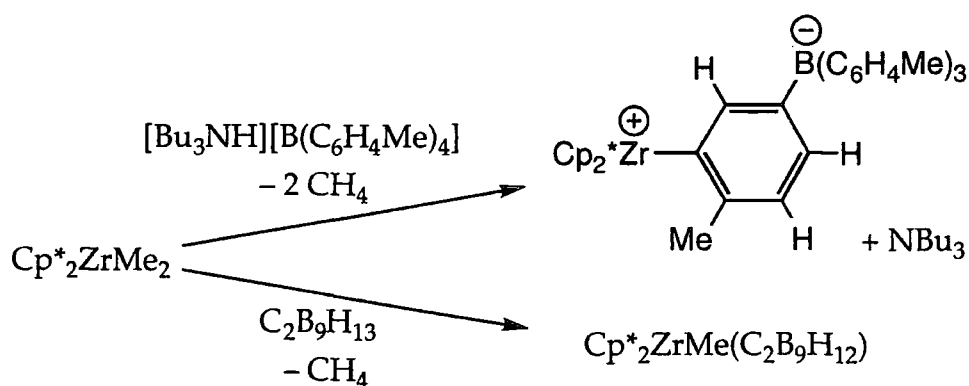


Figure 1.16.

A breakthrough in this aspect was the introduction of perfluorinated tetraphenylborates as 'non-coordinating' counterions.^{49,50} Hence the ion pairs $[\text{Cp}''_2\text{ZrMe}]^+[\text{B}(\text{C}_6\text{F}_5)_4]^-$ (Cp'' =substituted/linked Cp or indenyl) formed from the dimethyl precursor $\text{Cp}''_2\text{ZrMe}_2$ ^{51,52} (Figure 1.17) were the first well-defined zirconocene catalysts to polymerise propene and higher olefins at high rates without addition of an activator. Similar activities for ethylene and propene polymerisation were subsequently observed by Bochmann *et al* for cationic benzyl analogues.⁵³

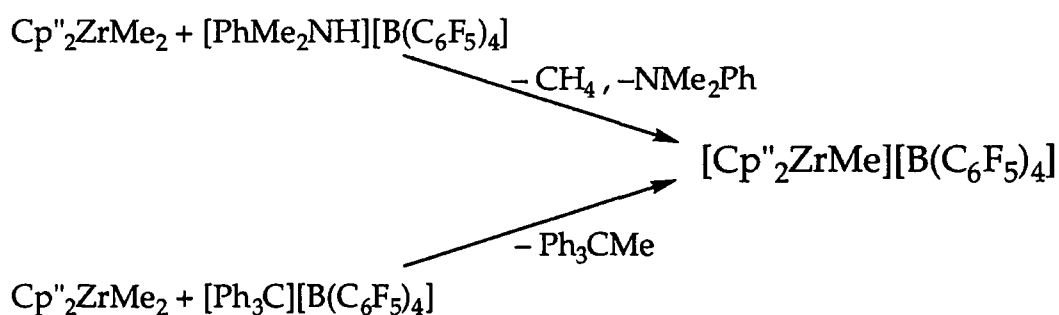


Figure 1.17. (Ref. 49–52)

Furthermore, Marks and co-workers have shown that the base-free complexes $\text{Cp}''_2\text{ZrMe}^+\text{MeB}(\text{C}_6\text{F}_5)_3^-$ (Cp'' =Cp, Cp*, Me₂C₅H₃), obtained by abstraction of Me⁻ from $\text{Cp}''_2\text{ZrMe}_2$ by the powerful Lewis acid B(C₆F₅)₃, are highly active α -olefin polymerisation catalysts.⁵⁴ A number of structural

determinations reveal ion pairing between the metal and the counterion, for example in $[(\eta\text{-Me}_2\text{C}_5\text{H}_3)_2(\text{Me})\text{Zr}^+\cdots\text{Me-B}(\text{C}_6\text{F}_5)_3^-]$.

Two possible mechanisms for α -olefin polymerisation have been proposed. The Cossee mechanism^{55a} involves initial coordination of the olefin onto a vacant site followed by direct migratory insertion into the polymer chain, and has been demonstrated by Grubbs for titanocene hexenyl complexes.^{55b} The Green-Rooney-Ivin mechanism⁵⁶ involves an initial agostic interaction between one of the α -hydrogens and the metal and results in α -hydrogen elimination from the polymer chain to form a hydrido-alkylidene intermediate. A metathesis-type reaction then ensues with an olefin to give a metallacyclobutane species, which undergoes reductive elimination from the metal centre to extend the polymer chain.

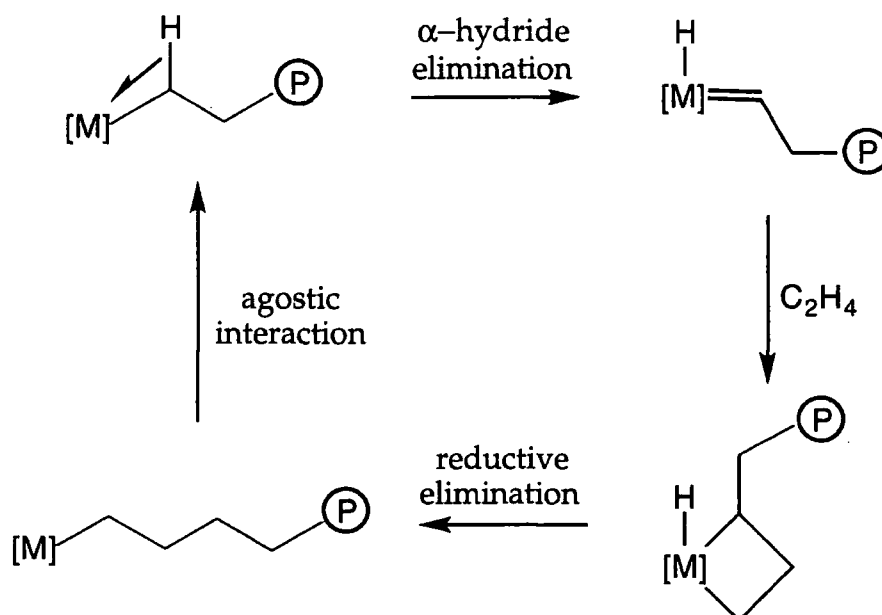


Figure 1.18. The Green-Rooney-Ivin Mechanism (P=polymer chain)

1.4.2. Reagents in Organic Synthesis

Zirconocene reagents have successfully been employed in recent years in organic synthesis to facilitate the efficient coupling of a wide variety of unsaturated organic substrates.⁵⁷ In particular, Negishi has demonstrated that a "Cp₂Zr" equivalent, generated by the treatment of Cp₂ZrCl₂ with 2 n-BuLi in THF,⁵⁸ has proved to be effective in converting a variety of enynes and diynes into the corresponding zirconabicycles in high yields;⁵⁸⁻⁶⁰ cyclopentenones are ultimately afforded upon addition of CO. These reactions proceed *via* the initial formation at -78°C of the bis(n-butyl) species Cp₂Zr(n-Bu)₂, which is unstable at ambient temperatures with respect to butane evolution and generation of the trigonal intermediate [Cp₂Zr(but-1-ene)]. The olefin ligand is readily displaced *in situ* in the presence of unsaturated hydrocarbons. For example, reaction in the presence of stilbene yields Cp₂Zr(η²-PhCH=CHPh) in 80% yield. For reactions of alkynes in the presence of phosphines, the expected zirconocene-(alkyne)(phosphine) complex is afforded. However, in the absence of a phosphine, the reaction is dominated by the formation of an alkyne-alkyne coupled zirconacyclopentadiene product.⁶¹ In addition, the formation of substituted zirconacycles is highly selective: alkyl substituents in alkenes and alkynes strongly prefer to be β to the metal, while aryl alkenyl, alkynyl and silyl groups favour the α position.^{57b} These are presumably due to steric and electronic factors respectively. This reactivity is summarised in Figure 1.19.

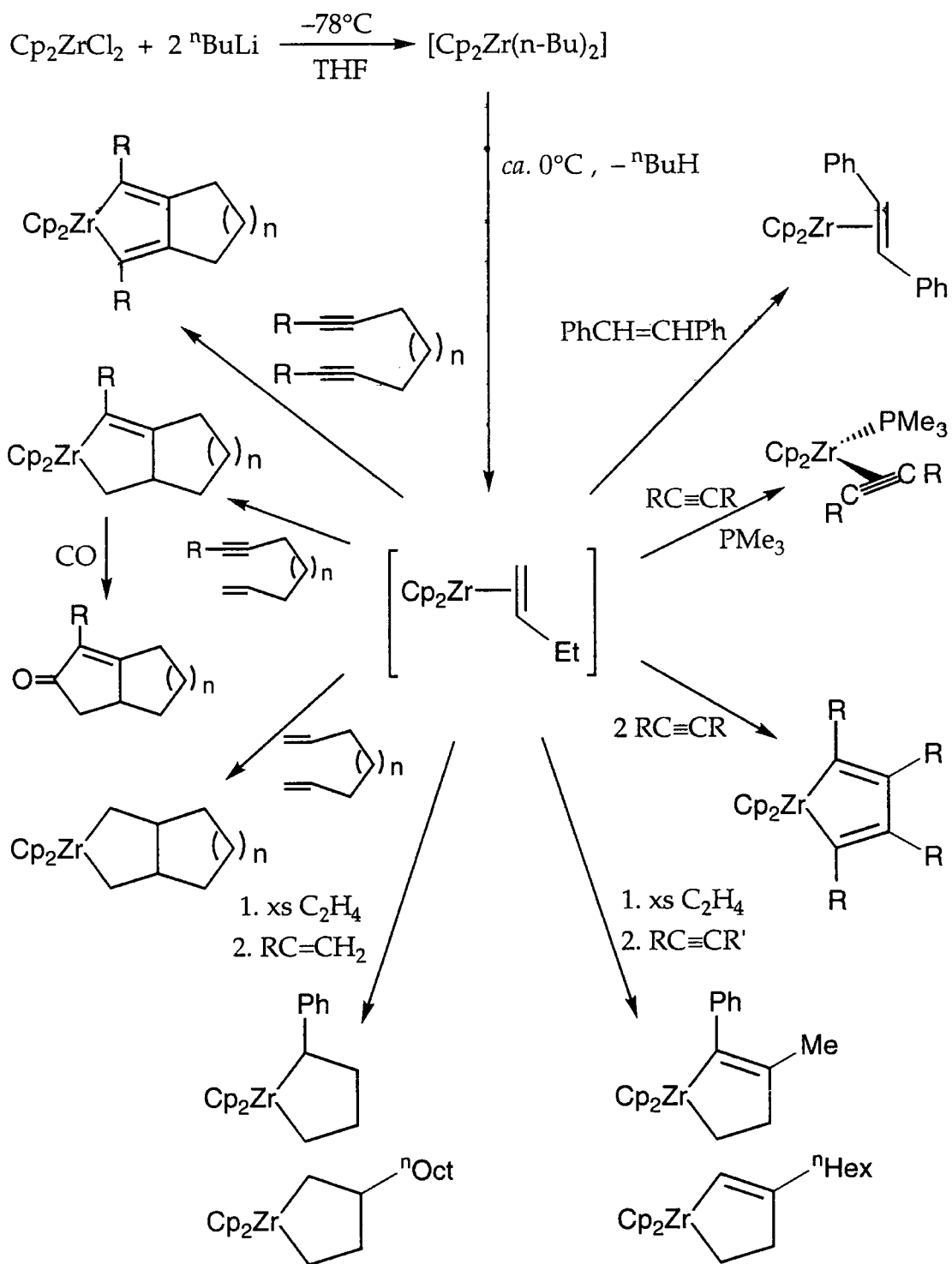


Figure 1.19.

1.4.3. Alkylidene Complexes

The ROMP of norbornene and 3,4-di(isopropylidene)cyclobutene by titanocene methylidene species has been reported by Grubbs and co-workers, in the latter case producing a novel polymer with cross-conjugated olefins in its backbone.⁶² Hessen recently described an α -abstraction process from the bis(neopentyl) complexes $\text{Cp}''_2\text{Ti}(\text{CH}_2\text{CMe}_3)_2$ ($\text{Cp}''=\text{Cp}$, $\text{C}_5\text{H}_4\text{Me}$) to afford reactive titanocene neopentylidene intermediates at ambient temperatures.⁶³ These are stabilised by PMe_3 to yield the alkylidene species $\text{Cp}''_2\text{Ti}(\text{=CHCMe}_3)(\text{PMe}_3)$ and can activate the aromatic and aliphatic C-H bonds of $\text{R}'\text{H}$ ($\text{R}'\text{H}=\text{benzene}$, p -xylene) to produce $\text{Cp}''_2\text{Ti}(\text{CH}_2\text{CMe}_3)\text{R}'$ (Figure 1.20).

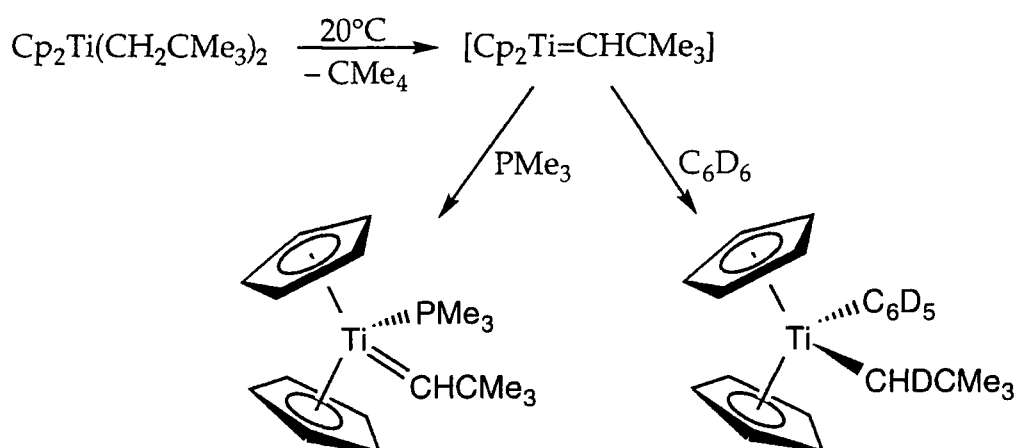


Figure 1.20.

1.5. Reactivity of Group 6 Bis(imido) Complexes

1.5.1. Olefin Polymerisation Catalysts

The synthetic entry into bis(arylimido) chromium(VI) chemistry was recently established by Gibson *et al* using the imido exchange reaction between $\text{Cr}(\text{N}^t\text{Bu})_2\text{Cl}_2$ and 2 equivalents of 2,6-*i*-Pr₂C₆H₃NH₂.⁶⁴ Treatment of the amide product $\text{Cr}(\text{N}-2,6\text{-}i\text{-Pr}_2\text{C}_6\text{H}_3)_2(\text{NH}^t\text{Bu})\text{Cl}$ with excess BCl_3 readily affords the dichloride $\text{Cr}(\text{N}-2,6\text{-}i\text{-Pr}_2\text{C}_6\text{H}_3)_2\text{Cl}_2$, which can be converted to the dialkyl derivatives $\text{Cr}(\text{N}-2,6\text{-}i\text{-Pr}_2\text{C}_6\text{H}_3)_2(\text{CH}_2\text{R})_2$ (R=H, Ph) in good yield by reaction with the appropriate Grignard reagent. Well-defined cationic ethylene polymerisation catalysts are subsequently generated upon the treatment of these dialkyl species and $\text{Cr}(\text{N}^t\text{Bu})_2(\text{CH}_2\text{Ph})_2$ with the borate salts $[\text{Ph}_3\text{C}][\text{B}(\text{C}_6\text{F}_5)_4]$ or $[\text{PhMe}_2\text{NH}][\text{B}(\text{C}_6\text{F}_5)_4]$.⁶⁵

1.5.2. Precursors to Alkylidene Complexes as ROMP Initiators

The synthesis of complexes of type $\text{Mo}(\text{NR})(=\text{CHR}')(\text{OR}'')_2$ (typically R=2,6-*i*-Pr₂C₆H₃, R'=^tBu, CMe₂Ph, R''=^tBu, CMe(CF₃)₂, C(CF₃)₃) *via* bis(imido) dialkyl derivatives was originally reported by Schrock and co-workers.^{9,66} The resultant four-coordinate molybdenum imido alkylidene complexes are of considerable technological importance due to their role in the well-defined ring-opening metathesis polymerisation (ROMP) of strained cyclic olefins.⁶⁷ Osborn demonstrated the use of the electron-withdrawing alcohol (CF₃)₂CHOH to protonate and subsequently eliminate an imido ligand from $\text{Mo}(\text{N}^t\text{Bu})_2(\text{CH}_2^t\text{Bu})_2$ to afford analogous ROMP catalysts.⁶⁸

$\text{Mo}(\text{N}-2,6\text{-}i\text{-Pr}_2\text{C}_6\text{H}_3)(=\text{CH}^t\text{Bu})(\text{O}^t\text{Bu})_2$ is inactive for the metathesis of ordinary alkenes but has outstanding activity and functional group tolerance

as a ROMP initiator. Reaction with norbornene affords the living, polymeric $\text{Mo}(\text{N}-2,6\text{-}i\text{Pr}_2\text{C}_6\text{H}_3)([\text{=CHC}_5\text{H}_8\text{CH}]_n\text{=CH}^t\text{Bu})(\text{O}^t\text{Bu})_2$ with a narrow mass distribution⁶⁹ (Figure 1.21). In the presence of another monomer which contains the (CO_2Me) functional group, a block copolymer is formed which can be cleaved from the metal with benzaldehyde.⁷⁰ These ROMP catalysts also offer a remarkable degree of microstructural control over the resultant polymer by changes in the ancillary ligands.^{68,71,72}

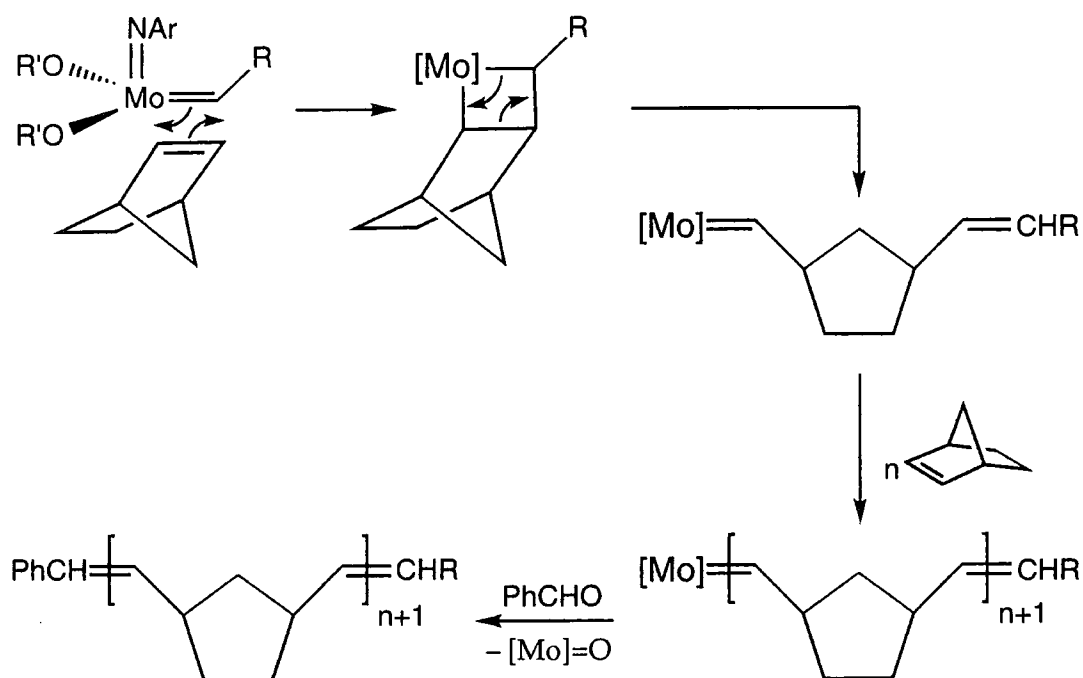


Figure 1.21.

1.6. Summary and Objectives

The qualitative molecular orbital approach introduced by Gibson⁷ highlights relationships between complexes containing a variety of different π -donor ligands. This therefore offers an opportunity to identify new systems of potential use in polymerisation catalysis and organic synthesis. Of particular relevance to this work is the isolobal relationship between bent metallocenes of the Group 4 metals and half-sandwich imido complexes of the Group 5 metals.

Chapter 2 describes investigations into the alkylation of half-sandwich vanadium imido derivatives and the isolation of several novel products. Chapter 3 aims to evaluate the steric and electronic influence of the imido substituent in a series of niobium complexes and reports on the successful stabilisation of previously inaccessible species. Syntheses of tantalum(V) dialkyl analogues are detailed in Chapter 4 and subsequent studies include examples of reactivity at the imido ligand. Finally, attempts to develop and explore the oxidative coupling chemistry at the half-sandwich tantalum imido fragment are discussed in Chapter 5.

1.7. References

1. (a) W.A. Nugent, B.L. Haymore, *Coord. Chem. Rev.*, 1980, **31**, 123; (b) D.E. Wigley, *Prog. Inorg. Chem.*, 1994, **42**, 239.
2. D.S. Glueck, F.J. Hollander, R.G. Bergman, *J. Am. Chem. Soc.*, 1989, **111**, 2719.
3. B.L. Haymore, E.A. Maatta, R.A.D. Wentworth, *J. Am. Chem. Soc.*, 1979, **101**, 2063.
4. A.A. Danapoulos, G. Wilkinson, T. Sweet, M.B. Hursthouse, *J. Chem. Soc. Chem. Commun.*, 1993, 495.
5. (a) W.A. Nugent, R.L. Harlow, *Inorg Chem.*, 1979, **18**, 2030; (b) B.L. Barnett, C. Kruger, *Angew. Chem., Int. Ed. Engl.*, 1971, **10**, 910.
6. J.T. Anhaus, T.P. Kee, M.H. Schofield, R.R. Schrock, *J. Am. Chem. Soc.*, 1990, **112**, 1642.
7. V.C. Gibson, *J. Chem. Soc. Dalton Trans.*, 1994, 1607. V.C. Gibson, *Angew. Chem., Int. Ed. Engl.*, 1994, **33**, 1656.
8. J.M. Mayer, D.L. Thorn, T.H. Tulip, *J. Am. Chem. Soc.*, 1985, **107**, 7454.
9. C.J. Schaverien, J.C. Dewan, R.R. Schrock, *J. Am. Chem. Soc.*, 1986, **108**, 2771; J.S. Murdzek, R.R. Schrock, *Organometallics*, 1987, **6**, 1373.
10. D.N. Williams, J.P. Mitchell, A.D. Poole, U. Siemeling, W. Clegg, D.C.R. Hockless, P.A. O'Neil, V. C. Gibson, *J. Chem. Soc., Dalton Trans.*, 1992, 739.
11. J.W. Lauher and R. Hoffman, *J. Am. Chem. Soc.*, 1976, **98**, 1729.
12. (a) A.D. Poole, V.C. Gibson, W. Clegg, *J. Chem. Soc., Chem. Commun*, 1992, 237. (b) J.K. Cockcroft, V.C. Gibson, J.A.K. Howard, A.D. Poole, U. Siemeling, C. Wilson, *J. Chem. Soc., Chem. Commun*, 1992, 1668.
13. D.S. Williams, M.H. Schofield, J.T. Anhaus, R.R. Schrock, *J. Am. Chem. Soc.*, 1990, **112**, 6729.
14. P.W. Dyer, V.C. Gibson, J.A.K. Howard, B. Whittle, C. Wilson, *Polyhedron*, 1995, **14**, 103.
15. F.W. Hartner Jr., J. Schwartz, S.M. Clift, *J. Am. Chem. Soc.*, 1983, **105**, 460; S.M. Clift, J. Schwartz, *J. Am. Chem. Soc.*, 1984, **106**, 8300.
16. T. Takahashi, D.R. Swanson, E.-I. Negishi, *Chem. Let.*, 1987, 623.

17. K. Mashima, S. Fujikawa, Y. Tanaka, H. Urata, T. Oshiki, E. Tanaka, A. Nakamura, *Organometallics*, 1995, **14**, 2633.
18. (a) P.J. Walsh, F.J. Hollander, R.G. Bergman, *J. Am. Chem. Soc.*, 1988, **110**, 8729; (b) P.J. Walsh, F.J. Hollander, R.G. Bergman, *Organometallics*, 1993, **12**, 3705.
19. P.J. Walsh, A.M. Baranger, R.G. Bergman, *J. Am. Chem. Soc.*, 1992, **114**, 1708.
20. C.C. Cummins, S.M. Baxter, P.T. Wolczanski, *J. Am. Chem. Soc.*, 1988, **110**, 8731.
21. (a) D.D. Devore, J.D. Lichtenhan, F. Takusagawa, E.A. Maatta, *J. Am. Chem. Soc.*, 1987, **109**, 7408; (b) E.A. Maatta, *Inorg. Chem.*, 1984, **23**, 2560.
22. (a) F. Preuss, H. Becker, J. Kaub, W.S. Sheldrick, *Z. Naturforsch*, 1988, **43b**, 1195; (b) F. Preuss, G. Overhoff, H. Becker, H.J. Häusler, W. Frank, G. Reiß, *Z. Anorg. Allg. Chem.*, 1993, **619**, 1827; (c) F. Preuss, H. Becker, T. Wieland, *Z. Naturforsch*, 1990, **45b**, 191.
23. F. Preuss, H. Becker, H.J. Häusler, *Z. Naturforsch*, 1987, **42b**, 881.
24. J.-K.F. Buijink, J.H. Teuben, H. Kooijman, A.L. Spek, *Organometallics*, 1994, **13**, 2922.
25. J. De With, A.D. Horton, A.G. Orpen, *Organometallics*, 1990, **9**, 2207.
26. J. de With, A.D. Horton, *Angew. Chem., Int. Ed. Engl.*, 1993, **32**, 903.
27. J. De With, A.D. Horton, A.G. Orpen, *Organometallics*, 1993, **12**, 1493.
28. (a) U. Siemeling, V.C. Gibson, *J. Organomet. Chem.*, 1992, **426**, C25; (b) U. Siemeling, V.C. Gibson, *J. Chem. Soc., Chem. Commun*, 1992, 1670.
29. D.M. Antonelli, M.L.H. Green, P. Mountford, *J. Organomet. Chem.*, 1992, **438**, C4.
30. M.L.H. Green, D.M. Michaelidou, P. Mountford, A.J. Suárez, L.-L. Wong, *J. Chem. Soc. Dalton Trans.*, 1993, 1593.
31. S. Schmidt, J. Sundermeyer, *J. Organomet. Chem.*, 1994, **472**, 127.
32. M.V. Galakhov, M. Gómez, G. Jiménez, M.A. Pellinghelli, P. Royo, A. Tiripichio, *Organometallics*, 1995, **14**, 2943.
33. J.C. Green, M.L.H. Green, J.T. James, P.C. Konidaris, G.H. Maunder, P. Mountford, *J. Chem. Soc., Chem. Commun*, 1992, 1361.

34. S.R. Huber, T.C. Baldwin, D.E. Wigley, *Organometallics*, 1993, **12**, 91.
35. D.S. Glueck, J. Wu, F.J. Hollander, R.G. Bergman, *J. Am. Chem. Soc.*, 1991, **113**, 2041.
36. R.I. Michelman, R.G. Bergman, R.A. Andersen, *J. Am. Chem. Soc.*, 1991, **113**, 5100 ; R.I. Michelman, R.G. Bergman, R.A. Andersen, *Organometallics*, 1993, **12**, 2741.
37. For recent reviews, see: (a) W Kaminsky, H. Sinn, Eds. 'Transition Metals and Organometallics as Catalysts for Olefin Polymerisation', Springer, New York, 1988; (b) A. Zambelli, C. Pellicchia, L. Oliva, *Makromol. Chem., Makromol. Symp.*, 1991, **48/49**, 297. For cationic complexes: R.F. Jordan, *Adv. Organomet. Chem.*, 1991, **32**, 325.
38. W. P. Long, D. S. Breslow, *J. Am. Chem. Soc.*, 1960, **82**, 1953.
39. G. Henrici-Olive, S. Olive, *Angew. Chem., Int. Ed. Engl.*, 1967, **6**, 790.
40. G. Fink, W. Zoller, *Makromol. Chem.*, 1981, **182**, 3265.
41. L. Clawson, J. Soto, S. Buchwald, M.L. Steigerwald, R. H. Grubbs, *J. Am. Chem. Soc.*, 1985, **107**, 3377.
42. A.K. Zevirova, A.E. Shilov, *Dokl. Acad. Nauk. SSSR*, 1961, **136**, 599; F.S. Dyachkovskii, A.K. Shilov, A.E. Shilov, *J. Polym. Sci., Part C: Polym. Symp.*, 1967, **16**, 2333.
43. H. Sinn, W Kaminsky, H.-J. Vollmer, R. Woldt, *Angew. Chem., Int. Ed. Engl.*, 1980, **19**, 390; (b) W. Kaminsky, M. Miri, H. Sinn, R. Woldt, *Makromol. Chem. Rapid. Commun.*, 1983, **4**, 417; (c) W. Kaminsky, H. Luker, *Makromol. Chem. Rapid. Commun.*, 1984, **5**, 225.
44. W Kaminsky, K. Kulper, H. H. Brintzinger, F. R. W. P. Wild, *Angew. Chem., Int. Ed. Engl.*, 1985, **24**, 507.
45. For recent review of stereospecific olefin polymerisation with chiral catalysts see: H. H. Brintzinger, D. Fischer, R. Mülhaupt, B. Rieger, R.M. Waymouth, *Angew. Chem., Int. Ed. Engl.*, 1995, **34**, 1143.
46. J. J. Eisch, A. M. Piotrowski, S. K. Brownstein, E. J. Gabe, F. L. Lee, *J. Am. Chem. Soc.*, 1985, **107**, 7219.
47. (a) R.F. Jordan, W.E. Dasher, S.F. Echols, *J. Am. Chem. Soc.*, 1986, **108**, 1718; (b) R.F. Jordan, C.S. Bajgur, R. Willet, B. Scott, *J. Am. Chem. Soc.*, 1986, **108**, 7410.

48. G. G. Hlatky, H. W. Turner, R. R. Eckman, *J. Am. Chem. Soc.*, 1989, **111**, 2728.
49. G. G. Hlatky, D.J. Upton, H. W. Turner, *Eur. Pat. Appl.*, 1988, 211004; *US Pat. Appl.*, 1990, 459921; *Chem. Abstr.*, 1991, **115**, 256897v.
50. X. Yang, C.L. Stern, T.J. Marks, *Organometallics*, 1991, **10**, 840.
51. J.A. Ewen, M.J. Elder, *Macromol. Chem., Macromol. Symp.*, 1993, **66**, 179, J.A. Ewen, M.J. Elder, *Eur. Pat. Appl.*, 1991, 426637, 426638, J.A. Ewen, M.J. Elder, *Chem. Abstr.*, 1991, **115**, 136987c, 136988d.
52. J.C.W. Chien, W.M. Tsai, M.D. Rausch, *J. Am. Chem. Soc.*, 1991, **113**, 8570.
53. (a) M. Bochmann, S.J. Lancaster, *Organometallics*, 1993, **12**, 633; (b) M. Bochmann, S.J. Lancaster, *Angew. Chem., Int. Ed. Engl.*, 1994, **33**, 1643.
54. X. Yang, C.L. Stern, T.J. Marks, *J. Am. Chem. Soc.*, 1991, **113**, 3623; *J. Am. Chem. Soc.*, 1994, **116**, 10015.
55. (a) E.G. Arlman, P. Cossee, *J. Catal.*, 1964, **3**, 99, (b) L. Clawson, J. Soto, S.L. Buchwald, M.L. Steigerwald, R.H. Grubbs, *J. Am. Chem. Soc.*, 1985, **107**, 3377.
56. (a) K.J. Ivin, J.J. Rooney, C.D. Stewart, M.L.H. Green, J.R. Mahtab, *J. Chem. Soc., Chem. Commun.*, 1978, 604, (b) M. Brookhart, M.L.H. Green, *J. Organomet. Chem.*, 1983, **250**, 395.
57. For recent reviews, see: (a) E. Negishi, p.1163, 'Comprehensive Organic Synthesis', Vol. 5, Ed. L. Paquette, Pergamon Press, New York, 1991; (b) E. Negishi, T. Takahashi, *Acc. Chem. Res.*, 1994, **27**, 124; (c) S.L. Buchwald, R.B. Nielsen, *Chem Rev.*, 1988, **88**, 1047; (d) R.D. Broene, S.L. Buchwald, *Science*, 1993, **261**, 1696.
58. E. Negishi, F.E. Cederbaum, T. Takahashi, *Tetrahedron Lett.*, 1986, **27**, 2829.
59. (a) E. Negishi, S.J. Holmes, J.M. Tour, J.A. Miller, *J. Am. Chem. Soc.*, 1985, **107**, 2568; (b) E. Negishi, D.R. Swanson, F.E. Cederbaum, T. Takahashi, *Tetrahedron Lett.*, 1987, **28**, 917; (c) E. Negishi, H. Sawada, J.M. Tour, Y. Wei, *J. Org. Chem.*, 1988, **53**, 913; (d) E. Negishi, S.J. Holmes, J.M. Tour, J.A. Miller, D.R. Swanson, F.E. Cederbaum, T. Takahashi, *J. Am. Chem. Soc.*, 1989, **111**, 3336.
60. (a) W.A. Nugent, D.L. Thorn, R.L. Harlow, *J. Am. Chem. Soc.*, 1987, **109**, 2788; (b) P.J. Fagan, W.A. Nugent, *J. Am. Chem. Soc.*, 1988, **110**, 2310; (c) T.V. Rajanbabu, W.A. Nugent, D.F. Taber, P.J. Fagan, *J. Am. Chem. Soc.*, 1988, **110**, 7128.

61. T. Takahashi, E. Negishi, D.R. Swanson, *Chem. Lett.*, 1987, 623.
62. (a) L.R. Gilliom, R.H. Grubbs, *J. Am. Chem. Soc.*, 1986, **108**, 733; (b) T.M. Swager, R.H. Grubbs, *J. Am. Chem. Soc.*, 1987, **109**, 894.
63. H. van der Heijden, B. Hessen, *J. Chem. Soc., Chem. Commun*, 1995, 145.
64. M.P. Coles, C.I. Dalby, V.C. Gibson, W. Clegg, M.R.J. Elsegood, *Polyhedron*, 1995, **14**, 2455.
65. M.P. Coles, C.I. Dalby, V.C. Gibson, W. Clegg, M.R.J. Elsegood, *J. Chem. Soc., Chem. Commun*, 1995, 1709.
66. J.S. Murdzek, R.R. Schrock, G.C. Bazan, J. Robbins, M. DiMare, M. O'Regan, *J. Am. Chem. Soc.*, 1990, **112**, 3875.
67. For recent reviews, see R.R. Schrock, *Acc. Chem. Res.*, 1990, **23**, 158; V.C. Gibson, *Adv. Mater.*, 1994, **6**, 37.
68. G. Schoettel, J. Kress, J.A. Osborn, *J. Chem. Soc., Chem. Commun*, 1989, 1062.
69. J.S. Murdzek, R.R. Schrock, *Macromolecules*, 1987, **20**, 2640.
70. R.R. Schrock, S.A. Krouse, K. Knoll, J. Feldman, J.S. Murdzek, D.C. Yang, *J. Mol. Catal.*, 1988, **46**, 243.
71. (a) G. Bazan, R.R. Schrock, E. Khosravi, W.J. Feast, V.C. Gibson, *Polymer. Commun.*, 1989, **30**, 257; (b) W.J. Feast, V.C. Gibson, E.L. Marshall, *J. Chem. Soc., Chem. Commun*, 1992, 1157.
72. (a) D.H. McConville, J.R. Wolf, R.R. Schrock, *J. Am. Chem. Soc.*, 1993, **115**, 4413; (b) J.H. Oskam, R.R. Schrock, *J. Am. Chem. Soc.*, 1993, **115**, 11831.

Chapter 2

Synthesis of Half-Sandwich Vanadium Arylimido Dichlorides and their Reactivity towards Alkylating Agents

2.1. Introduction

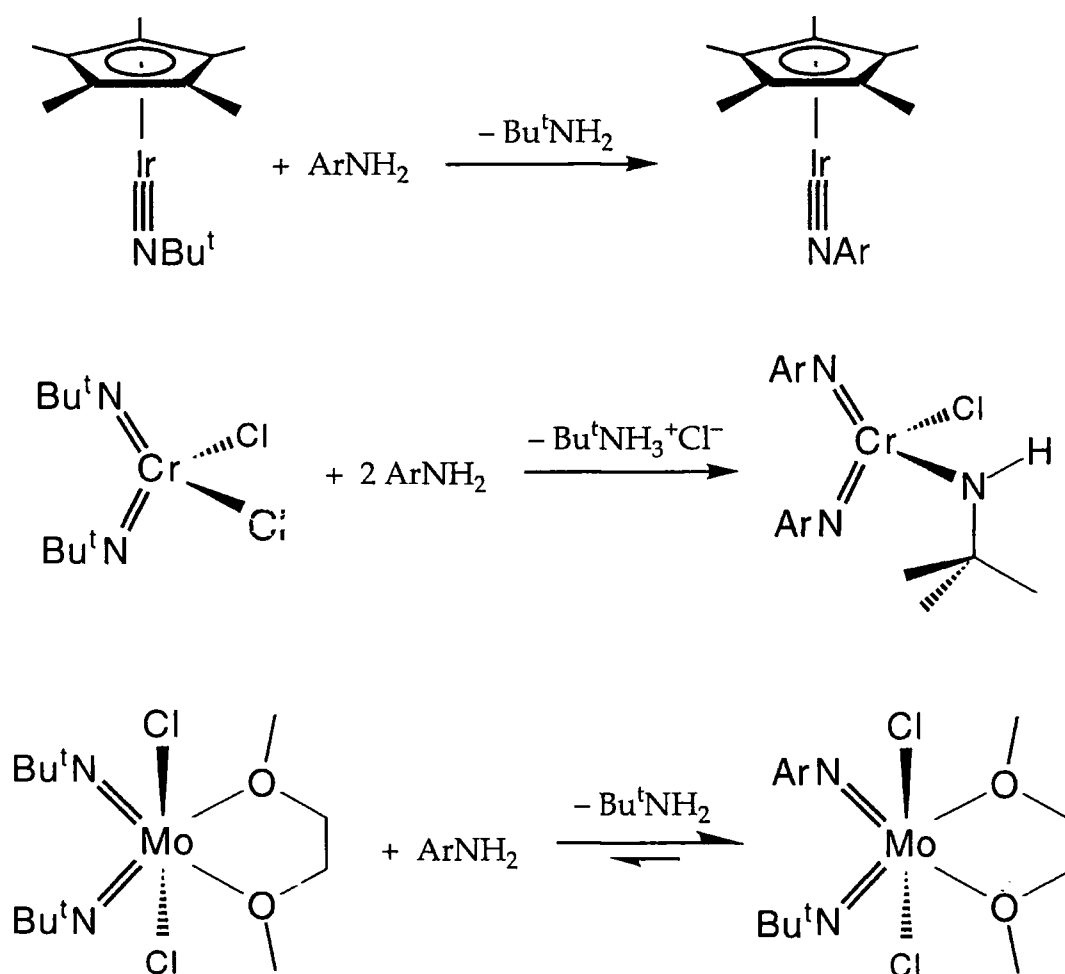
The apparent isolobal relationship across the first row of the transition metals between the $[\text{Cp}_2\text{Ti}]$, $[\text{CpV}(\text{NR})]$ and $[\text{Cr}(\text{NR})_2]$ fragments has recently been investigated.^{1,2}

The use of titanocene derivatives as precursors in α -olefin polymerisation is well established.³ Studies by this group have demonstrated that the $\text{CpV}(\text{N-p-tolyl})\text{Cl}_2/\text{Et}_2\text{AlCl}$ and $\text{Cr}(\text{N}^t\text{Bu})_2\text{Cl}_2/\text{Et}_2\text{AlCl}$ systems are active in the polymerisation of ethylene.⁴ In addition, this group has demonstrated that the reaction of $\text{Cr}(\text{N}^t\text{Bu})_2(\text{CH}_2\text{Ph})_2$ with a suitable alkyl abstracting reagent generates the well-defined cationic species $[\text{Cr}(\text{N}^t\text{Bu})_2(\text{CH}_2\text{Ph})]^+$, which is also catalytically active in ethylene polymerisation.^{1a} This correlation in reactivity with the titanocene congeners lends further support to the isolobal relationship.

Hence the first objective of this study was to synthesise new $\text{CpV}(\text{NR})\text{Cl}_2$ derivatives with different arylimido substituents in order to evaluate their effect on olefin polymerisation activity in dual-component systems. Attempts to prepare half-sandwich vanadium imido dialkyl species, which would be precursors to the corresponding alkyl cations, are also described, together with structural characterisation of the relevant products. Lastly, an undesirable feature of the half-sandwich vanadium imido dual-component catalyst is that the high activity is only short-lived, and results described herein will propose an explanation and a potential solution to this problem.

2.2. A Convenient Synthesis of CpV(NR)Cl₂ Derivatives: Imido Ligand Exchange using a Tert-Butylimido Precursor

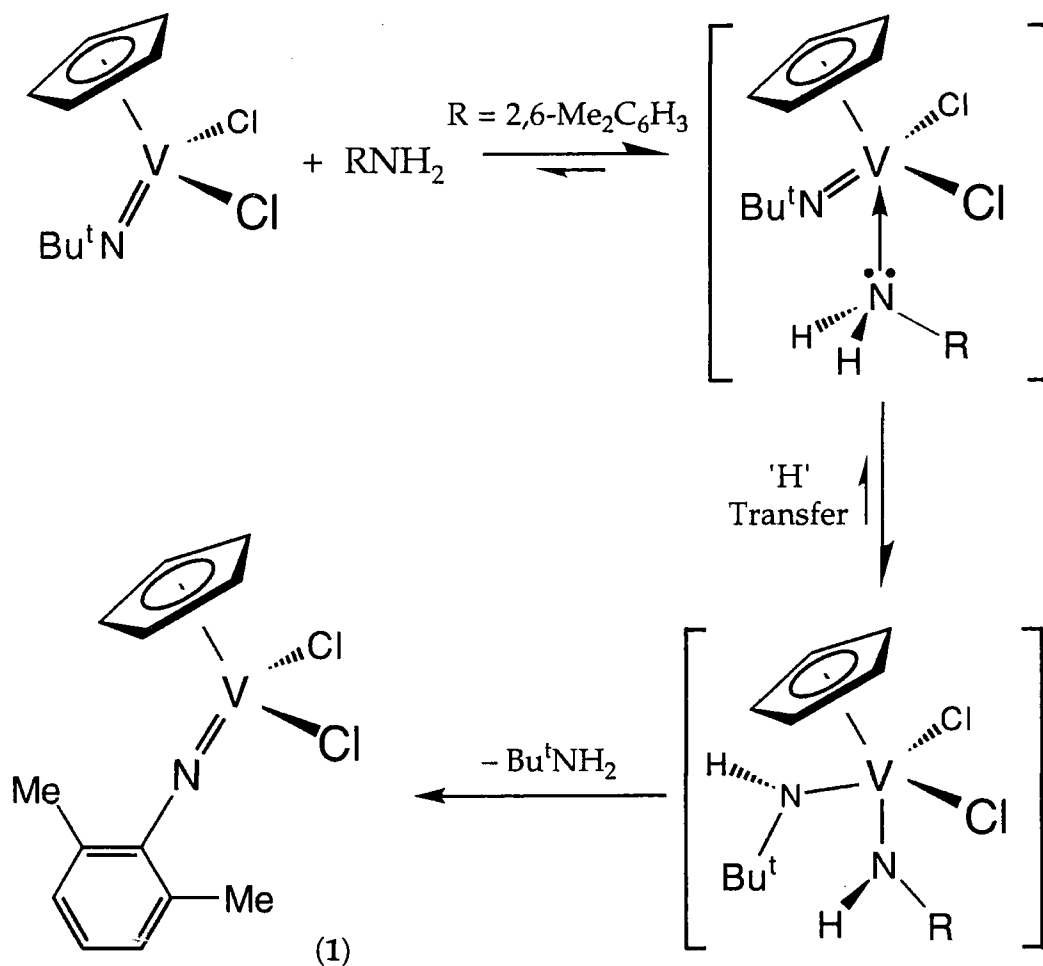
Imido ligand exchange reactions have been demonstrated by Bergman and co-workers for the Cp*Ir(NR)⁵ and (η⁶-arene)Os(NR)⁶ systems and more recently by this group in [CpNb(NR)] and [M(RN)₂] (M=Cr, Mo) chemistry (Scheme 2.1).^{1b,7,8} In these transformations, the greater basicity of the t-butyl nitrogen atom relative to the aryl nitrogen is believed to be crucial.⁷ For the purpose of this study, the multigram synthesis of CpV(N^tBu)Cl₂ has previously been reported⁹ and this therefore represents a suitable precursor to other half-sandwich vanadium imido complexes.



Scheme 2.1. Examples of Imido Exchange Reactions (Ar=2,6-ⁱPr₂C₆H₃).

2.2.1. Reaction of $\text{CpV}(\text{N}^t\text{Bu})\text{Cl}_2$ with 2,6-Dimethylaniline:Preparation and Molecular Structure of $\text{CpV}(\text{N}-2,6\text{-Me}_2\text{C}_6\text{H}_3)\text{Cl}_2$ (1)

Prolonged heating of a 1,2-dichloroethane solution of $\text{CpV}(\text{N}^t\text{Bu})\text{Cl}_2$ with one equivalent of 2,6-dimethylaniline afforded $\text{CpV}(\text{N}-2,6\text{-Me}_2\text{C}_6\text{H}_3)\text{Cl}_2$ (1) as a deep red crystalline solid in high yield. This reaction is thought to proceed via a five-coordinate amine adduct, which then undergoes intramolecular proton transfer to the *t*-butyl nitrogen to give a bis-amide intermediate.⁷ Further proton transfer then occurs to release *t*-butylamine and give the arylimido complex.



Scheme 2.2. Postulated Mechanism for Formation of 1

^1H NMR and mass spectral evidence indicate that the reaction is slow due to the reversible formation of other kinetically favoured organometallic species such as $\text{CpV}(\text{N-2,6-Me}_2\text{C}_6\text{H}_3)(\text{NH}^t\text{Bu})\text{Cl}$ and binuclear $[\text{CpV}(\text{N-2,6-Me}_2\text{C}_6\text{H}_3)(\mu\text{-Cl})]_2$. Thus these species are typically observed in the crude product mixture when the reaction is insufficiently heated. In these cases, moderate yields of **1** can nevertheless be obtained by treatment of the mixture with the mild chlorinating agent BCl_3 , a procedure used by Wilkinson in the $[\text{Cr}(\text{N}^t\text{Bu})_2]$ system.¹⁰

Elemental analysis corresponds to the empirical formula of $\text{C}_{13}\text{H}_{14}\text{NCl}_2\text{V}$. In the ^1H NMR spectrum, the ortho methyl and Cp groups give rise to singlets at 2.39 and 5.83 ppm respectively, and the aryl protons appear as the expected triplet and doublet resonances between 6.4 and 6.6 ppm.

*Molecular Structure of $\text{CpV}(\text{N-2,6-Me}_2\text{C}_6\text{H}_3)\text{Cl}_2$ (**1**)*

X-ray quality crystals were grown from a pentane solution at -20°C . The molecular structure is shown in Figure 2.1 and the structural parameters and crystal data are collected in Appendix A1.

The molecule is monomeric and isostructural with the previously crystallographically characterised half-sandwich niobium and tantalum imido dichlorides.¹¹ The V–N bond length [$1.684(9)\text{\AA}$] is typical for vanadium–(terminal imido) complexes¹² and the V–N– C_{ipso} angle shows a small deviation from linearity [$166.8(7)^\circ$]. The allyl-ene distortion of the Cp ring is evident with the metal displaced towards C(11) which eclipses the V–N bond (see p. 7). The imido phenyl ring is approximately orthogonal to the V– $\text{Cp}_{\text{centroid}}$ vector to avoid repulsion between the ortho methyl groups and the Cp ring.

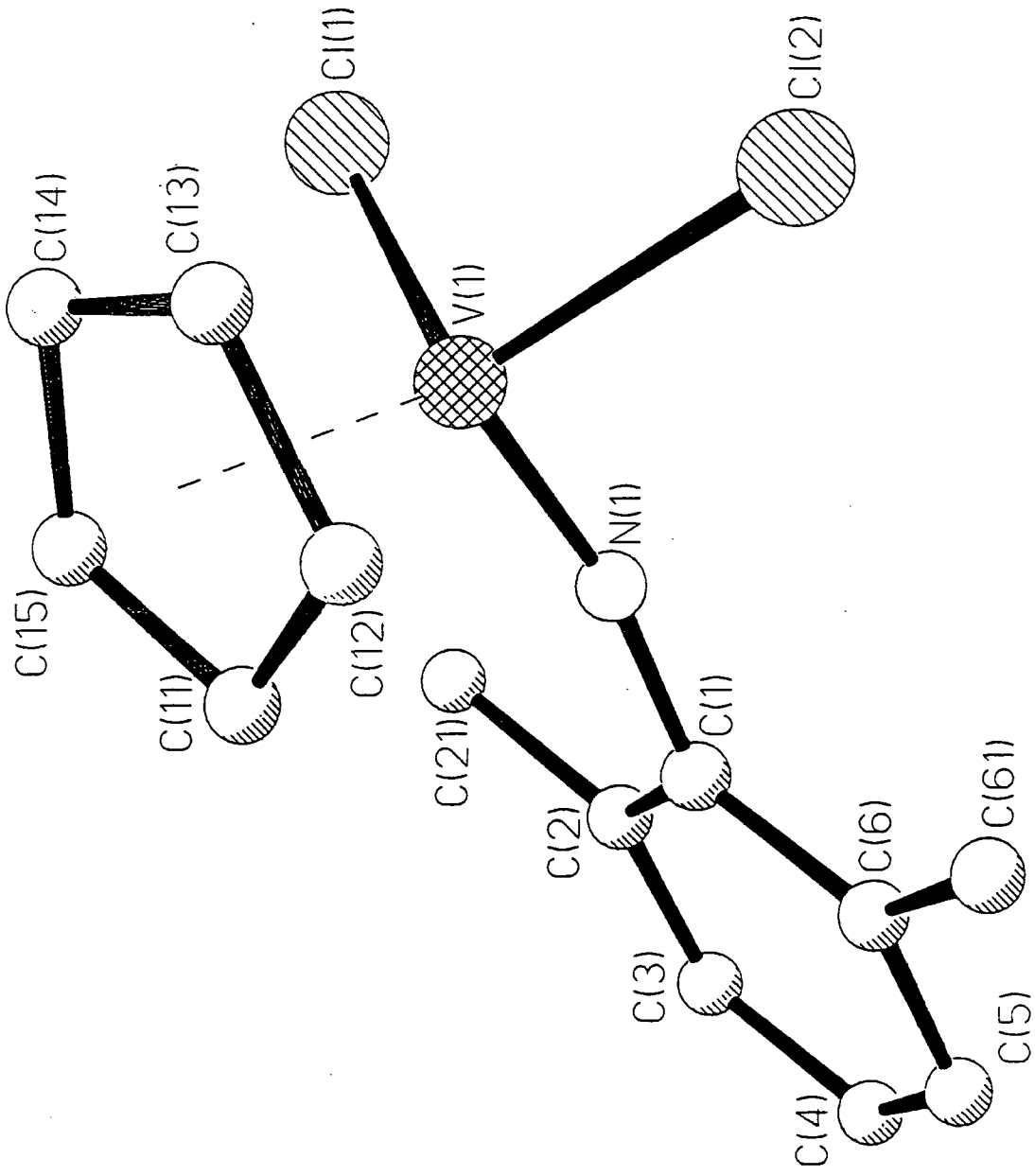
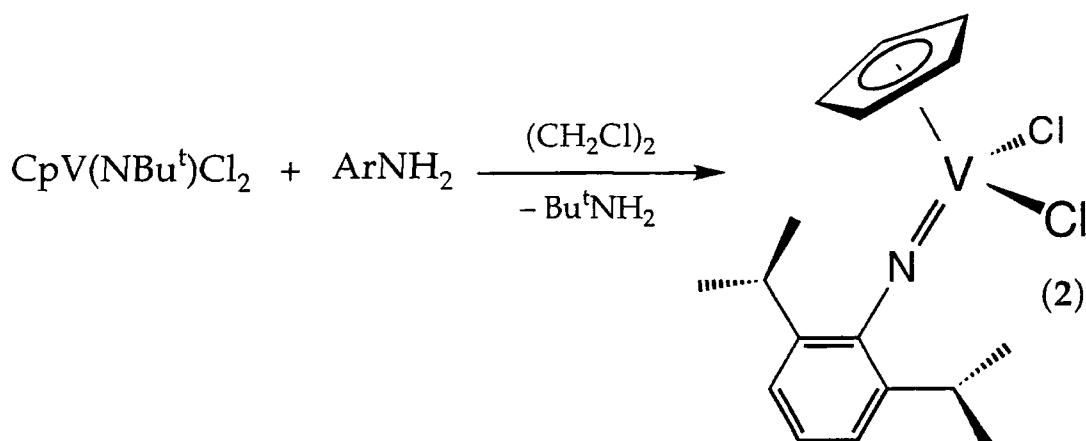


Figure 2.1. Molecular structure of CpV(N-2,6-Me₂C₆H₃)Cl₂ (1).

2.2.2. Reaction of $\text{CpV}(\text{N}^t\text{Bu})\text{Cl}_2$ with 2,6-Diisopropylaniline:

Preparation of $\text{CpV}(\text{N-2,6-}^i\text{Pr}_2\text{C}_6\text{H}_3)\text{Cl}_2$ (2)

$\text{CpV}(\text{N-2,6-}^i\text{Pr}_2\text{C}_6\text{H}_3)\text{Cl}_2$ (2) was prepared by the reaction of $\text{CpV}(\text{N}^t\text{Bu})\text{Cl}_2$ with 2,6-diisopropylaniline in hot 1,2-dichloroethane (70°C) for 2 weeks. Although the reaction is again slow, the product can be isolated as a orange-red crystalline solid in excellent yield (typically 85-90%).



Scheme 2.3. $\text{Ar} = 2,6\text{-}^i\text{Pr}_2\text{C}_6\text{H}_3$.

During this work, 2 was also prepared by Teuben and Buijink *via* treatment of VOCl_3 with $(2,6\text{-}^i\text{Pr}_2\text{C}_6\text{H}_3)\text{NCO}$ followed by reaction with CpSiMe_3 .²

2.3. Alkylation Studies on $\text{CpV}(\text{NR})\text{Cl}_2$ Complexes

The next aim of this investigation was to prepare dialkyl derivatives containing no β -hydrogens, which would subsequently be reacted with a suitable alkyl abstractor eg. $[\text{PhMe}_2\text{NH}][\text{B}(\text{C}_6\text{F}_5)_4]$ to generate the cationic alkyl complexes.¹³

Previous attempts by Teuben and co-workers to synthesise half-sandwich vanadium imido dialkyl compounds yielded only intractable oily mixtures of apparently partially alkylated and reduced [$\text{CpV}(\text{N}-2,6\text{-iPr}_2\text{C}_6\text{H}_3)$] fragments.^{2b} Nevertheless, a number of complexes, some of which possess novel and surprising structures, have been isolated during the course of this work.

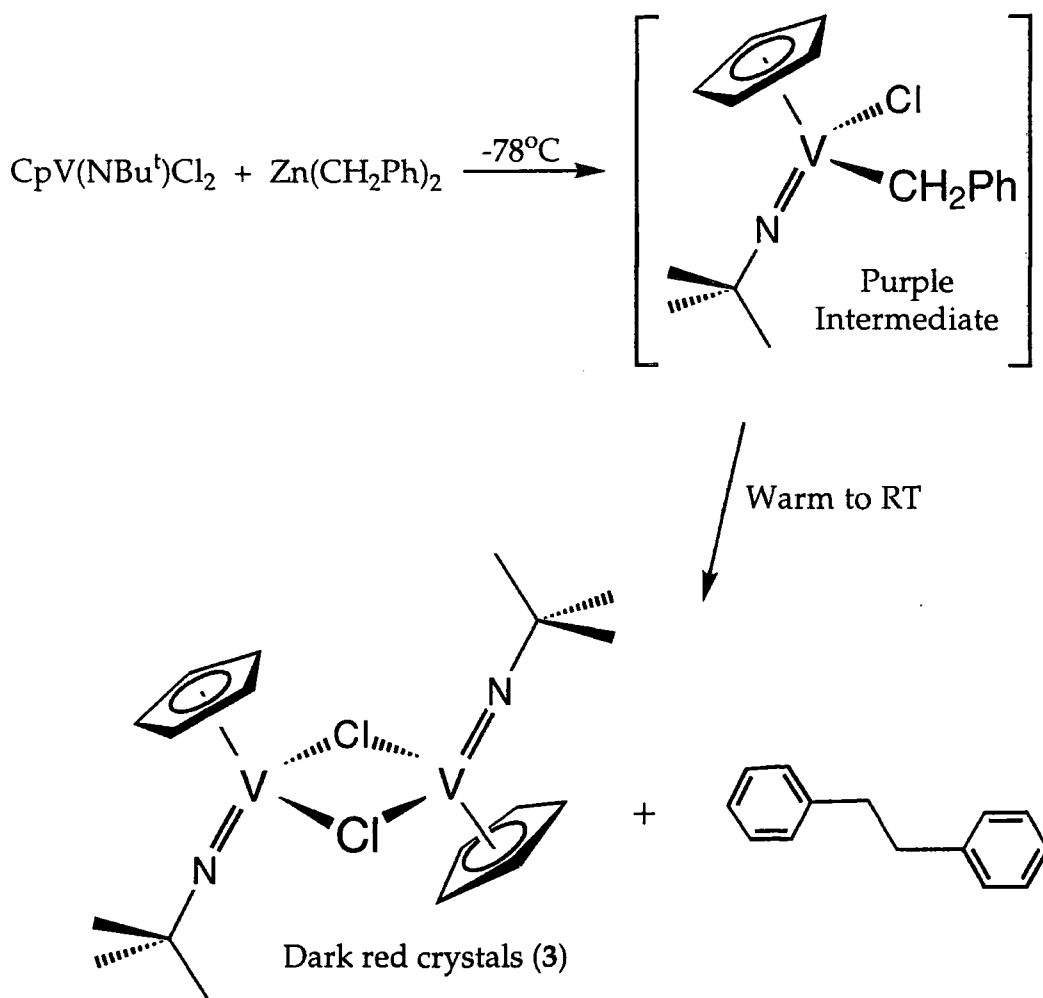
2.3.1. Reaction of $\text{CpV}(\text{N}^t\text{Bu})\text{Cl}_2$ with $\text{Zn}(\text{CH}_2\text{Ph})_2$:

Preparation of $[\text{CpV}(\text{N}^t\text{Bu})(\mu\text{-Cl})_2]$ (3)

The mild alkylating reagent dibenzyl zinc was employed in an attempt to avoid reduction of the vanadium centre. Hence cold toluene (*ca.* -78°C) was added to an equimolar mixture of $\text{CpV}(\text{N}^t\text{Bu})\text{Cl}_2$ and $\text{Zn}(\text{CH}_2\text{Ph})_2$ and stirred at -78°C for 30 minutes. During this period an intense purple coloration was observed, then on warming to room temperature the colour of the solution changed to dark red. After extraction and recrystallisation from pentane, a dark red microcrystalline solid was obtained in moderate yield.

The ^1H NMR spectrum of the solid, however, revealed no evidence for benzyl ligation; instead a broad singlet at 1.20ppm and a very broad resonance at 6.2ppm were observed. Indeed, the elemental analysis, mass spectral and NMR data were all consistent with the previously characterised vanadium(IV) dimer $[\text{CpV}(\text{N}^t\text{Bu})(\mu\text{-Cl})_2]$ (3). Its paramagnetism implies that there is no bonding interaction between the metals and this is supported by the V–V distance of 3.184(4)Å in the molecular structure.^{14a}

The nature of 3 implies that a reductive process has occurred. In order to gain insight into the mechanism for its formation, the reaction was repeated at -78°C and maintained at this temperature throughout in an attempt to identify the intermediate giving rise to the purple solution.



Scheme 2.4. Postulated Mechanism for the Formation of 3

The subsequent extraction was carefully performed at *ca.* -40°C using pentane and purple crystals were then obtained upon cooling the solution to -78°C . It was anticipated that once isolated in crystalline form, the purple product would be sufficiently stable to allow handling at ambient temperatures. However, upon drying *in vacuo* at room temperature, they transformed into a dark red oily solid. The ^1H NMR spectrum of this product contained resonances in a 1:1 ratio for the vanadium(IV) dimer 3 and a molecule of 1,2-diphenylethane. Hence, it would appear that the purple intermediate is the monobenzyl species $[\text{CpV}(\text{N}^t\text{Bu})(\text{CH}_2\text{Ph})\text{Cl}]$, which undergoes reductive dimerisation at ambient temperatures to generate the dark red dimer 3 and diphenylethane.

The suggested reaction pathway is summarised in Scheme 2.4 and has special relevance to the following section.

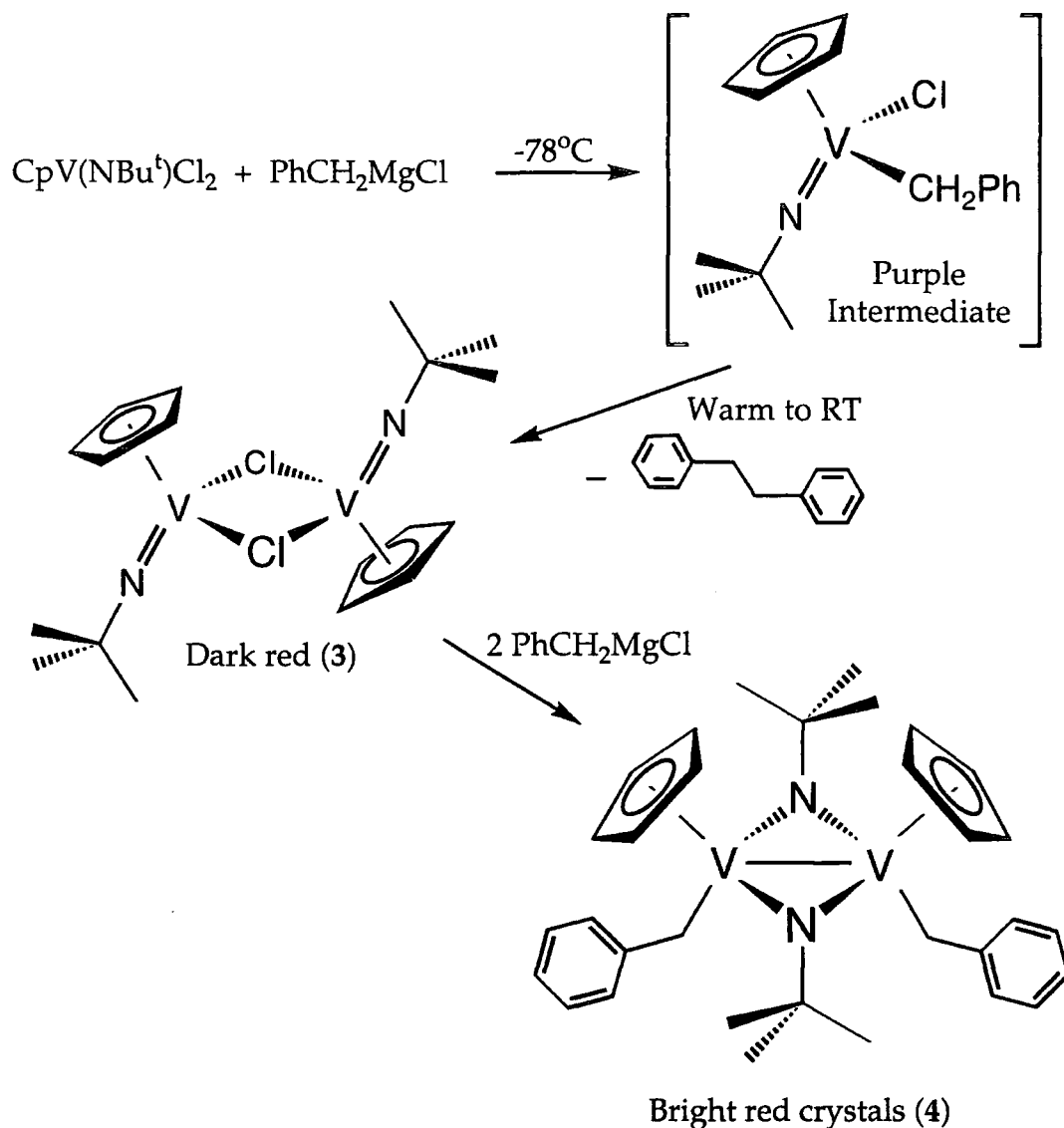
2.3.2. Reaction of $\text{CpV}(\text{N}^t\text{Bu})\text{Cl}_2$ with PhCH_2MgCl :

Preparation of $[\text{CpV}(\text{CH}_2\text{Ph})(\mu\text{-N}^t\text{Bu})]_2$ (4)

Benzyl magnesium chloride was chosen as the alkylating agent since $\text{Zn}(\text{CH}_2\text{Ph})_2$ evidently did not facilitate the metathesis of both chloride groups.

Two equivalents of PhCH_2MgCl were added dropwise to a diethyl ether solution of $\text{CpV}(\text{N}^t\text{Bu})\text{Cl}_2$ at -78°C . A purple coloration characteristic of the intermediate $[\text{CpV}(\text{N}^t\text{Bu})(\text{CH}_2\text{Ph})\text{Cl}]$ was observed immediately and on warming to room temperature, a dark red solution was afforded. However, in contrast to the reaction with $\text{Zn}(\text{CH}_2\text{Ph})_2$, bright red crystals were obtained, albeit in low yield, and the ^1H NMR spectrum of the crystals revealed the presence of metal-bound benzyl ligands. A structural analysis on suitable crystals revealed the structure to be $[\text{CpV}(\text{CH}_2\text{Ph})(\mu\text{-N}^t\text{Bu})]_2$ (4) (see 2.3.2.1). The elemental analysis was consistent with the stoichiometry of $\text{C}_{32}\text{H}_{42}\text{N}_2\text{V}_2$ and the mass spectrum showed a cluster for the fragment of the molecular ion after losing a benzyl unit.

The mechanism for the formation of 4 is thought to proceed *via* the initial generation of the dimer $[\text{CpV}(\text{N}^t\text{Bu})(\mu\text{-Cl})]_2$ (3), which presumably causes the observed dark red colouration. The subsequent reaction of two equivalents of PhCH_2MgCl with 3, accompanied by redistribution of the ancillary ligands, affords the isolated product 4 with bridging imido groups. This postulated mechanism is summarised in Scheme 2.5. The significance in the isolation of the dimer 4 is discussed in Section 2.5.



Scheme 2.5. Postulated Mechanism for the Formation of 4

2.3.2.1. Molecular Structure of $[\text{CpV}(\text{CH}_2\text{Ph})(\mu\text{-N}^t\text{Bu})_2]$ (4)

Bright red crystals suitable for structural analysis were grown by cooling a saturated acetonitrile solution of 4 at -20°C . The molecular structure is shown in Figure 2.2. Selected bond lengths and angles are collected in Table 2.1 and the crystal data are given in Appendix A2.

The molecule is binuclear with the *t*-butylimido groups bridging between two $[\text{CpV}(\text{CH}_2\text{Ph})]$ fragments and a virtually planar V_2N_2 core

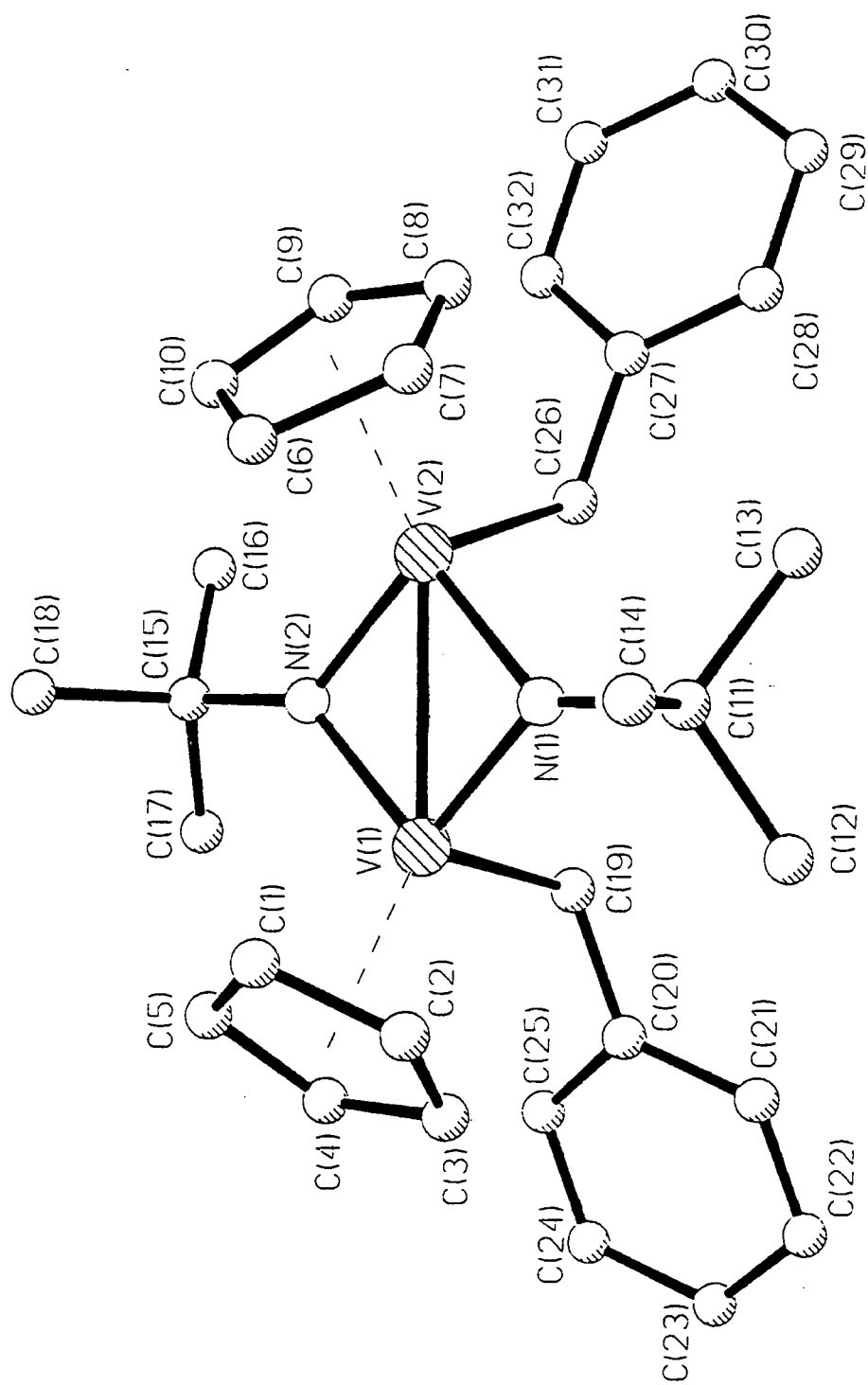


Figure 2.2. Molecular structure of $[\text{CpV}(\text{CH}_2\text{Ph})(\mu\text{-N}'\text{Bu})]_2$ (4).

V(1)–N(2)	1.853(5)	V(2)–C(6)	2.266(8)
V(1)–N(1)	1.854(5)	V(2)–C(7)	2.302(7)
V(1)–C(19)	2.141(7)	V(2)–C(10)	2.316(8)
V(1)–C(1)	2.249(7)	V(2)–C(8)	2.341(7)
V(1)–C(5)	2.326(8)	V(2)–C(9)	2.342(8)
V(1)–C(2)	2.336(7)	N(1)–C(11)	1.497(8)
V(1)–C(4)	2.351(7)	N(2)–C(15)	1.500(8)
V(1)–C(3)	2.367(7)	C(19)–C(20)	1.499(9)
V(1)–V(2)	2.519(2)	C(26)–C(27)	1.500(9)
V(2)–N(1)	1.861(5)	V(1)–C _{pcentroid} (1)	2.008(8)
V(2)–N(2)	1.868(5)	V(2)–C _{pcentroid} (2)	2.007(8)
V(2)–C(26)	2.141(7)		
N(2)–V(1)–N(1)	95.1(2)	C(26)–V(2)–V(1)	103.5(2)
N(2)–V(1)–C(19)	99.1(2)	C(11)–N(1)–V(1)	137.0(4)
N(1)–V(1)–C(19)	99.8(3)	C(11)–N(1)–V(1)	137.0(4)
N(2)–V(1)–V(2)	47.7(2)	V(1)–N(1)–V(2)	85.4(2)
N(1)–V(1)–V(2)	47.4(2)	C(15)–N(2)–V(1)	137.6(4)
C(19)–V(1)–V(2)	103.0(2)	C(15)–N(2)–V(2)	137.2(4)
N(1)–V(2)–N(2)	94.3(2)	V(1)–N(2)–V(2)	85.2(2)
N(1)–V(2)–C(26)	100.2(2)	C(20)–C(19)–V(1)	126.5(5)
N(2)–V(2)–C(26)	99.5(2)	C(27)–C(26)–V(2)	127.0(4)
N(1)–V(2)–V(1)	47.2(2)	V(1)–V(2)–C _{pcentroid} (2)	144.0(8)
N(2)–V(2)–V(1)	47.2(2)	V(2)–V(1)–C _{pcentroid} (1)	143.9(8)

Table 2.1.

Selected bond lengths (Å) and angles (°) for [CpV(CH₂Ph)(μ-N^tBu)]₂ (4)

[mean deviation 0.017Å]. The Cp rings are orientated in a *cis* arrangement, as are the two benzyl groups.

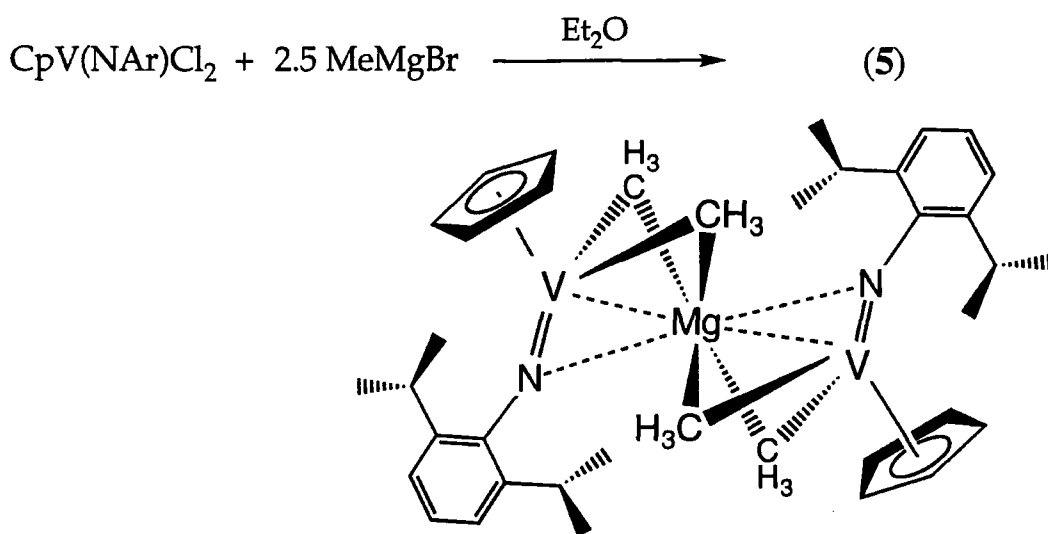
The V–N bond lengths [mean 1.859(5)Å] are noticeably longer than for vanadium-(terminal imido) complexes [1.60–1.68Å],¹² but they are similar to the analogous bridging V–N distances in [CpV(μ-N-p-tolyl)Me]₂ [mean 1.850(3)Å],^{2b} [V(μ-N-p-tolyl)(CH₂Ph)₂]₂ [mean 1.849(3)Å]¹⁵ and [V(μ-N^tBu)(CH₂CMe₃)(O^tBu)]₂ [mean 1.840(5)Å].^{14b} The V(1)–V(2) distance of 2.519(2)Å lies within the range normally associated with a single vanadium-vanadium bond,¹⁶ thus providing an explanation for the diamagnetism of this formally vanadium(IV) d¹ complex. Work by Floriani and co-workers on the chemistry of the cyclodivanadazene core [V₂(μ-NR)₂]⁴⁺ yielded d¹ diamagnetic alkyl and aryl derivatives which contained single V–V bonds. *Ab initio* calculations on the closed shell singlet (V–V bond) and open shell singlet showed the former electronic configuration to be 45kcal mol⁻¹ more stable,¹⁵ hence it is apparent that diamagnetism in complex 4 supports spin-pairing *via* either V–V bond formation or anti-ferromagnetic interactions.

The elongation of the V–CH₂ distances [mean 2.141(7)Å] and the η¹ bonding mode of the benzyl ligand in 4 differ significantly from Floriani's [V(μ-N-p-tolyl)(CH₂Ph)₂]₂ which displays η¹ and η² bonded benzyl ligands [V–CH₂ 2.082(3) and 2.065(2)Å respectively]. This is presumably a consequence of the greater steric constraint imposed on the benzyl ligand in 4 by the bulky t-butyl and Cp moieties.

2.3.3. Reaction of $\text{CpV}(\text{N}-2,6\text{-}^i\text{Pr}_2\text{C}_6\text{H}_3)\text{Cl}_2$ with MeMgBr in Et_2O :Preparation of $[\text{CpV}(\text{N}-2,6\text{-}^i\text{Pr}_2\text{C}_6\text{H}_3)(\mu\text{-Me})_2]_2(\mu\text{-Mg})$ (5)

2.5 equivalents of MeMgBr were added dropwise to a diethyl ether solution of $\text{CpV}(\text{N}-2,6\text{-}^i\text{Pr}_2\text{C}_6\text{H}_3)\text{Cl}_2$ at -78°C . The mixture was allowed to warm to room temperature and stirred overnight to give a deep red supernatant solution and white precipitate. Extraction followed by recrystallisation of the crude product from pentane afforded a dark red crystalline solid.

The paramagnetic nature of the product, implied by the absence of signals in the ^1H NMR spectrum, suggested that a vanadium(IV) species with d^1 configuration had been isolated, rather than the targeted vanadium(V) dimethyl complex. An X-ray crystallographic analysis showed the product to be the unusual magnesium-containing species 5 (2.3.3.1). Elemental analysis is consistent with this stoichiometry and the mass spectrum showed an envelope at 667 m/z for the parent ion.



Scheme 2.6. $\text{Ar}=2,6\text{-}^i\text{Pr}_2\text{C}_6\text{H}_3$.

The isolation of 5 was obviously unexpected; a possible mechanism for its formation may involve generation of the vanadium(IV) methyl species

[CpV(N-2,6-*i*Pr₂C₆H₃)Me], perhaps *via* initial formation of [CpV(N-2,6-*i*Pr₂C₆H₃)Me₂], followed by incorporation of MgMe₂. One can envisage the magnesium dimethyl to arise from the Schlenk equilibrium:¹⁷



Scheme 2.7.

The requirement for an additional equivalent of MeMgBr as the source of the complexed magnesium is consistent with the relatively low yield obtained.

2.3.3.1. Molecular Structure of [CpV(N-2,6-*i*Pr₂C₆H₃)(μ-Me)₂]₂(μ-Mg) (5)

Red X-ray quality crystals were grown from a saturated pentane solution at -5°C. The molecular structure is shown in Figure 2.3. Selected bond lengths and angles are collected in Table 2.2 and the crystal data are given in Appendix A3.

5 crystallises as a trimetallic V₂Mg cluster in the centrosymmetric space group P2₁/c, with the magnesium atom located at the centre of inversion. The structure consists of two methyl groups bridging between the vanadium atom of the [CpV(N-2,6-*i*Pr₂C₆H₃)] fragment and the magnesium core. The V-Mg distance of 2.594(1)Å is very similar to other proposed metal-Mg bonds^{18,19} and therefore, to our knowledge, constitutes the first example of a V-Mg bond. The N-Mg distance of 2.366(6)Å is also within the range for a genuine bonding interaction²⁰ and this would result in a bridging imido unit. However, the V-N distance of 1.724(6)Å (1.60-1.68Å in terminal imides,¹² 1.84-1.85Å in bridging imides^{2b}) and the V-N-C_{ipso} angle of 160.6(5)° suggests that the imido moiety is approaching a terminal bonding mode and the N-Mg interaction is therefore weak.

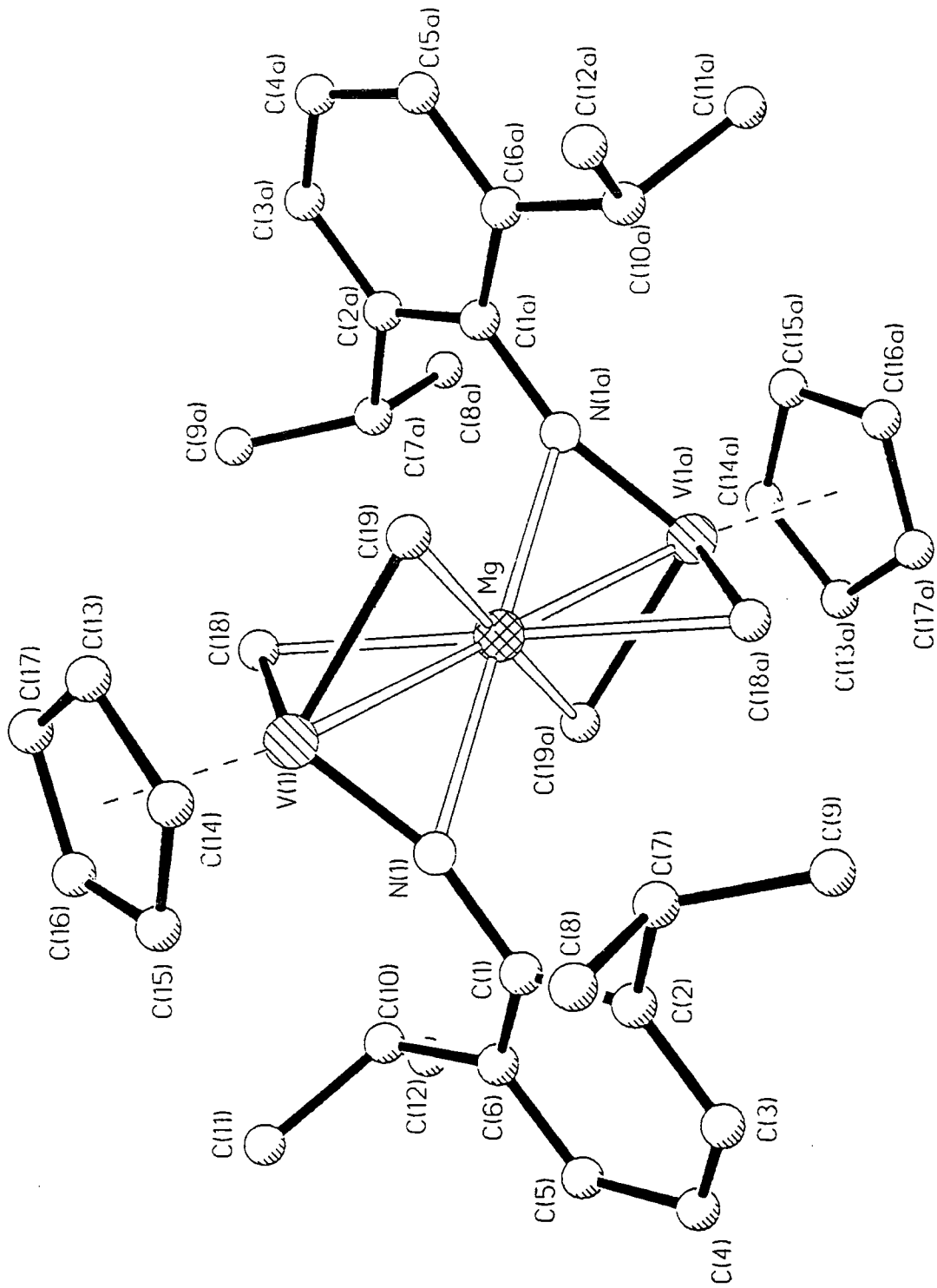


Figure 2.3. Molecular structure of $[\text{CpV}(\text{N-2,6-}^i\text{Pr}_2\text{C}_6\text{H}_3)(\mu\text{-Me})_2(\mu\text{-Mg})]_2$ (5).

V(1)–N(1)	1.724(6)	V(1)–Mg	2.594(1)
V(1)–C(18)	2.200(7)	Mg–N(1)	2.366(6)
V(1)–C(19)	2.227(7)	Mg–C(19)	2.382(7)
V(1)–C(15)	2.295(8)	Mg–C(18)	2.408(7)
V(1)–C(14)	2.295(7)	Mg–H(18c)	2.04
V(1)–C(16)	2.295(7)	Mg–H(19b)	2.35
V(1)–C(13)	2.344(8)	N(1)–C(1)	1.382(9)
V(1)–C(17)	2.348(7)	V(1)–C _p centroid	1.986(8)
C(18)–V(1)–N(1)	100.5(3)	C(19)–Mg–V(1)	53.0(2)
C(19)–V(1)–N(1)	101.3(3)	C(19a)–Mg–V(1)	127.0(2)
C(18)–V(1)–C(19)	91.0(3)	C(18a)–Mg–V(1)	128.0(2)
N(1)–V(1)–Mg	62.7(2)	C(18)–Mg–V(1)	52.0(2)
C(18)–V(1)–Mg	59.6(2)	N(1)–Mg–V(1a)	139.7(1)
C(19)–V(1)–Mg	58.6(2)	N(1a)–Mg–V(1a)	40.3(1)
N(1)–Mg–N(1a)	180.0	C(19)–Mg–V(1a)	127.0(2)
N(1)–Mg–C(19)	80.6(2)	C(19a)–Mg–V(1a)	53.0(2)
N(1a)–Mg–C(19)	99.4(2)	C(18a)–Mg–V(1a)	52.0(2)
C(19)–Mg–C(19a)	180.0	C(18)–Mg–V(1a)	128.0(2)
N(1)–Mg–C(18a)	101.2(2)	V(1)–Mg–V(1a)	180.0
N(1a)–Mg–C(18a)	78.8(2)	C(1)–N(1)–V(1)	160.6(5)
C(19)–Mg–C(18a)	97.6(2)	V(1)–C(18)–Mg	68.4(2)
C(19a)–Mg–C(18a)	82.4(2)	Mg–C(18)–H(18a)	106.1(4)
N(1)–Mg–C(18)	78.9(2)	Mg–C(18)–H(18b)	116.2(6)
N(1a)–Mg–C(18)	101.1(2)	Mg–C(18)–H(18c)	54.7(4)
C(19)–Mg–C(18)	82.4(2)	V(1)–C(19)–Mg	68.4(2)
C(19a)–Mg–C(18)	97.6(2)	Mg–C(19)–H(19a)	112.5(5)
C(18a)–Mg–C(18)	180.0	Mg–C(19)–H(19c)	126.6(5)
N(1)–Mg–V(1)	40.3(1)	Mg–C(19)–H(19b)	76.6(4)
N(1a)–Mg–V(1)	139.7(1)		

Table 2.2.

Selected bond lengths (Å) and angles (°) for [CpV(NAr)(μ-Me)₂]₂(μ-Mg) (5)

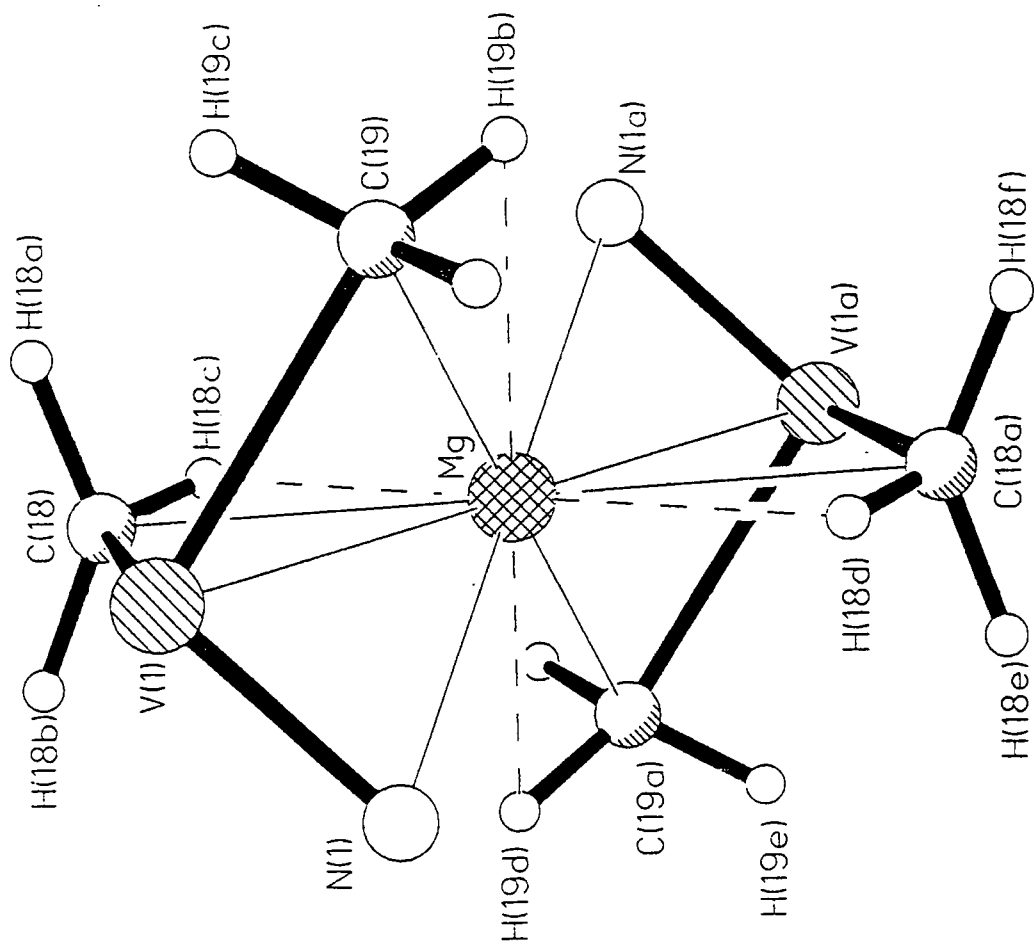


Figure 2.4. Core of 5 showing agostic interactions (dashed lines).

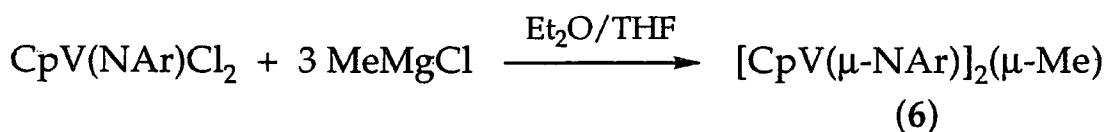
The bridging methyl groups are located slightly closer to the vanadium ($V-C_{\text{methyl}}$: 2.200(7) and 2.227(7)Å, $Mg-C_{\text{methyl}}$: 2.382(7) and 2.408(7)Å) and the $V-C_{\text{methyl}}$ distances are longer than those reported for vanadium complexes with terminal alkyl groups (2.04-2.08Å)^{2,14,21}. The two $V-C_{\text{methyl}}-Mg$ angles are identical ($68.4(2)^\circ$) and are typical for methyl groups bridging between two metals.^{18,22} All the bridging methyl hydrogens were located in the difference density maps and the two highly distorted $Mg-C-H$ angles (55° and 77°) and the particularly short $Mg-H$ separations (2.04Å and 2.35Å) for H(18c) and H(19b) respectively, suggest the presence of multiple $Mg-C-H$ agostic interactions (Figure 2.4). However, the positions of these hydrogens were not refined and neutron diffraction experiments are planned to confirm their location.

Ring slippage of the Cp group is apparent, with the metal displaced towards C(14), C(15) and C(16) (*cf.* 2.2.1). Lastly, the presence of the eight-coordinate magnesium core (excluding possible agostic interactions), with bonding distances in the range 2.366-2.594Å, appears to lend significant stability to this unusual product.

2.3.4. Reaction of $CpV(N-2,6-iPr_2C_6H_3)Cl_2$ with $MeMgCl$ in THF/Et₂O:

Preparation of $[CpV(\mu-N-2,6-iPr_2C_6H_3)]_2(\mu-Me)$ (6)

Reaction of 3 equivalents of methylmagnesium chloride in tetrahydrofuran with a diethyl ether solution of $CpV(N-2,6-iPr_2C_6H_3)Cl_2$ for 12 hours afforded very dark red crystals of 6 in moderate yield (Scheme 2.8). However, no discrete signals were observed in the ¹H NMR spectrum and the absolute structure of 6 was confirmed by X-ray crystallography (2.3.4.1).



Scheme 2.8. Ar = 2,6-*i*Pr₂C₆H₃.

The novel connectivity of **6** is highlighted by the presence of one methyl and two bulky 2,6-diisopropylphenylimido units as *bridging* groups. In addition, the two metal centres are formally mixed-valenced i.e. V(III) and V(IV). The elemental analysis corresponds to the formula C₃₅H₄₇N₂V₂ and peaks for the parent ion and the daughter fragment [CpV(N-2,6-*i*Pr₂C₆H₃)]₂, at 597 and 582 m/z respectively, are observed in the mass spectrum.

The mechanism for the formation of **6** is unclear. Differences to the reaction which afforded complex **5** include the presence of THF and the use of methylmagnesium chloride instead of the bromide analogue, and both these factors are known to influence the Schlenk equilibrium.

2.3.4.1. Molecular Structure of [CpV(μ-N-2,6-*i*Pr₂C₆H₃)]₂(μ-Me) (**6**)

Dark red diamond crystals were grown from a pentane solution at -20°C. The molecular structure is shown in Figure 2.5. Selected bond lengths and angles are collected in Table 2.3 and the crystal data are given in Appendix A4.

The crystal structure of **6** consists of a single methyl [C(35)] and two arylimido groups bridging between two [CpV] units. The distances V(1)-C(35) (2.215(4)Å), V(2)-C(35) (2.310(4)Å) and the V(1)-C(35)-V(2) angle (61.8(1)°) are comparable with **5** and other related complexes.^{18,22} Hydrogens in the bridging methyl group were located in the Fourier difference maps and they do not exhibit close contacts with the vanadium centres.

The V-N distances (av. 1.885(4)Å) are longer than in **5** and are indicative of the decrease in bond order which results from the bridging

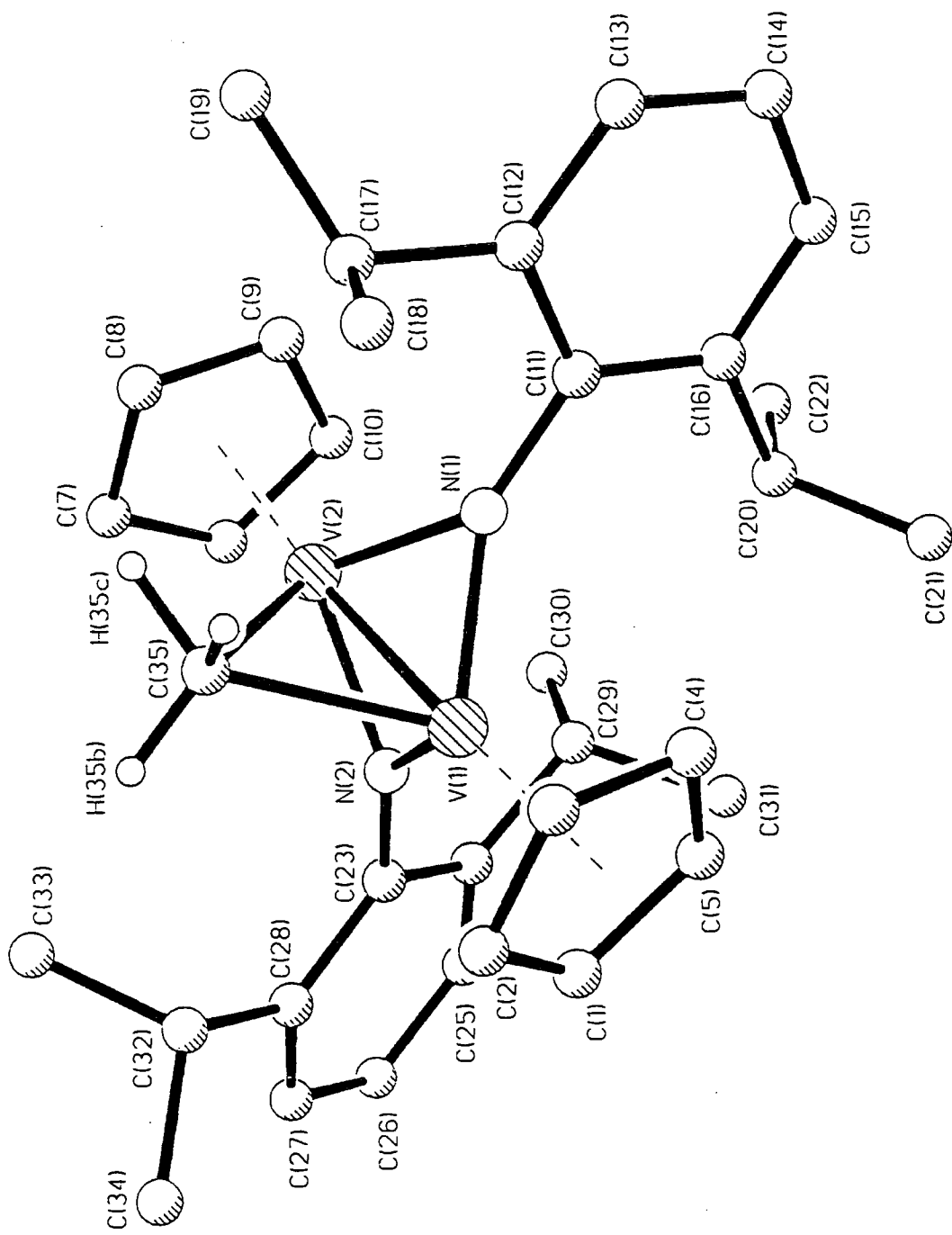


Figure 2.5. Molecular structure of $[\text{CpV}(\mu\text{-N-2,6-Pr}_2\text{C}_6\text{H}_3)]_2(\mu\text{-Me})$ (6).

V(1)–N(1)	1.867(3)	V(2)–C(10)	2.284(4)
V(1)–N(2)	1.882(4)	V(2)–C(9)	2.289(4)
V(1)–C(35)	2.215(4)	V(2)–C(7)	2.302(4)
V(1)–C(5)	2.293(4)	V(2)–C(8)	2.304(4)
V(1)–C(1)	2.301(4)	V(2)–C(6)	2.305(4)
V(1)–C(4)	2.308(4)	V(2)–C(35)	2.310(4)
V(1)–C(3)	2.310(4)	N(1)–C(11)	1.407(5)
V(1)–C(2)	2.310(4)	N(2)–C(23)	1.409(5)
V(1)–V(2)	2.324(1)	V(1)–C _{pcentroid} (1)	1.961(4)
V(2)–N(2)	1.894(3)	V(2)–C _{pcentroid} (2)	1.972(4)
V(2)–N(1)	1.896(3)		
N(1)–V(1)–N(2)	94.9(1)	N(1)–V(2)–V(1)	51.29(9)
N(1)–V(1)–C(35)	86.8(2)	C(35)–V(2)–V(1)	57.1(1)
N(2)–V(1)–C(35)	88.6(2)	C(11)–N(1)–V(1)	143.8(2)
N(1)–V(1)–V(2)	52.43(9)	C(11)–N(1)–V(2)	139.9(2)
N(2)–V(1)–V(2)	52.26(9)	V(1)–N(1)–V(2)	76.3(1)
C(35)–V(1)–V(2)	61.1(1)	C(23)–N(2)–V(1)	142.4(2)
N(2)–V(2)–N(1)	93.5(1)	C(23)–N(2)–V(2)	141.6(2)
C(35)–V(2)–N(2)	85.5(1)	V(1)–N(2)–V(2)	76.0(1)
C(35)–V(2)–N(1)	83.4(1)	V(1)–C(35)–V(2)	61.8(1)
N(2)–V(2)–V(1)	51.76(9)		

Table 2.3.

Selected bond lengths (Å) and angles (°) for [CpV(μ-NAr)]₂(μ-Me) (6)

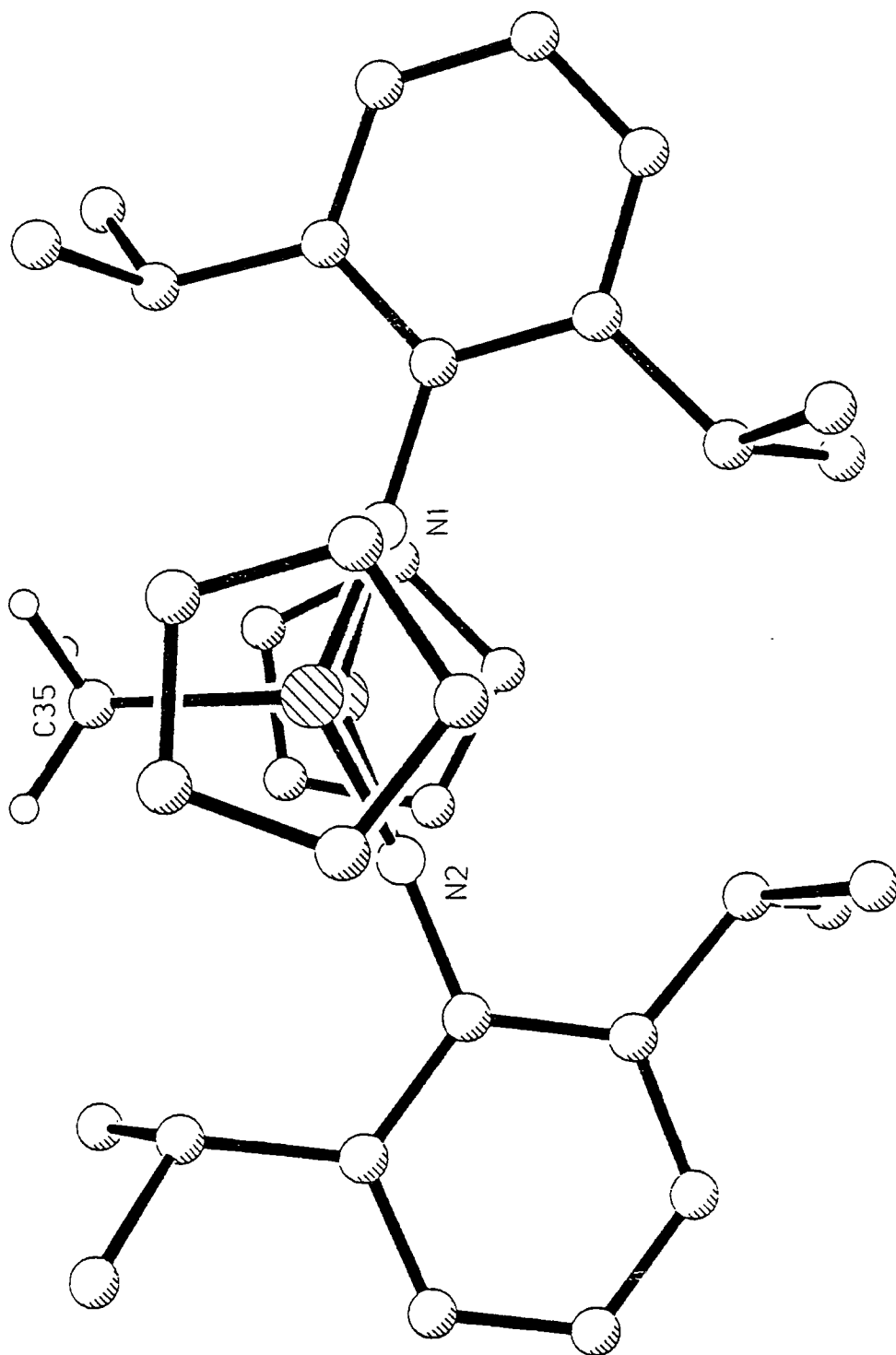


Figure 2.6. View of 6 along V-V vector.

nature of the imido substituents. The V(1)-V(2) distance of 2.324(1)Å is well within the range for a bonding interaction,¹⁶ and the V-Cp_{centroid} vectors are co-axial with the V-V bond. Finally, the bridging methyl and imido groups are spaced equally around the V-V vector such that C(35), N(1) and N(2) are approximately 120° to each other (Figure 2.6).

A comparison of the key bond distances and angles for the structures determined in this chapter is collected in Table 2.4.

2.3.5. Other Reactions of CpV(NR)Cl₂ towards Grignard Reagents

Reactions of CpV(N-2,6-Me₂C₆H₃)Cl₂ with excess MeMgBr in Et₂O and excess MeMgCl in Et₂O/THF were performed in order to compare with the analogous 2,6-diisopropylphenyl reactions and ascertain if the steric bulk of the arylimido group significantly influences the nature of the products. In both cases, orange-red solids were isolated. Their infra-red spectra were very similar to the corresponding [N-2,6-ⁱPr₂C₆H₃] derivatives but in the absence of NMR spectroscopy and X-ray crystallography as diagnostic techniques, it is not possible to predict their precise structures with confidence.

CpV(N-2,6-ⁱPr₂C₆H₃)Cl₂ has also been treated with 2 equivalents of benzyl and neopentyl Grignard reagents respectively, but both resulted in intractable oily mixtures of presumably partially alkylated and reduced [CpV(N-2,6-ⁱPr₂C₆H₃)] fragments (by ¹H NMR spectroscopy).

	V-N (Å)	V-N-C _{ipso} (°)	V-N-M (°)	V-M (Å)	V-C _α (Å)	V-C _α -X (°)	V-Cp _{centroid} (Å)
CpV(NPh)Cl ₂	1.653(4)	169.1(4)	—	—	—	—	1.968(8)
CpV(N-2,6-Me ₂ C ₆ H ₃)Cl ₂	1.684(9)	166.8(7)	—	—	—	—	1.963(3)
[CpV(CH ₂ Ph)(μ-N ^t Bu)] ₂ ^a	av. 1.860(5)	av. 137.4(4)	85.3(2)	2.519(2)	2.141(7)	126.5(5) 126.9(4)	2.007(9)
[CpV(N-2,6- <i>i</i> -Pr ₂ C ₆ H ₃)(μ-Me) ₂] ₂ (μ-Mg) ^b	1.724(6)	160.6(5)	77.0(2)	2.594(1)	2.200(7) 2.227(7)	av. 68.4(2)	1.986(8)
[CpV(μ-N-2,6- <i>i</i> -Pr ₂ C ₆ H ₃)] ₂ (μ-Me) ^c	av. 1.885(3)	av. 141.9(2)	76.2(1)	2.324(1)	2.215(4) 2.310(4)	61.8(1)	1.966(4)

^a M = V, X = Ph, ^b M = X = Mg, ^c M = X = V.

Table 2.4. Key Structural Parameters of Half-Sandwich Vanadium Imido Complexes

2.4. Studies on Half-Sandwich Vanadium Imido Complexes as Catalyst Precursors for Ethylene Polymerization

The polymerisation of ethylene using the $\text{CpV}(\text{N-}i\text{p-tolyl})\text{Cl}_2/\text{DEAC}$ system has recently been demonstrated.⁴ The short-lived nature of the active species prompted investigations into the activity of the dichlorides $\text{CpV}(\text{NR})\text{Cl}_2$ ($\text{R}=\text{tBu}$, 2,6- $i\text{Pr}_2\text{C}_6\text{H}_3$, 2,6- $\text{Me}_2\text{C}_6\text{H}_3$) in conjunction with DEAC. It was anticipated that steric protection provided by the ortho substituents of the imido ligand at the vanadium centre may increase the longevity of the active species.

The results of the polymerisation runs, carried out under a flow of ethylene at 25°C in toluene, are collected in Table 2.5. On addition of DEAC, colour changes are observed for $\text{CpV}(\text{N}^t\text{Bu})\text{Cl}_2$ (dark red to brown/green), $\text{CpV}(\text{N-}2,6\text{-}i\text{Pr}_2\text{C}_6\text{H}_3)\text{Cl}_2$ (dark red to orange/red) and $\text{CpV}(\text{N-}2,6\text{-Me}_2\text{C}_6\text{H}_3)\text{Cl}_2$ (dark red to black/red). All three systems resulted in the fast formation and appearance of polyethylene, within 45 seconds to 1 minute of introducing ethylene. The results of the tert-butyylimido system can be considered as a benchmark, since its activity is essentially the same as for the *p*-tolylimido analogue.²³ The activities for the catalysts derived from $\text{CpV}(\text{N-}2,6\text{-}i\text{Pr}_2\text{C}_6\text{H}_3)\text{Cl}_2$ and $\text{CpV}(\text{N-}2,6\text{-Me}_2\text{C}_6\text{H}_3)\text{Cl}_2$ are comparable, but they are marginally lower than for the tert-butyylimido catalyst. Hence the arylimido substituents unexpectedly lead to a decrease in catalytic activity.

In run 1a–2b, the polymer forms as a 'stringy' thread. By contrast, run 3a and 3b produce polymer which is dispersed throughout the solution, and this suggests that the nature of the polymerisation process is quite different. All the polymers show very similar melt temperatures by DSC, in the range 131–136°C.

Run	Catalyst Precursor (mmol)	DEAC (mmol/ equivs)	Time (mins)	Yield (g)	Activity (g mmol ⁻¹ hr ⁻¹)
1a	CpV(N ^t Bu)Cl ₂ (0.13)	2.6/20	20	0.11	2.5
1b	CpV(N ^t Bu)Cl ₂ (0.12)	2.4/20	20	0.15	3.6
2a	CpV(N-2,6- iPr ₂ C ₆ H ₃)Cl ₂ (0.14)	2.8/20	30	0.12	1.7
2b	CpV(N-2,6- iPr ₂ C ₆ H ₃)Cl ₂ (0.14)	2.8/20	30	0.13	1.9
3a	CpV(N-2,6- Me ₂ C ₆ H ₃)Cl ₂ (0.16)	3.3/20	30	0.10	1.2
3b	CpV(N-2,6- Me ₂ C ₆ H ₃)Cl ₂ (0.16)	3.3/20	30	0.09	1.1

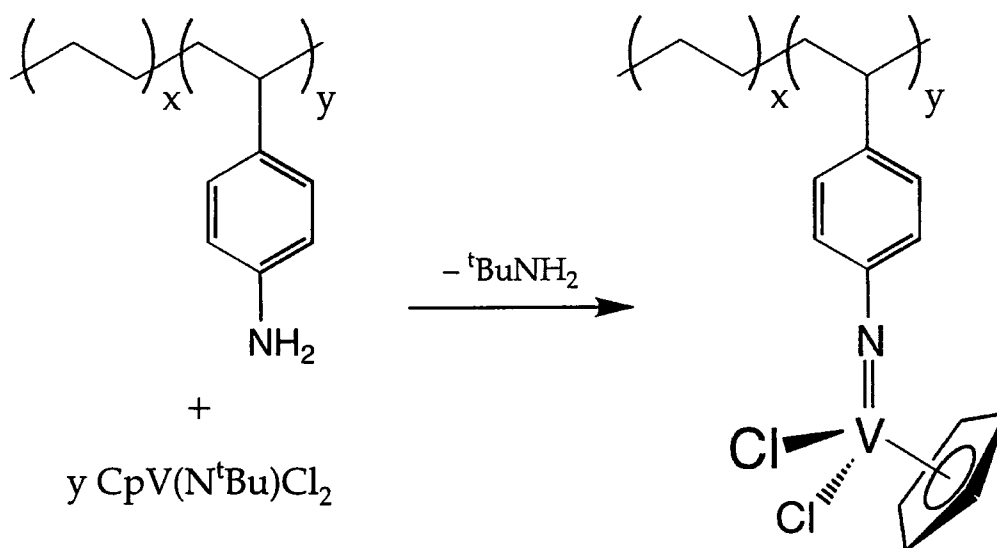
Table 2.5. Conditions: toluene solution, 25°C, 1 bar of ethylene.

Solutions containing equimolar mixtures of [PhNMe₂H][B(C₆F₅)₄] and [CpV(N-2,6-*i*Pr₂C₆H₃)(μ-Me)₂]₂(μ-Mg) (5) or [CpV(μ-N-2,6-*i*Pr₂C₆H₃)]₂(μ-Me) (6) were also evaluated for polymerisation activity in the presence of ethylene. However, no polymer was observed in these tests.

2.5. Implications and Solutions

The short-lived nature of the active species in the $\text{CpV}(\text{N-p-tolyl})\text{Cl}_2/\text{DEAC}$ system is obviously unattractive with respect to the application of the process. A possible mechanism for deactivation involves dimerisation or coupling of the active species, and the isolation of a number of dimeric and bimetallic complexes in this investigation strongly supports this hypothesis.

To prevent such coupling processes, the complex can in theory be supported onto a polymeric backbone using the imido exchange strategy (Scheme 2.9).



Scheme 2.9.

To test the viability of this approach, the reaction of $\text{CpV}(\text{N}^t\text{Bu})\text{Cl}_2$ with parent aniline was investigated. This afforded the desired $\text{CpV}(\text{NPh})\text{Cl}_2$ complex (7) which was structurally characterised (Appendix A5). Next, a 9:1 styrene:4-aminostyrene co-polymer was synthesised according to the procedure reported by Suzuki and co-workers.²⁴ The half-sandwich vanadium imido species was then introduced by treating the copolymer with $\text{CpV}(\text{N}^t\text{Bu})\text{Cl}_2$ in $(\text{CH}_2\text{Cl})_2$ at 80°C for 10 days to afford a black glutinous

solid. After removal of all volatile components under reduced pressure, this solid was washed thoroughly with dichloromethane to remove all traces of residual $\text{CpV}(\text{N}^t\text{Bu})\text{Cl}_2$ and dried *in vacuo* overnight.

Although no characterising data were obtained for this black solid/polymer, preliminary polymerisation tests on the solid with 20 equivalents of DEAC under 1 atmosphere of ethylene gave 0.73g of polymer and an activity of 17.7g/mmol/hr. This is substantially higher than the value obtained for the unsupported vanadium catalysts. In addition, the amount of polymer appeared to increase steadily throughout the run, which is in stark contrast to the fast deactivation of the unsupported systems.

Future work will focus on thorough characterisation of the supported catalyst. Nevertheless it appears that the strategy of supporting the vanadium complex to preclude dimerisation of the active species and increase the activity of the system has been successful.

2.6. Summary

$\text{CpV}(\text{NR})\text{Cl}_2$ ($\text{R}=2,6\text{-Me}_2\text{C}_6\text{H}_3$ (1), $2,6\text{-}^i\text{Pr}_2\text{C}_6\text{H}_3$ (2)) compounds have been prepared in high yield *via* imido ligand exchange reactions. In theory, other imido substituents can be introduced by treatment of $\text{CpV}(\text{N}^t\text{Bu})\text{Cl}_2$ with the corresponding amine. The crucial requirement is a nitrogen atom on the amine which is less basic than the tert-butyl nitrogen.

The reactions of half-sandwich vanadium imido dichlorides with alkylating agents have yielded a number of surprising and interesting products. Their nature can be attributed to the tendency for monomeric vanadium(V) species with appropriate ancillary ligands to undergo facile elimination-dimerisation processes at ambient temperatures. Hence, this suggests that the fast deactivation of the $\text{CpV}(\text{NR})\text{Cl}_2/\text{DEAC}$ catalyst systems may also be due to coupling of the active species, and this has been addressed by supporting the catalyst precursor on a polystyrene backbone. Preliminary results show that an increase in the activity and longevity of the system has been achieved.

The novel structures of $[\text{CpV}(\text{N-}2,6\text{-}^i\text{Pr}_2\text{C}_6\text{H}_3)(\mu\text{-Me})_2]_2(\mu\text{-Mg})$ (5) and $[\text{CpV}(\mu\text{-N-}2,6\text{-}^i\text{Pr}_2\text{C}_6\text{H}_3)]_2(\mu\text{-Me})$ (6), featuring bridging methyl and imido substituents, have been elucidated. 5 also possesses the first crystallographically characterised V–Mg bond and multiple agostic interactions.

2.7. References

1. (a) M.P. Coles, C.I. Dalby, V.C. Gibson, W. Clegg, M.R.J. Elsegood, *J. Chem. Soc. Chem. Commun.*, 1995, 1709. (b) M.P. Coles, C.I. Dalby, V.C. Gibson, W. Clegg, M.R.J. Elsegood, *Polyhedron*, 1995, 14, 2455.
2. (a) J.-K.F. Buijink, J.H. Teuben, H. Kooijman, A.L. Spek, *Organometallics*, 1994, 13, 2922. (b) J.-K.F. Buijink, Ph.D Thesis, University of Groningen, 1995.
3. For a review see: R.F. Jordan, *Adv. Organomet. Chem.*, 1991, 32, 325.
4. M.P. Coles, V.C. Gibson, *Polymer Bulletin*, 1994, 33, 529.
5. D.S. Glueck, Jianxin Wu, F.J. Hollander, R.G. Bergman, *J. Am. Chem. Soc.*, 1991, 113, 2041.
6. R.I. Michelman, R.G. Bergman, R.A. Andersen, *Organometallics*, 1993, 12, 2741.
7. (a) M. Jolly, J.P. Mitchell, V. C. Gibson, *J. Chem. Soc., Dalton Trans.*, 1992, 1331. (b) M. Jolly, Ph.D Thesis, University of Durham, 1994.
8. A. Bell, W. Clegg, P.W. Dyer, M.J. Elsegood, V.C. Gibson, E.L. Marshall, *J. Chem. Soc., Chem. Commun.*, 1994, 2247. A. Bell, W. Clegg, P.W. Dyer, M.J. Elsegood, V.C. Gibson, E.L. Marshall, *J. Chem. Soc., Chem. Commun.*, 1994, 2547.
9. F. Preuss, H. Becker, H.J. Häusler, *Z. Naturforsch*, 1987, 42b, 881.
10. A.A. Danopoulos, W.-H. Leung, G. Wilkinson, B. Hussain-Bates, M.B. Hursthouse, *Polyhedron*, 1990, 21, 2625.
11. D.N. Williams, J.P. Mitchell, A.D. Poole, U. Siemeling, W. Clegg, D.C.R. Hockless, P.A. O'Neil, V. C. Gibson, *J. Chem. Soc., Dalton Trans.*, 1992, 739.
12. W.A. Nugent, J.M. Mayer, 'Metal-Ligand Multiple Bonds', Wiley Interscience, New York, 1988.
13. M. Bochmann, S.J. Lancaster, *Organometallics*, 1993, 12, 633 and references therein.
14. (a) F. Preuss, H. Becker, J. Kaub, W.S. Sheldrick, *Z. Naturforsch*, 1988, 43b, 1195. (b) F. Preuss, G. Overhoff, H. Becker, H.J. Häusler, W. Frank, G. Reiß, *Z. Anorg. Allg. Chem.*, 1993, 619, 1827.
15. G.A. Solan, P.G. Cozzi, C. Floriani, A. Chiesi-Villa, C. Rizzoli, *Organometallics*, 1994, 13, 2572.

16. F.A. Cotton, M.J. Millar, *J. Am. Chem. Soc.*, 1977, **99**, 7886. H. Vahrenkamp, *Chem. Ber.*, 1978, **111**, 3472.
17. W. Schlenk, *Chem. Ber.*, 1929, **62**, 920.
18. Ni-Mg bond of 2.615Å : W. Kaschube, K.R. Pörschke, K. Angermund, C. Krüger, G. Wilke, *Chem. Ber.*, 1988, **121**, 1921.
19. (a) Co-Mg bonds of 2.565 and 2.480Å : K. Jonas, G. Koepe, C. Krüger, *Angew. Chem. Int. Ed. Engl.*, 1986, **25**, 9. (b) Mo-Mg bonds of 2.853 and 2.737Å : M.L.H. Green, G.A. Moser, I. Packer, F. Petit, R.A. Forder, K. Prout, *J. Chem. Soc., Chem. Commun.*, 1974, 839.
20. For example see H. Viebrock, E. Weiss, *J. Organomet. Chem.*, 1994, **464**, 121 and references therein.
21. J. De With, A.D. Horton, A.G. Orpen, *Organometallics*, 1990, **9**, 2207.
22. S.K. Noh, S.C. Sendlinger, C. Janiak, K.H. Theopold, *J. Am. Chem. Soc.*, 1989, **111**, 9127. S.K. Noh, R.A. Heintz, S.C. Sendlinger, C. Janiak, K.H. Theopold, *Angew. Chem., Int. Ed. Engl.*, 1990, **29**, 775.
23. V.C. Gibson, M.P. Coles, unpublished results.
24. K. Suzuki, K. Yamaguchi, A. Hirao, S. Nakahama, *Macromol.*, 1989, **22**, 2607, sample synthesised by Dr C.I. Dalby.

Chapter 3

Investigation into the Steric and Electronic Effects of the Imido Substituent in the Half-Sandwich Niobium Arylimido System

3.1. Introduction

The chemistry of the $[\text{CpM}(\text{NR})]$ systems ($\text{M}=\text{Group 5 metal}$; $\text{R}=\text{alkyl, aryl}$) has received considerable attention due to their 'isolobal' relationship with the bent metallocene fragment $[\text{Cp}_2\text{M}]$ ($\text{M}=\text{Group 4 metal}$).¹⁻³ A variety of half-sandwich niobium imido derivatives have been synthesised, including novel alkylidene and benzyne complexes, and their stability appears to be largely dependent upon the steric influence of the cyclopentadienyl and imido ligands. In order to investigate the importance of the steric properties of the imido substituent and also to explore electronic influences, we decided to examine the 2-tert-butylphenylimido and 2,6-dichlorophenylimido systems. The 2-tert-butylphenylimido ligand allows considerable steric flexibility since the t-butyl moiety can be orientated away from a congested environment. The 2,6-dichlorophenylimido group was chosen to hopefully probe any electronic effects when compared with the 2,6-di-isopropylphenylimido ligand.

3.1.1. Steric Influence of the Imido Moiety :

Synthesis and Reactivity of $\text{CpNb}(\text{N}-2\text{-}^t\text{BuC}_6\text{H}_4)\text{Cl}_2$

This section describes a synthetic route to the niobium half-sandwich imido complex $\text{CpNb}(\text{N}-2\text{-}^t\text{BuC}_6\text{H}_4)\text{Cl}_2$ and discusses the synthesis, characterisation and, in particular, the stability of derivatives of this system.

3.1.2. Reaction of CpNbCl_4 with $\text{Me}_3\text{SiNH}(2\text{-}^t\text{BuC}_6\text{H}_4)$ and 2,6-Lutidine:

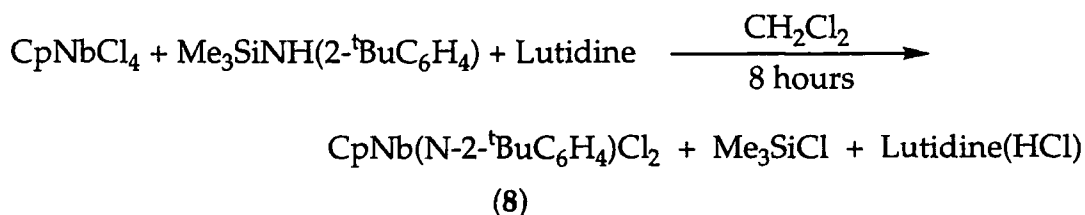
Preparation of $\text{CpNb}(\text{N}-2\text{-}^t\text{BuC}_6\text{H}_4)\text{Cl}_2$ (8)

The recently established procedure by Poole using the mono(silylated) aniline and 2,6-lutidine was employed.² To a stirred suspension of CpNbCl_4

in CH_2Cl_2 was added one equivalent of 2,6-lutidine, followed by the dropwise addition of one equivalent of $\text{Me}_3\text{SiNH}(2\text{-}^t\text{BuC}_6\text{H}_4)$ at 0°C . The mixture was stirred at room temperature for 8 hours to afford a clear red solution before the solvent was removed under reduced pressure to give an orange-yellow solid.

However, attempts to isolate $\text{CpNb}(\text{N}-2\text{-}^t\text{BuC}_6\text{H}_4)\text{Cl}_2$ (**8**) from the 2,6-lutidinium hydrochloride by-product with pentane, toluene or diethyl ether were unsuccessful. Extraction of **8** was finally achieved using boiling *n*-heptane; an orange solution formed and this was filtered from the solid residue which was identified as 2,6-lutidinium hydrochloride by infra red spectroscopy. Recrystallisation from heptane afforded long needle-like orange crystals in high yield (85%). The reaction is summarised in Scheme 3.1.

The ^1H NMR spectrum for compound **8** shows singlets for the *t*-butyl and Cp groups; the predicted two doublets and two triplets for the aromatic protons are also clearly resolved. The ^{13}C [^1H] NMR spectrum shows the Cp carbons not as the expected doublet, but as a doublet of pentets. This can be explained by the two- and three-bond coupling constants ($^2J_{\text{CH}}$ and $^3J_{\text{CH}}$) being identical, a phenomenon observed in other niobium species such as $\text{CpNb}(\text{N}-2,6\text{-}^i\text{Pr}_2\text{C}_6\text{H}_3)\text{Cl}_2$ and $\text{Cp}_2\text{Nb}(\text{Et})(\text{C}_2\text{H}_4)$.⁴



Scheme 3.1.

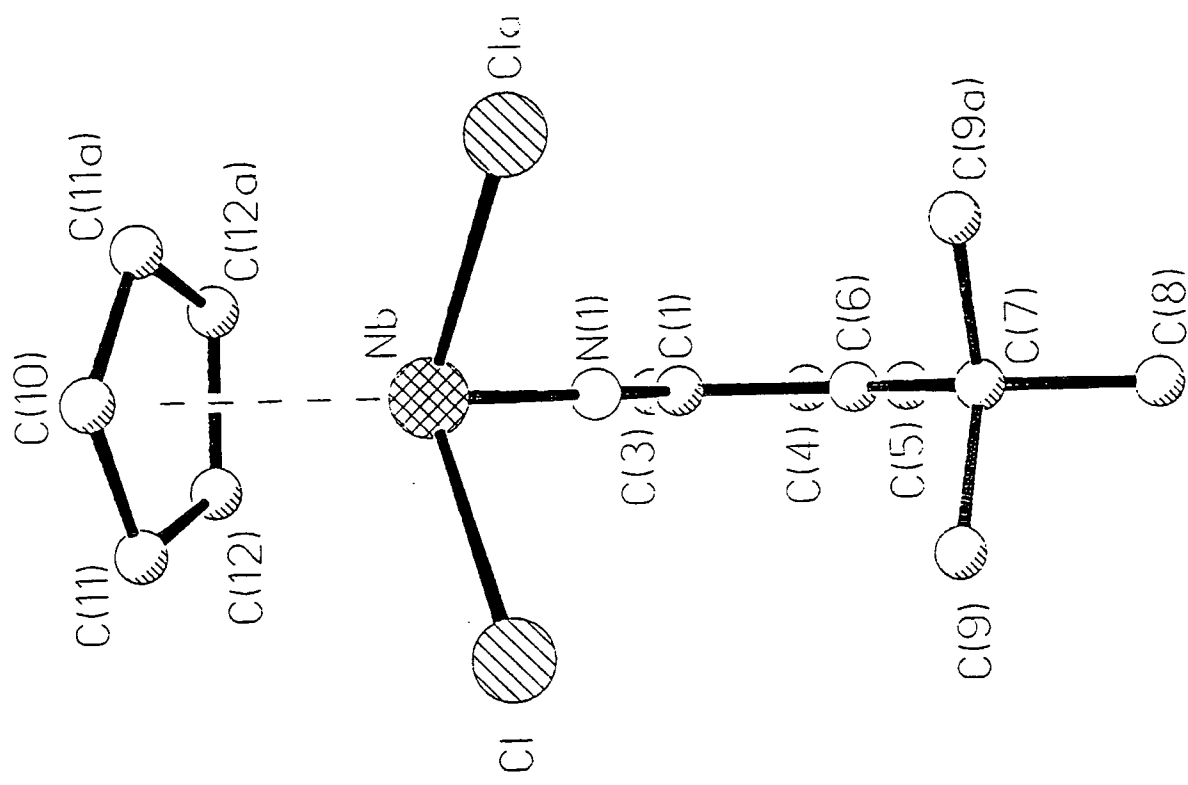
3.1.2.1. Molecular Structure of CpNb(N-2-^tBuC₆H₄)Cl₂ (8)

The structure of **8** was investigated primarily to determine the preferred orientation of the arylimido moiety and for comparison with the related [N-2,6-ⁱPr₂C₆H₃] derivative.

Red crystals were grown from a saturated solution of **8** in *n*-heptane at room temperature. Different views of the molecule are shown in Figure 3.1 and bond lengths and angles are collected in Table 3.1. Structural parameters are given in Appendix A6.

The molecule possesses a mirror plane of symmetry which bisects the Cl-Nb-Cl angle. The important difference between **8** and CpNb(N-2,6-ⁱPr₂C₆H₃)Cl₂ lies in the orientation of the aryl ring which for **8** aligns in the mirror plane; consequently the *t*-butyl group is accommodated in this plane and points *away* from the Cp ring. By contrast, the 2,6-disubstituted aryl ring in CpNb(N-2,6-ⁱPr₂C₆H₃)Cl₂ is orientated perpendicular to this alignment in order to avoid steric repulsion between the Cp ring and one of the ortho groups.^{1a} Hence in this system, replacement of the two chloride ligands by bulky ancillary ligands would result in unfavourable steric interactions with the ortho iso-propyl substituents. However, such destabilisation could be circumvented in the 2-*tert*-butylphenyl imido analogue because the single *tert*-butyl moiety can be positioned into a cavity in line with the mirror plane 'beneath' the ancillary substrates and remote from the Cp ring (see Figure 3.1).

The following reactivity studies on CpNb(N-2-^tBuC₆H₄)Cl₂ will explore this effect upon complex stability.



View along mirror plane

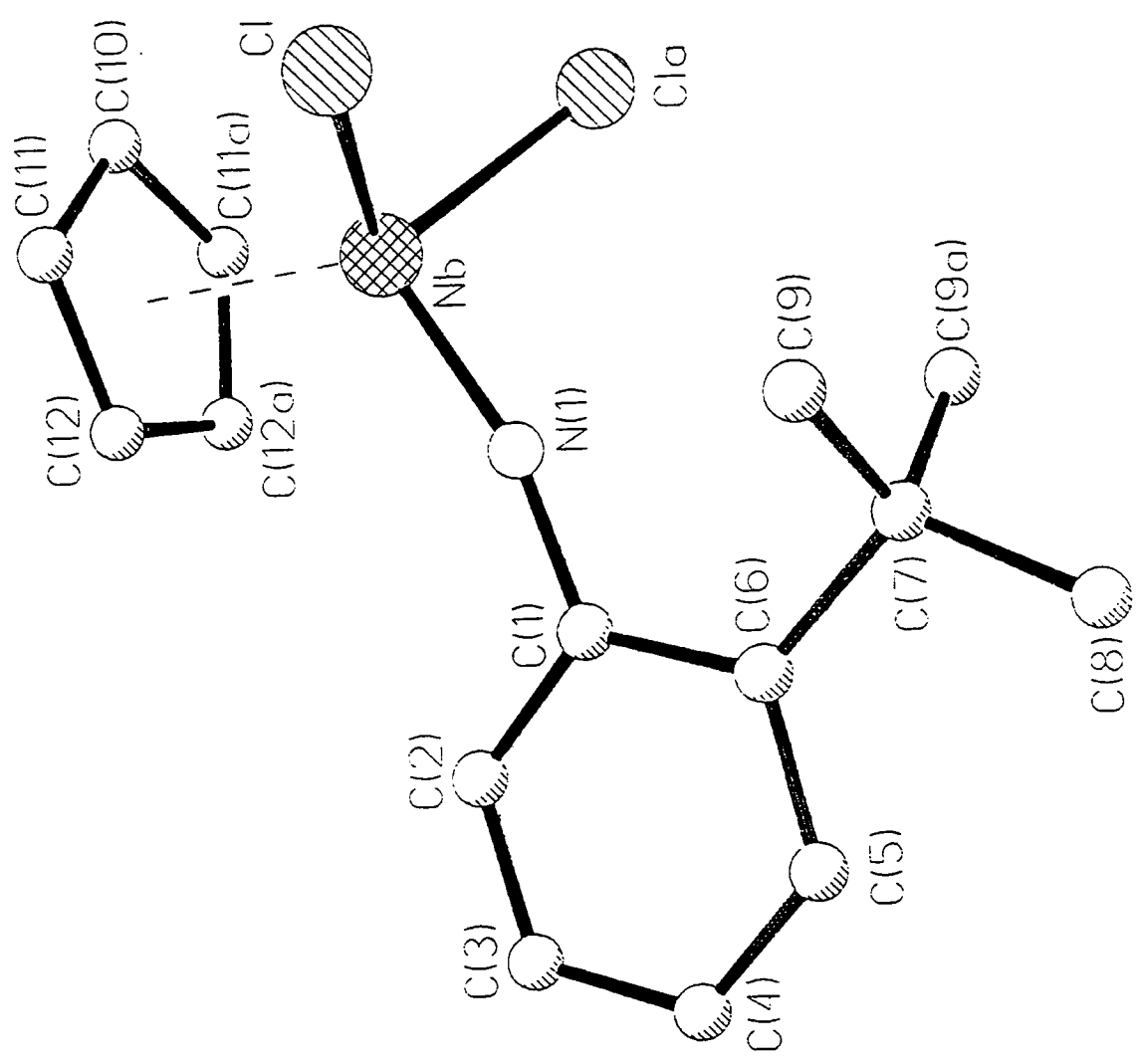


Figure 3.1. Molecular structure of CpNb(N-2-¹BuC₆H₄)Cl₂ (8).

Nb-N(1)	1.782(3)	C(3)-C(4)	1.374(7)
Nb-Cl	2.3455(8)	C(4)-C(5)	1.385(7)
Nb-C(12)	2.379(3)	C(5)-C(6)	1.397(6)
Nb-C(11)	2.464(3)	C(6)-C(7)	1.531(6)
Nb-C(10)	2.523(4)	C(10)-C(11)	1.404(4)
N(1)-C(1)	1.394(5)	C(11)-C(12)	1.409(5)
C(1)-C(2)	1.397(6)	C(12)-C(12a)	1.420(7)
C(1)-C(6)	1.423(6)	Nb-C _{pcentroid}	2.128(5)
C(2)-C(3)	1.375(6)		
N(1)-Nb-Cl	101.76(7)	C(10)-C(11)-C(12)	108.4(3)
Cl-Nb-Cl _a	104.58(4)	C(11)-C(12)-C(12a)	107.6(2)
C(1)-N(1)-Nb	165.1(3)	N(1)-Nb-C _{pcentroid}	119.7(2)
C(11)-C(10)-C(11a)	108.0(4)	Cl-Nb-C _{pcentroid}	113.6(2)

Table 3.1.

Selected bond lengths (Å) and angles (°) for CpNb(N-2-^tBuC₆H₄)Cl₂ (8)

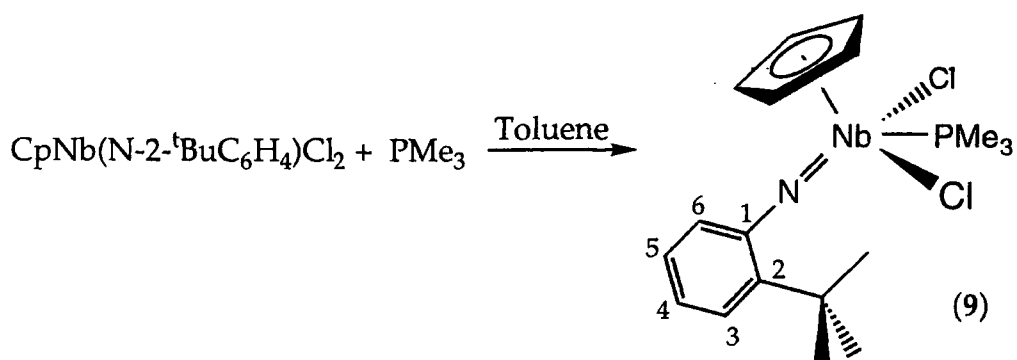
3.1.3. Reaction of CpNb(N-2-^tBuC₆H₄)Cl₂ with PMe₃ :

Preparation of CpNb(N-2-^tBuC₆H₄)(PMe₃)Cl₂ (9)

Species of general formula CpNb(NR)Cl₂ are coordinatively unsaturated and readily react with PMe₃ to give the corresponding 5-coordinate adduct.^{1a} However, facile loss of PMe₃ from CpNb(N-2,6-ⁱPr₂C₆H₃)(PMe₃)Cl₂ *in vacuo* prompted attempts to prepare the (N-2-^tBuC₆H₄) congener.

CpNb(N-2-^tBuC₆H₄)Cl₂ readily binds PMe₃ in toluene to afford CpNb(N-2-^tBuC₆H₄)(PMe₃)Cl₂ (9) as a yellow powder. Analysis of this

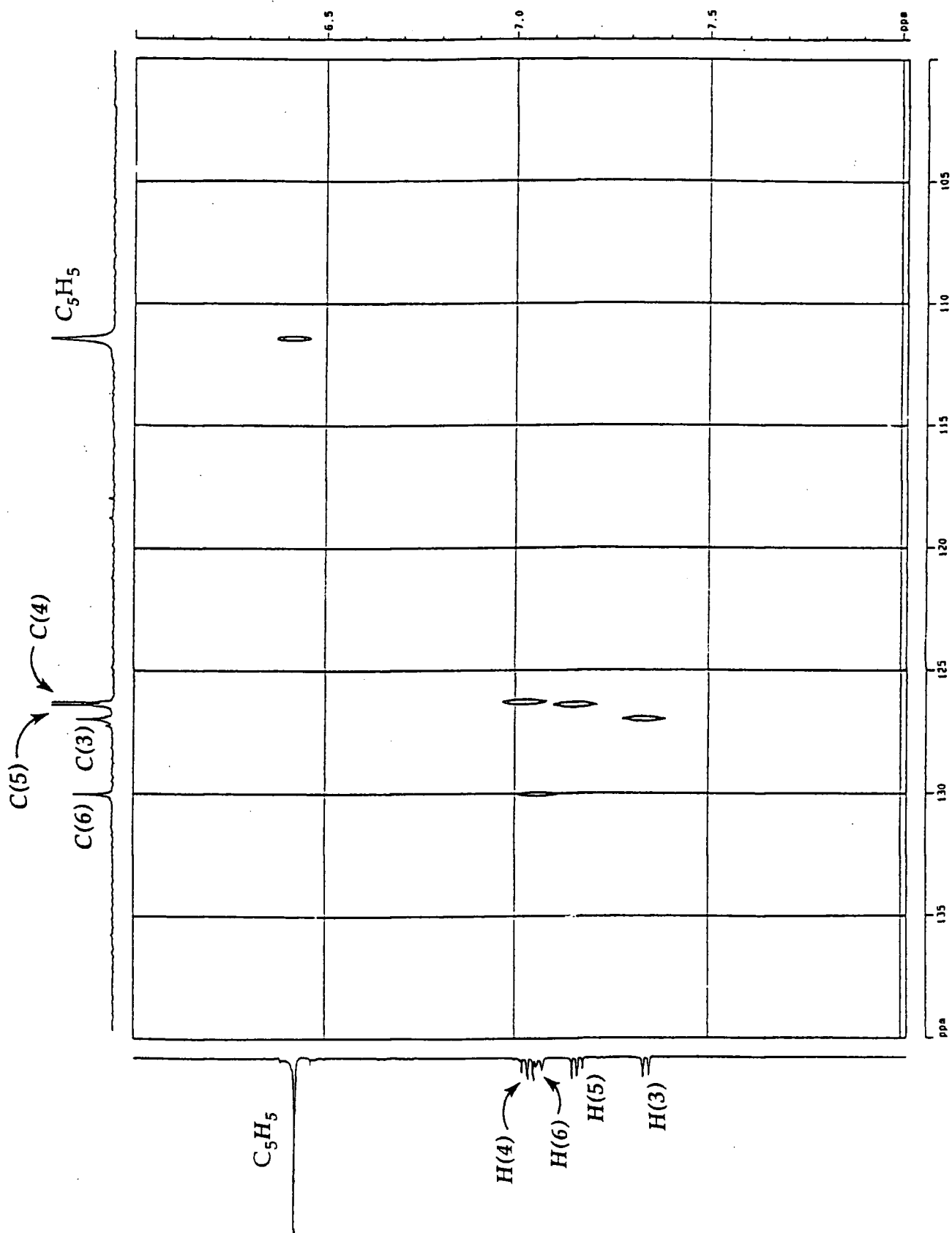
powder by ^1H NMR spectroscopy reveals the presence of residual toluene, which can be removed by prolonged drying *in vacuo*. Recrystallisation of the powder from toluene yielded small yellow crystals.



Scheme 3.2.

The stability of **9** *in vacuo* is in direct contrast to $\text{CpNb}(\text{N}-2,6\text{-}^i\text{Pr}_2\text{C}_6\text{H}_3)(\text{PMe}_3)\text{Cl}_2$; the lability of the phosphine in the latter was accounted for by steric considerations.² The steric bulk of the tert-butyl and the isopropyl moieties are comparable, therefore it appears that the ability of the tert-butyl group to rotate away from the crowded PMe_3 environment does indeed have a major influence on the stability of **9**, especially since the phosphine in related compounds lies adjacent to the imido group and a chloride ligand.^{1a}

Furthermore, the chemical shift (1.54ppm) for the PMe_3 protons of **9** in CDCl_3 implies that the phosphine is strongly bound,^{1a} compared to the value obtained for $\text{CpNb}(\text{N}-2,6\text{-}^i\text{Pr}_2\text{C}_6\text{H}_3)(\text{PMe}_3)\text{Cl}_2$ (1.13ppm). The aryl region in the ^1H spectrum is well resolved and shows four distinct resonances which have been shifted slightly downfield compared to the precursor **8**. These aromatic protons and the corresponding aryl ring carbons have been carefully assigned using a combination of nOe, $^1\text{H}[^1\text{H}]$ COSY and $^1\text{H}[^{13}\text{C}]$ HETCOR (Spectrum 3.1) NMR spectroscopic techniques.



Spectrum 3.1. $^1\text{H}[^{13}\text{C}]$ HETCOR NMR Spectrum (CD_2Cl_2) of $\text{CpNb}(\text{N}-2\text{-}^t\text{BuC}_6\text{H}_4)(\text{PMe}_3)\text{Cl}_2$ (9) : Cp and aryl region.

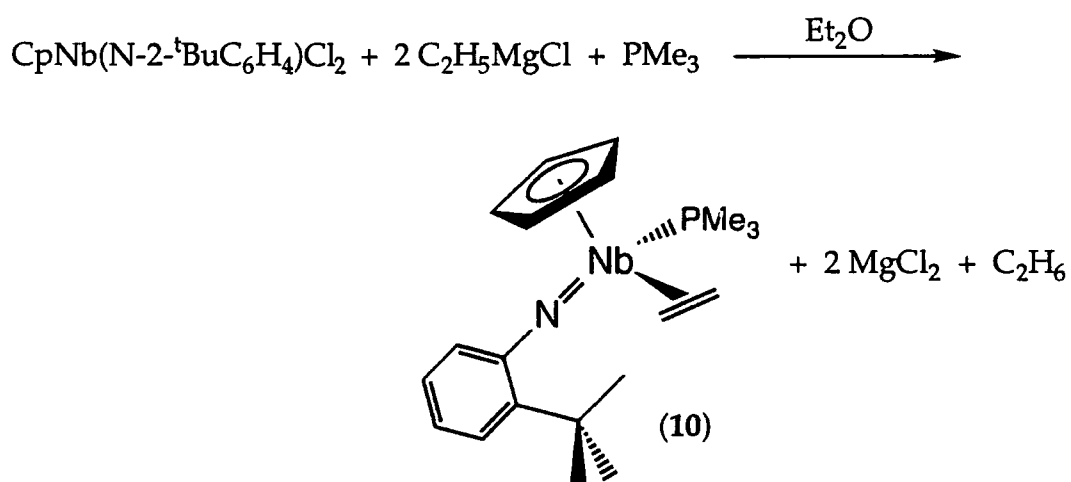
3.1.4. Formation of Phosphine-Stabilised Half-Sandwich Niobium Imido Olefin Complexes

Certain transition metal complexes have the ability to stabilise highly reactive organic fragments and to activate stable molecules toward attack. In addition, species combining imido ligands and neutral organic molecules at a single Group 5 metal centre are rare.^{1b,1c,6} Therefore, attempts were made to prepare olefin derivatives for comparison with the analogous complexes $\text{CpNb}(\text{N-2,6-}^i\text{Pr}_2\text{C}_6\text{H}_3)(\eta^2\text{-C}_2\text{H}_3\text{R})(\text{PMe}_3)$ [$\text{R} = \text{H}, \text{CH}_3$].^{1b}

3.1.4.1. Reaction of $\text{CpNb}(\text{N-2-}^t\text{BuC}_6\text{H}_4)\text{Cl}_2$ with $\text{C}_2\text{H}_5\text{MgCl}$ in the presence of trimethylphosphine :

Preparation of $\text{CpNb}(\text{N-2-}^t\text{BuC}_6\text{H}_4)(\eta^2\text{-C}_2\text{H}_4)(\text{PMe}_3)$ (10)

Treatment of a diethyl ether solution of $\text{CpNb}(\text{N-2-}^t\text{BuC}_6\text{H}_4)\text{Cl}_2$ with two equivalents of $\text{C}_2\text{H}_5\text{MgCl}$ and PMe_3 yielded bright orange crystals of $\text{CpNb}(\text{N-2-}^t\text{BuC}_6\text{H}_4)(\eta^2\text{-C}_2\text{H}_4)(\text{PMe}_3)$ (10) in high yield :



Scheme 3.3

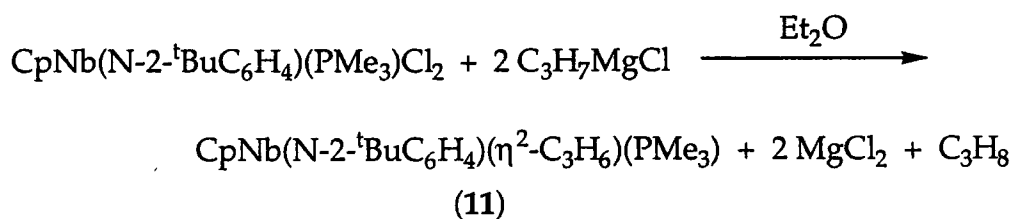
The ^1H NMR spectrum of 10 features multiplets at 0.57, 1.19, 1.42 and 1.67ppm due to the olefinic protons. Their complexity is caused by the presence of a static ethylene ligand in a chiral metal environment, hence

giving rise to an ABCD spin system. The ^{13}C NMR spectrum shows two ethylene resonances at 26.43 and 30.35ppm, with only the latter displaying coupling to phosphorus ($^2J_{\text{CP}}=13\text{Hz}$); hence this carbon is lying adjacent (*endo*) to the PMe_3 ligand.

The mechanism for the formation of **10** is thought to proceed *via* an unstable metal diethyl species, which undergoes β -elimination of ethane to generate the phosphine-stabilised ethylene product.²

**3.1.4.2. Reaction of $\text{CpNb}(\text{N}-2\text{-}^t\text{BuC}_6\text{H}_4)(\text{PMe}_3)\text{Cl}_2$ with $n\text{-C}_3\text{H}_7\text{MgCl}$:
Preparation of $\text{CpNb}(\text{N}-2\text{-}^t\text{BuC}_6\text{H}_4)(\eta^2\text{-C}_3\text{H}_6)(\text{PMe}_3)$ (**11**)**

Compound **11** was afforded in high yield (86%) as large deep red crystals from the reaction of a diethyl ether solution of the PMe_3 adduct **9** with two equivalents of $n\text{-C}_3\text{H}_7\text{MgCl}$.



Scheme 3.4.

Elemental analysis on **11** indicates a stoichiometry of $\text{C}_{21}\text{H}_{33}\text{NNbP}$ and the mass spectrum shows envelopes at m/z 423 and 381, which are attributed to the parent ion and the daughter fragment $[\text{CpNb}(\text{N}-2\text{-}^t\text{BuC}_6\text{H}_4)(\text{PMe}_3)]$ respectively. Complex **11** is extremely air-sensitive but is stable in solution at room temperature for several weeks, in contrast to the 2,6-di(isopropyl)phenyl analogue which readily decomposes. The difference in the steric nature of the imido substituents is again believed to be the significant factor.

The ^1H NMR spectrum reveals a mixture of four isomers (**11a-11d** : **a** is the most abundant; **d** is the least abundant), as is the case for $\text{CpNb}(\text{N}-2,6\text{-}$

$^i\text{Pr}_2\text{C}_6\text{H}_3)(\eta^2\text{-C}_3\text{H}_6)(\text{PMe}_3)$. The assignment of resonances for each isomer was made on the basis of the relative intensities for each set of peaks; homonuclear decoupling NMR experiments were required to assign resonances to **11d**. The isomerism can be explained by the possibility for four propylene binding orientations at the metal centre, though it is unusual for all four isomers to be observed in room temperature solutions of metal propylene complexes. The four species exist as two rotamer pairs, each related by a 180° rotation of the propylene ligand. One would predict the methyl group of the olefin for the most abundant isomer **11a** to orientate towards the imido unit and away from the Cp ring, since stereochemical models show that this is the least hindered environment for the ligand.

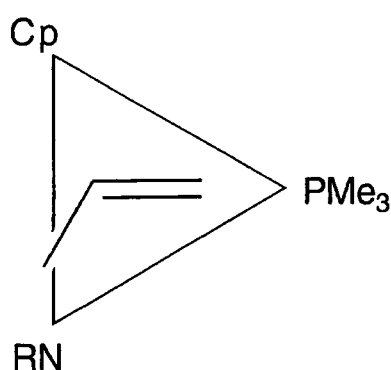


Figure 3.2. Proposed triad representation⁷ of isomer **11a** ($\text{R}=2\text{-}^t\text{BuC}_6\text{H}_4$).

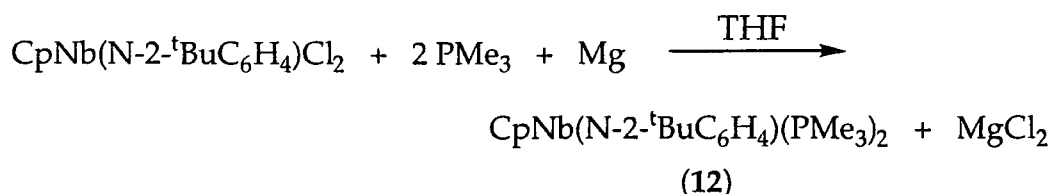
3.1.5. Reduction of $\text{CpNb}(\text{N-}2\text{-}^t\text{BuC}_6\text{H}_4)\text{Cl}_2$ with Magnesium in the Presence of Trimethylphosphine :

Preparation of $\text{CpNb}(\text{N-}2\text{-}^t\text{BuC}_6\text{H}_4)(\text{PMe}_3)_2$ (**12**)

Bis(phosphine) complexes of Group 4 bent metallocenes undergo facile loss of one or both phosphine ligands under very mild conditions in the presence of reactive substrates. They have been shown to react with alkynes to form synthetically useful metallacyclopentadienes.⁸ Work was undertaken to prepare the half-sandwich niobium imido congener which may also display versatile synthetic chemistry due to the isolobal relationship. The

generation of a relatively stable bis(phosphine) complex would be in contrast to $\text{CpNb}(\text{N-2,6-}i\text{Pr}_2\text{C}_6\text{H}_3)(\text{PMe}_3)_2$, which readily loses PMe_3 and decomposes *in vacuo*.²

Magnesium reduction of a THF solution of $\text{CpNb}(\text{N-2-}^t\text{BuC}_6\text{H}_4)\text{Cl}_2$ in the presence of PMe_3 yielded the complex **12**. Subsequent recrystallisation from pentane afforded shiny, dark green, extremely air and moisture sensitive crystals in high yield (74%) :

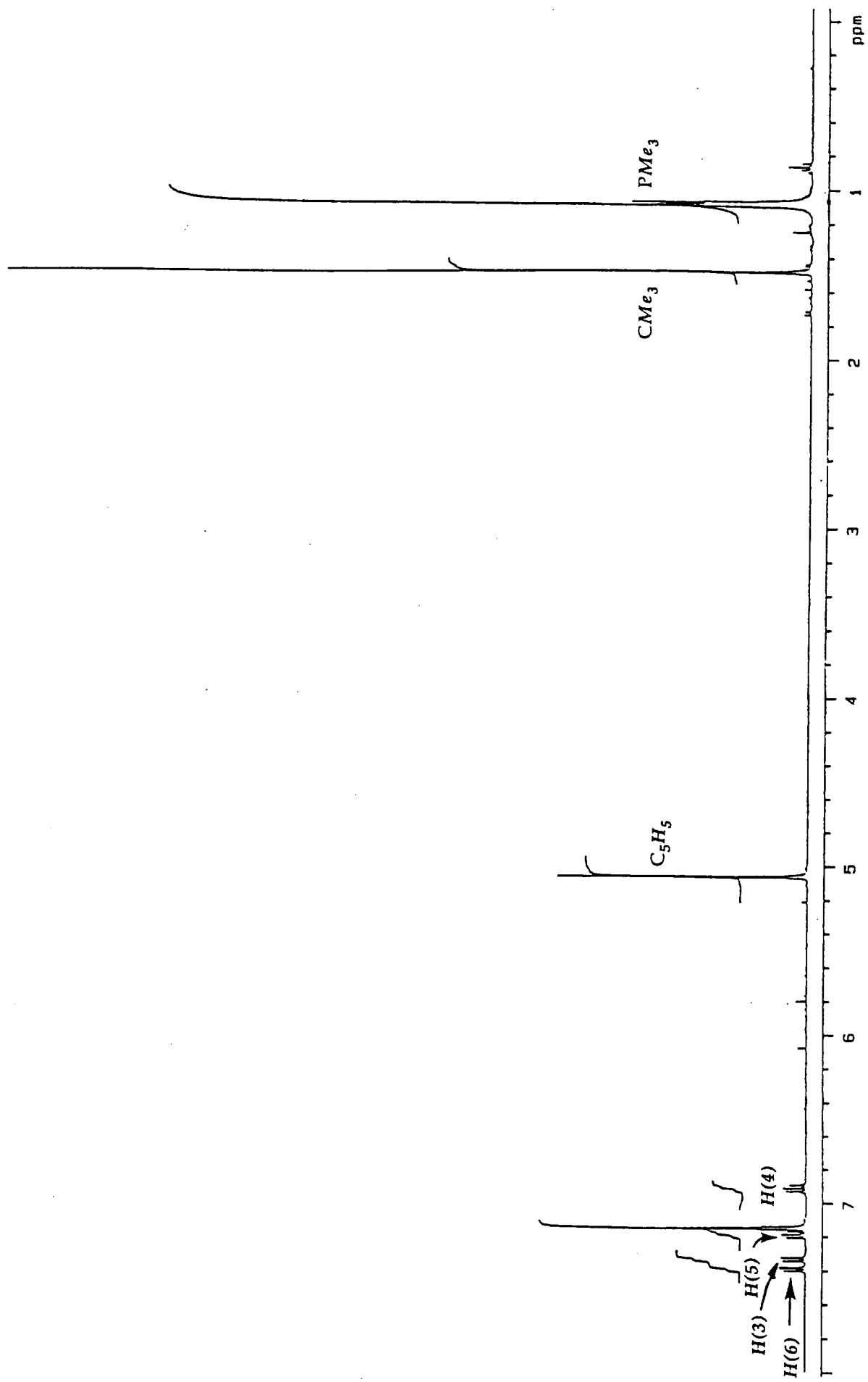


Scheme 3.5.

Unlike $\text{CpNb}(\text{N-2,6-}i\text{Pr}_2\text{C}_6\text{H}_3)(\text{PMe}_3)_2$, **12** is stable indefinitely under reduced pressure; this again underlines the steric versatility of the 2-tert-butylphenyl group. The stability of the sterically crowded $\text{Cp}^*\text{Nb}(\text{N-2,6-}i\text{Pr}_2\text{C}_6\text{H}_3)(\text{PMe}_3)_2$ derivative under the same conditions can be attributed to the electron-donating effect of the Cp^* ring.^{1c}

In the ^1H NMR spectrum of **12** (Spectrum 3.2), the PMe_3 doublet appears at 1.09ppm. Singlets at 1.48 and 5.06ppm have been assigned to the t-butyl and Cp protons respectively. The Cp resonance is shifted significantly upfield compared to the starting material **8** (5.80ppm), indicative of the change in the oxidation state of the metal, from Nb(V) to Nb(III). Signals for the aryl protons appear in the region 6.91-7.39ppm.

The mass spectrum for **12** exhibits an envelope at m/z 457 due to the molecular ion. A peak at m/z 381 has been assigned to the $[\text{M-PMe}_3]^+$ fragment. However, another envelope at m/z 913 corresponding to the dimeric species can also be detected. Detailed analysis of the data, using time resolved selected ion monitoring of the signals at m/z 457 and m/z 913 concluded that the intensities of the two species are intrinsically linked.



Spectrum 3.2. 400MHz ^1H NMR Spectrum (C_6D_6) of $\text{CpNb}(\text{N}-2\text{-}^t\text{BuC}_6\text{H}_4)(\text{PMe}_3)_2$ (12).

Furthermore, one would expect to see intensities due to the more volatile monomer appearing first on the time scale if it was present in the sample, but this is not the case. Therefore, the evidence clearly suggests that the complex is dimeric in the solid state. This dimer presumably consists of the two imido units bridging between two $[\text{CpNb}(\text{PMe}_3)_2]$ fragments.

3.1.6. Reaction of $\text{CpNb}(\text{N}-2\text{-}^t\text{BuC}_6\text{H}_4)(\text{PMe}_3)_2$ (12) with Alkynes

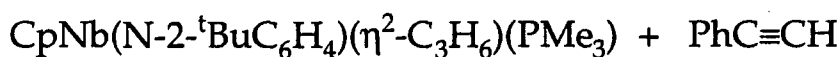
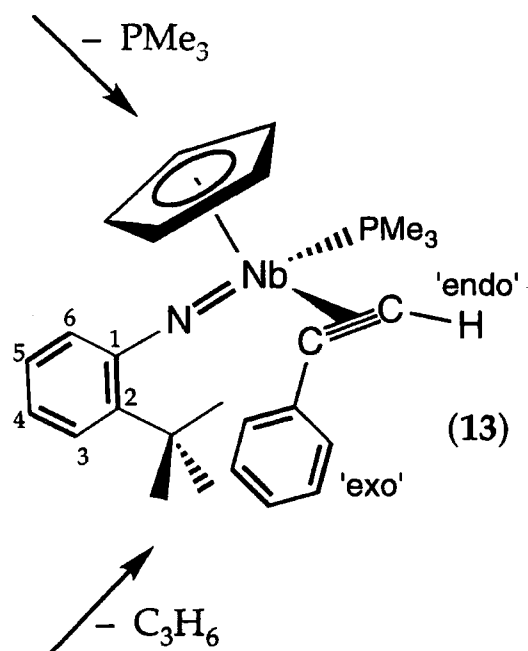
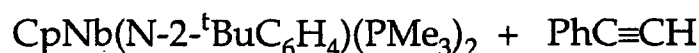
In the reaction of $\text{Cp}_2\text{Ti}(\text{PMe}_3)_2$ with acetylenes, the mono-phosphine complexes $\text{Cp}_2\text{Ti}(\text{RC}\equiv\text{CR})(\text{PMe}_3)$ are initially generated and the corresponding metallacyclopentadienes are subsequently formed.^{8a,b} For the analogous reaction of $\text{Cp}_2\text{Zr}(\text{PMePh}_2)_2$ with $\text{EtC}\equiv\text{CEt}$, only the metallacyclopentadiene species is isolated, although the conversion presumably proceeds via the $[\text{Cp}_2\text{Zr}(\text{EtC}\equiv\text{CEt})(\text{PMePh}_2)]$ intermediate.^{8c}

Hence our study focused on the isolation of both the acetylene mono-phosphine and the metallacyclopentadiene complexes in the half-sandwich niobium imido system. In addition, $\text{CpNb}(\text{N}-2,6\text{-}^i\text{Pr}_2\text{C}_6\text{H}_3)(\text{PhC}\equiv\text{CPh})(\text{PMe}_3)$ has been reported to be relatively unstable due to steric congestion in the coordination sphere and has not yet been isolated.² Therefore the synthesis of the 2-*t*-butylphenylimido derivative would further confirm its steric versatility.

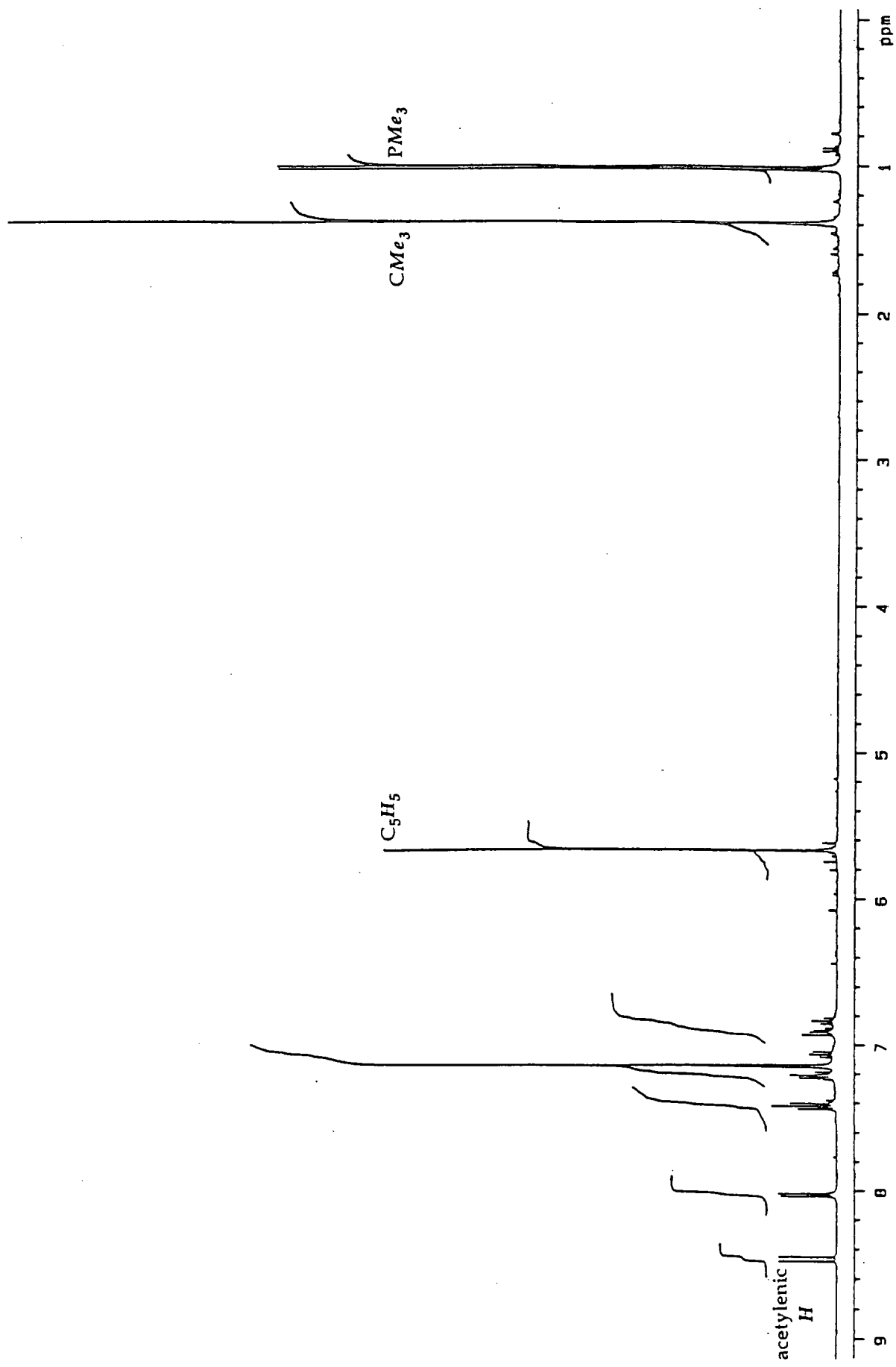
3.1.6.1. Preparation of $\text{CpNb}(\text{N}-2\text{-}^t\text{BuC}_6\text{H}_4)(\text{PhC}\equiv\text{CH})(\text{PMe}_3)$ (13)

The phenylacetylene complex is obtained as a yellow crystalline solid upon treatment of a pentane solution of $\text{CpNb}(\text{N}-2\text{-}^t\text{BuC}_6\text{H}_4)(\text{PMe}_3)_2$ with one equivalent of the alkyne at room temperature. The complex can also be prepared *via* the displacement of propene from $\text{CpNb}(\text{N}-2\text{-}^t\text{BuC}_6\text{H}_4)(\eta^2\text{-C}_3\text{H}_6)(\text{PMe}_3)$ (11) with $\text{PhC}\equiv\text{CH}$, although prolonged heating is required to achieve substantial conversion and the reaction is less clean.

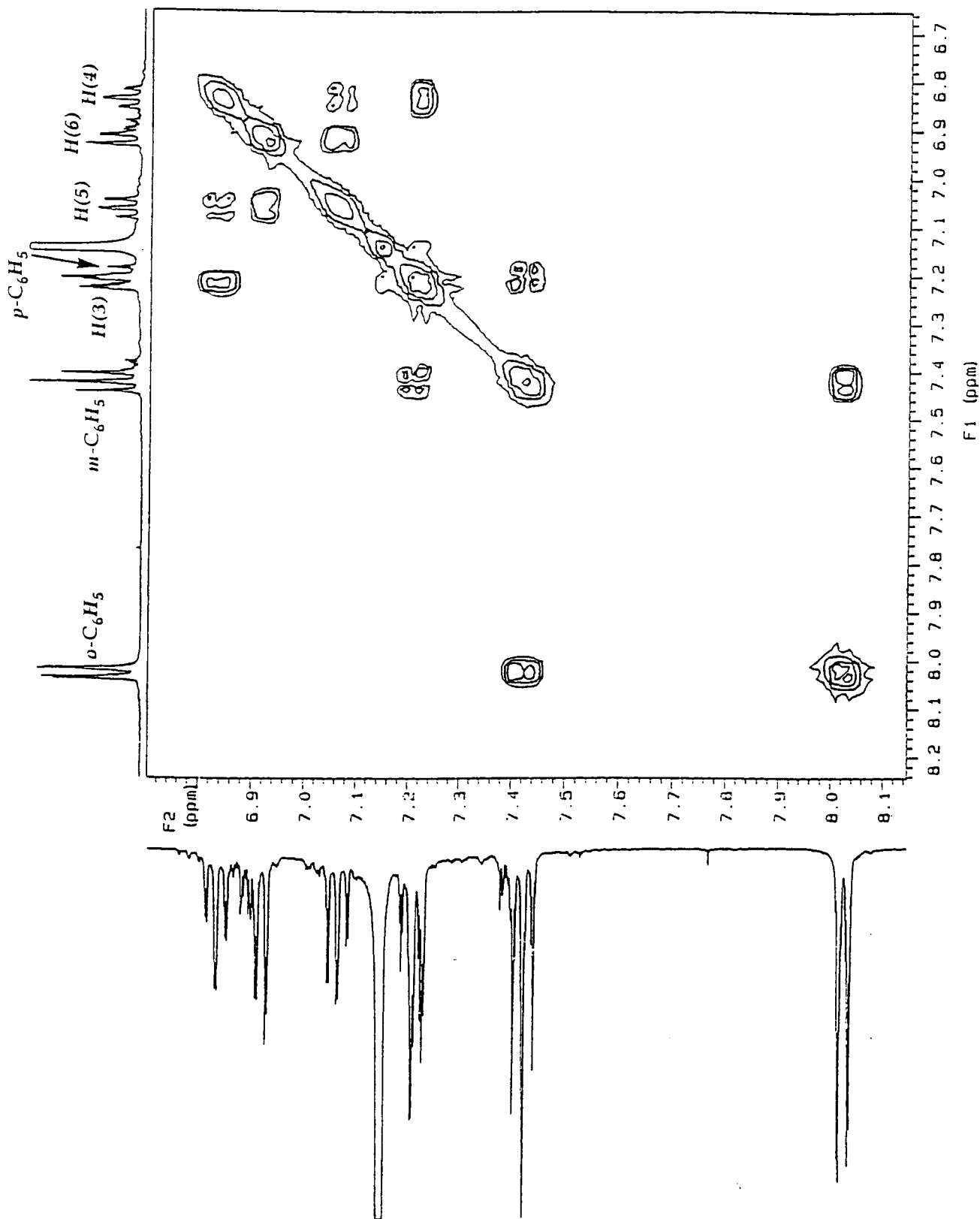
In the ^1H NMR spectrum for **13** (Spectrum 3.3), the terminal acetylenic proton appears as a doublet at 8.47ppm with coupling to phosphorus ($^3J_{\text{PH}}=12\text{Hz}$). The ortho protons of the phenylacetylene ring, compared to the uncoordinated alkyne, have also shifted significantly downfield to 8.03ppm. A doublet of doublets at 143.53ppm in the ^{13}C NMR spectrum has been assigned to the terminal acetylenic carbon which displays coupling to the acetylenic proton ($^1J_{\text{CH}}=179\text{Hz}$) and the phosphorus nucleus ($^2J_{\text{CP}}=29\text{Hz}$). This relatively large phosphorus coupling, in comparison to the phenylacetylenic carbon (157.44ppm, $^2J_{\text{CP}}=22\text{Hz}$), is indicative of the orientation where the unsubstituted end of the alkyne is in the *endo* position i.e. adjacent to the phosphine; the phenyl ring is in the *exo* position and lies remote to the PMe_3 group⁹ (Scheme 3.6). **13** has also been characterised by using nOe, COSY (Spectrum 3.4) and HETCOR NMR techniques.



Scheme 3.6.



Spectrum 3.3. 400MHz ^1H NMR Spectrum (C_6D_6) of $\text{CpNb}(\text{N}-2\text{-}^i\text{BuC}_6\text{H}_4)(\text{PhC}\equiv\text{CH})(\text{PMe}_3)$ (13).

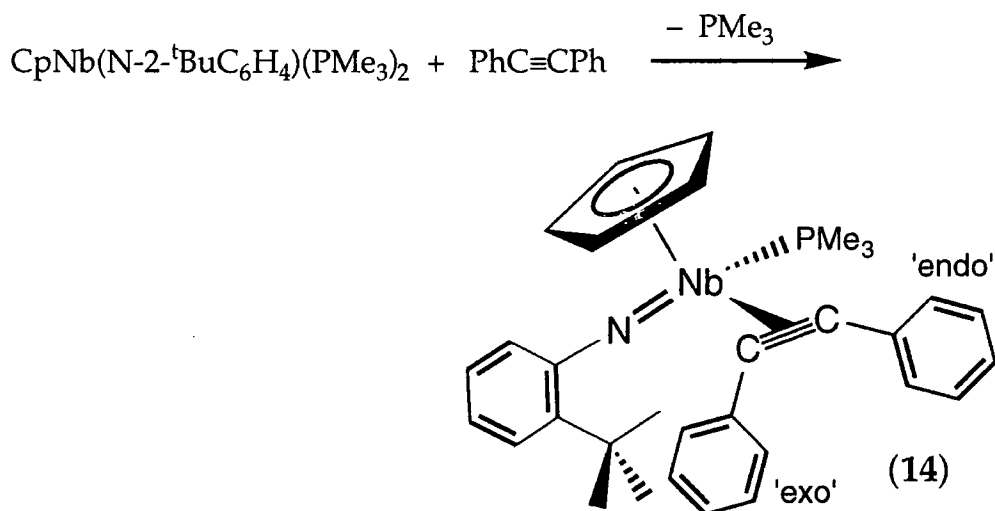


Spectrum 3.4. $^1\text{H}[^1\text{H}]$ COSY NMR Spectrum (C_6D_6) of
 $\text{CpNb}(\text{N}\text{-}2\text{-}^t\text{BuC}_6\text{H}_4)(\text{PhC}\equiv\text{CH})(\text{PMe}_3)$ (13) : aryl hydrogens.

Attempts to displace the second phosphine by treating $\text{CpNb}(\text{N}-2\text{-}^t\text{BuC}_6\text{H}_4)(\text{PMe}_3)_2$ with excess phenylacetylene only yielded complex **13**; formation of the desired metallacyclopentadiene was not observed. The reasons behind this probably have a steric origin, although the increased interaction between the basic phosphine and the more electrophilic Nb centre in **13**, compared to Zr in the bent metallocene complexes, may also be important.

3.1.6.2. Preparation and Molecular Structure of $\text{CpNb}(\text{N}-2\text{-}^t\text{BuC}_6\text{H}_4)(\text{PhC}\equiv\text{CPh})(\text{PMe}_3)$ (14**); Structural Comparisons with Isolobal Complexes**

$\text{CpNb}(\text{N}-2\text{-}^t\text{BuC}_6\text{H}_4)(\text{PhC}\equiv\text{CPh})(\text{PMe}_3)$ (**14**) was formed after prolonged warming of a pentane solution of $\text{CpNb}(\text{N}-2\text{-}^t\text{BuC}_6\text{H}_4)(\text{PMe}_3)_2$ with one equivalent of diphenylacetylene:



Scheme 3.7.

The severity of the conditions compared to the phenylacetylene reaction reflects the increase in steric congestion in the complex. As expected,

a metallacyclopentadiene was not observed upon treatment of **14** with excess $\text{PhC}\equiv\text{CPh}$.

NMR spectroscopic assignment of **14** was made using ^1H , ^{13}C , COSY and HETCOR NMR experiments and by comparison with $\text{Mo}(\text{N}^t\text{Bu})_2(\text{PhC}\equiv\text{CPh})(\text{PMe}_3)$.⁹ Resonances for the acetylenic carbons appear at 157.4 and 162.0 ppm in the ^{13}C NMR spectrum; only the former displays coupling to phosphorus ($^2J_{\text{CP}}=22.1\text{Hz}$) and therefore this corresponds to the endo position. These ^{13}C shifts are intermediate between the ranges typically observed for 2-electron (110–120 ppm) and 4-electron alkyne ligands (190–210 ppm).¹⁰ This may be indicative of partial donation of electron density from the orthogonal π -system of the alkyne ligand, since in a pseudo-tetrahedral environment, π -donor ligands compete with each other for the available empty metal orbitals of d_{π} symmetry. Similar intermediate ^{13}C NMR shifts for the acetylenic carbons are also a feature of the isolobal complexes $\text{Cp}_2\text{Zr}(\text{PhC}\equiv\text{CPh})(\text{PMe}_3)$ (141.6, 156.4 ppm)¹¹ and $\text{Mo}(\text{N}^t\text{Bu})_2(\text{PhC}\equiv\text{CPh})(\text{PMe}_3)$ (149.4, 154.6 ppm).⁹

Crystals of **14** suitable for an X-ray structural determination were grown from a pentane solution at 0°C . The molecular structure is shown in Figure 3.3. Selected interatomic distances and angles are collected in Table 3.2 and the crystal data are given in Appendix A7.

Key structural parameters are collected in Table 3.3 together with those for the isolobal complexes $\text{Cp}_2\text{Zr}(\text{PhC}\equiv\text{CPh})(\text{PMe}_3)$,¹¹ $\text{CpNb}(\eta^4\text{-C}_4\text{H}_6)(\text{PhC}\equiv\text{CPh})(\text{PMe}_3)$ ^{12§} and $\text{Mo}(\text{N}^t\text{Bu})_2(\text{PhC}\equiv\text{CPh})(\text{PMe}_3)$.⁹

The molecular geometry of **14** is pseudo-tetrahedral, with a $\text{Cp}_{\text{centroid}}\text{-Nb-N}$ angle of 121.5° and $\text{Cp}_{\text{centroid}}\text{-Nb-P}$ angle of 111.5° . The angle at the

§ The 1,3-butadiene ligand possesses two π -symmetry orbitals, is capable of forming one σ and two π bonds with a metal and can donate up to four electrons. Therefore it can be considered to be isolobal and 'isonumeral' with the imido unit.⁷

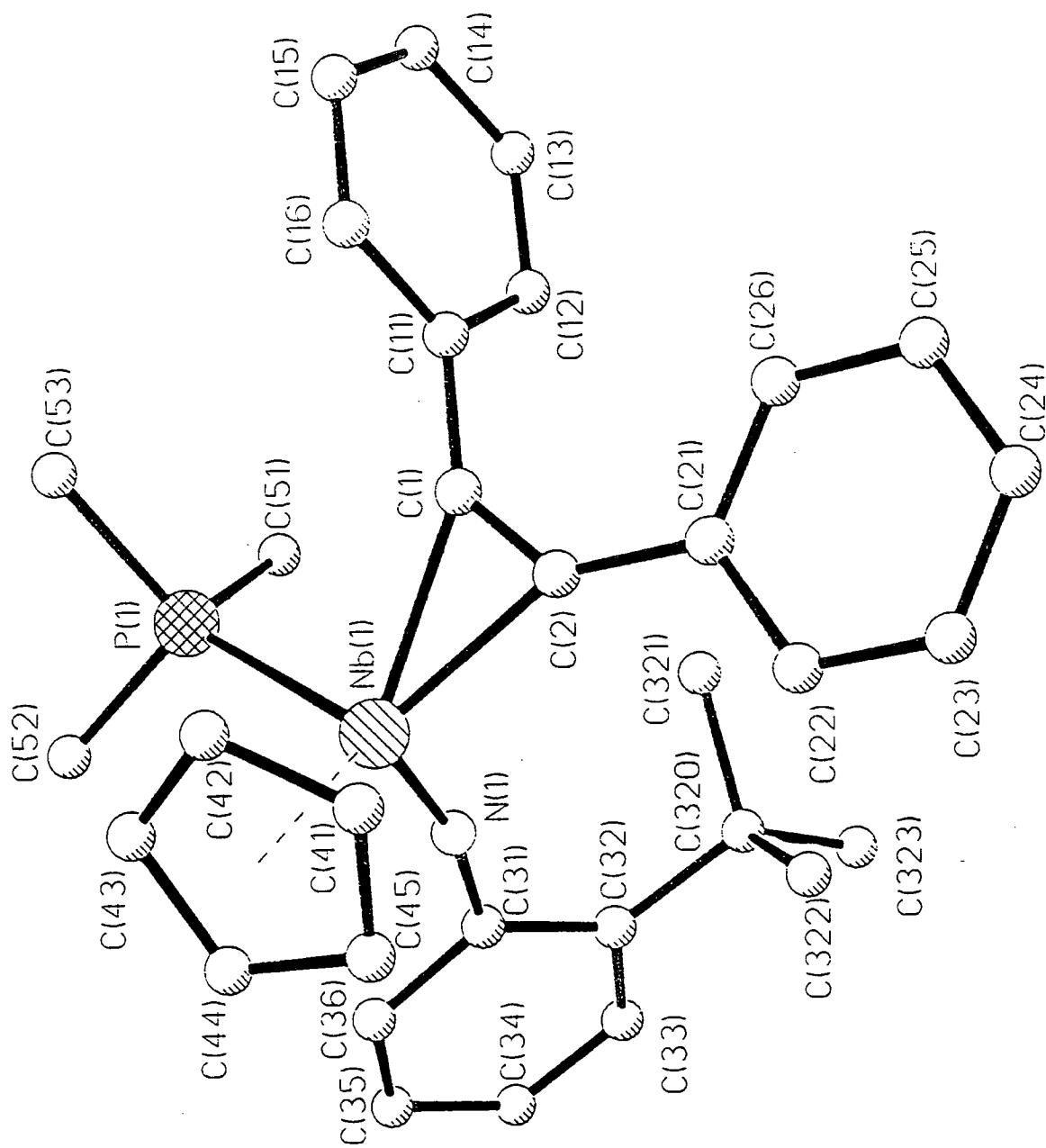


Figure 3.3. Molecular structure of CpNb(N-2-'BuC₆H₄)(PhC≡CPh)(PMe₃) (14).

Nb(1)–N(1)	1.813(3)	P(1)–C(53)	1.830(5)
Nb(1)–C(2)	2.144(3)	N(1)–C(31)	1.392(4)
Nb(1)–C(1)	2.200(3)	C(1)–C(2)	1.309(5)
Nb(1)–C(45)	2.435(3)	C(1)–C(11)	1.457(5)
Nb(1)–C(41)	2.453(4)	C(2)–C(21)	1.469(5)
Nb(1)–C(43)	2.469(4)	C(41)–C(42)	1.400(6)
Nb(1)–C(44)	2.472(4)	C(41)–C(45)	1.419(6)
Nb(1)–C(42)	2.479(4)	C(42)–C(43)	1.395(6)
Nb(1)(1)–P(1)	2.546(1)	C(43)–C(44)	1.391(6)
P(1)–C(52)	1.812(4)	C(44)–C(45)	1.404(6)
P(1)–C(51)	1.815(4)	Nb(1)–C _p centroid	2.154(4)
N(1)–Nb(1)–C(2)	105.9(1)	C(11)–C(1)–Nb(1)	152.2(2)
N(1)–Nb(1)–C(1)	109.5(1)	C(1)–C(2)–C(21)	136.0(3)
C(1)–Nb(1)–C(2)	35.1(1)	C(1)–C(2)–Nb(1)	74.8(2)
N(1)–Nb(1)–P(1)	88.5(1)	C(21)–C(2)–Nb(1)	149.0(2)
C(2)–Nb(1)–P(1)	116.1(1)	P(1)–Nb(1)–C _p centroid	111.5(1)
C(1)–Nb(1)–P(1)	81.2(1)	N(1)–Nb(1)–C _p centroid	121.5(1)
C(31)–N(1)–Nb(1)	166.3(2)	C(1)–Nb(1)–C _p centroid	127.1(1)
C(2)–C(1)–C(11)	137.7(3)	C(2)–Nb(1)–C _p centroid	111.8(1)
C(2)–C(1)–Nb(1)	70.1(2)		

Table 3.2. Selected bond lengths (Å) and angles (°) for CpNb(N-2-^tBuC₆H₄)(PhC≡CPh)(PMe₃) (14)

Parameters	Cp ₂ Zr(PhC≡CPh) (PMe ₃) ¹¹	CpNb(N-2-tBuC ₆ H ₄) (PhC≡CPh)(PMe ₃)	CpNb(η ⁴ -C ₄ H ₆) (PhC≡CPh)(PMe ₃) ¹²	Mo(N ^t Bu) ₂ (PhC≡CPh) (PMe ₃) ⁹
Cendo-Cexo ^{a,b} (Å)	1.36(6)	1.309(5)	1.281(1)	1.31(1)
M-Cendo ^a (Å)	2.25(4)	2.200(3)	2.214(1)	2.158(9)
M-Cexo ^b (Å)	2.20(4)	2.144(3)	2.187(1)	2.081(8)
M-P (Å)	2.70(1)	2.546(1)	2.554(1)	2.465(3)
M-X ^c (Å)	—	2.15(1) [Cp], 1.81(1) [N]	2.13(1) [Cp]	1.761(7), 1.759(7)
X-M-X ^c (°)	127.4	121.5	—	117.6

^a Cendo refers to the metal-bound acetylenic carbon closest from the PMe₃ ligand. ^b Cexo refers to the metal-bound acetylenic carbon furthest from the PMe₃ ligand. ^c X = Cp ring centroid(s) and/or N, where appropriate.

Table 3.3. Comparison of Key Structural Parameters of Isobalally Related Alkyne Complexes

imido nitrogen [166.3(2)°] is virtually identical to that found in CpNb(N-2-*t*BuC₆H₄)Cl₂ (**2**) [165.1(3)°]. The Nb–N bond length [1.813(3)Å] is substantially longer than for **2** [1.782(3)Å] reflecting the lower formal oxidation state of the metal in the alkyne complex. The phenyl ring of the imido moiety is rotated by 51.1° relative to its position in CpNb(N-2-*t*BuC₆H₄)Cl₂ but nevertheless the *t*-butyl substituent is accommodated in a cavity beneath the alkyne ligand (see 3.1.2.1). Hence the ability of the 2-*t*-butylphenylimido group to position the bulky alkyl unit into an area of minimum steric repulsion appears to be the overriding factor for the successful isolation and relative stability of **14**.

The phosphorus atom of the PMe₃ ligand is displaced by only 0.021Å out of the Nb–C(1)–C(2) plane, which confirms the bent metallocene-like characteristics of the half-sandwich niobium imido fragment. A triad representation⁷ which illustrates the alkyne orientation is shown in Figure 3.4.

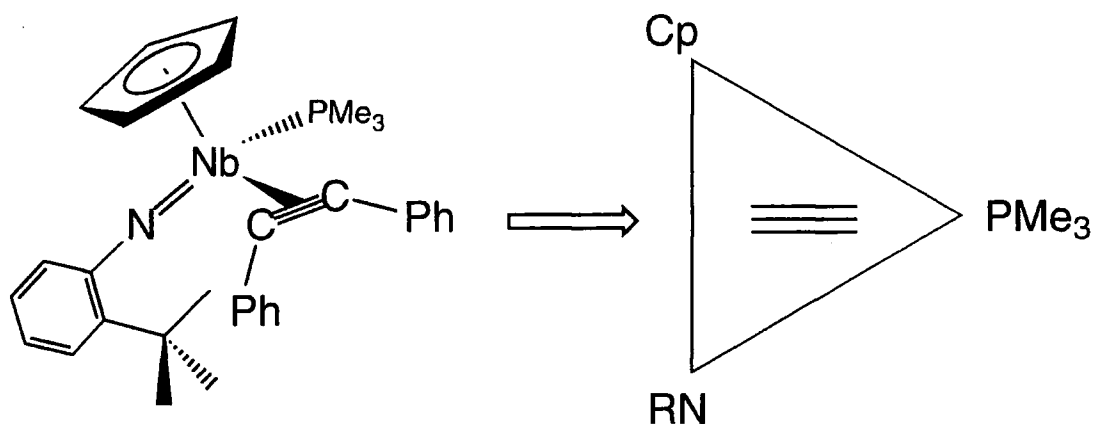


Figure 3.4.

For the alkyne ligand, the ipso carbons also lie in the Nb–C(1)–C(2) plane. The phenyl rings, however, are tilted out of this plane; the endo ring by 79.1° and the exo ring by 6.4°. This uneven distortion and the asymmetric

coordination of the acetylene [Nb–C(1)/endo 2.200(3)Å, Nb–C(2)/exo 2.144(3)Å] are both likely consequences of the steric constraints imposed by the phosphine ligand. These features are also displayed by the related complexes in Table 3.3. The C(1)–C(2) distance of 1.309(5)Å is indicative of significant back donation (compared with C–C bond length in free acetylene and ethylene: 1.20 and 1.33Å respectively); thus the interaction with the metal approaches a metallacyclopropene description. The phenyl rings substantiate this by bending away from the metal centre [mean angle of 137° between C≡C bond and ipso carbons].

In summary, the similarities in the structural parameters of CpNb(N-2-^tBuC₆H₄)(PhC≡CPh)(PMe₃) (**14**) and CpNb(η⁴-C₄H₆)(PhC≡CPh)(PMe₃) appear to validate the proposed relationship between the imido and 1,3-butadiene ligands. The comparable key bond lengths and angles and the distinctive orientation of the alkyne ligand for the complexes in Table 3.3 provides further support for the isolobal relationship between the [Cp₂Zr], [CpNb(NR)] and [Mo(NR)₂] fragments. The slight deviations in the metal–ligand distances may be attributed to differences in the ionic radii, electronegativity and steric crowding of the metals (see 3.2.4.1).

3.2. Introduction

Many derivatives of $\text{CpNb}(\text{N}-2,6\text{-}^i\text{Pr}_2\text{C}_6\text{H}_3)\text{Cl}_2$ have been previously reported and their chemical and structural behaviour have been compared with the isolobal zirconocene analogues.^{1,2} In order to evaluate the effects of electron-withdrawing substituents on the arylimido ligand upon the stability of these half-sandwich niobium imido complexes, 2,6-dichlorophenylimido derivatives were targeted. The high electronegativity of the chloro substituents is expected to increase the acidity of the metal centre and aid in the stabilisation of basic substrates. In addition, the chlorine substituents at the ortho positions are relatively small compared to branched alkyl groups such as the isopropyl fragment and therefore steric congestion at the metal should be decreased.

3.2.1. Electronic Influence of the Imido Moiety :

Synthesis and Reactivity of $\text{CpNb}(\text{N}-2,6\text{-Cl}_2\text{C}_6\text{H}_3)\text{Cl}_2$

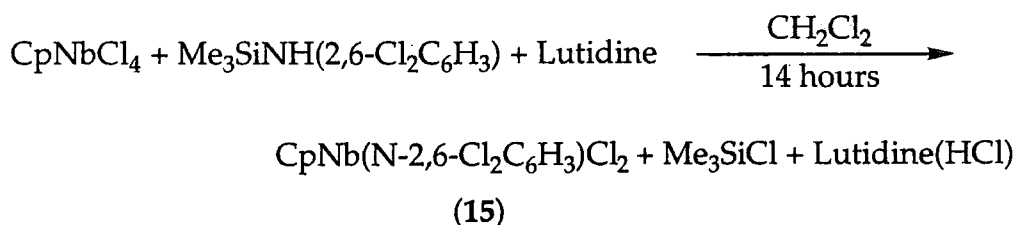
This section describes the synthesis, characterisation and reactivity of the new imido complex $\text{CpNb}(\text{N}-2,6\text{-Cl}_2\text{C}_6\text{H}_3)\text{Cl}_2$, together with comparisons with the corresponding $[\text{N}-2,6\text{-}^i\text{Pr}_2\text{C}_6\text{H}_3]$ derivatives.

3.2.2. Reaction of CpNbCl_4 with $\text{Me}_3\text{SiNH}(2,6\text{-Cl}_2\text{C}_6\text{H}_3)$ and 2,6-Lutidine:

Preparation of $\text{CpNb}(\text{N}-2,6\text{-Cl}_2\text{C}_6\text{H}_3)\text{Cl}_2$ (15)

The established procedure using 2,6-lutidine was employed^{1a} (Scheme 3.8). Reaction of CpNbCl_4 and 2,6-lutidine in CH_2Cl_2 with $\text{Me}_3\text{SiNH}(2,6\text{-Cl}_2\text{C}_6\text{H}_3)$ at room temperature for 14 hours afforded a clear orange-red solution. On removal of the volatile components under reduced pressure an

orange solid was obtained, but attempts to extract $\text{CpNb}(\text{N-2,6-Cl}_2\text{C}_6\text{H}_3)\text{Cl}_2$ (**15**) with petroleum ether, pentane or boiling heptane all failed. However, extraction with acetonitrile eventually afforded a red solution, which was filtered from the lutidinium hydrochloride, concentrated and cooled to -40°C to yield **15** as an orange-red solid. The extraction was problematic due to the persistent contamination of **15** by the lutidinium salt. **15** is also sparingly soluble in diethyl ether and toluene.



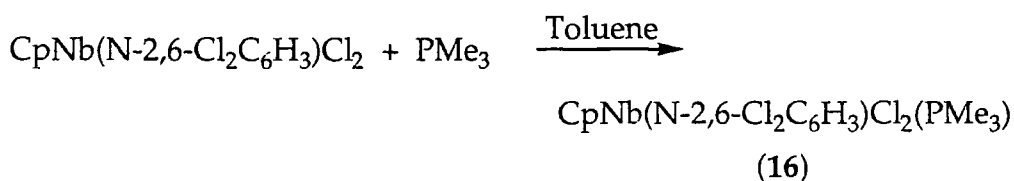
Scheme 3.8.

The ^1H NMR spectrum shows a singlet resonance for the Cp ring and a triplet and doublet for the para and meta protons respectively on the phenyl ring. A doublet of pentets is observed for the Cp carbons in the proton coupled ^{13}C spectrum and this again implies that the two- and three-bond coupling constants ($^2\text{J}_{\text{CH}}$ and $^3\text{J}_{\text{CH}}$) are identical. The relative intensities of the signals around m/z 389 in the mass spectrum are virtually identical to the theoretical isotope cluster abundance and satisfactory elemental analysis has also been obtained. Structurally, complex **15** is expected to be monomeric and similar to $\text{CpNb}(\text{N-2,6-}^i\text{Pr}_2\text{C}_6\text{H}_3)\text{Cl}_2$.

3.2.3. Reaction of CpNb(N-2,6-Cl₂C₆H₃)Cl₂ with PMe₃ :Preparation of CpNb(N-2,6-Cl₂C₆H₃)(PMe₃)Cl₂ (16)

It has been shown that phosphine adducts are readily formed by the treatment of PMe₃ with CpNb(NR)Cl₂. Attempts to generate the PMe₃ adduct of CpNb(N-2,6-Cl₂C₆H₃)Cl₂ were undertaken to ascertain the electronic effect of the imido moiety by comparison with analogous complexes.

At room temperature, treatment of a toluene solution of compound 15 with PMe₃ immediately afforded a yellow precipitate. The supernatant solution was filtered from the yellow solid, which was collected and dried *in vacuo*.



Scheme 3.9.

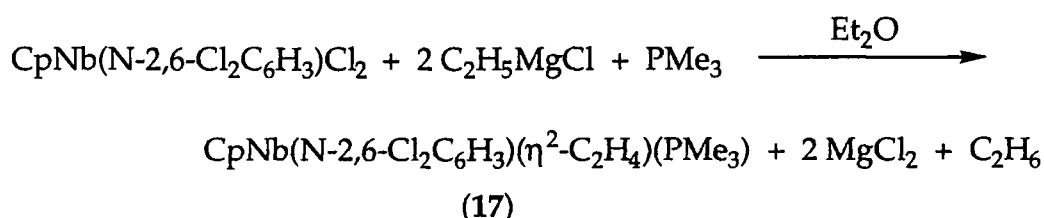
An envelope at *m/z* 389 in the mass spectrum of 16 has been accredited to the species [M-PMe₃]⁺. The stability of this complex *in vacuo* compared to CpNb(N-2,6-ⁱPr₂C₆H₃)Cl₂ is again noted. In the ¹H NMR spectrum, the shift of the PMe₃ protons at 1.57ppm implies that the base is strongly bound,² and this is thought to be a result of the lack of steric crowding around the metal due to the small chlorine substituents on the phenylimido moiety. However, the assumption that this shift also correlates to an increase in the acidity of the metal centre as predicted is debatable. If this was so, one would have expected a larger downfield shift for 16 compared to CpNb(N-2-^tBuC₆H₄)(PMe₃)Cl₂ (9) (1.54ppm). The shift of the

PMe₃ doublet at 1.58ppm for the related complex CpNb(NMe)Cl₂(PMe₃)⁵ which bears a small and electron-donating methylimido group, demonstrates that the chemical shift is influenced by both electronic and steric factors.

3.2.4. Reaction of CpNb(N-2,6-Cl₂C₆H₃)Cl₂ with C₂H₅MgCl in the presence of Trimethylphosphine :

Preparation of CpNb(N-2,6-Cl₂C₆H₃)(η²-C₂H₄)(PMe₃) (17)

The reaction of a diethyl ether solution of CpNb(N-2,6-Cl₂C₆H₃)Cl₂ with 2 equivalents of ethylmagnesium chloride in the presence of excess PMe₃ for 24 hours afforded a red solid after the removal of volatile components. Extraction from the magnesium chloride residue with pentane afforded a red solution, which was concentrated and cooled to -30°C to give small red crystals of compound 17 (Scheme 3.10). Hot heptane (60°C) may also be used to extract and recrystallise 17 .



Scheme 3.10.

The ¹H NMR spectrum for 17 shows a doublet at 0.98ppm for the coordinated PMe₃ and a singlet at 5.38ppm for the Cp ring. Resonances for the *p*- and *m*-C₆H₃ protons appear as a triplet at 6.17ppm and a doublet at 6.91ppm respectively. In addition, a broad peak at 1.78ppm is observed, and this is assigned to the ethylene ligand. Variable temperature experiments down to -70°C served to further broaden the signal, while warming to 70°C only achieved a slight sharpening. Two very broad resonances are present

between 25-30ppm in the ^{13}C NMR spectrum, and these have been attributed to the olefinic carbons. The dynamic behaviour of the olefin, compared to the static ligand in the $[\text{N-2,6-}^i\text{Pr}_2\text{C}_6\text{H}_3]$ analogue, can be rationalised by considering the reduction in congestion in the metal coordination sphere as a consequence of the sterically undemanding nature of the ortho chloride groups. This would therefore allow for the relatively free rotation of the olefin.

3.2.4.1. Molecular Structure of $\text{CpNb}(\text{N-2,6-Cl}_2\text{C}_6\text{H}_3)(\eta^2\text{-C}_2\text{H}_4)(\text{PMe}_3)$ (17)

Red needle crystals suitable for X-ray analysis were grown upon slow cooling of a saturated heptane solution from 60°C to room temperature. The molecular structure is shown in Figure 3.5. Bond lengths and angles are collected in Table 3.4 and the crystal data are given in Appendix A8.

The molecular geometry of 17 is pseudo-tetrahedral; for example, the $\text{Cp}_{\text{centroid}}\text{-Nb-P}$ angle is 110.7°. The Nb-N bond length of 1.819(2)Å is at the long end of the range expected for a niobium-(terminal imido) bonding interaction.¹³ This is likely to be a result of the decrease in the electrophilic nature of the metal centre arising from the lowering of its formal oxidation state.

The angle at the nitrogen (174.0(2)°) is typical for a pseudo-linear imido moiety with a sp -hybridised nitrogen atom. The phenyl ring of the imido group is orientated such that one of the ortho-chlorines points at the Cp ring. This is presumably more energetically favoured than the perpendicular alignment, which would result in repulsion between the two chlorines of the imido moiety and the phosphine and ethylene ligands. The C(15)-C(16) distance of 1.431(4)Å supports the view that a metallacyclopropane

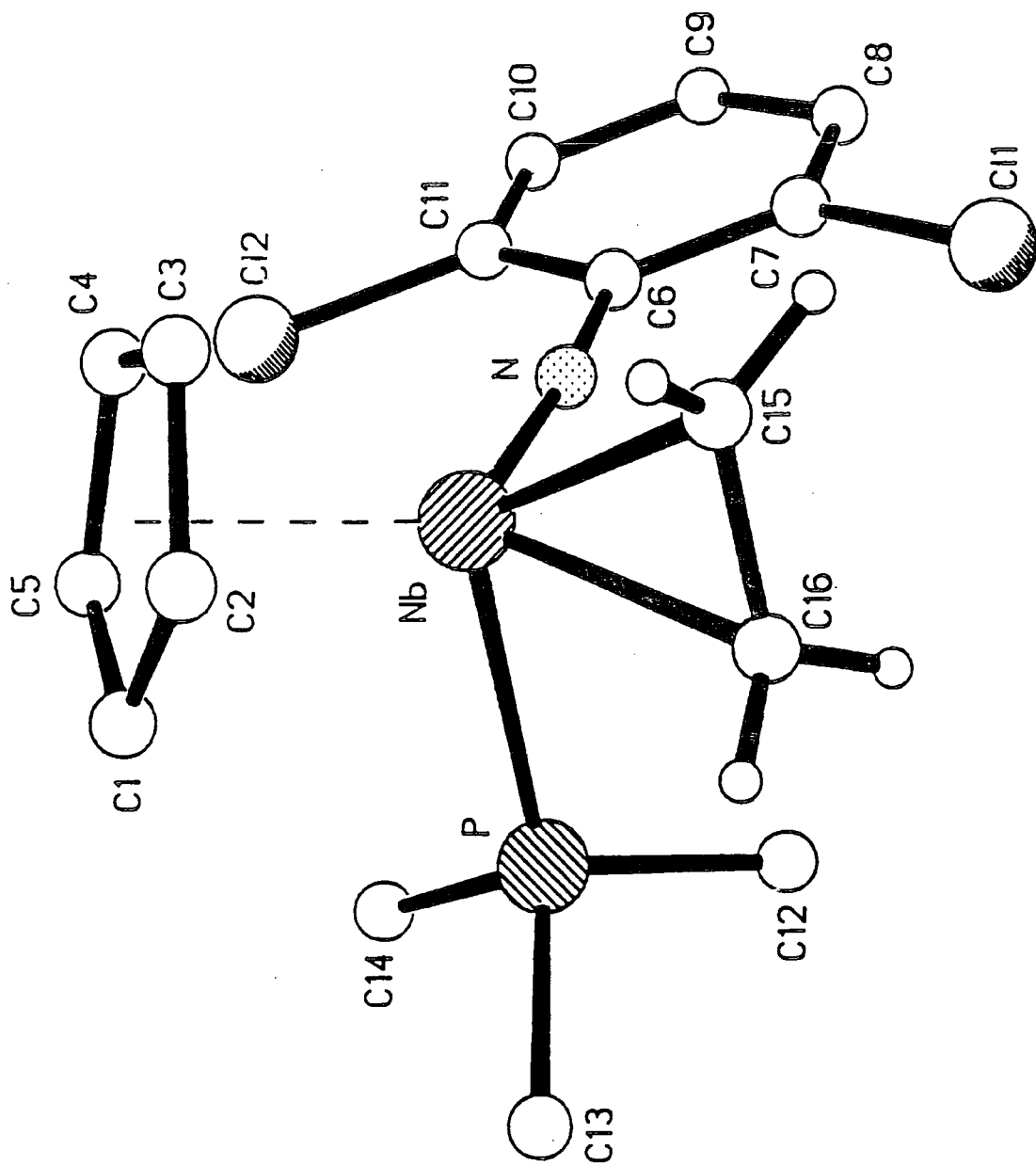


Figure 3.5. Molecular structure of CpNb(N-2,6-Cl₂C₆H₃)(η²-C₂H₄)(PMe₃) (17).

Nb-N	1.819(2)	C(15)-C(16)	1.431(4)
Nb-C(15)	2.240(3)	N-C(6)	1.360(3)
Nb-C(16)	2.278(3)	C(6)-C(11)	1.412(3)
Nb-C(4)	2.388(2)	C(6)-C(7)	1.414(3)
Nb-C(5)	2.418(3)	Cl(1)-C(7)	1.736(3)
Nb-C(3)	2.436(3)	C(7)-C(8)	1.390(4)
Nb-C(1)	2.519(3)	C(8)-C(9)	1.371(4)
Nb-C(2)	2.534(3)	C(9)-C(10)	1.382(4)
Nb-P	2.5316(7)	C(10)-C(11)	1.387(4)
C(1)-C(2)	1.401(5)	Cl(2)-C(11)	1.733(3)
C(1)-C(5)	1.404(5)	P-C(13)	1.818(3)
C(2)-C(3)	1.402(4)	P-C(12)	1.822(3)
C(3)-C(4)	1.398(4)	P-C(14)	1.824(3)
C(4)-C(5)	1.398(4)	Nb-C _{pcentroid}	2.154(4)
N-Nb-C(15)	101.2(1)	C(6)-N-Nb	174.0(2)
N-Nb-C(16)	107.3(1)	C(16)-C(15)-Nb	73.0(2)
C(15)-Nb-C(16)	36.9(1)	C(15)-C(16)-Nb	70.1(2)
N-Nb-P	91.30(6)	P-Nb-C _{pcentroid}	110.7(2)
C(15)-Nb-P	114.4(1)	N-Nb-C _{pcentroid}	129.3(2)
C(16)-Nb-P	87.8(1)		

Table 3.4. Selected bond lengths (Å) and angles (°) for CpNb(N-2,6-Cl₂C₆H₃)(η²-C₂H₄)(PMe₃) (17)

description is appropriate for the interaction (compared with C–C bond length in free ethylene and ethane: 1.33 and 1.54 Å respectively).

The Nb, P, C(15) and C(16) atoms virtually all lie in the plane (mean displacement 0.049 Å) which bisects the Cp_{centroid}–Nb–N angle (deviation from orthogonality 5.2°). This alignment is further evidence of the bent metallocene-like frontier orbitals for the [CpNb(N-2,6-Cl₂C₆H₃)] fragment, and is illustrated using the triad representation in Figure 3.6.⁷

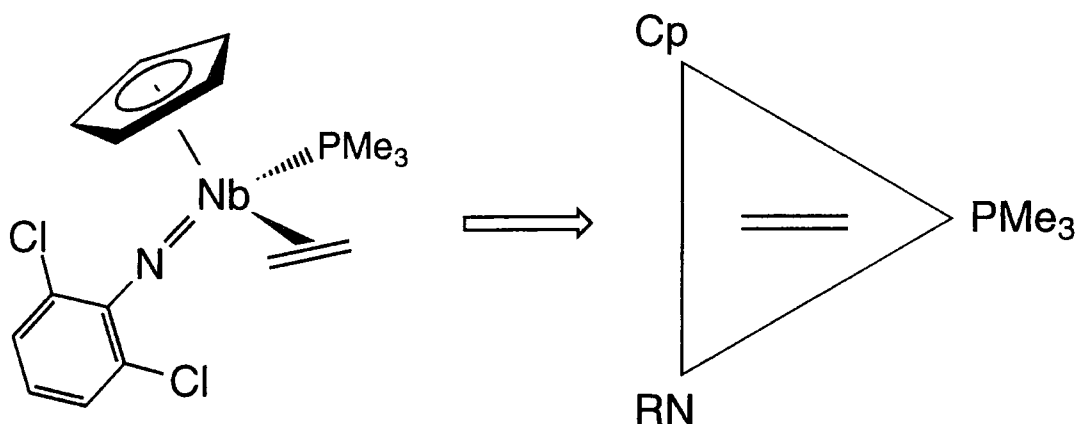


Figure 3.6.

The key bond lengths and angles are collected in Table 3.5, together with the corresponding parameters for the structurally related Cp₂Zr(C₂H₄)(PMe₃)¹⁴ and Mo(N^tBu)₂(C₃H₆)(PMe₃)⁹ complexes. The alkenes bind unsymmetrically to the metal centres in all three complexes, and this reflects the close proximity of the PMe₃ ligand to the endo carbon of the alkene. It is also noticeable that the phosphine and olefin metal-ligand distances decrease across the row from left to right. This trend is not wholly accounted for by the decrease in ionic radii from Zr to Mo, but may also be a consequence of the alleviation in steric congestion within the metal coordination sphere arising from replacement of the rigid, planar Cp rings with imido groups. Lastly, the shorter C–C bond lengths for the alkene

Parameters	Cp ₂ Zr(C ₂ H ₄) (PMe ₃) ¹³	CpNb(N-2,6-Cl ₂ C ₆ H ₃) (C ₂ H ₄)(PMe ₃)	Mo(N ^t Bu) ₂ (C ₃ H ₆) (PMe ₃) ⁹
Cendo-Cexo ^{a,b} (Å)	1.486(8)	1.431(4)	1.418(6)
M-Cendo ^a (Å)	2.373(8)	2.278(3)	2.228(4)
M-Cexo ^b (Å)	2.344(8)	2.240(3)	2.182(3)
M-P (Å)	2.693(2)	2.532(1)	2.445(1)
M-X ^c (Å)	2.22	2.152(4) [Cp], 1.819(2) [N]	1.774(3), 1.765(3)
X-M-X ^c (°)	129.3	129.3	123.0

^a Cendo refers to the metal-bound acetylenic carbon closest from the PMe₃ ligand. ^b Cexo refers to the metal-bound acetylenic carbon furthest from the PMe₃ ligand. ^c X = Cp ring centroid(s) and/or N, where appropriate.

Table 3.5. Comparison of Key Structural Parameters of Isobalably Related Alkene Complexes

ligand going from Zr to Mo imply reduced metal-to-ligand back donation, an observation consistent with the higher electronegativity of the later transition metals.

3.2.4.2. Reactivity of $\text{CpNb}(\text{N-2,6-Cl}_2\text{C}_6\text{H}_3)(\eta^2\text{-C}_2\text{H}_4)(\text{PMe}_3)$ with Alkynes

$\text{CpNb}(\text{N-2,6-Cl}_2\text{C}_6\text{H}_3)(\eta^2\text{-C}_2\text{H}_4)(\text{PMe}_3)$ (**17**) was treated with alkynes in an attempt to displace the olefin ligand and form acetylene-bound complexes.

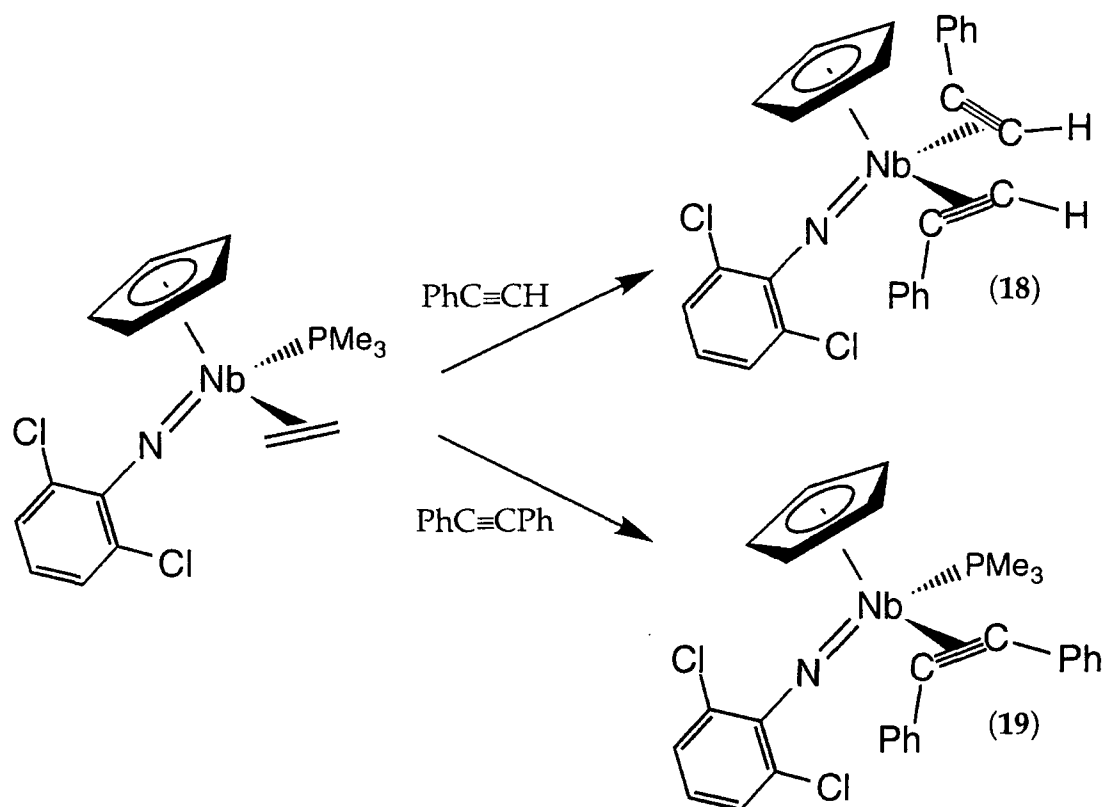
With PhC≡CH : Reaction of **17** with excess PhC≡CH at room temperature in C_6D_6 was monitored by ^1H and ^{31}P NMR spectroscopy. After one week, a mixture of products was observed. While one set of the new signals corresponded to the expected phosphine-stabilised alkyne complex, other peaks could be assigned to species where one or two phenylacetylene molecules have displaced the ethylene *and/or the phosphine ligands* [small complex multiplets observed at 2–4ppm in ^1H NMR spectrum]. Warming the sample to 60°C eventually yielded a single species: only one resonance in the Cp region (singlet at 5.66ppm) was present in the ^1H NMR spectrum, in which unbound ethylene and PMe_3 were observed; the ^{31}P NMR spectrum also displayed no evidence of phosphine ligation. This species is tentatively assigned as $\text{CpNb}(\text{N-2,6-Cl}_2\text{C}_6\text{H}_3)(\text{PhC}\equiv\text{CH})_2$ (**18**), since no multiplets corresponding to a bound ethylene ligand are observed. The 'dialkyne' species apparently generated is expected to be the (α , α' -Ph) isomer, since Negishi noted that, due to electronic factors, aryl groups strongly favour the α positions in the related bis-cyclopentadienyl zirconacyclopentadiene complexes.¹⁵

These observations prompted the preparative scale reaction of $\text{CpNb}(\text{N-2,6-Cl}_2\text{C}_6\text{H}_3)(\eta^2\text{-C}_2\text{H}_4)(\text{PMe}_3)$ with excess $\text{PhC}\equiv\text{CH}$ at elevated temperatures. However, attempts to isolate the red-brown product by filtration and drying *in vacuo* caused the solid to decompose to an unidentifiable intractable oil.

The presumed generation of the dialkyne species **18**, albeit *in situ*, is surprising considering the absence of further reaction of $\text{CpNb}(\text{N-2-}^t\text{BuC}_6\text{H}_4)(\text{RC}\equiv\text{CR})(\text{PMe}_3)$ with alkynes. Its formation is likely to be facilitated by the sterically undemanding chlorine substituents which help to reduce congestion in the coordination sphere of the metal centre. Nevertheless, the inability to isolate the complex suggests that the niobium–ligand combination present in the dialkyne complex is inherently unstable.

With PhC≡CPh : Prolonged warming of a C_6D_6 solution of $\text{CpNb}(\text{N-2,6-Cl}_2\text{C}_6\text{H}_3)(\eta^2\text{-C}_2\text{H}_4)(\text{PMe}_3)$ (**17**) and diphenylacetylene afforded resonances in the ^1H NMR spectrum consistent with the formation of $\text{CpNb}(\text{N-2,6-Cl}_2\text{C}_6\text{H}_3)(\text{PhC}\equiv\text{CPh})(\text{PMe}_3)$ (**19**), plus other as yet unidentified species. Isolation of the products was not pursued.

With C₂H₄ : Given the apparent displacement of the PMe_3 ligand in the reaction of **17** with $\text{PhC}\equiv\text{CH}$, the analogous reaction with excess ethylene was attempted in order to form a bis-ethylene/metallacyclopentane species. Unfortunately, no reaction was observed even after prolonged heating at 60°C .



Scheme 3.11. Postulated products from reactions of 17 with alkynes.

3.2.5. Attempted Formation of $\text{CpNb}(\text{N}-2,6\text{-Cl}_2\text{C}_6\text{H}_3)(\text{PMe}_3)_2$

In order to ascertain the electronic effect of the ortho chlorines on the $[\text{CpNb}(\text{N}-2,6\text{-Cl}_2\text{C}_6\text{H}_3)]$ fragment, our studies targeted the bisphosphine derivative. Its isolation would allow for comparisons with the stability and reactivity of $\text{CpNb}(\text{N}-2\text{-}^t\text{BuC}_6\text{H}_4)(\text{PMe}_3)_2$ (12).

However, treatment of a THF solution of $\text{CpNb}(\text{N}-2,6\text{-Cl}_2\text{C}_6\text{H}_3)\text{Cl}_2$ with activated magnesium in the presence of PMe_3 yielded a brown/black intractable solid which was totally insoluble in all common solvents. The apparent failure to form the desired product may be indicative of attack by the magnesium at the relatively nucleophilic chlorines of the imido moiety.



3.3. Studies on $\text{CpNb}(\text{N}-2\text{-}^t\text{BuC}_6\text{H}_4)\text{Cl}_2$ and $\text{CpNb}(\text{N}-2,6\text{-Cl}_2\text{C}_6\text{H}_3)\text{Cl}_2$ as Catalyst Precursors for Ethylene Polymerization

3.3.1. Introduction

Through our understanding of the isolobal relationship between Cp and imido units it was envisaged that a number of the half-sandwich niobium imido complexes described in this section may function as catalyst precursors for the polymerization of α -olefins. Therefore, a programme of work was undertaken to investigate potential catalyst systems analogous to the classical homogeneous systems such as $\text{Cp}_2\text{TiCl}_2/\text{Et}_2\text{AlCl}$.

This study describes the treatment of the complexes $\text{CpNb}(\text{N}-2\text{-}^t\text{BuC}_6\text{H}_4)\text{Cl}_2$ (8) and $\text{CpNb}(\text{N}-2,6\text{-Cl}_2\text{C}_6\text{H}_3)\text{Cl}_2$ (15) with the alkylating agents diethylaluminium chloride (DEAC) and methylaluminoxane (MAO) in the presence of ethylene, in attempts to form polyethylene. Part of this work has already been reported.¹⁶

3.3.2. Catalysis Results

The dual component systems were evaluated for catalytic activity over different time periods and molar ratios of co-catalyst, and the results are collected in Table 3.6. Addition of DEAC to $\text{CpNb}(\text{N}-2\text{-}^t\text{BuC}_6\text{H}_4)\text{Cl}_2$ in toluene gave an immediate colour change from orange to brown, and this is presumably due to the formation of alkylated metal species. During the runs, a brown-black precipitate would suddenly become visible, on average two minutes after the introduction of ethylene. The majority of the polymer formed seemed to occur in this initial period; indeed, the amount of polymer did not significantly increase for extended runs. The implication for this is that the active species has a short life-time and decomposes or deactivates very quickly. Increasing the ratio of DEAC resulted in marginally greater

activities as expected. However, it should be noted that the calculated activities are considerably lower than that found for the classical $\text{Cp}_2\text{TiCl}_2/\text{DEAC}$ control run.

The $\text{CpNb}(\text{N-2,6-Cl}_2\text{C}_6\text{H}_3)\text{Cl}_2/\text{DEAC}$ system was also studied, but unexpectedly, no polymer was produced. This may be attributed to likely interaction between the Lewis acidic aluminium alkyls and the electronegative chloro groups.

Catalyst Precursor (mmol)	Activator (mmol/ equivs)	Time (mins)	Yield (g)	Activity (g mmol ⁻¹ hr ⁻¹) ^a
Cp_2TiCl_2 (0.078)	DEAC (0.234/3)	60	1.44	18.5
$\text{CpNb}(\text{N-2-}^t\text{Bu-C}_6\text{H}_4)\text{Cl}_2$ (0.04)	DEAC (0.120/3)	60	0.02	0.5
$\text{CpNb}(\text{N-2-}^t\text{Bu-C}_6\text{H}_4)\text{Cl}_2$ (0.125)	DEAC (1.875/15)	50	0.06	0.6
$\text{CpNb}(\text{N-2-}^t\text{Bu-C}_6\text{H}_4)\text{Cl}_2$ (0.120)	DEAC (3.60/30)	15	0.06	2.0
$\text{CpNb}(\text{N-2-}^t\text{Bu-C}_6\text{H}_4)\text{Cl}_2$ (0.125)	DEAC ^b (1.875/15)	60	0.07	0.6
$\text{CpNb}(\text{N-2-}^t\text{Bu-C}_6\text{H}_4)\text{Cl}_2$ (0.04)	MAO ^c (12/300)	60	0.05	1.3

Table 3.6. (^a all runs in toluene under 1 bar of ethylene, ^b 1ml of CH_2Cl_2 added, ^c reaction at 60°C).

3.4. Summary

Significant differences to the $[\text{CpNb}(\text{N}-2,6\text{-}^i\text{Pr}_2\text{C}_6\text{H}_3)]$ derivatives have been observed in the chemistry of the $[\text{CpNb}(\text{N}-2\text{-}^t\text{BuC}_6\text{H}_4)]$ system, notably in the isolation and relative stability of the PMe_3 adduct **9**, the bis(phosphine) species **12** and the alkyne complexes **13** and **14**. These have been attributed to the nature of the unsymmetric 2-*t*-butylphenylimido ligand, which appears to have the ability, by rotating around the nitrogen-carbon bond, to position the bulky *t*-butyl group in a region of minimum steric hindrance and maximum stability for the molecule overall.

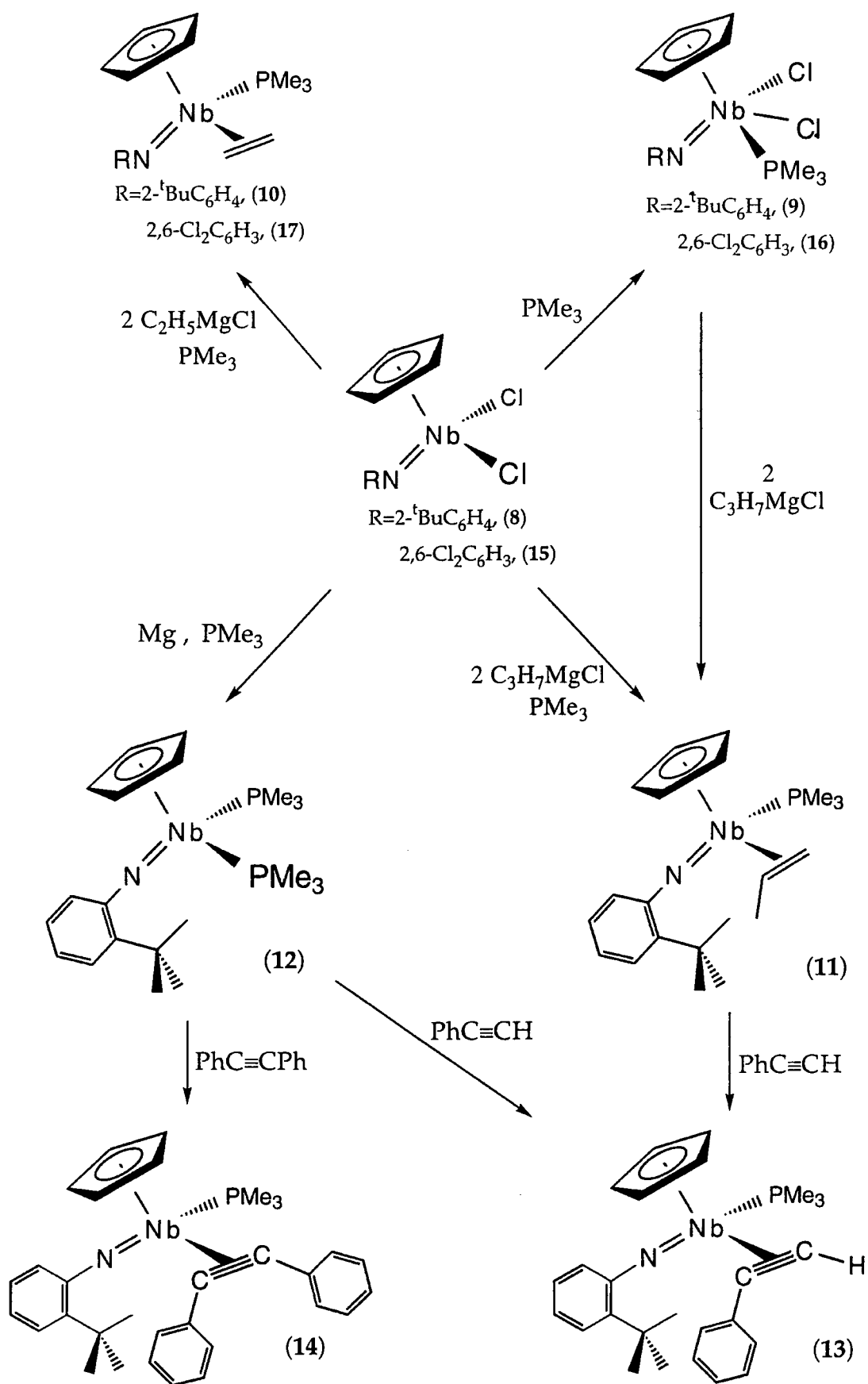
Contrasts between the $[\text{CpNb}(\text{N}-2,6\text{-Cl}_2\text{C}_6\text{H}_3)]$ complexes and their $[\text{N}-2,6\text{-}^i\text{Pr}_2\text{C}_6\text{H}_3]$ counterparts include the stability of **16** *in vacuo* and the fluxional behaviour of **17**. However, such dissimilarities do not warrant the claim that the 2,6-dichlorophenyl imido ligand has induced an increase in the electrophilicity of the niobium centre; since steric arguments alone can account for the differences. The synthesis and study of other imido moieties, such as $[\text{NC}_6\text{F}_5]$ and $[\text{N}-2,4,6\text{-(CF}_3)_3\text{C}_6\text{H}_2]$, may be pursued to achieve this.

$\text{CpNb}(\text{N}-2\text{-}^t\text{BuC}_6\text{H}_4)\text{Cl}_2$ (**8**), $\text{CpNb}(\text{N}-2\text{-}^t\text{BuC}_6\text{H}_4)(\text{PhC}\equiv\text{CPh})(\text{PMe}_3)$ (**14**) and $\text{CpNb}(\text{N}-2,6\text{-Cl}_2\text{C}_6\text{H}_3)(\eta^2\text{-C}_2\text{H}_4)(\text{PMe}_3)$ (**17**) have been characterised by X-ray crystallography. The structures of **8** and **14** confirm the uncrowded location of the *t*-butyl substituent. The orientation of the diphenylacetylene ligand in **14** and the ethylene molecule in **17**, plus the core geometry of the respective structures, serve to support the isolobal relationship between the $[\text{Cp}_2\text{Zr}]$ and $[\text{CpNb}(\text{NR})]$ fragments.

The $\text{CpNb}(\text{N}-2\text{-}^t\text{BuC}_6\text{H}_4)\text{Cl}_2/\text{DEAC}$ dual-component system has shown activity in the polymerisation of ethylene. However, the low activity

suggests that the [CpNb(NR)] system is inherently inferior to the metallocene analogues.

In conclusion, a number of half-sandwich imido complexes of niobium have been prepared and isolated containing a variety of ancillary ligands, and they are illustrated in Scheme 3.12.

Scheme 3.12. Reactivity of $\text{CpNb}(\text{NR})\text{Cl}_2$ ($\text{R} = 2\text{-}^t\text{BuC}_6\text{H}_4$, $2,6\text{-Cl}_2\text{C}_6\text{H}_3$)

3.5. References

1. (a) D.N. Williams, J.P. Mitchell, A.D. Poole, U. Siemeling, W. Clegg, D.C.R. Hockless, P.A. O'Neil, V. C. Gibson, *J. Chem. Soc., Dalton Trans.*, 1992, 739. (b) A.D. Poole, V.C. Gibson, W. Clegg, *J. Chem. Soc., Chem. Commun*, 1992, 237. (c) U. Siemeling, V.C. Gibson, *J. Organomet. Chem.*, 1992, **426**, C25. (d) J.K. Cockcroft, V.C. Gibson, J.A.K. Howard, A.D. Poole, U. Siemeling, C. Wilson, *J. Chem. Soc., Chem. Commun*, 1992, 1668.
2. A.D. Poole, Ph. D. Thesis, University of Durham, 1992.
3. J. Sundermeyer, D. Runge, *Angew. Chem., Int. Ed. Engl.*, 1994, **33**, 1255.
4. L.J. Guggenberger, P. Meakin, F.N. Tebbe, *J. Am. Chem. Soc.*, 1974, **96**, 5420.
5. D.N. Williams, Ph. D. Thesis, University of Durham, 1990.
6. (a) S.M. Rocklage, R.R. Schrock, *J. Am. Chem. Soc.*, 1980, **102**, 7808. (b) Y.-W. Chao, P.A. Wexler, D.E. Wigley, *Inorg. Chem.*, 1989, **28**, 3860.
7. V.C. Gibson, *J. Chem. Soc., Dalton Trans.*, 1994, 1607. V.C. Gibson, *Angew. Chem., Int. Ed. Engl.*, 1994, **33**, 1565.
8. (a) L.B. Kool, M.D. Rausch, H.G. Alt, M. Herberhold, U. Thewalt, B. Wolf, *Angew. Chem., Int. Ed. Engl.*, 1985, **24**, 394. (b) L.B. Kool, M.D. Rausch, H.G. Alt, M. Herberhold, B. Honold, U. Thewalt, *J. Organomet. Chem.*, 1987, **320**, 37. (c) G. Wilkinson, F.G.A. Stone, E.W. Abel, 'Comprehensive Organometallic Chemistry', Vol. 3, Pergamon, Oxford, 1982, and references therein.
9. (a) P.W. Dyer, V.C. Gibson, J.A.K. Howard, B. Whittle, C. Wilson, *J. Chem. Soc., Chem. Commun*, 1992, 1666. (b) P.W. Dyer, V.C. Gibson, J.A.K. Howard, B. Whittle, C. Wilson, *Polyhedron*, 1995, **14**, 103
10. J.L. Templeton, B.C. Ward, *J. Am. Chem. Soc.*, 1980, **102**, 3288.
11. T. Takahashi, D.R. Swanson, E. Negishi, *Chem. Let.*, 1987, 623.
12. G.E. Herberich, U. Englert, K. Linn, P. Roos, J. Runsink, *Chem. Ber.*, 1991, **124**, 975.
13. W.A. Nugent, J.M. Mayer, 'Metal-Ligand Multiple Bonds', Wiley Interscience, New York, 1988.

14. H.G. Alt, C.E. Denner, U. Thewalt, M.D. Rausch, *J. Organomet. Chem.*, 1988, **356**, C83.
15. E. Negishi, T. Takahashi, *Acc. Chem. Res.*, 1994, **27**, 124.
16. M.P. Coles, V.C. Gibson, *Polymer Bulletin*, 1994, **33**, 529.

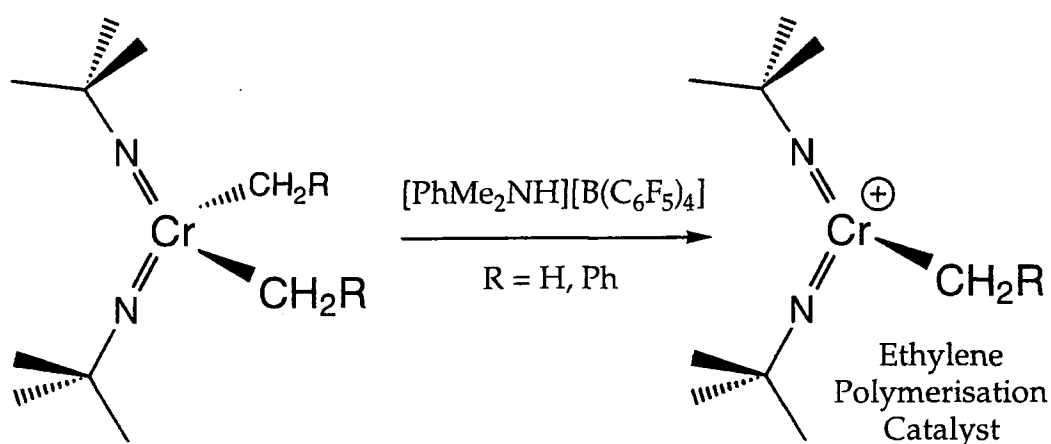
Chapter 4

Synthesis and Reactivity of Tantalum(V) Alkyl Complexes

4.1. Introduction

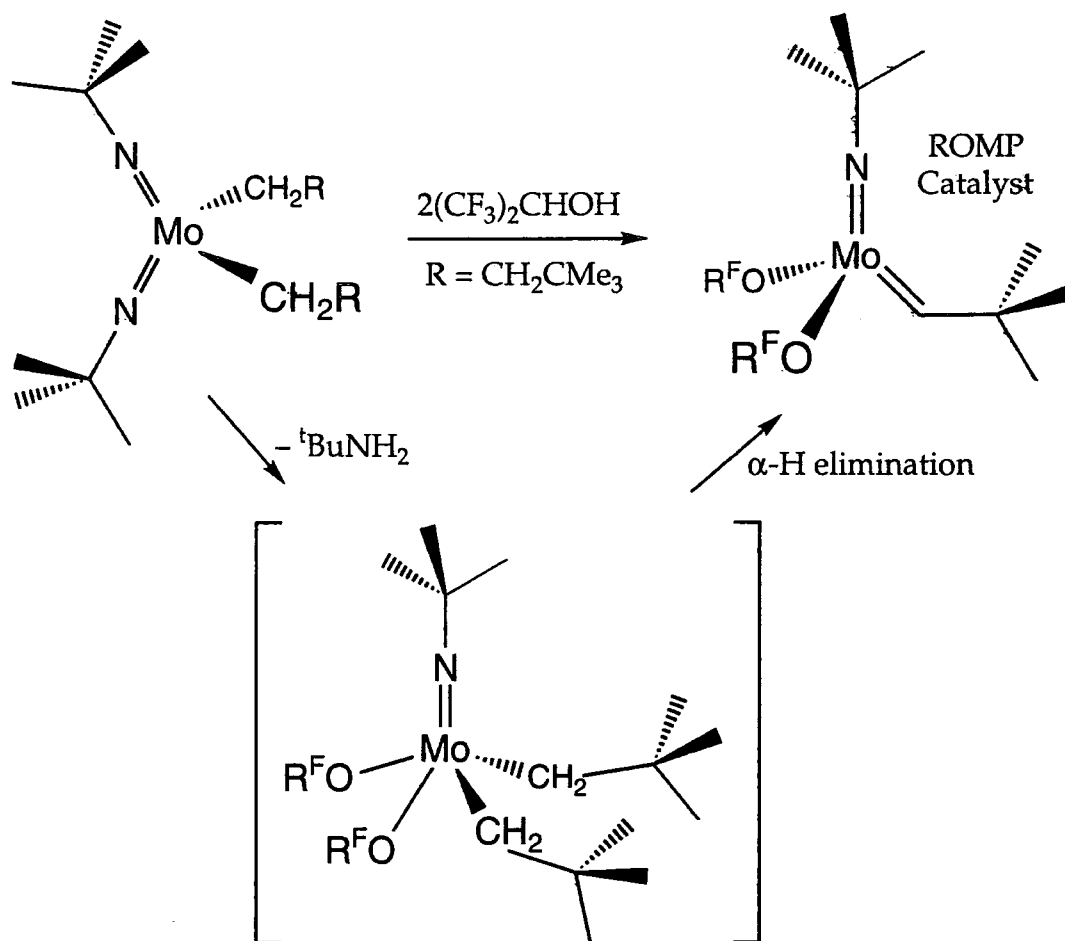
The isolobal relationship between the Group 4 bent metallocene, Group 5 half-sandwich imido and Group 6 bis-imido fragments has recently attracted considerable interest.¹⁻³

One significant result of this has been the development in this laboratory of bis-imido chromium dialkyl complexes as catalyst precursors for the polymerisation of ethylene (Scheme 4.1).^{1b}



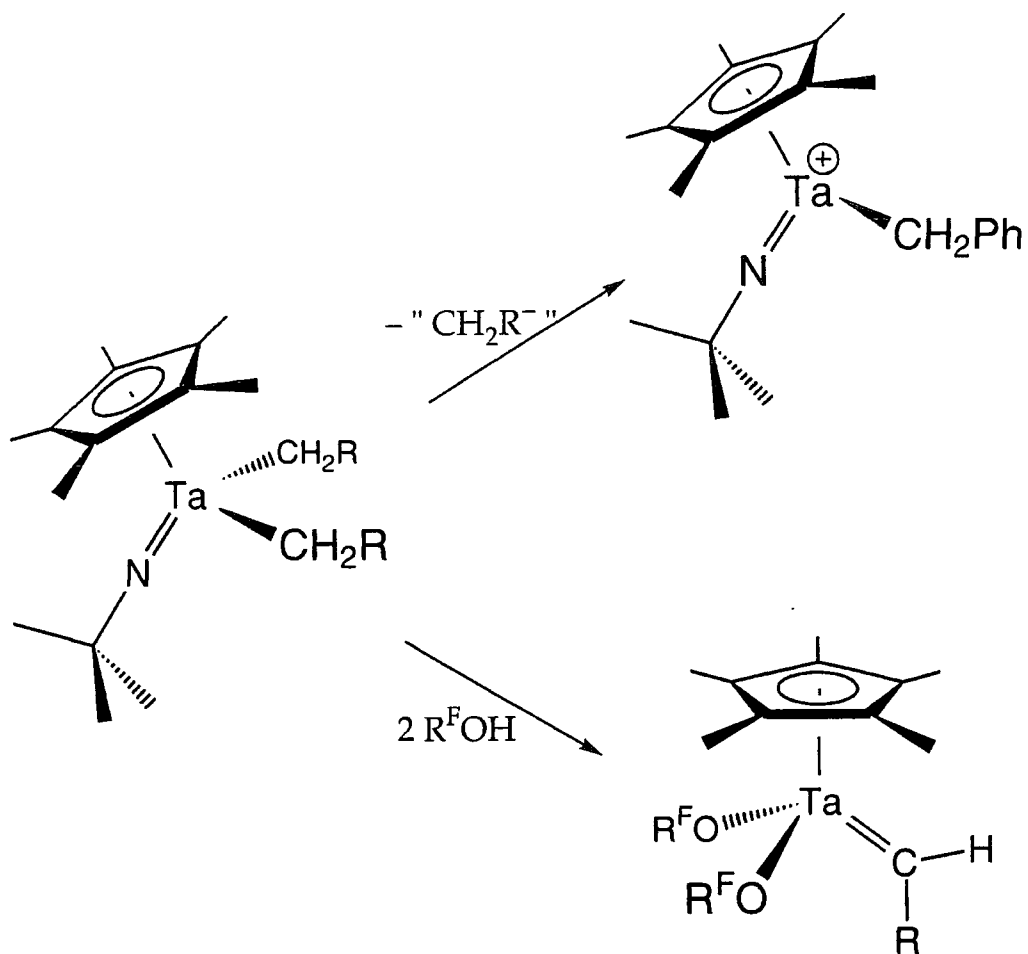
Scheme 4.1.

Using closely related bis(imido) molybdenum derivatives, Osborn generated alkylidene species which are active for the ring-opening metathesis polymerisation (ROMP) of strained olefins (Scheme 4.2).⁴



Scheme 4.2.

Therefore the aim of these studies was the synthesis of Group 5 half-sandwich imido dialkyl species which could act as precursors either for the polymerisation of α -olefins or for ring-opening metathesis polymerisation (Scheme 4.3). Pentamethylcyclopentadienyl tantalum *t*-butylimido derivatives were targeted because they are readily prepared and should be relatively stable.⁵ Hence, this chapter describes the synthesis and characterisation of a number of complexes with general formula $\text{Cp}^*\text{Ta}(\text{N}^t\text{Bu})(\text{CH}_2\text{R})_2$ as a prelude to studies into their stoichiometric and catalytic reactivity.

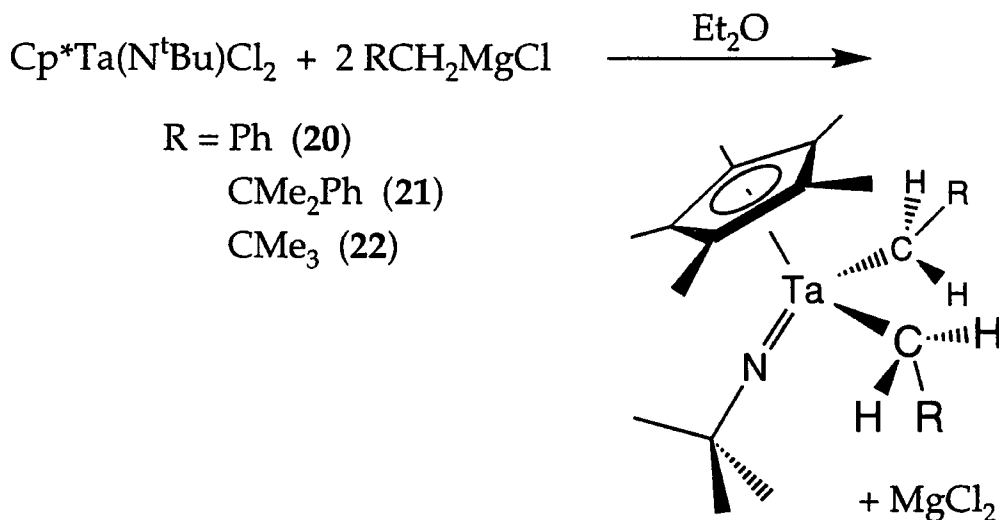


Scheme 4.3. Schematic representation of Objectives.

4.2. Synthesis of Cp*Ta(N^tBu)(CH₂R)₂ [R = Ph (20) , CMe₂Ph (21) , CMe₃ (22)] : Evidence for Multiple Agostic Interactions

While interactions of alkyl ligand C–H bonds with coordinatively unsaturated transition metal centres have become well established,⁶ multiple interactions of this type at a single metal centre remain relatively rare and are restricted to very low electron count complexes such as Cp*Ti(CH₂Ph)₃⁷ (formally 12e⁻) or complexes of the rare earth elements eg. Cp*₂M(CH(SiMe₃)₂) (M=Y,⁸ Nd⁹).

The dialkyl complexes in this investigation can be prepared by the reaction of $\text{Cp}^*\text{Ta}(\text{N}^t\text{Bu})\text{Cl}_2$ ^{3b} with two equivalents of the appropriate Grignard reagent in diethyl ether:

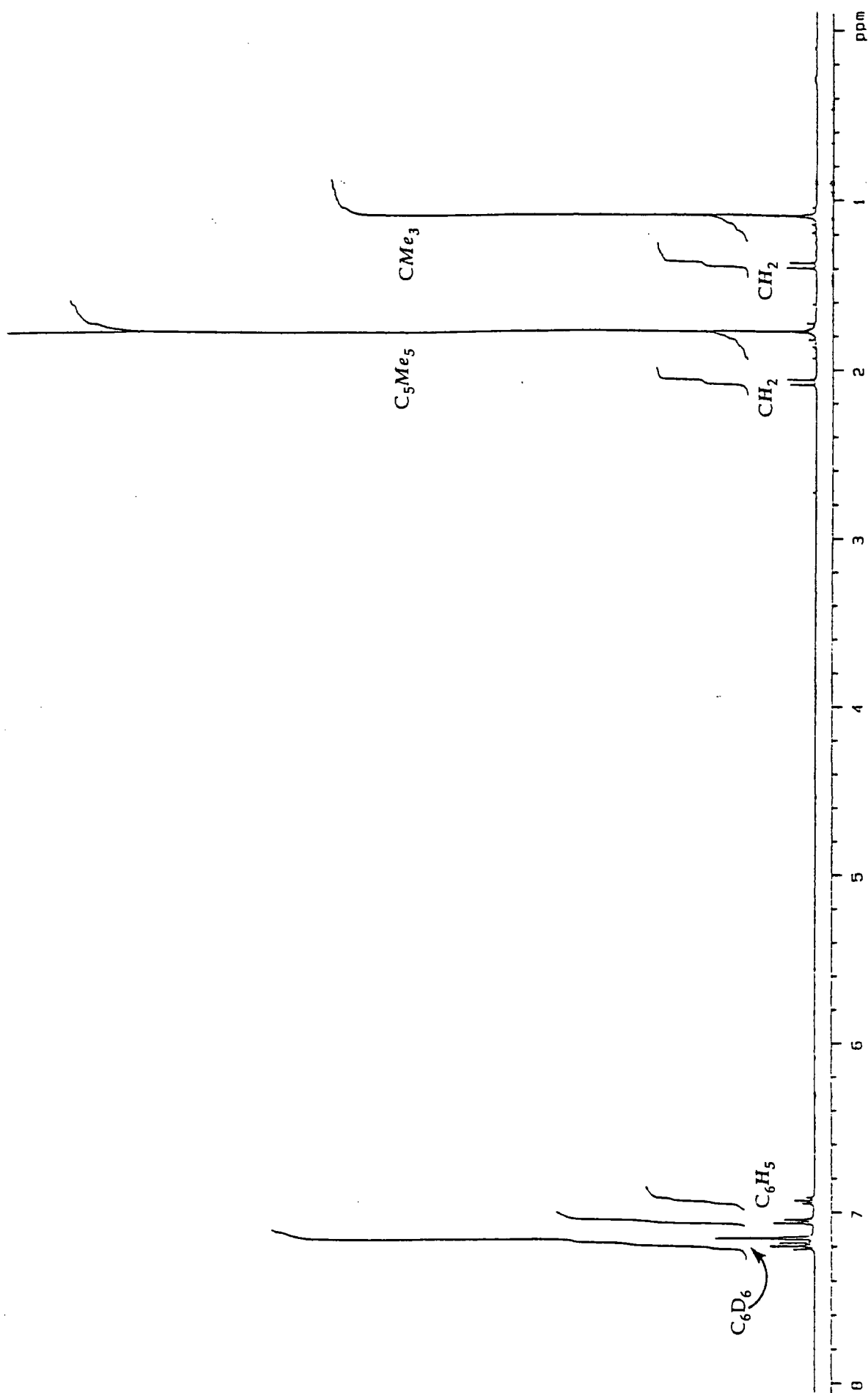


Scheme 4.4.

Analytically pure $\text{Cp}^*\text{Ta}(\text{N}^t\text{Bu})(\text{CH}_2\text{Ph})_2$ (20) was obtained in high yield by filtration and removal of volatile components *in vacuo*. A doublet of doublets is observed for the diastereotopic methylene protons in the ^1H NMR spectrum (Spectrum 4.1) and the $^1J_{\text{CH}}$ coupling constant for the metal-bound methylene group is 119Hz.

Pure samples of $\text{Cp}^*\text{Ta}(\text{N}^t\text{Bu})(\text{CH}_2\text{CMe}_2\text{Ph})_2$ (21) can only be obtained after recrystallisation of the crude product from acetonitrile. In the ^1H and ^{13}C NMR spectra, the neophyl methyl groups ($\text{CH}_2\text{CMe}_2\text{Ph}$) are inequivalent, while the $^1J_{\text{CH}}$ for the methylenes is 109Hz. This relatively low value may be attributed to an average of a terminal sp^3 C-H bond ($^1J_{\text{CH}} = 120\text{-}130\text{Hz}$)¹⁰ and a 3-centre M-C-H agostic interaction ($^1J_{\text{CH}} = 70\text{-}100\text{Hz}$),^{10, 11} and suggests that there is some interaction between the metal centre and the C-H bond.

$\text{Cp}^*\text{Ta}(\text{N}^t\text{Bu})(\text{CH}_2\text{CMe}_3)_2$ (22) was purified by extraction of the crude product into pentane followed by recrystallisation from acetonitrile. The methylene doublets appear at -0.61 and 1.39ppm; the latter signal is partially



Spectrum 4.1. 400MHz ^1H NMR Spectrum (C_6D_6) of $\text{Cp}^*\text{Ta}(\text{NtBu})(\text{CH}_2\text{Ph})_2$ (20).

obscured by the neopentyl methyl resonance. The even lower $^1J_{\text{CH}}$ value of 106 Hz for the methylenes strongly implies the presence of agostic interactions in **22**, and further evidence is provided by an X-ray structural determination in 4.2.1.

	^1H (ppm)	^{13}C (ppm)	$^1J_{\text{CH}}$ (Hz)
$\text{Cp}^*\text{Ta}(\text{N}^t\text{Bu})(\text{CH}_2\text{Ph})_2$ (20)	1.38, 2.07	71.3	119
$\text{Cp}^*\text{Ta}(\text{N}^t\text{Bu})(\text{CH}_2\text{CMe}_3\text{Ph})_2$ (21)	-0.42, 1.58	91.5	109
$\text{Cp}^*\text{Ta}(\text{N}^t\text{Bu})(\text{CH}_2\text{CMe}_3)_2$ (22)	-0.61, 1.39	90.4	106

Table 4.1.

Key NMR parameters for methylene groups in $\text{Cp}^*\text{Ta}(\text{N}^t\text{Bu})(\text{CH}_2\text{R})_2$

4.2.1. Molecular Structure of $\text{Cp}^*\text{Ta}(\text{N}^t\text{Bu})(\text{CH}_2\text{CMe}_3)_2$ (**22**)

A saturated acetonitrile solution of **22** was cooled at -20°C overnight to afford pale yellow needle-like crystals. The molecular structure is shown in Figure 4.1. Selected bond lengths and angles are collected in Table 4.2 and the crystal data are given in Appendix A9.

The molecule is pseudo-tetrahedral with a mean N-Ta-C $_{\alpha}$ angle of 104.4° and a C(11)-Ta-C(16) angle of 101.8° . The Ta-N bond length [$1.788(2)\text{\AA}$] is within the expected range for a tantalum imido complex¹² and the angle at the nitrogen is close to linearity [$170.7(2)^\circ$].

Two hydrogens, one on each of the two neopentyl methylene groups, lie in close contact [mean 2.48\AA] with the metal centre giving rise to highly distorted Ta-C(11)-H(11b) and Ta-C(16)-H(16b) angles of 88° and 99° respectively. These values, and the shorter Ta-H(11b) distance, indicate that

Ta(1)–N(1)	1.788(2)	Ta(1)–H(11a)	2.675(4)
Ta(1)–C(11)	2.199(3)	Ta(1)–H(11b)	2.390(4)
Ta(1)–C(16)	2.208(3)	Ta(1)–H(16a)	2.695(4)
Ta(1)–C(4)	2.425(3)	Ta(1)–H(16b)	2.575(4)
Ta(1)–C(5)	2.429(3)	C(1)–C(2)	1.410(4)
Ta(1)–C(3)	2.503(3)	C(1)–C(5)	1.426(5)
Ta(1)–C(1)	2.527(3)	C(1)–C(6)	1.501(5)
Ta(1)–C(2)	2.554(3)	C(2)–C(3)	1.416(4)
N(1)–C(21)	1.455(4)	C(2)–C(7)	1.501(4)
C(11)–C(12)	1.554(4)	C(3)–C(4)	1.422(4)
C(11)–H(11a)	0.98(4)	C(3)–C(8)	1.494(4)
C(11)–H(11b)	1.00(4)	C(4)–C(5)	1.427(4)
C(16)–C(17)	1.533(5)	C(4)–C(9)	1.488(5)
C(16)–H(16a)	0.91(4)	C(5)–C(10)	1.506(5)
C(16)–H(16b)	1.01(4)	Ta(1)–C _p centroid	2.175(3)
N(1)–Ta(1)–C(11)	103.6(1)	Ta(1)–C(11)–H(11a)	108(2)
N(1)–Ta(1)–C(16)	105.0(1)	Ta(1)–C(11)–H(11b)	88(2)
C(11)–Ta(1)–C(16)	101.8(1)	C(17)–C(16)–Ta(1)	126.7(2)
C(21)–N(1)–Ta(1)	170.7(2)	Ta(1)–C(16)–H(16a)	113(2)
C(12)–C(11)–Ta(1)	128.8(2)	Ta(1)–C(16)–H(16b)	99(2)

Table 4.2. Selected bond lengths (Å) and angles (°) for Cp*Ta(N^tBu)(CH₂CMe₃)₂ (**22**)

the Ta-H(11b) agostic interaction is the stronger one (H(11b) and H(16b) were found in the Fourier difference map and their positions were freely refined). These parameters compare well with the related complex $\text{CpNb}(\text{N}-2,6\text{-}i\text{Pr}_2\text{C}_6\text{H}_3)(\text{CH}_2\text{CMe}_3)_2$ [$\text{Nb}-\text{H}_\alpha$ mean 2.36\AA , $\text{Nb}-\text{C}_\alpha-\text{H}_\alpha$ 87° and 89°]¹³ and the isolobal $\text{Mo}(\text{N}-2,6\text{-}i\text{Pr}_2\text{C}_6\text{H}_3)(\text{N}^t\text{Bu})(\text{CH}_2\text{CMe}_3)_2$ [$\text{Mo}-\text{H}_\alpha$ mean 2.40\AA , $\text{Mo}-\text{C}_\alpha-\text{H}_\alpha$ 91° and 98°].¹⁴

The Cp^* ring is bonded in an η^5 fashion, although close examination of the Ta-C_{ring} distances reveals that a significant ring-slip distortion is apparent. Indeed, a view along the ring normal-metal vector (Figure 4.2) shows that the metal is displaced towards C(4) and C(5), which are staggered with respect to the Ta-N bond. This phenomenon is also present in $\text{CpNb}(\text{N}-2,6\text{-}i\text{Pr}_2\text{C}_6\text{H}_3)(\text{CH}_2\text{CMe}_3)_2$ but contrasts with the structures of other half-sandwich transition metal imido complexes in which the metal is displaced towards a ring carbon which eclipses the metal-imido bond (see 2.2.1).^{1a}

Although one of the two agostic interactions appears weak, their presence in **22**, together with the Cp^* ring slippage, pose a question as to the electron count of the complex. Agostics apart, **22** is formally a $16e^-$ complex. Addition of 4 more electrons from the two agostic C-H bonds (by interaction with the metal via donation of the C-H bonding pair of electrons) would result in a $20e^-$ species. However, the actual situation seems to lie in between these two extremes. For example, distortion of the cyclopentadienyl ring is often found when it is in direct competition with an imido group for available metal d_π symmetry orbitals.^{1a,15,16} While the distortion in **22** cannot be regarded as a total adjustment to an allyl-ene configuration, it may nevertheless be attributed to a ligand-based filled π orbital on the Cp^* ring.

The angle from the Ta-C(11)-C(16) plane to the Ta-C(11)-H(11b) and Ta-C(16)-H(16b) planes are 16.1° and 42.5° respectively. In other words, the agostic interactions, in particular the latter, lie *out* of the 'equatorial' binding plane. It has been shown for the isolobal bent metallocenes that metal-ligand

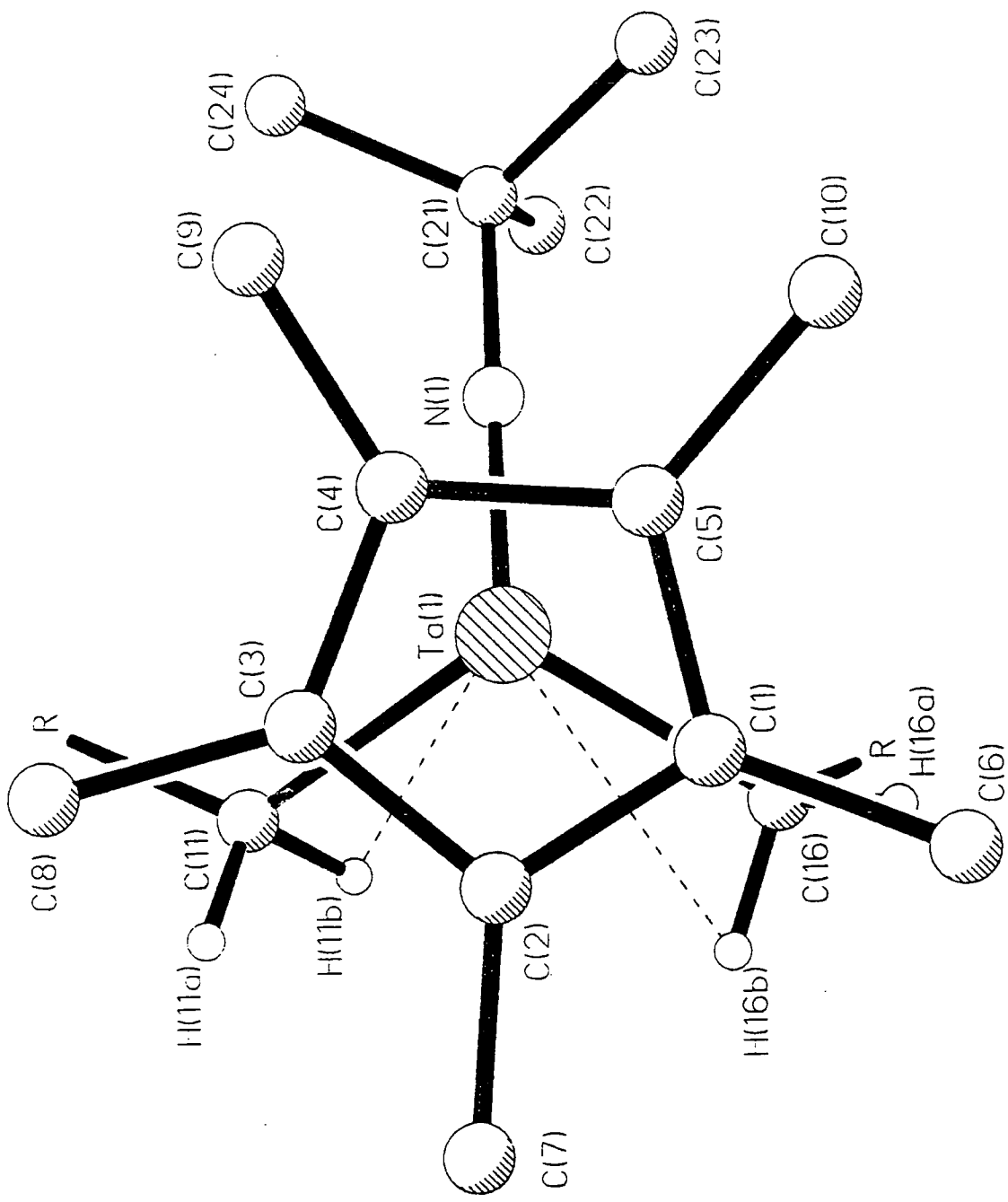


Figure 4.2. View of 22 along ring normal-metal vector (R=CMe₃).

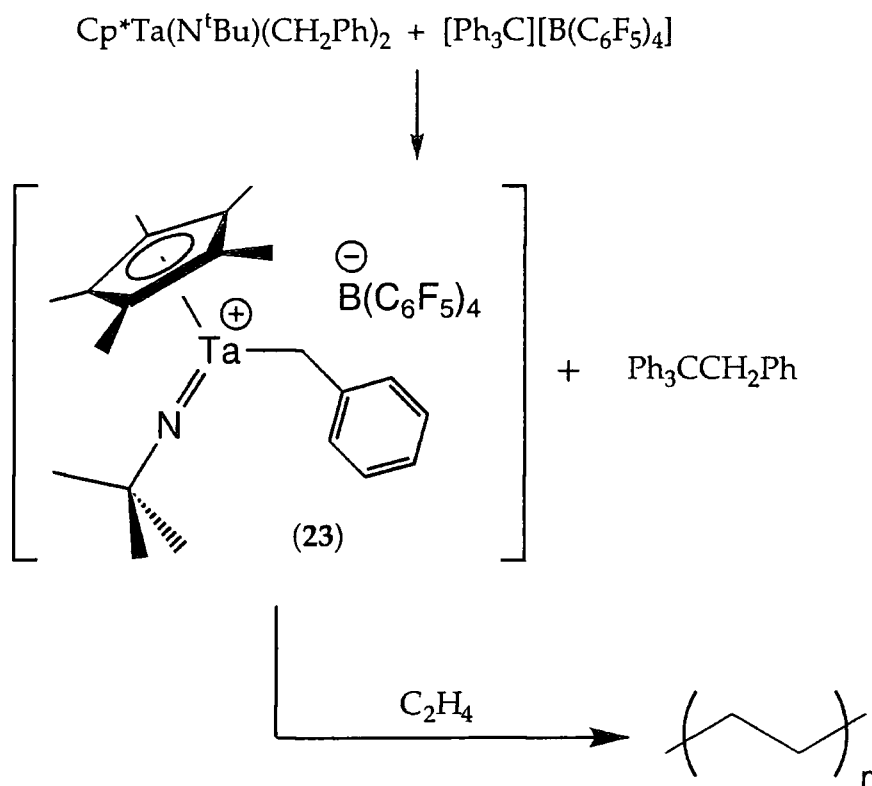
interactions outside this binding plane lead to destabilisation of metal-Cp ring bonding interactions.¹⁷ Therefore this is likely to have a detrimental effect on the metal-Cp* bonding in **22**, through competition with the agostic contacts. Finally, the t-butyl substituents of the neopentyl group actually point *towards* the imido moiety, thus implying that there is an electronic preference for this orientation as a result of the agostic interactions (Figure 4.2).

4.3. Reactivity of Cp*Ta(N^tBu)(CH₂Ph)₂ (**20**)

4.3.1. Alkyl Abstraction Reactions; Generation of [Cp*Ta(N^tBu)(CH₂Ph)]⁺ in the Presence of Ethylene

[Ph₃C][B(C₆F₅)₄] and [PhMe₂NH][B(C₆F₅)₄]¹⁸ have been used to abstract alkyl groups from bent metallocene dialkyl complexes to form the corresponding mono-alkyl cations, which are widely accepted as the active initiating species for α -olefin polymerisation.¹⁹

*Reaction of Cp*Ta(N^tBu)(CH₂Ph)₂ (**20**) with [Ph₃C][B(C₆F₅)₄]* : **20** was treated with one equivalent of [Ph₃C][B(C₆F₅)₄] in C₆D₆ under 3 atmospheres of ethylene. By ¹H NMR spectroscopy, the starting bisbenzyl **20** was quickly consumed. Resonances which can be assigned to the mono-benzyl cation [Cp*Ta(N^tBu)(CH₂Ph)]⁺ became visible; in particular singlets for the t-butyl (1.26ppm), Cp* (2.26ppm) and methylene groups (2.96ppm) and a doublet for the ortho-phenyl protons (6.78ppm). After 12 hours at room temperature, a white precipitate formed in the reaction solution and the ethylene intensity in the ¹H NMR spectrum had decreased by ~50% ; it was apparent that the ethylene had been polymerised (Scheme 4.5).

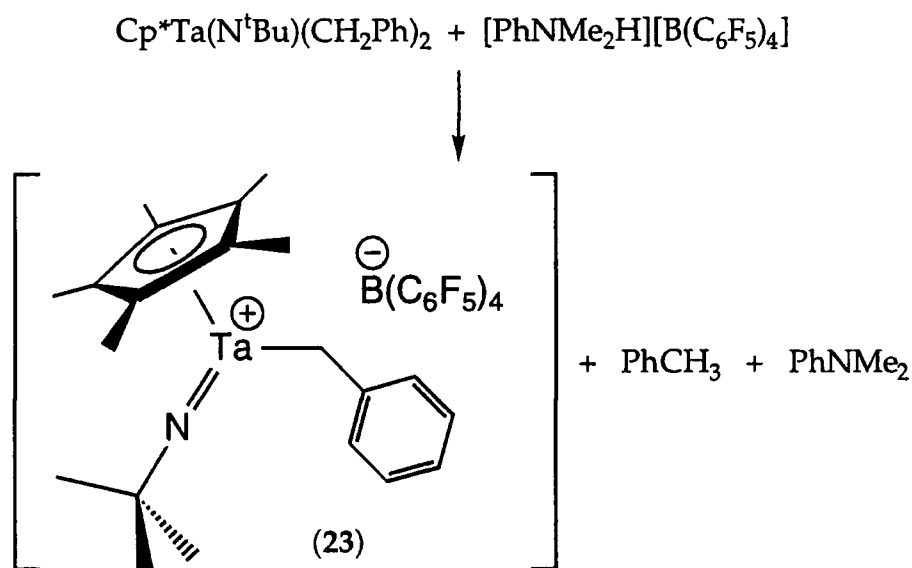


Scheme 4.5.

The slow formation of polyethylene was also accompanied by the appearance of several as yet unidentified peaks between 0–3ppm. The symmetry of some of the small multiplets in this region may be indicative of the formation of species which have undergone limited step-wise insertion of ethylene, as observed by Bercaw for permethylscandocene alkyl complexes,²⁰ but further work is obviously required to verify this. Bercaw attributes the slow rate of ethylene insertion in the $[\text{Cp}_2\text{ScR}]$ system to a ground-state stabilisation by a Sc- $\beta(\text{C-H})$ agostic interaction, and since such interactions have already been observed with the electrophilic tantalum centre in this study (*vide supra*), a similar explanation may account for the slow formation of polyethylene in this system.

Reaction of $\text{Cp}^*\text{Ta}(\text{N}^t\text{Bu})(\text{CH}_2\text{Ph})_2$ (**20**) with $[\text{PhMe}_2\text{NH}][\text{B}(\text{C}_6\text{F}_5)_4]$: The analogous reaction of **20** with $[\text{PhMe}_2\text{NH}][\text{B}(\text{C}_6\text{F}_5)_4]$ yielded identical resonances for the benzyl cation (Scheme 4.6).

This suggests that the interaction between the tantalum centre and the basic N,N-dimethylaniline which is generated is small, and this is in stark contrast to the $[\text{Cr}(\text{N}^t\text{Bu})_2]$ system.^{1b} However, the interaction seems sufficient to hinder approach by incoming ethylene; no polymer was observed in this case. Moreover, it is apparent that there is negligible interaction between the metal centre and ethylene, since in the absence of ethylene the ^1H NMR spectrum is essentially identical. In the ^{13}C NMR spectrum, the abundance of signals in the aromatic region precluded efforts to assign the bonding mode of the benzyl ligand as η^1 or η^2 .²¹ The oily nature of the products has prevented satisfactory analyses being obtained for $[\text{Cp}^*\text{Ta}(\text{N}^t\text{Bu})(\text{CH}_2\text{Ph})]^+[\text{B}(\text{C}_6\text{F}_5)_4]^-$ (**23**).



Scheme 4.6.

4.3.2. Reaction of $\text{Cp}^*\text{Ta}(\text{N}^t\text{Bu})(\text{CH}_2\text{Ph})_2$ with Alcohols

Osborn has demonstrated the formation of molybdenum alkylidene complexes by the protonation and subsequent elimination of an imido moiety from molybdenum bis-imido dialkyls with the highly acidic alcohol $(\text{CF}_3)_2\text{CHOH}$.⁴ Similar alkylidenes have also been generated in an analogous manner using pentafluorophenol.¹⁴ In this study, a number of acidic alcohols have been investigated for their reactivity towards **20**.

4.3.2.1. Reaction of $\text{Cp}^*\text{Ta}(\text{N}^t\text{Bu})(\text{CH}_2\text{Ph})_2$ with Pentafluorophenol:

Preparation of $[\text{Cp}^*\text{Ta}(\text{CH}_2\text{Ph})(\text{OC}_6\text{F}_5)(\mu\text{-O})]_2$ (**24**)

Two molar equivalents of $\text{C}_6\text{F}_5\text{OH}$ were added to a toluene solution of **20** at -78°C and this was stirred overnight to afford a bright red solution. After filtration and cooling to -30°C , bright yellow hexagonal crystals were obtained. However, the crystals turned opaque immediately after the solution was decanted. ^1H NMR data on the crystals confirmed the presence of the Cp^* ring and doublets at 2.80 and 2.97 ppm corresponded to the diastereotopic methylenes of a single benzyl ligand. The ^{19}F NMR spectrum suggested ligation of the $[\text{OC}_6\text{F}_5]$ moiety, and elemental analysis confirmed that the reaction had resulted in the elimination of the *t*-butyl imido substituent.

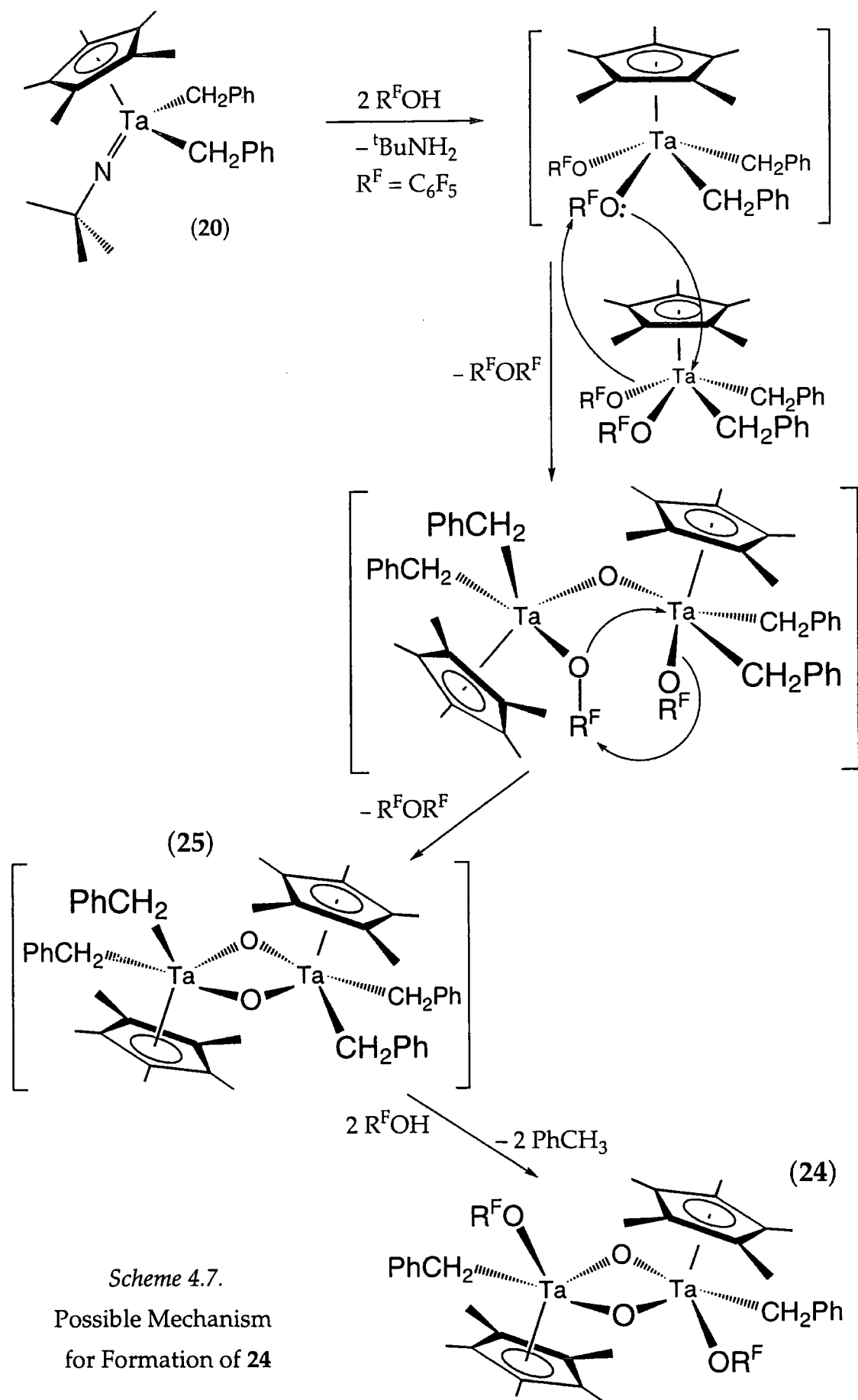
A crystallographic determination was deemed necessary to elucidate the structure. When more hexagonal crystals were grown, the solution was decanted only *after* they were covered with highly viscous perfluoroether oil used in the oil drop method for crystal mounting purposes. On this occasion, the crystals remained intact and the structural analysis revealed the complex to be the dimeric tantalum(V) molecule $[\text{Cp}^*\text{Ta}(\text{CH}_2\text{Ph})(\text{OC}_6\text{F}_5)(\mu\text{-O})]_2$ (**24**).

The presence of an oxo bridge was unexpected, and presumably results from loss of bis(pentafluorophenyl) ether. A possible mechanism for its formation is shown in Scheme 4.7, involving the protonation and subsequent elimination of the imido moiety as *t*-butylamine to form $[\text{Cp}^*\text{Ta}(\text{CH}_2\text{Ph})_2(\text{OC}_6\text{F}_5)_2]^\S$ followed by a bimolecular condensation process. [The complex nature of the ^{19}F NMR spectrum of the reaction residue precluded the identification of the perfluorinated ether.] Finally, reaction of the dimer **25** with one equivalent of pentafluorophenol per tantalum yields the isolated product. The low yield obtained (22%) is consistent with the insufficient molar quantity of $\text{C}_6\text{F}_5\text{OH}$ needed to generate the product effectively. The speculative nature of the mechanism must be stressed at this point.

It would appear that the inability of the Cp^* ring to provide steric protection for the metal centre and the highly electrophilic nature of the Ta(V) centre, arising from phenoxide ligation, combine to hinder the formation and stabilisation of an alkylidene species.

Although the reaction of **20** with $\text{C}_6\text{F}_5\text{OH}$ proceeded, there was no reaction with $2,6\text{-}^t\text{Bu}_2\text{C}_6\text{H}_3\text{OH}$ or $(\text{CF}_3)_2\text{CMeOH}$ even at 60°C . These alcohols may be insufficiently acidic or too bulky to allow protonation of the imido group. Compared to the $[\text{Mo}(\text{NR})_2]$ system, the rigid and sterically demanding nature of the Cp^* ring may also be a contributing factor.

§ ^1H NMR monitoring of the reaction in C_6D_6 shows the appearance of *tert*-butylamine before resonances for toluene are observed, hence this suggests that the imido group is protonated before the benzyl ligand.



Scheme 4.7.
Possible Mechanism
for Formation of 24

4.3.2.2. Molecular Structure of $[\text{Cp}^*\text{Ta}(\text{CH}_2\text{Ph})(\text{OC}_6\text{F}_5)(\mu\text{-O})]_2$ (24)

Yellow crystals of 24 were grown from a toluene solution at -30°C . The molecular structure is shown in Figure 4.3. Selected bond lengths and angles are collected in Table 4.3 and the crystal data are given in Appendix A10.

The dimeric structure has an inversion centre which lies equidistant between O(1), O(2) and Ta, Ta(a). The tantalum atom is in a highly distorted square pyramidal environment because of the steric influence of the Cp^* ring.

The remarkably long phenoxide Ta–O(1) bond length of $2.005(8)\text{\AA}$ is greater than the largest previously reported Ta(V)– OC_{sp^2} distance.²² The oxo Ta–O(2) distance is also very long [$1.957(7)\text{\AA}$]. These elongated bonding interactions can be rationalised by considering the fierce competition for the vacant d_π symmetry orbitals of the electrophilic Ta(V) centre. There are three oxygen atoms per metal, each attempting to participate in p_π – d_π interactions with the metal via π donation from their lone pairs, as well as the Cp^* ligand which is an extremely strong π -donor. The Ta– Cp^* interaction is not distorted and appears to dominate, hence it is apparent that any metal–oxygen p_π – d_π interactions will be relatively weak, and this will intrinsically lengthen the tantalum–oxygen bonds. In addition, the lone pair in the oxygen p_π orbital is expected to be delocalised into the highly electron-withdrawing pentafluorophenyl ring, thus removing electron density away from the phenoxide oxygen and further reducing its capacity for π -donation to the metal. This latter factor presumably results in the marginally longer phenoxide Ta–O(1) bond length compared to the oxo Ta–O(2) distance.

Close scrutiny of the structure of 24 shows severe steric congestion around each tantalum atom, and this seems to be alleviated by the twist angle of 102.9° between the pentafluorophenyl ring [C(1)–C(6)] and the benzyl ring [C(8)–C(13)] (Figure 4.3.b).

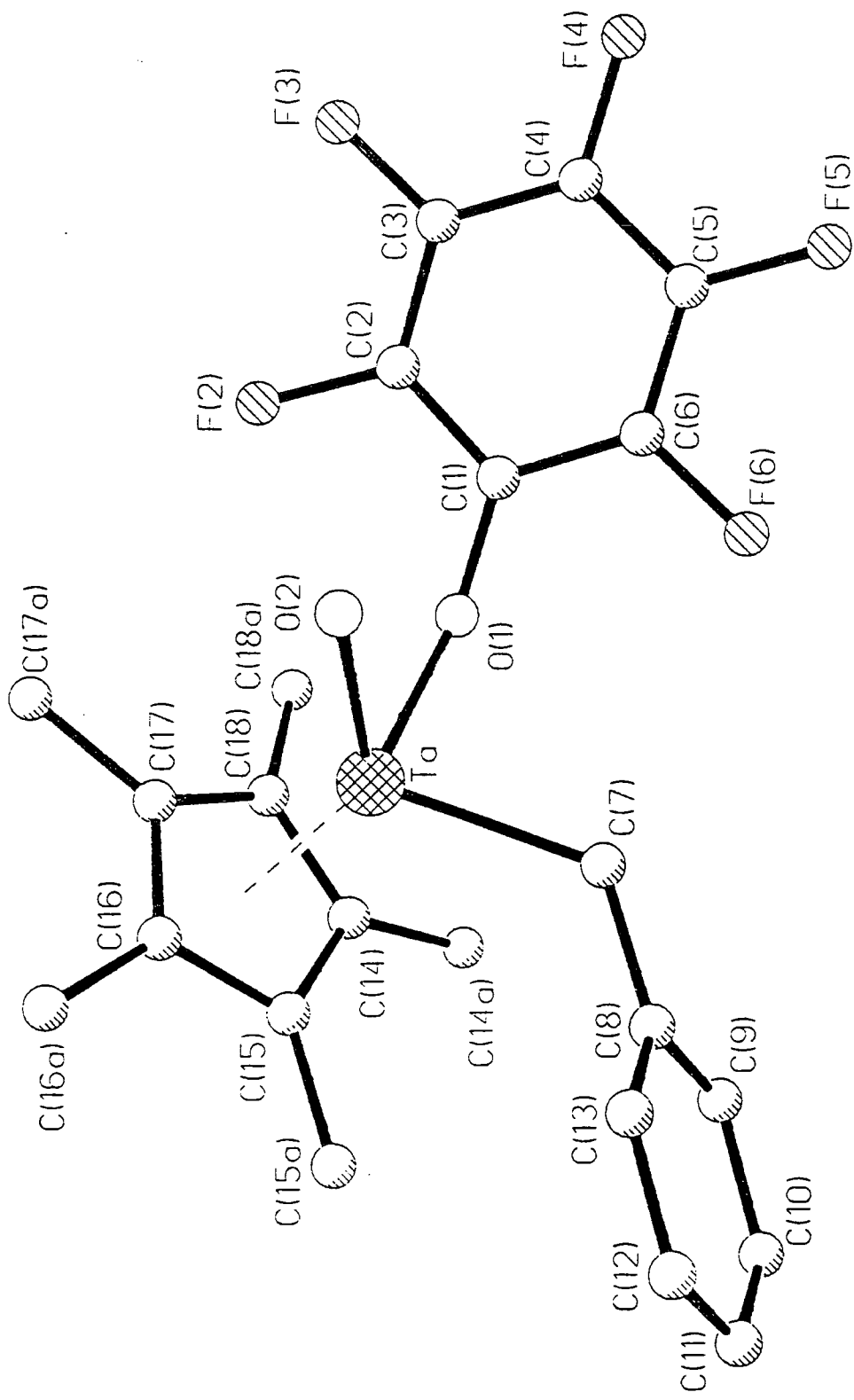
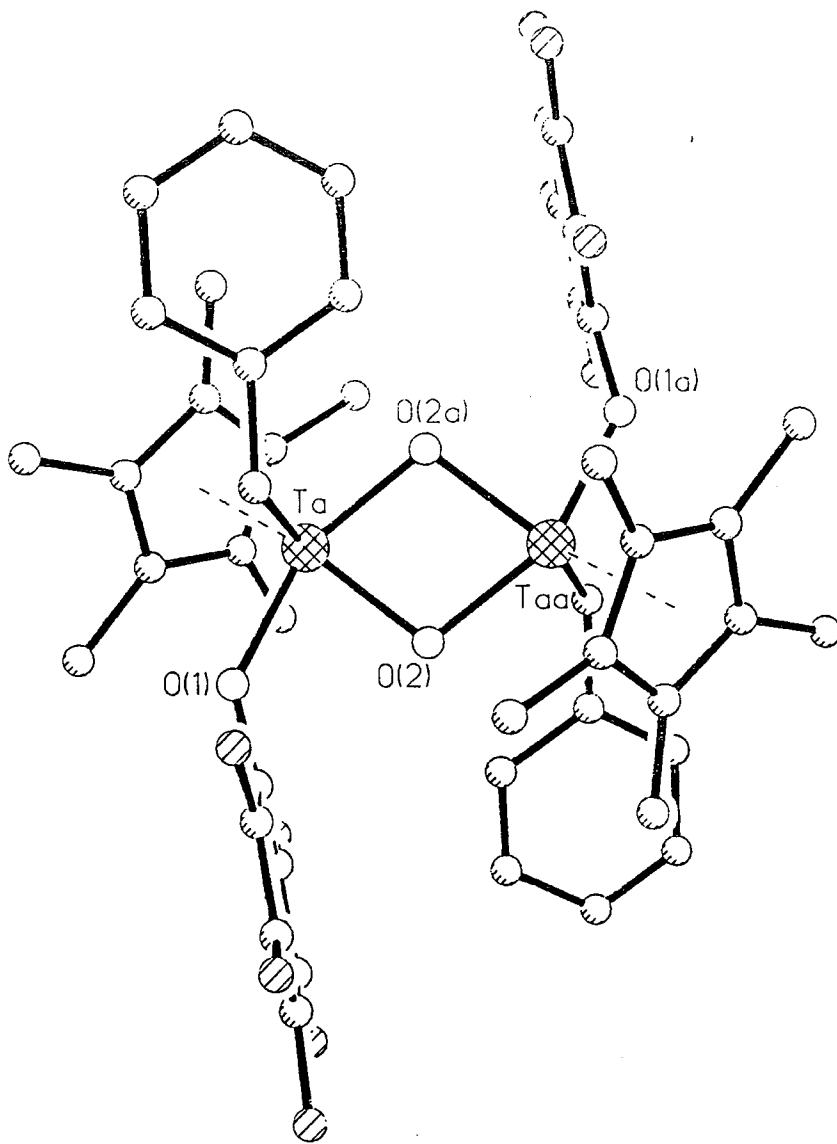


Figure 4.3. Molecular structure of $[\text{Cp}^*\text{Ta}(\text{CH}_2\text{Ph})(\text{OC}_6\text{F}_5)(\mu\text{-O})]_2$ (24). (a) Asymmetric unit.

Ta-O(2a)	1.950(8)	F(4)-C(4)	1.37(1)
Ta-O(2)	1.957(7)	F(5)-C(5)	1.33(2)
Ta-O(1)	2.005(8)	F(6)-C(6)	1.32(2)
Ta-C(7)	2.20(1)	O(1)-C(1)	1.33(1)
Ta-C(17)	2.39(1)	C(7)-C(8)	1.50(2)
Ta-C(16)	2.45(1)	C(14)-C(18)	1.40(2)
Ta-C(18)	2.48(2)	C(14)-C(15)	1.44(2)
Ta-C(15)	2.53(1)	C(15)-C(16)	1.45(2)
Ta-C(14)	2.56(1)	C(16)-C(17)	1.40(2)
F(2)-C(2)	1.35(2)	C(17)-C(18)	1.40(2)
F(3)-C(3)	1.34(2)	Ta-C _p centroid	2.17(2)
O(2a)-Ta-O(2)	76.7(3)	O(1)-Ta-C(7)	83.2(4)
O(2a)-Ta-O(1)	150.8(4)	C(1)-O(1)-Ta	139.8(8)
O(2)-Ta-O(1)	80.7(3)	Taa-O(2)-Ta	103.3(3)
O(2a)-Ta-C(7)	89.1(4)	C(8)-C(7)-Ta	125.2(8)
O(2)-Ta-C(7)	113.4(4)		

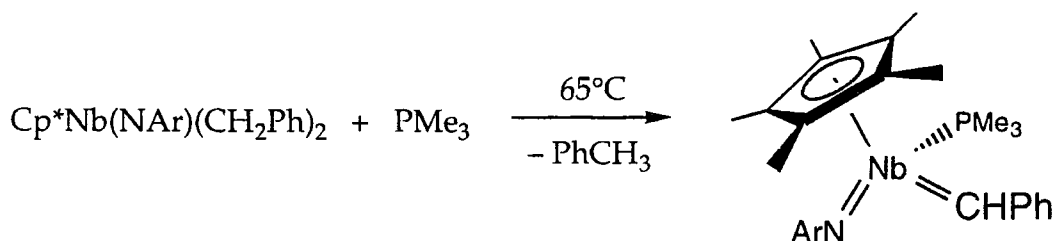
Table 4.3. Selected bond lengths (Å) and angles (°) for [Cp*Ta(CH₂Ph)(OC₆F₅)(μ-O)]₂ (**24**)



(b) Illustration of twist angle between aryl rings.

4.3.3. Attempted Reaction of $\text{Cp}^*\text{Ta}(\text{N}^t\text{Bu})(\text{CH}_2\text{Ph})_2$ with Trimethylphosphine

The benzylidene complex $\text{Cp}^*\text{Nb}(\text{N}-2,6\text{-}i\text{Pr}_2\text{C}_6\text{H}_3)(\eta^1\text{-CHPh})(\text{PMe}_3)$ was prepared in this group by the reaction of $\text{Cp}^*\text{Nb}(\text{N}-2,6\text{-}i\text{Pr}_2\text{C}_6\text{H}_3)(\text{CH}_2\text{Ph})_2$ with PMe_3 at elevated temperatures:²³



Scheme 4.8. Ar = 2,6-*i*Pr₂C₆H₃.

Therefore it was hoped that a stable tantalum benzylidene complex could be similarly prepared by a phosphine-assisted α -abstraction and elimination of a molecule of toluene. However, a solution of **20** and five equivalents of PMe_3 in C_6D_6 showed no sign of reaction after several weeks at 60°C . This is presumably because the bulky Cp^* and *t*-butyl substituents prevent the phosphine from approaching the metal centre; a prerequisite for the reaction to proceed.⁵

4.4. Reactivity of $\text{Cp}^*\text{Ta}(\text{N}^t\text{Bu})(\text{CH}_2\text{CMe}_2\text{Ph})_2$ (**21**)

The reaction of a C_6D_6 solution of **21** with $\text{Ph}_3\text{C B}(\text{C}_6\text{F}_5)_4$, in an attempt to form and observe the corresponding neophyl cation, was not clean (*cf.* 4.3.1) and resulted in a highly complicated ^1H NMR spectrum.

4.4.1. Reaction of $\text{Cp}^*\text{Ta}(\text{N}^t\text{Bu})(\text{CH}_2\text{CMe}_2\text{Ph})_2$ with Pentafluorophenol:

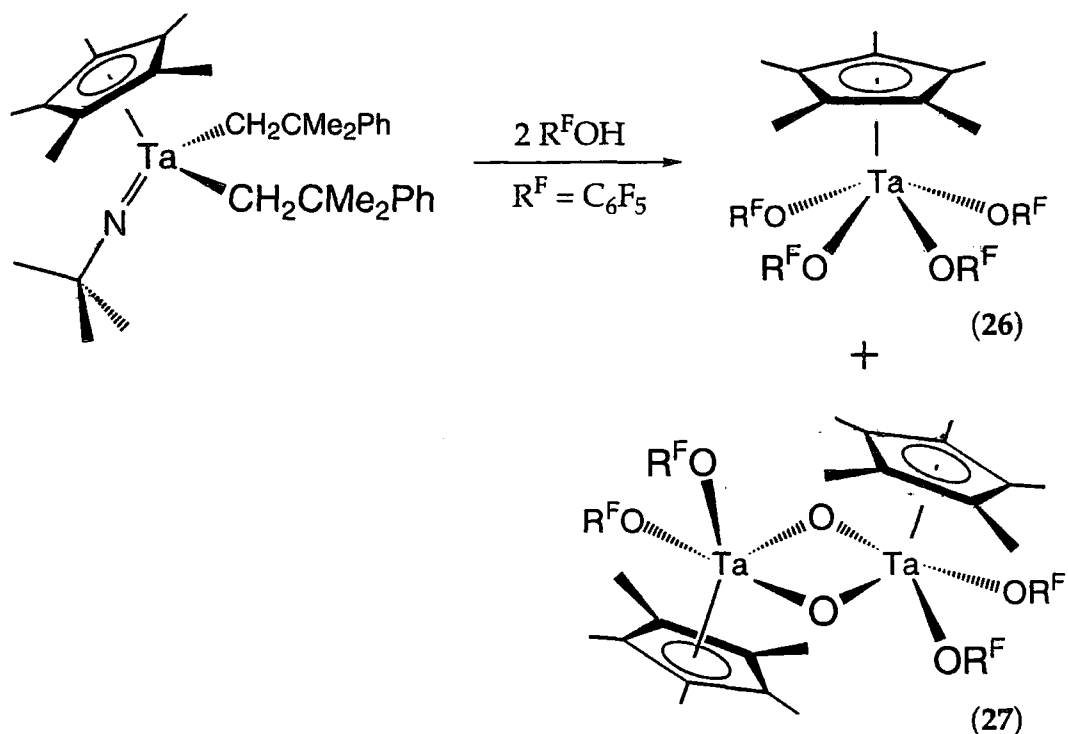
Preparation of $\text{Cp}^*\text{Ta}(\text{OC}_6\text{F}_5)_4$ (**26**) and $[\text{Cp}^*\text{Ta}(\text{OC}_6\text{F}_5)_2(\mu\text{-O})]_2$ (**27**).

Treatment of $\text{Cp}^*\text{Ta}(\text{N}^t\text{Bu})(\text{CH}_2\text{CMe}_2\text{Ph})_2$ (**21**) with two equivalents of $\text{C}_6\text{F}_5\text{OH}$ at 60°C for 10 days yielded a yellow solution from which a small

crop of yellow needle crystals was isolated. Analysis of the crystals by ^1H and ^{13}C NMR spectroscopy suggested that not only the *t*-butylimido but also the *neophyl* groups had been removed. Elemental analysis confirmed that the compound contained no nitrogen and resonances in the ^{19}F NMR spectrum pointed to the presence of $[\text{C}_6\text{F}_5]$ units. The nature of the crystals was confirmed as $\text{Cp}^*\text{Ta}(\text{OC}_6\text{F}_5)_4$ (**26**) by X-ray crystallography (*vide infra*).

The mother liquor from the reaction was then concentrated and cooled to -30°C to give a second crop of **26** [75%] plus another product **27** [25%]. Complexes **26** and **27** have very similar solubilities in toluene and pure **27** was only afforded after several recrystallisations. Spectroscopic analysis of **27** implied that it had similar ancillary ligands to **26** and again no nitrogen was found by elemental analysis. An X-ray structural determination (4.4.1.2) identified **27** as $[\text{Cp}^*\text{Ta}(\text{OC}_6\text{F}_5)_2(\mu\text{-O})]_2$ (Scheme 4.9).

A possible mechanism for the formation of **26** involves the reaction of $\text{Cp}^*\text{Ta}(\text{N}^t\text{Bu})(\text{CH}_2\text{CMe}_2\text{Ph})_2$ with four molecules of $\text{C}_6\text{F}_5\text{OH}$ and the elimination of *t*-butylamine and two molecules of PhCMe_3 . The reaction pathway to **27** is thought to be analogous to the possible mechanism described in Scheme 4.7, with the resultant species $[\text{Cp}^*\text{Ta}(\text{CH}_2\text{CMe}_2\text{Ph})(\text{OC}_6\text{F}_5)(\mu\text{-O})]_2$ reacting with yet another equivalent of $\text{C}_6\text{F}_5\text{OH}$ per tantalum to yield the final product. Another hypothetical mechanism for the formation of $[\text{Cp}^*\text{Ta}(\text{OC}_6\text{F}_5)_2(\mu\text{-O})]_2$ (**27**) is the homocoupling of two molecules of $\text{Cp}^*\text{Ta}(\text{OC}_6\text{F}_5)_4$ (**26**) with the elimination of $\text{C}_6\text{F}_5\text{OC}_6\text{F}_5$. However, this is unlikely because the ratios of **26** and **27** in a d_6 -benzene solution did not alter over several months.



Scheme 4.9.

Significantly, the *t*-butyl imido group has again shown a susceptibility to react. This phenomenon in half-sandwich Group 5 metal imido chemistry is very rare for the imido moiety, which is normally envisaged as a 'spectator' ligand; the highly acidic nature of pentafluorophenol is obviously a contributing factor.

4.4.1.1. Molecular Structure of Cp*Ta(OC₆F₅)₄ (26)

Yellow needle crystals suitable for structural analysis were obtained from the heptane reaction solution. The molecular structure is shown in Figure 4.4. Selected bond lengths and angles are collected in Table 4.4 and the crystal data are given in Appendix A11.

The molecule has a mirror axis through O(2) and O(3). The tantalum centre possesses a distorted square pyramidal geometry with the Cp* ring at

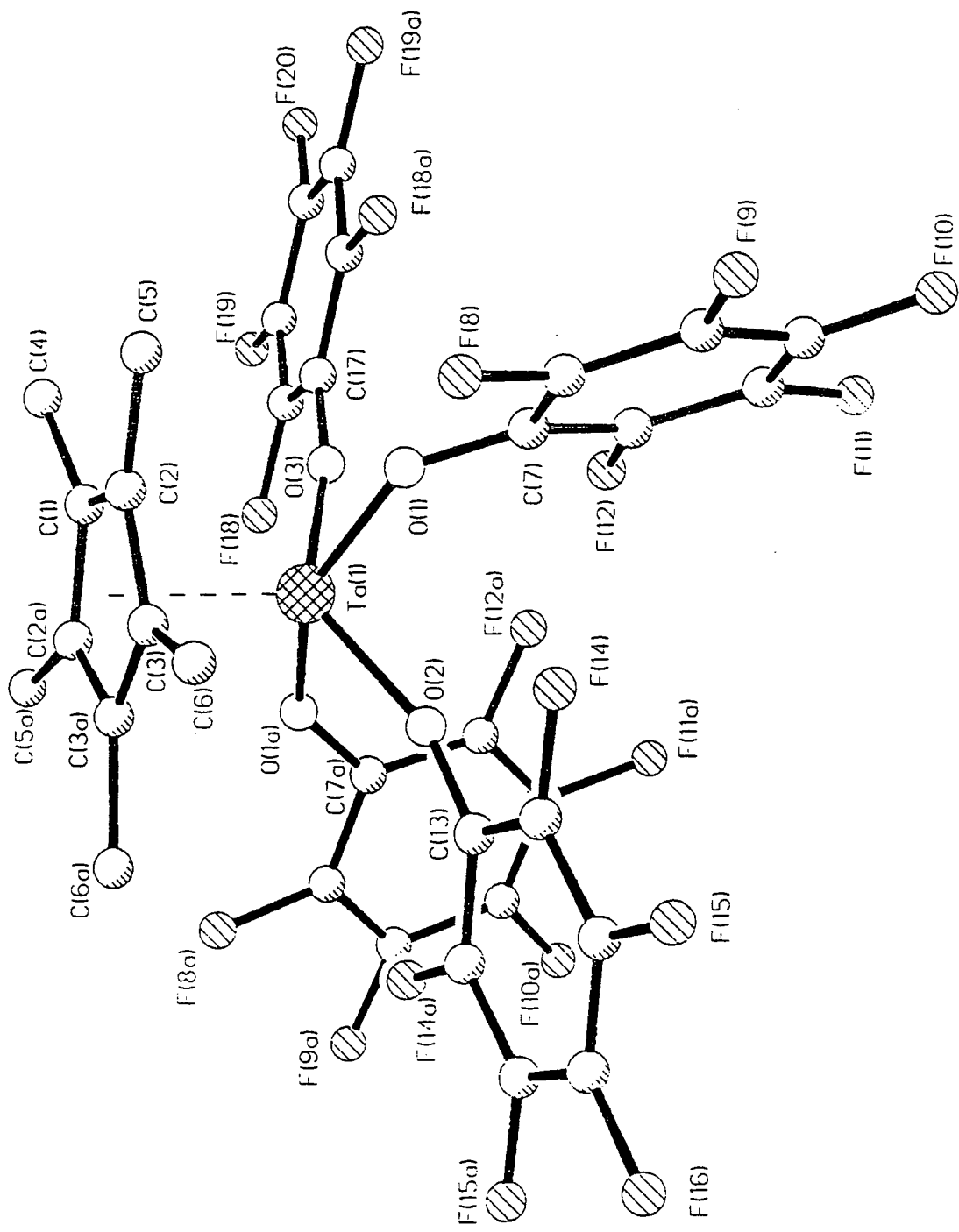
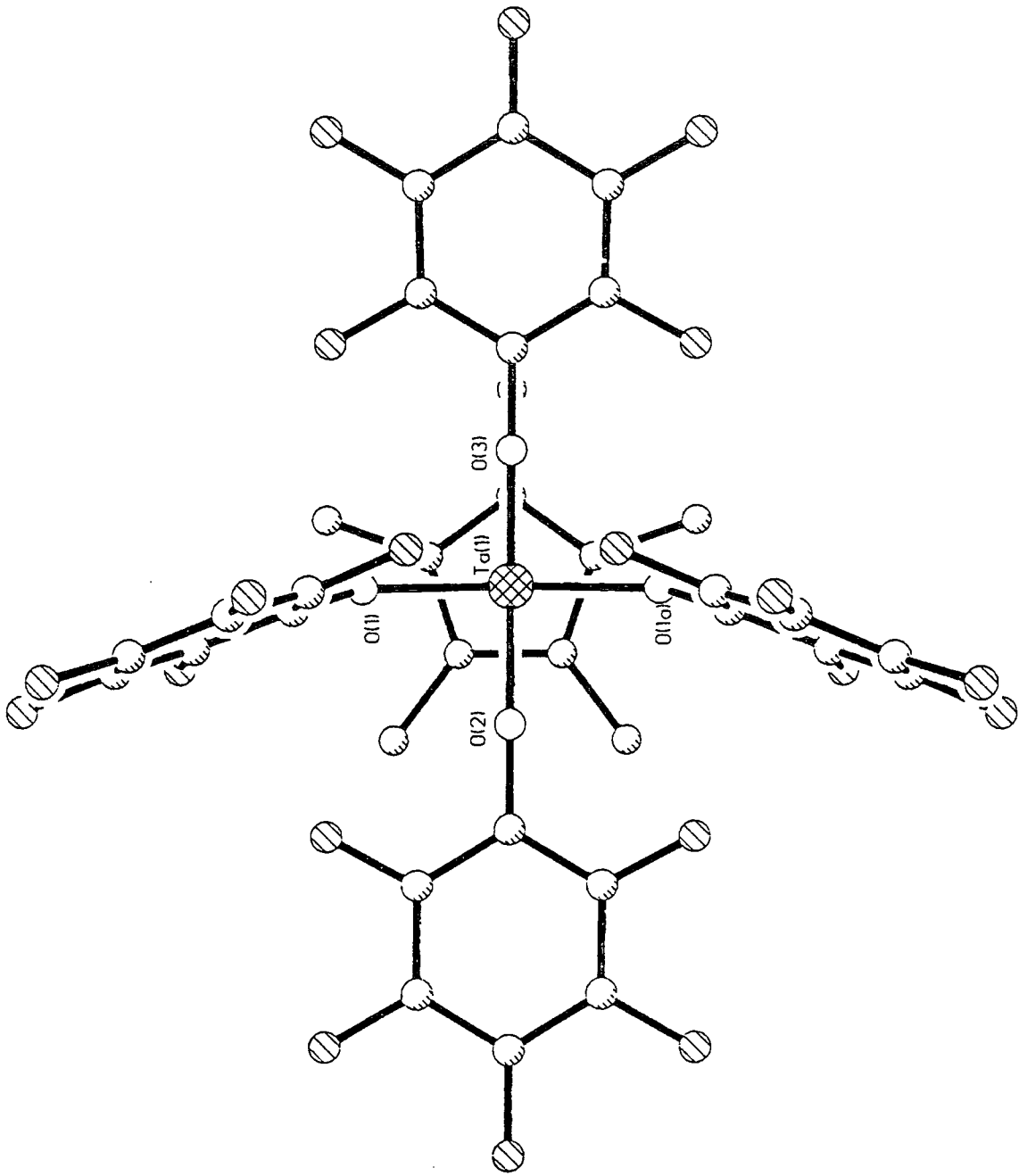


Figure 4.4. Molecular structure of Cp*Ta(OC₆F₅)₃ (26). (a) Square pyramid.

Ta(1)–O(3)	1.907(8)	C(7)–C(8)	1.40(1)
Ta(1)–O(2)	1.956(8)	C(8)–F(8)	1.354(9)
Ta(1)–O(1)	1.985(5)	C(8)–C(9)	1.37(1)
Ta(1)–O(1a)	1.985(5)	C(9)–F(9)	1.354(9)
Ta(1)–C(3a)	2.419(7)	C(9)–C(10)	1.38(1)
Ta(1)–C(3)	2.419(7)	C(10)–F(10)	1.34(1)
Ta(1)–C(1)	2.43(1)	C(10)–C(11)	1.36(1)
Ta(1)–C(2)	2.451(8)	C(11)–F(11)	1.35(1)
Ta(1)–C(2a)	2.451(8)	C(11)–C(12)	1.37(1)
C(1)–C(2)	1.42(1)	C(12)–F(12)	1.361(9)
C(2)–C(3)	1.42(1)	O(2)–C(13)	1.35(1)
C(3)–C(3a)	1.43(2)	O(3)–C(17)	1.33(1)
O(1)–C(7)	1.317(9)	Ta(1)–C _p centroid	2.21(1)
C(7)–C(12)	1.38(1)		
O(3)–Ta(1)–O(2)	133.3(3)	C(2)–C(1)–C(2a)	107.8(9)
O(3)–Ta(1)–O(1)	85.6(2)	C(1)–C(2)–C(3)	108.3(7)
O(2)–Ta(1)–O(1)	83.5(2)	C(2)–C(3)–C(3a)	107.7(4)
O(3)–Ta(1)–O(1a)	85.6(2)	C(7)–O(1)–Ta(1)	142.7(5)
O(2)–Ta(1)–O(1a)	83.5(2)	C(13)–O(2)–Ta(1)	160.2(7)
O(1)–Ta(1)–O(1a)	151.9(3)	C(17)–O(3)–Ta(1)	169.5(7)

Table 4.4. Selected bond lengths (Å) and angles (°) for Cp*Ta(OC₆F₅)₄ (26)



(b) Illustration of mirror plane and twist angle between aryl rings.

the apex and the oxygen atoms of four $[\text{OC}_6\text{F}_5]$ units at the corners of the square base.

The relatively long Ta–O bonds [1.907(8), 1.956(8) and 1.985(5)Å] are presumably the result of a combination of the competition between all the ligands present to participate in π interactions with vacant metal d_π symmetry orbitals, plus the delocalisation of the filled oxygen p_π orbital into the $[\text{C}_6\text{F}_5]$ ring density (see 4.3.2.2). The twist angle in **26** of the pentafluorophenyl rings with respect to each other is approximately 90° (Figure 4.4.b), which is comparable to the twist angles observed between the different phenyl rings in $[\text{Cp}^*\text{Ta}(\text{CH}_2\text{Ph})(\text{OC}_6\text{F}_5)(\mu\text{-O})]_2$ (**24**). This rotation evidently minimises the steric and electronic repulsion between the fluorine atoms.

4.4.1.2. Molecular Structure of $[\text{Cp}^*\text{Ta}(\text{OC}_6\text{F}_5)_2(\mu\text{-O})]_2$ (**27**)

Yellow crystals of **27** were isolated from a toluene solution at -20°C . The molecular structure is shown in Figure 4.5. Selected bond lengths and angles are collected in Table 4.5 and the crystal data are given in Appendix A12.

The molecule is a dimer with a highly distorted square pyramidal arrangement around each tantalum atom, but unlike $[\text{Cp}^*\text{Ta}(\text{CH}_2\text{Ph})(\text{OC}_6\text{F}_5)(\mu\text{-O})]_2$ (**24**), it possesses only C_i symmetry. A rationale for the noticeably long phenoxide Ta–O distances [1.939(6), 1.952(7), 1.971(6) and 2.014(6)Å] has already been provided (*vide supra*). The largest Ta–O distance in **27** is even greater than the longest in **24** [2.005(8)Å] and reflects the replacement of a benzyl group in **24** by an electron-withdrawing $[\text{OC}_6\text{F}_5]$ group, which is expected to intensify the competition between the ligands for the empty d_π metal orbitals.

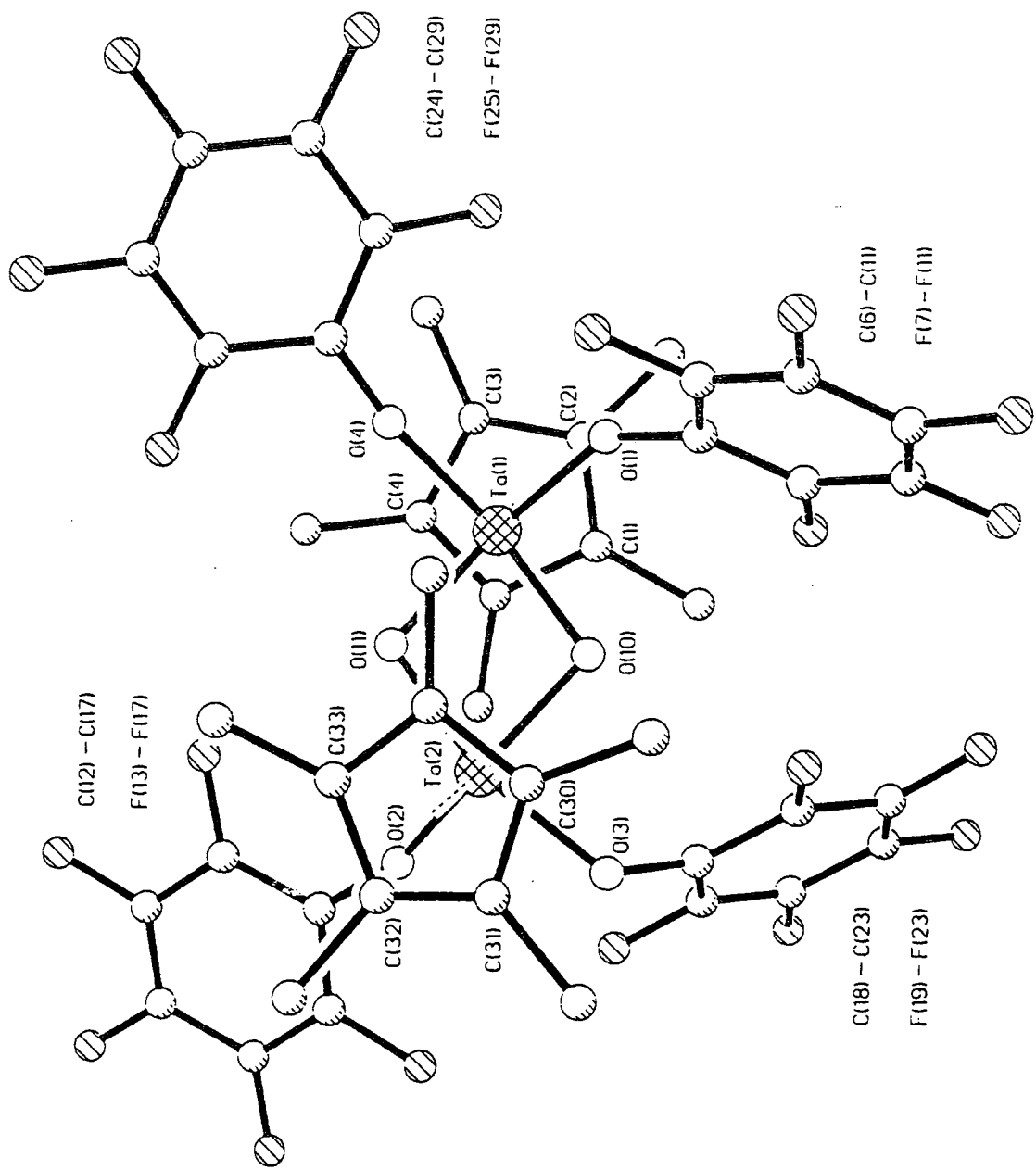


Figure 4.5. Molecular structure of $[\text{Cp}^*\text{Ta}(\text{OC}_6\text{F}_5)_2(\mu\text{-O})]_2$ (27).

Ta(1)–O(11)	1.918(6)	Ta(2)–O(3)	2.014(6)
Ta(1)–O(4)	1.952(7)	Ta(2)–C(34)	2.39(1)
Ta(1)–O(10)	1.969(6)	Ta(2)–C(30)	2.44(1)
Ta(1)–O(1)	1.971(6)	Ta(2)–C(33)	2.45(1)
Ta(1)–C(5)	2.41(1)	Ta(2)–C(32)	2.47(1)
Ta(1)–C(4)	2.43(1)	Ta(2)–C(31)	2.48(1)
Ta(1)–C(1)	2.458(9)	O(1)–C(6)	1.35(1)
Ta(1)–C(3)	2.464(9)	O(2)–C(12)	1.32(1)
Ta(1)–C(2)	2.482(9)	O(3)–C(18)	1.33(1)
Ta(2)–O(10)	1.933(6)	O(4)–C(24)	1.31(1)
Ta(2)–O(2)	1.939(6)	Ta(1)–C _p centroid	2.13(1)
Ta(2)–O(11)	1.961(6)	Ta(2)–C _p centroid	2.14(1)
O(11)–Ta(1)–O(4)	87.2(3)	O(10)–Ta(2)–O(3)	82.8(2)
O(11)–Ta(1)–O(10)	76.6(2)	O(2)–Ta(2)–O(3)	85.2(3)
O(4)–Ta(1)–O(10)	140.7(3)	O(11)–Ta(2)–O(3)	146.2(3)
O(11)–Ta(1)–O(1)	136.2(3)	Ta(1)–O(10)–Ta(2)	103.0(3)
O(4)–Ta(1)–O(1)	84.4(3)	Ta(1)–O(11)–Ta(2)	103.9(3)
O(10)–Ta(1)–O(1)	83.3(3)	C(6)–O(1)–Ta(1)	145.7(6)
O(10)–Ta(2)–O(2)	129.2(3)	C(12)–O(2)–Ta(2)	163.0(6)
O(10)–Ta(2)–O(11)	76.4(2)	C(18)–O(3)–Ta(2)	134.5(6)
O(2)–Ta(2)–O(11)	87.6(3)	C(24)–O(4)–Ta(1)	168.5(7)

Table 4.5.

Selected bond lengths (Å) and angles (°) for [Cp*Ta(OC₆F₅)₂(μ-O)]₂ (27)

The Ta(1)–O–Ta(2) angles of 103.0(3) and 103.9(3)° are almost identical to those in **24** [103.3(3)°] and are comparable with other Ta(V)–O–Ta(V) angles.²² The four relatively large Ta–O–C angles range from 134.5° to 168.5° and are presumably dependent on the steric constraint upon each pentafluorophenyl ring.

Compared with the twist angle between the phenyl rings in [Cp*Ta(CH₂Ph)(OC₆F₅)(μ-O)]₂ (**24**) (102.9°), those in **27** are relatively small [range 34.1°–57.3°, mean 42°]. This suggests that the large phenoxide Ta–O–C angles contribute to a reduction in unfavourable repulsive interactions in **27**. Hence, the large twist angle in **24** appears to be a result of the rigid tetrahedral geometry of the methylene carbon atoms (4.3.2.2).

Compared to Cp*Ta(OC₆F₅)₄ (**26**), which also exhibits high twist angles, the C₆F₅ rings in **27** obviously experience less steric congestion because of the presence of the Ta–O–Ta bridges.

4.5. Reactivity of Cp*Ta(N^tBu)(CH₂CMe₃)₂ (**22**)

Even at elevated temperatures, no reaction was observed between (CF₃)₂CMeOH or C₆F₅OH with **22** in C₆D₆. This surprising inactivity may have a steric origin; the Cp* and the three t-butyl groups form a virtual 'barrier' to the core of the molecule thus preventing attack at the metal centre and the imido nitrogen.

4.6. Summary

The dialkyl complexes $\text{Cp}^*\text{Ta}(\text{N}^t\text{Bu})(\text{CH}_2\text{R})_2$ [$\text{R}=\text{Ph}$ (**20**), CMe_2Ph (**21**), CMe_3 (**22**)] have been synthesised. The molecular structure of $\text{Cp}^*\text{Ta}(\text{N}^t\text{Bu})(\text{CH}_2\text{CMe}_3)_2$ reveals multiple agostic interactions and these are supported by spectroscopic evidence. Ring slippage of the Cp^* ligand is apparent and this is thought to arise from the competition between the imido, Cp^* ligands and the agostic interactions for the available metal orbitals of d_π symmetry.

The reactivity of the dialkyl derivatives has been investigated. An ethylene polymerisation catalyst is generated by the treatment of $\text{Cp}^*\text{Ta}(\text{N}^t\text{Bu})(\text{CH}_2\text{Ph})_2$ (**20**) with $[\text{Ph}_3\text{C}][\text{B}(\text{C}_6\text{F}_5)_4]$. In attempts to afford alkylidene species, reaction of **20** with excess $\text{C}_6\text{F}_5\text{OH}$ yielded the oxo-bridged dimer $[\text{Cp}^*\text{Ta}(\text{CH}_2\text{Ph})(\text{OC}_6\text{F}_5)(\mu\text{-O})]_2$ (**24**). Treatment of $\text{Cp}^*\text{Ta}(\text{N}^t\text{Bu})(\text{CH}_2\text{CMe}_2\text{Ph})_2$ (**21**) with excess $\text{C}_6\text{F}_5\text{OH}$ gave $\text{Cp}^*\text{Ta}(\text{OC}_6\text{F}_5)_4$ (**26**) and $[\text{Cp}^*\text{Ta}(\text{OC}_6\text{F}_5)_2(\mu\text{-O})]_2$ (**27**). These three phenoxide complexes have been crystallographically characterised and the similarities and differences between the structures have been discussed. The key features are the remarkably long pentafluorophenoxide Ta–O distances, which have been attributed to the fierce competition for the vacant d_π symmetry metal orbitals between the oxygen atoms (*via* π donation from their lone pairs) and the Cp^* ring. In addition, the delocalisation of the oxygen lone pair into the highly electron-withdrawing pentafluorophenyl ring is also expected to reduce the capacity of the oxygen atom to participate in $p_\pi\text{-}d_\pi$ interactions with the metal. Ultimately, the combination of the electrophilic nature of the d^0 tantalum centre and the high nucleophilicity of the metal phenoxide species ensures that the desired alkylidene species are not generated.

4.7. References

1. (a) D.N. Williams, J.P. Mitchell, A.D. Poole, U. Siemeling, W. Clegg, D.C.R. Hockless, P.A. O'Neil, V. C. Gibson, *J. Chem. Soc., Dalton Trans.*, 1992, 739. (b) M.P. Coles, C.I. Dalby, V.C. Gibson, W. Clegg, M.R.J. Elsegood, *J. Chem. Soc. Chem. Commun.*, 1995, 1709.
2. D.S. Williams, R.R. Schrock, *Organometallics*, 1993, **12**, 1148.
3. (a) J. Sundermeyer, D. Runge, *Angew. Chem., Int. Ed. Engl.*, 1994, **33**, 1255. (b) S. Schmidt, J. Sundermeyer, *J. Organomet. Chem.*, 1994, **472**, 127.
4. G. Schoettel, J. Kress, J.A. Osborn, *J. Chem. Soc. Chem. Commun.*, 1989, 1062.
5. A.D. Poole, Ph. D. Thesis, University of Durham, 1992.
6. For recent reviews, see: (a) M. Brookhart, M.L.H. Green, L. Wong, *Prog. Inorg. Chem.*, 1988, **36**, 1. (b) R.H. Crabtree, D.G. Hamilton, *Adv. Organomet. Chem.*, 1988, **28**, 299.
7. M. Mena, M.A. Pellinghelli, P. Royo, R. Serrano, A. Tiripicchio, *J. Chem. Soc. Chem. Commun.*, 1986, 1118.
8. K.H. den Haan, L.J. de Boer, J.H. Teuben, A.L. Spek, B. Kojicprodic, G.H. Hays, R. Huis, *Organometallics*, 1986, **5**, 1726.
9. G. Jeske, H. Lauke, H. Mauermann, P.N. Swepston, H. Schumann, T.J. Marks, *J. Am. Chem. Soc.*, 1985, **107**, 8091.
10. M. Brookhart, T.H. Whitesides, *Inorg Chem.*, 1976, **15**, 1550.
11. M. Brookhart, M.L.H. Green, *J. Organomet. Chem.*, 1983, **250**, 395.
12. (a) W.A. Nugent, R.L. Harlow, *J. Chem. Soc. Chem. Commun.*, 1978, 579. (b) L.R. Chamberlain, L.R. Rothwell, J.C. Huffman, *J. Chem. Soc. Chem. Commun.*, 1986, 1203.
13. A.D. Poole, D.N. Williams, A.M. Kenwright, V. C. Gibson, W. Clegg, D.C.R. Hockless, P.A. O'Neil, *Organometallics*, 1993, **12**, 2549.
14. A. Bell, W. Clegg, P.W. Dyer, M.J. Elsegood, V.C. Gibson, E.L. Marshall, *J. Chem. Soc., Chem. Commun.*, 1994, 2547.
15. M.L.H. Green, P.C. Konidaris, P. Mountford, S.J. Simpson, *J. Chem. Soc., Chem. Commun.*, 1992, 256.

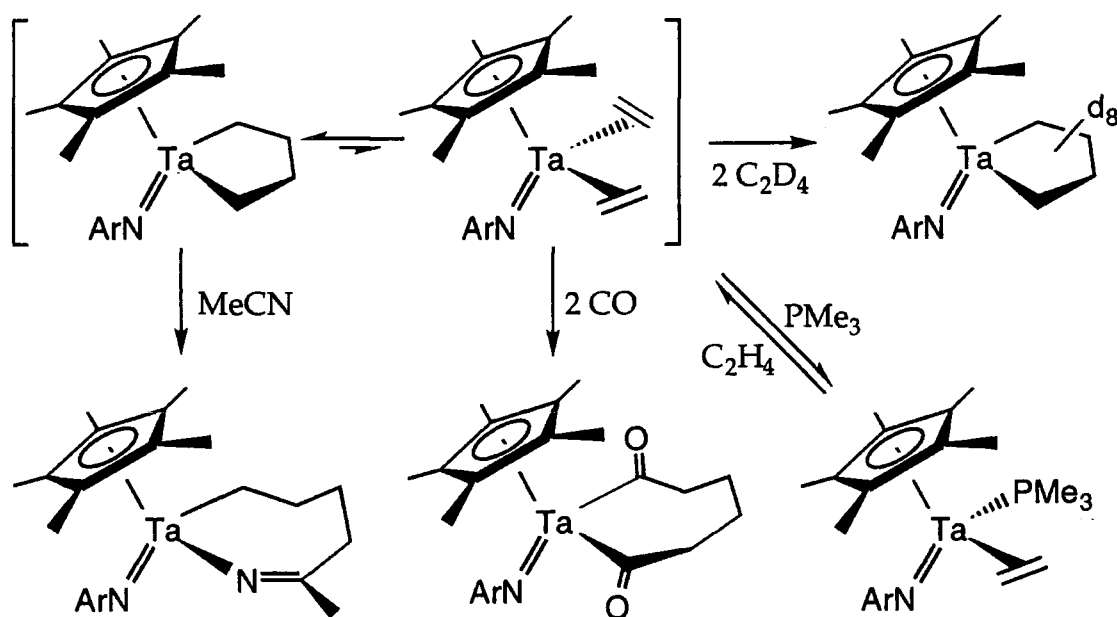
16. W.A. Hermann, G. Weichselbaumer, R.A. Paciello, R.A. Fischer, E. Herdtweck, J. Okuda, D.W. Marz, *Organometallics*, 1990, **9**, 489.
17. J.W. Lauher, R. Hoffman, *J. Am. Chem. Soc.*, 1976, **98**, 1729.
18. M. Bochmann, S.J. Lancaster, *Organometallics*, 1993, **12**, 633 and references therein, perfluorophenylborate salts prepared by Dr C.I. Dalby.
19. Z. Wu, R.F. Jordan, J.L. Peterson, *J. Am. Chem. Soc.*, 1995, **117**, 5867 and references therein.
20. B.J. Burger, M.E. Thompson, W.D. Cotter, J.E. Bercaw, *J. Am. Chem. Soc.*, 1990, **112**, 1566.
21. R.F. Jordan, R.E. LaPointe, N. Baenziger, G.D. Hinch, *Organometallics*, 1990, **9**, 1539 and references therein.
22. Cambridge Structural Database.
23. J.K. Cockcroft, V.C. Gibson, J.A.K. Howard, A.D. Poole, U. Siemeling, C. Wilson, *J. Chem. Soc., Chem. Commun.*, 1992, 1668.

Chapter 5

Studies Towards the C–C Coupling of Unsaturated Organic Molecules at the Half-Sandwich Tantalum Imido Fragment

5.1. Introduction

In recent years, zirconocene-based reagents have successfully been employed in organic synthesis to facilitate the efficient coupling of a wide variety of unsaturated organic substrates.^{1,2} Gibson *et al* have been studying the reactivity of half-sandwich imido complexes of the Group 5 metals and comparing their chemistry to the isolobally related bent metallocenes of the Group 4 metals.^{3,4} To date, while [CpM(NR)] derivatives of vanadium⁵ and niobium^{3d} have not displayed the ability to promote C-C coupling processes, the [Cp*Ta(N-2,6-*i*Pr₂C₆H₃)] fragment readily engages in oxidative coupling and novel insertion reactivity (Scheme 5.1).^{3e, 6}

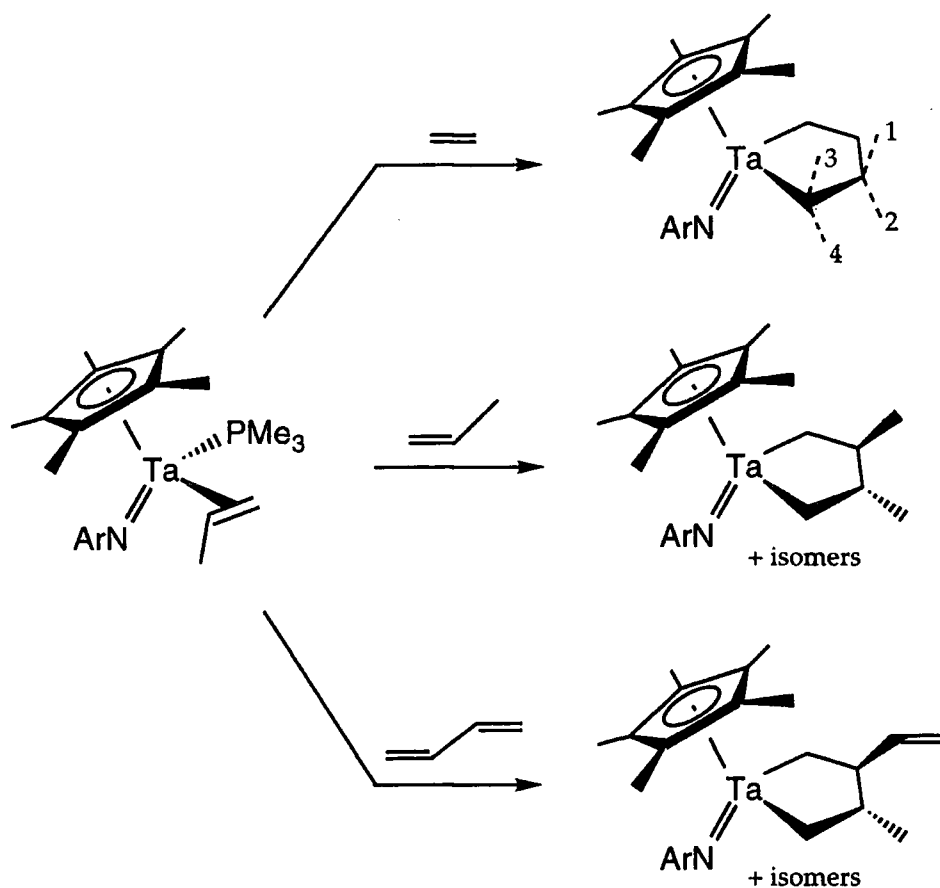


Scheme 5.1. Reactivity of Tantalacyclopentane complex (Ar=2,6-*i*Pr₂C₆H₃).

Spectroscopic evidence suggest that a metallacyclopentane description is the most appropriate for the Ta-C₄H₈ fragment. In behaviour reminiscent of zirconacyclopentanes, the half-sandwich imido tantalacyclopentane complex does not undergo facile β-H elimination to afford but-1-ene, even

upon prolonged heating at 120°C, due to conformational constraints which prevent the $\beta(\text{C-H})$ bonds from accessing the metal-centred LUMO.

Tertiary phosphine derivatives can also be used as precursors to the tantalacyclopentane complexes; treatment of $\text{Cp}^*\text{Ta}(\text{N-2,6-}i\text{Pr}_2\text{C}_6\text{H}_3)(\eta^2\text{-CH}_2\text{=CHMe})(\text{PMe}_3)$ with olefins displaces the phosphine ligand to yield the corresponding substituted metallacycle products (Scheme 5.2). The reaction with butadiene results in the incorporation of one double bond into the tantalacyclopentane ring to leave an exo-cyclic vinyl group. However, prolonged heating at 100°C does not eliminate the propene molecule to afford an η^4 -butadiene complex similar to $\text{Cp}_2\text{Zr}(\eta^4\text{-butadiene})$.⁷



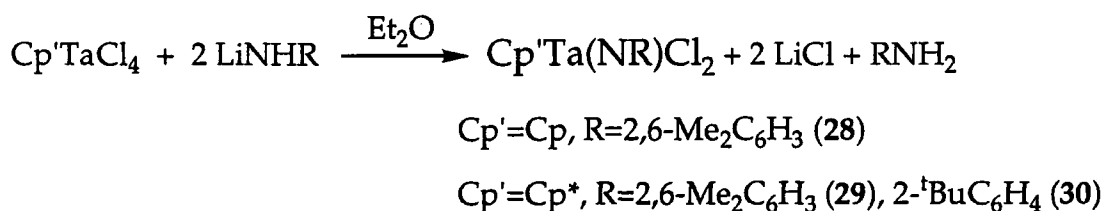
Scheme 5.2. Ar=2,6-*i*Pr₂C₆H₃.

Hence this investigation begins by examining the steric and electronic effects of the cyclopentadienyl and imido ligands upon the stability of the

tantalacyclopentane species, through the attempted synthesis of analogous complexes. The formation and reactivity of new C–C coupled products and related species are subsequently explored.

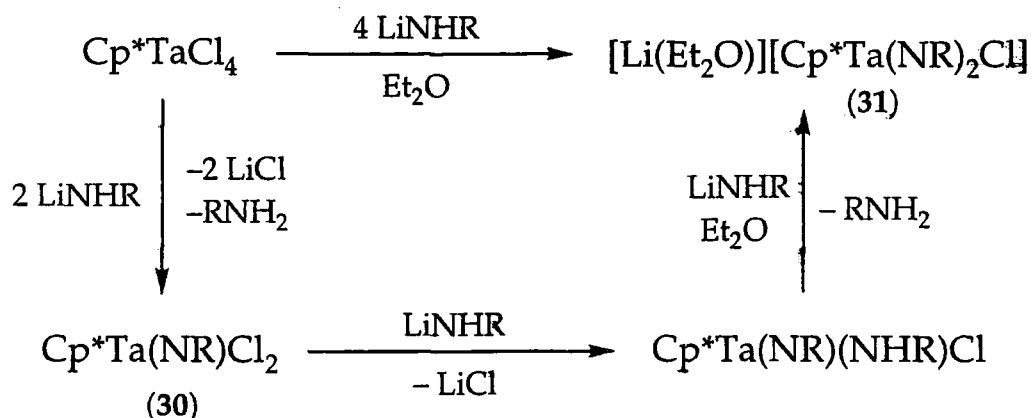
5.2. Synthesis of Cp'Ta(NR)Cl₂ and Related Complexes

A number of complexes of the general formula Cp'Ta(NR)Cl₂ were prepared as a prelude to their attempted conversion to tantalacyclopentanes. The observation that imido ligand exchange reactions of Cp*Ta(N^tBu)Cl₂⁸ with anilines to give the corresponding arylimido complexes do not proceed is initially surprising. The sterically congested nature of the t-butylimido species presumably prevents the formation of the initial 5-coordinate aniline adduct (see Section 2.1). However, complexes **28**, **29**⁹ and **30** can all be isolated as orange to red crystals *via* the route described by Wigley and co-workers¹⁰ (Scheme 5.3).



Scheme 5.3.

While moderate to high yields of **29** are commonly obtained (60-65%), the synthesis of **30** can be problematic due to contamination by a bright yellow crystalline side-product. This Et₂O-insoluble solid is tentatively assigned as the amide complex Cp*Ta(N-2-^tBuC₆H₄)(NH-2-^tBuC₆H₄)Cl, since its treatment with 1 equivalent of LiNH(2-^tBuC₆H₄) in diethyl ether affords the half-sandwich tantalum bis-imido complex [Li(OEt₂)] [Cp*Ta(N-2-^tBuC₆H₄)₂Cl] (**31**). **31** can also be obtained by the reaction of Cp*TaCl₄ with 4 equivalents of LiNH(2-^tBuC₆H₄) in Et₂O (Scheme 5.4).



Scheme 5.4. Postulated Reaction Pathway to 31 (R=2-^tBuC₆H₄).

5.2.1. Molecular Structure of [Li(OEt₂)] [Cp*Ta(N-2-^tBuC₆H₄)₂Cl] (31)

Long yellow crystals of **31** were grown from a saturated diethyl ether solution at -20°C. The molecular structure is shown in Figure 5.1. Selected bond lengths and angles are collected in Table 5.1 and the crystal data are given in Appendix A13.

The tantalum centre is in a pseudo-tetrahedral environment with a Cp*centroid-Ta(1)-Cl(1) angle of 109.7° and a Cp*centroid-Ta(1)-N(1) angle of 118.8°. The diethyl ether molecule which is bound to the lithium atom is disordered and hence only the oxygen atom is illustrated in the diagram. The degree of association of the [μ-Li(OEt₂)]⁺ fragment with N(1) and N(2) is comparable, as in the crystal structure of the 2,6-di(isopropyl)phenylimido analogue [Li(OEt₂)] [Cp*Ta(N-2,6-ⁱPr₂C₆H₃)₂Cl].¹⁰ Accordingly, the Ta-N bond lengths are identical (Ta(1)-N(1) 1.844(6) Å, Ta(1)-N(2) 1.848(6) Å) although the angles at the nitrogen atoms show a small difference (Ta(1)-N(1)-C(11) 165.9(5)°, Ta(1)-N(2)-C(21) 161.7(5)°). These Ta-N distances are similar to those found in [Li(OEt₂)] [Cp*Ta(N-2,6-ⁱPr₂C₆H₃)₂Cl] but are slightly longer than expected for tantalum-imido contacts, presumably due to diminished π donation to the tantalum centre arising from Li⁺ coordination.

Ta(1)–N(1)	1.844(6)	N(1)–C(11)	1.393(9)
Ta(1)–N(2)	1.848(6)	N(1)–Li(1)	2.06(2)
Ta(1)–Cl(1)	2.396(2)	N(2)–C(21)	1.41(1)
Ta(1)–C(3)	2.408(7)	N(2)–Li(1)	2.06(2)
Ta(1)–C(2)	2.443(7)	Li(1)–O(1')	1.92(2)
Ta(1)–C(4)	2.459(7)	Li(1)–O(1)	2.10(3)
Ta(1)–C(1)	2.478(7)	O(1)–O(1')	1.05(3)
Ta(1)–C(5)	2.493(7)	Ta(1)–C _p centroid	2.134(7)
N(1)–Ta(1)–N(2)	100.5(3)	O(1')–Li(1)–N(2)	137.6(9)
N(1)–Ta(1)–Cl(1)	106.2(2)	N(1)–Li(1)–N(2)	86.9(6)
N(2)–Ta(1)–Cl(1)	103.4(2)	O(1)–Li(1)–N(1)	130(1)
C(11)–N(1)–Ta(1)	165.9(5)	O(1)–Li(1)–N(2)	134(1)
C(11)–N(1)–Li(1)	98.3(6)	N(1)–Ta(1)–C _p centroid	118.8
C(21)–N(2)–Ta(1)	161.7(5)	N(2)–Ta(1)–C _p centroid	119.5
C(21)–N(2)–Li(1)	103.0(6)	Cl–Ta(1)–C _p centroid	109.7
O(1')–Li(1)–N(1)	134.8(8)		

Table 5.1. Selected bond lengths (Å) and angles (°) for [Li(OEt₂)]([Cp*Ta(N-2-^tBuC₆H₄)₂Cl]) (31)

The fierce competition to participate in $p\pi-d\pi$ interactions with the metal between the two imido ligands and the Cp^* ring, which are all strong π -donors, will also lead to lengthening of the Ta–N bonds.

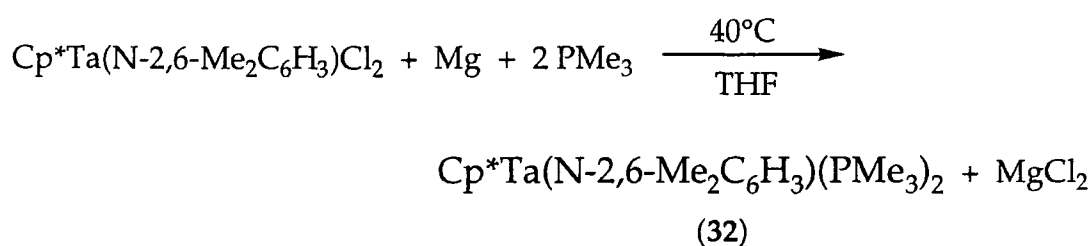
The planes of the 2-*t*-butylphenyl rings and the Cp^* ring are orientated approximately parallel to each other to avoid steric repulsion between the Cp^* methyl and the *tert*-butyl groups. Similarly, these *tert*-butyl substituents are positioned remote from the $[\mu-Li(OEt_2)]^+$ moiety and point in a similar direction to the Ta–Cl vector.

5.3. Reactivity of $Cp'Ta(NR)Cl_2$ Complexes

Reactions of $Cp'Ta(NR)Cl_2$ ($Cp'=Cp$, $R=^tBu$;⁸ $Cp'=Cp^*$, $R=^tBu$, 2,6- $Me_2C_6H_3$, 2- tBuC_6H_4) with 2 equivalents of ethylmagnesium chloride in diethyl ether under an atmosphere of ethylene were performed⁶ in order to generate the corresponding tantalacyclopentane. However, in all cases, only intractable oils containing several unidentifiable species (by 1H NMR) were obtained; the nature and the high solubilities of the products in aliphatic solvents precluded the isolation of any single species. These results were unexpected and indicate that the successful isolation of the desired tantalacyclopentane derivatives require highly specific ligation in the metal coordination sphere; factors which are investigated in the next section. Analogous reactions of $Cp'Ta(NR)Cl_2$ ($Cp'=Cp^*$, $R=2,6-Me_2C_6H_3$, 2- tBuC_6H_4) with 2 equivalents of ethylmagnesium chloride in the presence of diphenylacetylene yielded only unreacted diphenylacetylene and an intractable oil.

Coupling of alkyne ligands to form metallacyclopentadienes has been achieved using zirconocene bis(phosphine) complexes.¹¹ Hence it was

anticipated that the analogous reaction of half-sandwich tantalum imido bis(phosphine) compounds may also lead to the corresponding metallacycles. Hence, reduction of $\text{Cp}'\text{Ta}(\text{NR})\text{Cl}_2$ ($\text{Cp}'=\text{Cp}^*$, $\text{R}=\text{tBu}$, $2,6\text{-Me}_2\text{C}_6\text{H}_3$, $2\text{-tBuC}_6\text{H}_4$) with activated magnesium in the presence of PMe_3 was carried out at 40°C and this resulted in the isolation of $\text{Cp}^*\text{Ta}(\text{N-}2,6\text{-Me}_2\text{C}_6\text{H}_3)(\text{PMe}_3)_2$ (**32**), albeit in very low yield (Scheme 5.5). The use of Na/Hg amalgam as the reducing agent also gave very low yields for **32** and this consequently hindered investigations into its reactivity.



Scheme 5.5.

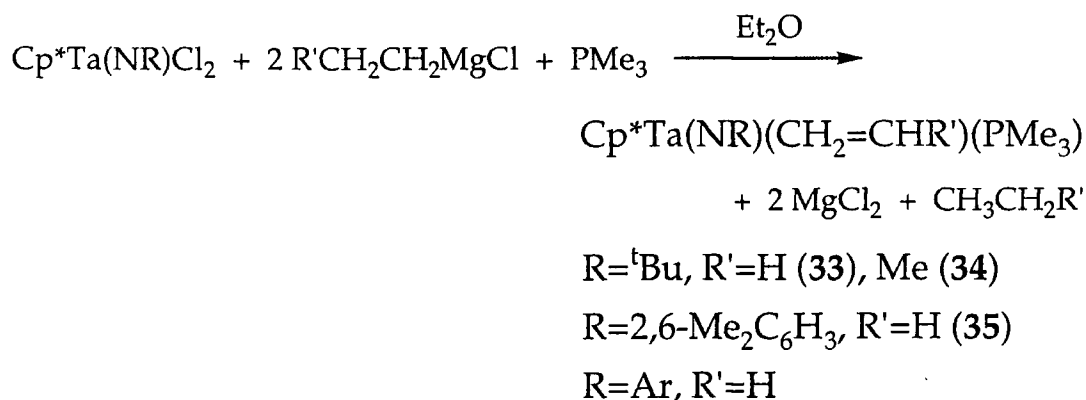
The ^1H NMR resonances for **32** are all shifted significantly downfield compared to the Ta(V) dichloride **29**, reflecting the decreased electrophilicity of the Ta(III) centre. The PMe_3 methyl protons give rise to a virtual triplet splitting pattern thus implying that the $^2\text{J}_{\text{PH}}$ and $^4\text{J}_{\text{PH}}$ coupling constants are of similar magnitude.

5.4. Synthesis of $\text{Cp}^*\text{Ta}(\text{NR})(\text{CH}_2=\text{CHR}')(\text{PMe}_3)$ Derivatives and their Reactivity with Unsaturated Hydrocarbons

In light of the apparent formation of metallacyclic species by treatment of $\text{Cp}^*\text{Ta}(\text{N-}2,6\text{-iPr}_2\text{C}_6\text{H}_3)(\text{CH}_2=\text{CHMe})(\text{PMe}_3)$ with olefins,⁶ reactions of analogous complexes containing different imido substituents towards

ethylene were undertaken in order to identify suitable Cp*/NR combinations to stabilise the desired tantalacyclopentane products.

The olefin complexes Cp*Ta(NR)(CH₂=CHR')(PMe₃) (R=^tBu, R'=H (33), Me (34); R=2,6-Me₂C₆H₃, R'=H (35), R=2,6-ⁱPr₂C₆H₃, R'=H^{3e}) are readily prepared by the treatment of the dichlorides with 2 equivalents of the appropriate Grignard reagent in the presence of PMe₃ (Scheme 5.6).



Scheme 5.6.

Complex 33 is isolated as an oily solid presumably as a consequence of the tert-butyl moiety. The ethylene ligands in 33 and 35 display an AA'MM' splitting pattern in their ¹H NMR spectra due to the chiral metal environment. Three of the four possible isomers of 34, depending on the orientation of the olefinic methyl group, can clearly be observed spectroscopically in a manner comparable to the analogous complex CpNb(N-2-^tBuC₆H₄)(CH₂=CHMe)(PMe₃) (11).⁴

5.4.1. Reaction of Ethylene with Cp*Ta(NR)(CH₂=CHR')(PMe₃) Complexes

The following complexes were treated with excess ethylene (*ca.* 5 equivalents) in d₆-benzene in sealed NMR tubes:

$Cp^*Ta(N^tBu)(CH_2=CH_2)(PMe_3)$ (33) : No reaction is observed at 60°C for four weeks. Severe heating of the sample at 100°C for one week eventually leads to *ca.* 67% conversion to a new species by 1H NMR spectroscopy: singlets are present at 1.33ppm (tBu) and 1.86ppm (Cp^*) and small broad multiplets are visible at 0.6, 2.2 and 2.4ppm (C_4H_8). Hence this species is tentatively assigned as the metallacycle $Cp^*Ta(N^tBu)(\sigma-1,4-C_4H_8)$ (36). However, the metallacycle continues to react with excess ethylene and after four weeks at 100°C, a solid residue appears in the sample. 1H NMR spectroscopy also indicates that several new species are formed. One may speculate that ethylene oligomerisation processes have occurred, possibly as a result of further olefin insertion into the tantalacyclopentane.

$Cp^*Ta(N^tBu)(CH_2=CHMe)(PMe_3)$ (34) : Decomposition of the tantalum species is observed over a period of several weeks at room temperature, suggesting that the substituted metallacycle which is expected to form is unstable and incompatible with the [$Cp^*/N(tBu)$] ligand combination.

$Cp^*Ta(N-2,6-Me_2C_6H_3)(CH_2=CH_2)(PMe_3)$ (35) : The reaction proceeds very slowly at 60°C with <5% conversion after 2 weeks to a new species by 1H NMR spectroscopy. Attempts to increase the rate of reaction by heating the tube to 100°C were not successful and led to decomposition. This implies that the [$Cp^*/N-2,6-Me_2C_6H_3$] ligand pair does not impart a stabilising effect on tantalacyclopentane species.

$Cp^*Ta(N-2,6-^iPr_2C_6H_3)(CH_2=CH_2)(PMe_3)$: The previously observed equilibrium⁶ is established⁶ after six weeks at 60°C, resulting in *ca.* 60% conversion to the tantalacyclopentane product. Although total conversion is not achieved, the rate of reaction and the relative stability of the product clearly demonstrate that, *of the systems investigated, the [$Cp^*/N-2,6-^iPr_2C_6H_3$]*

ligand combination uniquely provides the appropriate steric and electronic environment for the stabilisation and isolation of such metallacyclic complexes. This conclusion is applied to the work in Section 5.5.

5.4.2. Reaction of Alkynes with $\text{Cp}^*\text{Ta}(\text{NR})(\text{CH}_2=\text{CHR}')(\text{PMe}_3)$

The reactions of the following olefin complexes with an excess of various alkynes in C_6D_6 were investigated to compare the products with the niobium metallacyclopentadiene species (18) which was apparently generated from the treatment of $\text{CpNb}(\text{N}-2,6\text{-Cl}_2\text{C}_6\text{H}_3)(\text{CH}_2=\text{CH}_2)(\text{PMe}_3)$ (17) with excess phenylacetylene.⁴

Reaction of $\text{Cp}^\text{Ta}(\text{N}^t\text{Bu})(\text{CH}_2=\text{CHMe})(\text{PMe}_3)$ (34) with $\text{PhC}\equiv\text{CH}$:* After 3 weeks at 100°C , complete conversion to a single new species is observed by ^1H and ^{31}P NMR spectroscopy, and this is accompanied by the appearance of displaced propene. The product is assigned as the alkyne-phosphine complex $\text{Cp}^*\text{Ta}(\text{N}^t\text{Bu})(\text{PhC}\equiv\text{CH})(\text{PMe}_3)$ (37).

Reaction of $\text{Cp}^\text{Ta}(\text{N}-2,6\text{-Me}_2\text{C}_6\text{H}_3)(\text{CH}_2=\text{CH}_2)(\text{PMe}_3)$ (35) with $\text{PhC}\equiv\text{CPh}$:* An equilibrium is reached after heating the reaction at 100°C for 4 weeks. The olefin molecule is again displaced to presumably afford $\text{Cp}^*\text{Ta}(\text{N}-2,6\text{-Me}_2\text{C}_6\text{H}_3)(\text{PhC}\equiv\text{CPh})(\text{PMe}_3)$ (38) with *ca.* 60% conversion. Hence it is apparent from the formation of 37 and 38 that the Cp^*/NR combinations concerned facilitate the displacement of the olefin rather than the phosphine ligand in these systems.

Reaction of $\text{Cp}^\text{Ta}(\text{N}-2,6\text{-}^i\text{Pr}_2\text{C}_6\text{H}_3)(\text{CH}_2=\text{CH}_2)(\text{PMe}_3)$ with $\text{PhC}\equiv\text{CPh}$:*

As expected, a derivative which corresponds to $\text{Cp}^*\text{Ta}(\text{N}-2,6\text{-}^i\text{Pr}_2\text{C}_6\text{H}_3)(\text{PhC}\equiv\text{CPh})(\text{PMe}_3)$ (39) is observed as the major species after 3

weeks at 100°C, accompanied by the elimination of ethylene. Reaction of **39** with the excess alkyne continues slowly and after 3 months results in total displacement of PMe₃ and significant conversion to a new product (**40**). In the ¹H NMR spectrum, a singlet (1.86ppm) for the Cp* ring and doublet and septet resonances (1.52 and 5.05ppm respectively) for the *iso*-propyl group leads to the tentative assignment of **40** as Cp*Ta(N-2,6-*i*-Pr₂C₆H₃)(PhC≡CPh)₂. Identical resonances to those of **39** and **40** are also observed in Section 5.5.3.1, where further evidence for the assignment of **40** is presented.

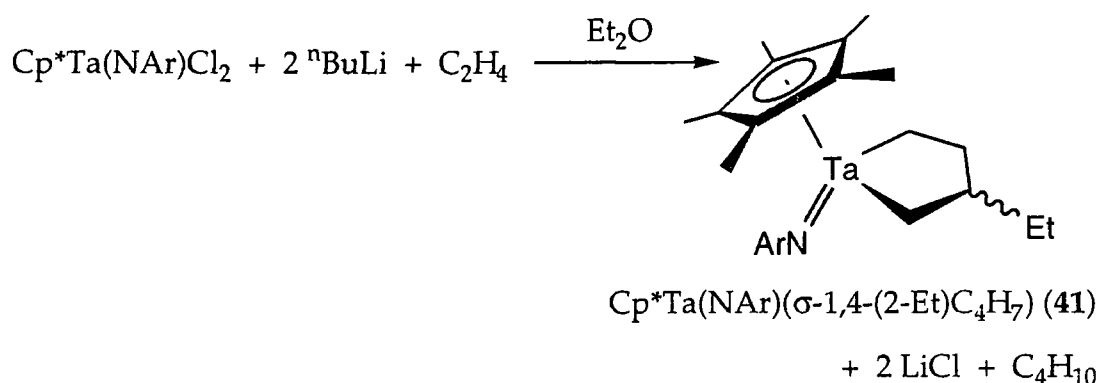
5.5. New C–C Coupled Products and Related Complexes of the [Cp*Ta(N-2,6-*i*-Pr₂C₆H₃)] System

As a consequence of results described in previous sections, it was decided to focus on the [Cp*Ta(N-2,6-*i*-Pr₂C₆H₃)] system, which has previously been shown to promote oxidative coupling processes to afford metallacyclic complexes. In zirconocene chemistry, Negishi and co-workers have extensively demonstrated analogous coupling reactivity in the effective conversion of a variety of alkenes, alkynes, enynes and diynes into the corresponding zirconacycles and -bicycles, *via* a zirconocene-(but-1-ene) derivative which is generated by the treatment of Cp₂ZrCl₂ with 2 equivalents of ⁿBuLi in THF² (see Section 1.4.2). Hence reactions of ⁿBuLi with the isolobal Cp*Ta(N-2,6-*i*-Pr₂C₆H₃)Cl₂ in the presence of π-donor ligands were investigated.

5.5.1. Reaction of Cp*Ta(N-2,6-*i*-Pr₂C₆H₃)Cl₂ with 2ⁿBuLi in the presence of Ethylene: Preparation of Cp*Ta(N-2,6-*i*-Pr₂C₆H₃)(σ-1,4-(2-Et)C₄H₇) (**41**)

Treatment of a diethyl ether solution of Cp*Ta(N-2,6-*i*-Pr₂C₆H₃)Cl₂ with 2 equivalents of n-butyllithium at -78°C results in a green solution. This

green species is presumed to be the di(*n*-butyl) complex (see Section 5.5.3). An atmosphere of ethylene is then introduced and the mixture is allowed to warm to room temperature, during which the green colouration is slowly replaced by a yellow solution and white precipitate. The substituted tantalacyclopentane complex $\text{Cp}^*\text{Ta}(\text{N-2,6-}i\text{Pr}_2\text{C}_6\text{H}_3)(\sigma\text{-1,4-(2-Et)C}_4\text{H}_7)$ (**41**) is isolated from the yellow solution as a bright orange crystalline solid in *ca.* 50% yield (Scheme 5.7). **41** can also be generated by the treatment of $\text{Cp}^*\text{Ta}(\text{N-2,6-}i\text{Pr}_2\text{C}_6\text{H}_3)(\eta^2\text{-CH}_2\text{=CHEt})(\text{PMe}_3)$ with ethylene; the synthesis and reactivity of this (but-1-ene)-phosphine complex is discussed in Section 5.5.3.



Scheme 5.7. Ar=2,6-*i*Pr₂C₆H₃.

The ¹H and ¹³C NMR spectra for **41** and $\text{Cp}^*\text{Ta}(\text{N-2,6-}i\text{Pr}_2\text{C}_6\text{H}_3)(\sigma\text{-1,4-C}_4\text{H}_8)$ ⁶ are comparable except for the metallacycle signals. Most significantly, the proton-coupled ¹³C NMR spectrum of **41** contains multiplets which can be assigned to the methine (doublets) and ethyl (triplets and quartets) groups, resonances which are absent in the corresponding spectrum for $\text{Cp}^*\text{Ta}(\text{N-2,6-}i\text{Pr}_2\text{C}_6\text{H}_3)(\sigma\text{-1,4-C}_4\text{H}_8)$. The mass spectrum contains envelopes at 575, 547 and 519 *m/z* which correspond to the parent ion and the $[\text{M}-\text{C}_2\text{H}_4]^+$ and $[\text{M}-\text{C}_4\text{H}_8]^+$ daughter fragments, while elemental analysis indicates the correct stoichiometry for **41**. The ethyl group is proposed to be in the β-position with respect to the metal since Negishi found that, due to steric reasons, alkyl

substituents strongly favour the β position in isolobal bis(cyclopentadienyl) zirconacyclopentanes.¹²

Figure 5.2. shows four isomers of **41** with the ethyl substituent in the β position. However, **a** and **b** are optical isomers of **c** and **d** respectively and hence spectroscopically indistinguishable. Therefore only *two* isomers of comparable intensities are observed in the ^1H and ^{13}C NMR spectra, and they correspond to the ethyl group pointing towards the Cp^* ring (**a** and **c**) and the imido ligand (**b** and **d**).

The NMR data for **41** are consistent with a metallacyclic character rather than a di-olefin product; in particular the eight ^{13}C NMR signals which have been assigned to the metallacyclic carbons appear in the range 27.6–61.8ppm and their $^1\text{J}_{\text{CH}}$ coupling constants of 120–125Hz are consistent with sp^3 -hybridised methylene units.

The mechanism for the formation of **41** is likely to be related to the analogous zirconocene pathway.^{2b} Hence the green di(*n*-butyl) complex is expected to undergo β -elimination of butane upon warming to room temperature and generate the 3-coordinate η^2 -(but-1-ene) intermediate $[\text{Cp}^*\text{Ta}(\text{N}-2,6\text{-}i\text{Pr}_2\text{C}_6\text{H}_3)(\text{CH}_2=\text{CHEt})]$ (see Section 5.5.3). This species is likely to exhibit significant metallacyclopropane character therefore preventing displacement of the olefin at this juncture. The metallacyclopentane is then formed by coupling of the intermediate with ethylene. This process is presumably reversible thus allowing access to the thermodynamically preferred form of **41** where the ethyl group occupies a β position (Scheme 5.10).

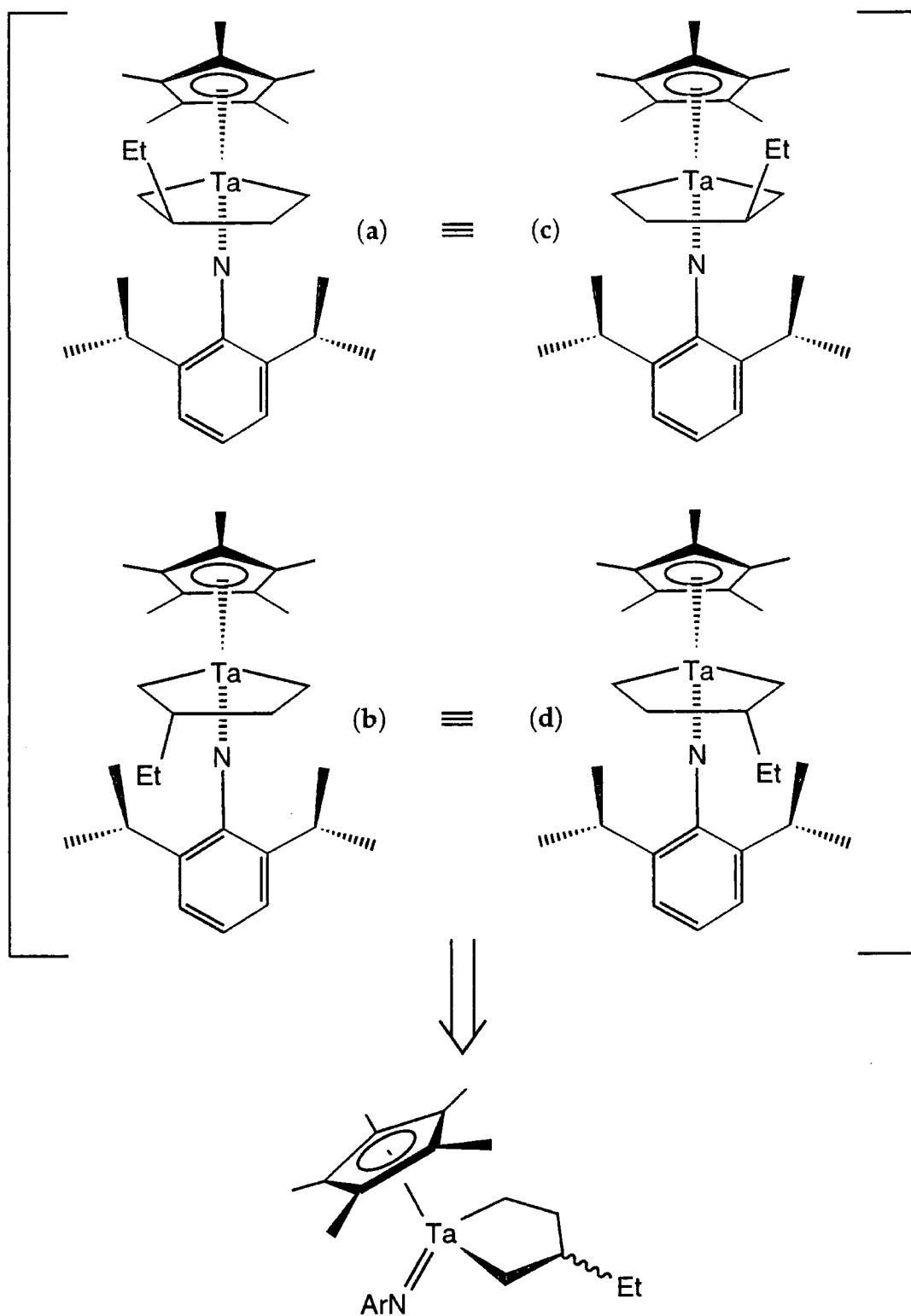


Figure 5.2. Postulated isomers of 41.

Given the presence of a large excess of ethylene in the reaction, the isolation of the ethylene-(but-1-ene) coupled species 41 was initially

surprising, since the but-1-ene ligand in the zirconocene analogue is readily displaced. However, the tantalacyclopentane nature of **41** means that the replacement of the but-1-ene ligand by a second molecule of C_2H_4 can only occur *via* $\beta(C-C)$ cleavage of the metallacycle; this is evidently energetically unfavourable under these reaction conditions.

Attempts to prepare analogous tantalacyclopentanes by the treatment of $Cp^*Ta(NR)Cl_2$ ($R=2,6-Me_2C_6H_3$ (**29**), $2-tBuC_6H_4$ (**30**)) with 2 $nBuLi$ and ethylene were unsuccessful and yielded unidentifiable oily solids. Reactions were also performed to generate the but-1-ene intermediate $[Cp^*Ta(N-2,6-iPr_2C_6H_3)(CH_2=CHEt)]$ in the presence of an excess of $PhC\equiv CR$ ($R=H, Ph$). This would hopefully afford the olefin-alkyne coupled complex or a metallacyclopentadiene, since this latter species is formed in the corresponding zirconocene system. Unfortunately, only unreacted alkyne and impure intractable oils were isolated from these experiments.

5.5.2. Reactivity of $Cp^*Ta(N-2,6-iPr_2C_6H_3)(\sigma-1,4-(2-Et)C_4H_7)$ (**41**)

Displacement of the but-1-ene ligand is observed in the treatment of **41** with PMe_3 at $100^\circ C$ to give $Cp^*Ta(N-2,6-iPr_2C_6H_3)(CH_2=CH_2)(PMe_3)$. This result implies that $\beta(C-C)$ cleavage processes are significantly more facile at these high temperatures (*vide supra*).

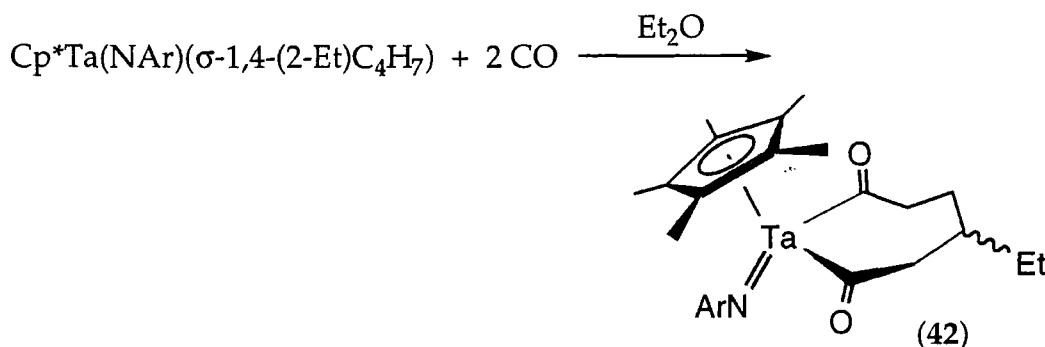
5.5.2.1. Reactivity of $Cp^*Ta(N-2,6-iPr_2C_6H_3)(\sigma-1,4-(2-Et)C_4H_7)$ with CO:

Preparation of $Cp^*Ta(N-2,6-iPr_2C_6H_3)[\sigma-1,6-C(O)(3-Et)C_4H_7C(O)]$ (**42**)

Like their acyclic counterparts, the metal-carbon bonds in metallacyclopentanes can insert carbon monoxide to afford acyl derivatives.

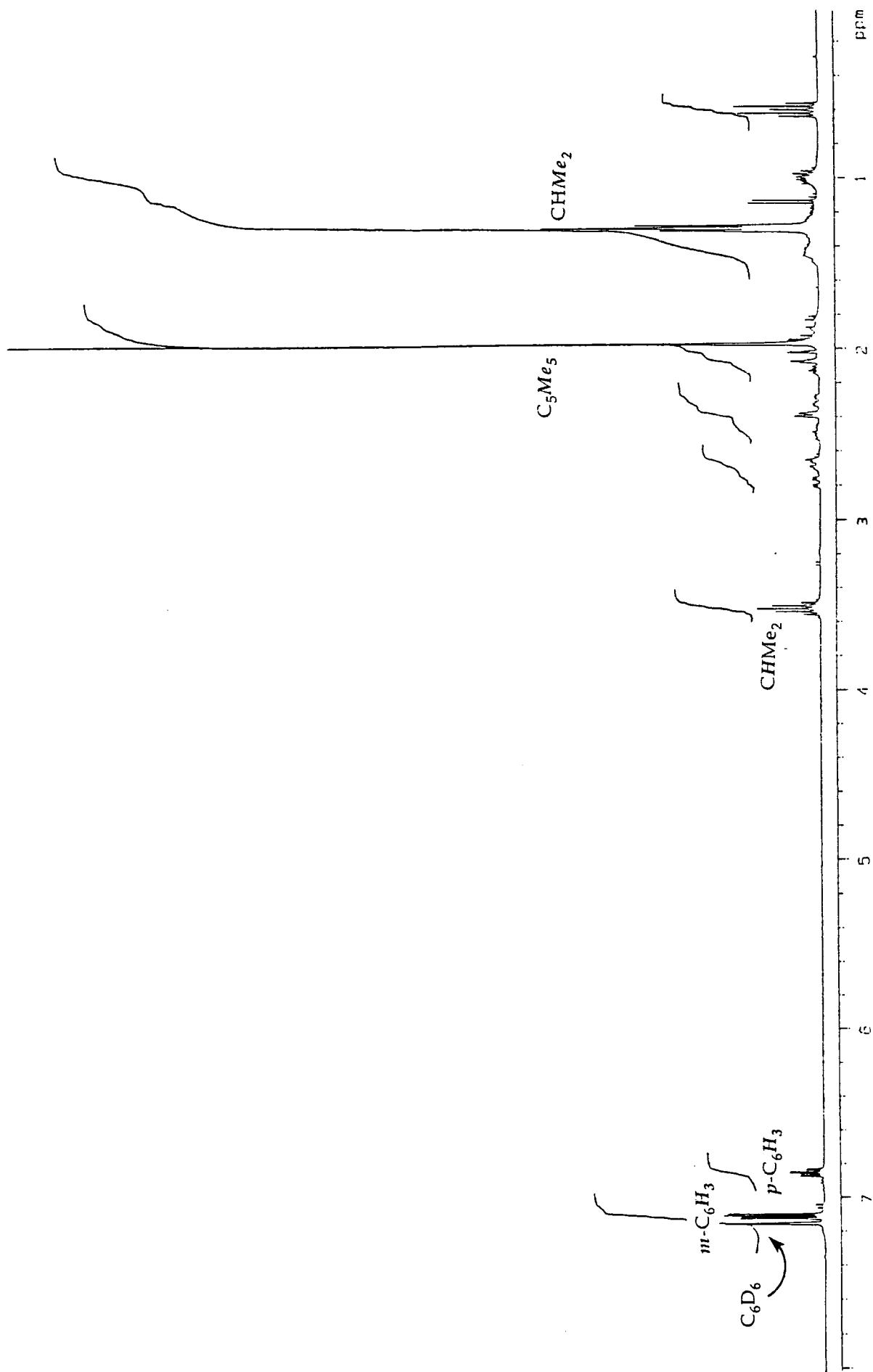
Grubbs¹³ demonstrated this with Ni(II) bis(phosphine) metallacyclopentanes which subsequently liberated cyclic ketones on decomposition.

An excess of carbon monoxide was condensed onto a frozen diethyl ether solution of $\text{Cp}^*\text{Ta}(\text{N}-2,6\text{-}i\text{Pr}_2\text{C}_6\text{H}_3)(\sigma\text{-}1,4\text{-}(2\text{-Et})\text{C}_4\text{H}_7)$ (**41**) at *ca.* -196°C . An intense red coloration was immediately observed as the mixture was allowed to warm up to room temperature, suggesting that the insertion process is extremely facile. Further stirring for 2 hours gave a deep orange solution of the diacyl complex $\text{Cp}^*\text{Ta}(\text{N}-2,6\text{-}i\text{Pr}_2\text{C}_6\text{H}_3)[\sigma\text{-}1,6\text{-C(O)}(3\text{-Et})\text{C}_4\text{H}_7\text{C(O)}]$ (**42**). **42** is subsequently isolated as a yellow/orange crystalline solid in 53% yield from a saturated Et_2O solution at -30°C (Scheme 5.8).



Scheme 5.8.

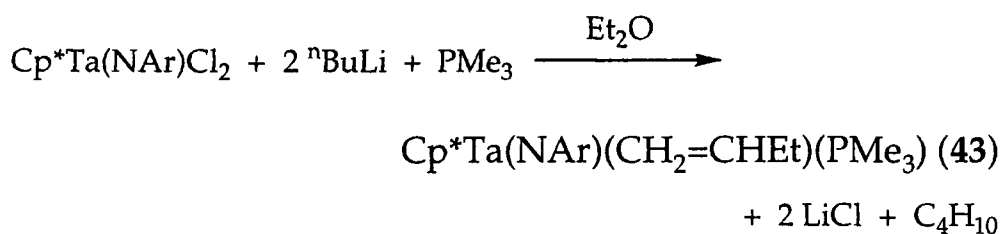
In the mass spectrum, an envelope at 631m/z corresponds to the molecular ion. A weak band at 1620cm^{-1} in the infra red spectrum has been attributed to an acyl $\nu(\text{CO})$ stretching vibration. Furthermore, the metallacyclic nature of the product dictates that, upon CO insertion into complex **41**, the ethyl substituent in **42** is situated exclusively γ to the metal. Two isomers are again observed by NMR spectroscopy (see Section 5.5.1), and four singlets in the range $132.6\text{-}134.0$ ppm in the ^{13}C NMR spectrum have been assigned to the acyl carbons. Such shifts are diagnostic of the $\text{C}=\text{O}$ bonding mode, because while η^1 -acyl resonances appear over a very wide range, the signals for an η^2 -acyl carbon are restricted to values between $248\text{-}392$ ppm.¹⁴ Hence η^1 -bonding modes are cautiously proposed for the acyl groups in **42**.



Spectrum 5.1. 400MHz ^1H NMR Spectrum (C_6D_6) of $\text{Cp}^*\text{Ta}(\text{N-2,6-}^i\text{Pr}_2\text{C}_6\text{H}_3)[\sigma\text{-1,6-C(O)(3-Et)C}_4\text{H}_7\text{C(O)}]$ (42).

5.5.3. Synthesis of $\text{Cp}^*\text{Ta}(\text{N-2,6-}i\text{Pr}_2\text{C}_6\text{H}_3)(\eta^2\text{-CH}_2\text{=CHEt})(\text{PMe}_3)$ (**43**)

The initial products from the decomposition of the green species which is afforded by the treatment of $\text{Cp}^*\text{Ta}(\text{N-2,6-}i\text{Pr}_2\text{C}_6\text{H}_3)\text{Cl}_2$ with 2 equivalents of *n*-butyllithium at -78°C have not been identified. However, we propose that this green species is the dialkyl $\text{Cp}^*\text{Ta}(\text{N-2,6-}i\text{Pr}_2\text{C}_6\text{H}_3)(n\text{Bu})_2$ and that decomposition yields the pseudo 3-coordinate species $[\text{Cp}^*\text{Ta}(\text{N-2,6-}i\text{Pr}_2\text{C}_6\text{H}_3)(\eta^2\text{-CH}_2\text{=CHEt})]$ and butane, since the phosphine-stabilised complex $\text{Cp}^*\text{Ta}(\text{N-2,6-}i\text{Pr}_2\text{C}_6\text{H}_3)(\eta^2\text{-CH}_2\text{=CHEt})(\text{PMe}_3)$ (**43**) is isolated in 58% yield when the reaction is performed in the presence of excess PMe_3 (Scheme 5.9 and 5.10). Interestingly, $\text{Cp}_2\text{Zr}(n\text{Bu})_2$ also displays similar reactivity,^{15,16} although for the titanocene analogue, the but-1-ene ligand is labile and $\text{Cp}_2\text{Ti}(\text{PMe}_3)_2$ is formed.¹⁶ This may be a result of the increased metal-carbon bond strength as the Group is descended, and may also reflect the enhanced back-bonding capacity of the heavier metals.



Scheme 5.9.

Triad representations¹⁷ of the four possible isomers of **43** (a–d), depending on the orientation of the ethyl substituent on the olefin, are shown in Figure 5.3. Three sets of resonances of comparable intensities are observed in the ^1H , ^{13}C and ^{31}P NMR spectra. These are thought to correspond to isomers **a**, **b** and **d**, since stereochemical models indicate that the environment of the but-1-ene ligand in **c**, compared to the other isomers, is energetically unfavourable due to steric repulsion between the ethyl group and the phosphine ligand and/or Cp^* ring.

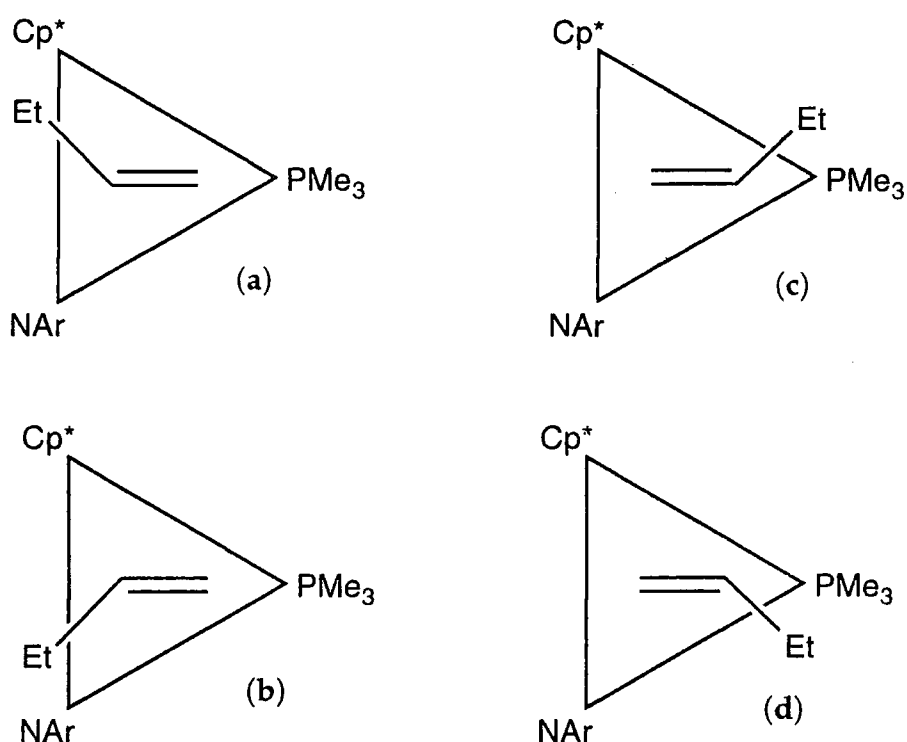


Figure 5.3. Triad Representation of the 4 Isomers of **43** (Ar=2,6-*i*Pr₂C₆H₃).

5.5.3.1. Reactivity of Cp*Ta(N-2,6-*i*Pr₂C₆H₃)(η^2 -CH₂=CHEt)(PMe₃) (**43**)

With excess C₂H₄: Slow elimination of the phosphine proceeds over 5 weeks at 60°C in d₆-benzene to eventually afford the substituted tantalacyclopentane Cp*Ta(N-2,6-*i*Pr₂C₆H₃)(σ -1,4-(2-Et)C₄H₇) (**41**). This again demonstrates that oxidative coupling products are stabilised by the [Cp*Ta(N-2,6-*i*Pr₂C₆H₃)] fragment. However, at elevated temperatures and in the presence of the displaced PMe₃, but-1-ene is subsequently released to give the ethylene-phosphine complex Cp*Ta(N-2,6-*i*Pr₂C₆H₃)(η^2 -CH₂=CH₂)(PMe₃); indeed, over 95% conversion to this species is observed after 8 weeks at 100°C. The elimination of but-1-ene rather than ethylene from **41** reflects the greater steric demand of the substituted olefin compared to C₂H₄.

With excess $\text{PhC}\equiv\text{CPh}$: The alkyne-phosphine complex $\text{Cp}^*\text{Ta}(\text{N-2,6-}i\text{Pr}_2\text{C}_6\text{H}_3)(\text{PhC}\equiv\text{CPh})(\text{PMe}_3)$ (**39**) and the tantalacyclopentadiene species $\text{Cp}^*\text{Ta}(\text{N-2,6-}i\text{Pr}_2\text{C}_6\text{H}_3)(\text{PhC}\equiv\text{CPh})_2$ (**40**), as postulated in Section 5.4.2 from the analogous reaction of $\text{Cp}^*\text{Ta}(\text{N-2,6-}i\text{Pr}_2\text{C}_6\text{H}_3)(\eta^2\text{-CH}_2=\text{CH}_2)(\text{PMe}_3)$ with $\text{PhC}\equiv\text{CPh}$, are generated after 8 weeks at 60°C and a further 2 days at 100°C respectively. This observation proves that the corresponding olefin ligands are not incorporated into the metallacyclic product and further supports the assignment of **40** as the tantalacyclopentadiene. Prolonged heating of the sample at 100°C eventually resulted in decomposition.

5.6. Summary

Investigations into the C–C oxidative coupling processes of half-sandwich tantalum imido systems concluded that the combination of ligands in the $[\text{Cp}^*\text{Ta}(\text{N-2,6-}i\text{Pr}_2\text{C}_6\text{H}_3)]$ fragment is particularly suitable for conferring stability upon corresponding metallacyclic derivatives. Hence, a number of new tantalacyclopentane complexes and related species, in particular those bearing the $\text{Cp}^*/\text{N-2,6-}i\text{Pr}_2\text{C}_6\text{H}_3$ moieties, have been prepared by the use of *n*-butyllithium.

A key feature of these reactions is the tendency for the but-1-ene ligand to be retained in the final product, while in the analogous zirconocene system, the but-1-ene is readily displaced by a variety of π -donor ligands. This difference indicates that the olefin ligands are more strongly bound in the tantalum complexes, possibly as a result of enhanced $d_\pi \rightarrow \pi^*$ back donation for the third row derivatives.

The chemistry of the $[\text{Cp}^*\text{Ta}(\text{N-2,6-}i\text{Pr}_2\text{C}_6\text{H}_3)]$ system described in this chapter is summarised in Scheme 5.10.

5.7. References

1. For recent reviews, see: (a) E. Negishi, 'Comprehensive Organic Synthesis', Ed. L. Paguette, Pergamon Press, New York, 1991, Vol.5, p.1163; (b) S.L. Buchwald, R.B. Nielson, *Chem. Rev.*, 1988, **88**, 1047; (c) R.D. Broene, S.L. Buchwald, *Science*, 1993, **261**, 1696.
2. (a) E. Negishi, F.E. Cederbaum, T. Takahashi, *Tetrahedron Lett.*, 1986, **27**, 2829; (b) E. Negishi, T. Takahashi, *Acc. Chem. Res.*, 1994, **27**, 124 and references therein.
3. (a) D.N. Williams, J.P. Mitchell, A.D. Poole, U. Siemeling, W. Clegg, D.C.R. Hockless, P.A. O'Neil, V. C. Gibson, *J. Chem. Soc., Dalton Trans.*, 1992, 739; (b) A.D. Poole, V.C. Gibson, W. Clegg, *J. Chem. Soc., Chem. Commun.*, 1992, 237; (c) U. Siemeling, V.C. Gibson, *J. Organomet. Chem.*, 1992, **426**, C25; (d) J.K. Cockcroft, V.C. Gibson, J.A.K. Howard, A.D. Poole, U. Siemeling, C. Wilson, *J. Chem. Soc., Chem. Commun.*, 1992, 1668; (e) A. D. Poole, Ph. D. Thesis, University of Durham, 1992.
4. Chapter 3 of this thesis.
5. J.-K.F. Buijink, J.H. Teuben, H. Kooijman, A.L. Spek, *Organometallics*, 1994, **13**, 2922.
6. V.C. Gibson, A.D. Poole, *J. Chem. Soc., Chem. Commun.*, 1995, 2261.
7. See G. Erker, C. Kruger, G. Muller, *Adv. Organomet. Chem.*, 1985, **24**, 1.
8. S. Schmidt, J. Sundermeyer, *J. Organomet. Chem.*, 1994, **472**, 127.
9. Reported during this work: M.V. Galakhov, M. Gómez, G. Jiménez, M.A. Pellinghelli, P. Royo, A. Tiripichio, *Organometallics*, 1994, **13**, 1564.
10. T.C. Baldwin, S.R. Huber, M.A. Bruck, D.E. Wigley, *Inorg. Chem.*, 1993, **32**, 5682.
11. (a) L.B. Kool, M.D. Rausch, H.G. Alt, M. Herberhold, U. Thewalt, B. Wolf, *Angew. Chem., Int. Ed. Engl.*, 1985, **24**, 394. (b) L.B. Kool, M.D. Rausch, H.G. Alt, M. Herberhold, B. Honold, U. Thewalt, *J. Organomet. Chem.*, 1987, **320**, 37.
12. (a) E. Negishi, Y. Nitto, J.C. Rousset, T. Seki, M. Saburi, T. Takahashi, *J. Am. Chem. Soc.*, 1991, **113**, 6266; (b) E. Negishi, M. Kageyama, V. Denisov, R. Hara, T. Takahashi, *Tetrahedron Lett.*, 1993, **34**, 687; (c) C. Coporet, E. Negishi, Z. Xi, T. Takahashi, *Tetrahedron Lett.*, 1994, **35**, 695
13. R.H. Grubbs, A. Miyashita, *J. Am. Chem. Soc.*, 1978, **100**, 7416.
14. L.D. Durfee, I.P. Rothwell, *Chem. Rev.*, 1988, **88**, 1059.

15. E. Negishi, S.J. Holmes, J.M. Tour, J.A. Miller, F.E. Cederbaum, D.R. Swanson, T. Takahashi, *J. Am. Chem. Soc.*, 1989, **111**, 3336.
16. P. Binger, P. Muller, R. Berm, A. Rufinska, B. Gabor, C. Kruger, P. Betz, *Chem. Ber.*, 1989, **122**, 1035.
17. V.C. Gibson, *J. Chem. Soc., Dalton Trans.*, 1994, 1607. V.C. Gibson, *Angew. Chem., Int. Ed. Engl.*, 1994, **33**, 1565.

Chapter 6

Experimental Details

6.1. General

6.1.1. Experimental and Characterisation Techniques

All manipulations of air and/or moisture sensitive materials were performed on a conventional vacuum/inert atmosphere line using standard Schlenk and cannular techniques, or in an inert atmosphere glove box.

Elemental analyses were performed by the microanalytical services of this department.

Infra red spectra were recorded on Perkin-Elmer 577 and 457 grating spectrophotometers using CsI windows. Absorptions abbreviated as: vs (very strong), s (strong), m (medium), w (weak), br (broad), sh (shoulder).

Mass spectra were recorded on a VG 7070E Organic Mass Spectrometer and performed by Dr M. Jones and Miss L.M. Turner.

Nuclear Magnetic Resonance spectra were recorded on the following instruments for the nuclei shown, unless stated otherwise (frequencies in parentheses): Bruker AMX500, ^1H (500.14 MHz), ^{13}C (125.76 MHz); Varian VXR400, ^1H (399.95 MHz), ^{13}C (100.58 MHz), ^{31}P (161.90 MHz), ^{19}F (376.29 MHz); Bruker AC250, ^1H (250.13 MHz), ^{13}C (62.90 MHz), ^{31}P (101.26 MHz), ^{19}F (235.34 MHz); Varian Gemini 200, ^1H (199.98 MHz). The following abbreviations have been used for band multiplicities : s (singlet), d (doublet), t (triplet), q (quartet), pent (pentet), sept (septet), m (multiplet). Chemical shifts are quoted in ppm for the following nuclei, unless stated otherwise (references in parentheses): ^1H (C_6D_6 : 7.15 ppm, C_7D_8 : 6.98 ppm, CDCl_3 : 7.26 ppm, CD_2Cl_2 : 5.35 ppm); ^{13}C (C_6D_6 : 128.0 ppm, CDCl_3 : 77.0 ppm, C_7D_8 : 125.2 ppm); ^{31}P (dilute aqueous H_3PO_4 , 0 ppm); ^{19}F (CFCl_3 : 0 ppm) (§ performed by Dr A.M. Kenwright and Mrs J.M. Say).

6.1.2. Purification and Preparation of Solvents and Reagents

The following NMR solvents were dried by vacuum distillation from phosphorus(V) oxide and stored under nitrogen or vacuum prior to use: benzene-d₆, toluene-d₈, chloroform-d, dichloromethane-d₂.

The following solvents were dried by prolonged reflux over a suitable drying agent, being freshly distilled and deoxygenated before use (drying agents in parentheses) : toluene (Na metal), petroleum ether 40-60°C (LiAlH₄), pentane (LiAlH₄), heptane (Na metal), tetrahydrofuran (sodium benzophenone ketyl), acetonitrile (CaH₂), dichloromethane (CaH₂), diethyl ether (LiAlH₄), 1,2-dichloroethane (CaH₂).

The following chemicals were prepared by previously published procedures: NaCp,¹ PMe₃,² CpNbCl₄,³ Me₃SiNHR (R=2,6-*i*Pr₂C₆H₃, 2-*t*BuC₆H₄, 2,6-Me₂C₆H₃),⁴ ⁿBu₃SnCp,⁵ CpSiMe₃,⁶ MAO,⁷ Zn(CH₂Ph)₂,⁸ CpTaCl₄,⁹ Cp*TaCl₄,¹⁰ PhMe₂CCH₂MgCl and Me₃CCH₂MgCl.¹¹

The following chemicals were obtained commercially and used as received unless stated otherwise : vanadium oxytrichloride (Aldrich), *t*-butylamine (Aldrich, distilled before use), 2,6-di(*isopropyl*)aniline (Aldrich, distilled before use), 2,6-dimethylaniline (Aldrich, distilled before use), zinc(II) chloride (Aldrich), benzylmagnesium chloride (Aldrich, 1.0M in diethyl ether), aniline (Aldrich, distilled before use), methylmagnesium bromide (Aldrich, 3.0M in diethyl ether), methylmagnesium chloride (Aldrich, 3.0M in tetrahydrofuran), diethylaluminium chloride (Aldrich, 1.8M in toluene), ethylene (Air Products), niobium pentachloride (Aldrich), chloromethylsilane (Aldrich, distilled before use), *n*-butyl lithium (Aldrich, 1.6M in hexane), 2,6-lutidine (Aldrich, distilled before use), 2-*t*-butylaniline

(Aldrich, distilled before use), 2,6-dichloroaniline (recrystallised in pentane), ethylmagnesium chloride (Aldrich, 2.0M in diethyl ether), n-propylmagnesium chloride (Aldrich, 2.0M in diethyl ether), magnesium turnings (Aldrich), phenylacetylene (Aldrich, distilled before use), diphenylacetylene (Aldrich), tantalum pentachloride (Fluka), pentafluorophenol (Fluorochem), carbon monoxide (Air Products).

6.2. Experimental Details for Chapter 2

6.2.1. Reaction of $\text{CpV}(\text{N}^t\text{Bu})\text{Cl}_2$ with 2,6-Dimethylaniline :

Preparation of $\text{CpV}(\text{N}-2,6\text{-Me}_2\text{C}_6\text{H}_3)\text{Cl}_2$ (1).

2,6-Dimethylaniline (1.20g, 9.89 mmol) was added to a stirred solution of $\text{CpV}(\text{N}^t\text{Bu})\text{Cl}_2$ (2.55g, 9.89 mmol) in 1,2-dichloroethane (120ml) at -30°C . The mixture was allowed to reach room temperature then heated at 75°C for 4 weeks. The resultant dark red solution was filtered and all volatile components were removed under reduced pressure to leave a red solid. Recrystallisation of the solid from pentane at -20°C afforded dark red crystals (Yield: 1.82g, 60%).

Elemental analysis for $\text{C}_{13}\text{H}_{14}\text{NCl}_2\text{V}$ (306.11) found (required) : %C = 50.84 (51.01), %H = 4.72 (4.61), %N = 4.56 (4.58).

Infra red data (Nujol, CsI, cm^{-1}) : 3090(w), 3070(w), 2710(w), 1575(m, sh), 1415(m), 1250(m), 1245(m), 1155(m), 1085(m, br), 1020(s), 1000(s), 960(w),

910(w), 860(vs), 810(vs), 800(m), 765(vs), 715(m), 575(w), 500(w), 460(m), 405(s), 395(s), 360(s), 315(s), 275(s, sh).

Mass spectral data (EI, m/z, ^{35}Cl) : 305 [M]⁺.

^1H NMR data (400MHz, C_6D_6 , 298K) : 2.39(s, 6H, *Me*), 5.83(s, 5H, C_5H_5), 6.50(t, 1H, $^3J_{\text{HH}}=7.4\text{Hz}$, *p*- C_6H_3), 6.56(d, 2H, $^3J_{\text{HH}}=7.2\text{Hz}$, *m*- C_6H_3).

^{13}C NMR data (126MHz, C_6D_6 , 298K) : 19.03(q, $^1J_{\text{CH}}=130\text{Hz}$, *Me*), 116.26(d, $^1J_{\text{CH}}=180\text{Hz}$, C_5H_5), 127.81(d, $^1J_{\text{CH}}=159\text{Hz}$, *m*- C_6H_3), 128.51(d, $^1J_{\text{CH}} = 161\text{Hz}$, *p*- C_6H_3), 139.49(s, *o*- C_6H_3), not resolved: *ipso*- C_6H_3 .

6.2.2. Reaction of $\text{CpV}(\text{N}^t\text{Bu})\text{Cl}_2$ with 2,6-Di(*isopropyl*)aniline :

Preparation of $\text{CpV}(\text{N-2,6-}^i\text{Pr}_2\text{C}_6\text{H}_3)\text{Cl}_2$ (2).

2,6-Di(*isopropyl*)aniline (0.48g, 2.68 mmol) was added to a stirred solution of $\text{CpV}(\text{N}^t\text{Bu})\text{Cl}_2$ (0.69g, 2.68 mmol) in 1,2-dichloroethane (60ml) at -30°C . The mixture was allowed to reach room temperature then stirred at 75°C for 2 weeks. The resultant dark red solution was filtered and the volatile components were removed under reduced pressure to leave a red solid. Recrystallisation of the solid from heptane (70°C), followed by concentration and cooling at -20°C afforded dark red crystals (Yield: 0.88g, 90%).

Elemental analysis for $\text{C}_{17}\text{H}_{22}\text{NCl}_2\text{V}$ (362.22) found (required) : %C = 56.33 (56.37), %H = 5.70 (6.12), %N = 3.60 (3.87).

Infra red data (Nujol, CsI , cm^{-1}) : 3090(w), 2700(w), 1570(m, sh), 1340(m), 1253(m, sh), 1217(w), 1090(m, br), 1047(m), 1020(m, br), 965(w), 925(m), 850(s),

812(vs), 795(vs), 855(vs), 718(m, sh), 560(w), 453(m), 425(m, sh), 390(s), 377(m), 307(s).

Mass spectral data (EI, m/z , ^{35}Cl) : 361 $[\text{M}]^+$.

^1H NMR data (400MHz, C_6D_6 , 298K) : 1.19(d, 12H, $^3J_{\text{HH}}=6.8\text{Hz}$, CHMe_2), 3.91(sept, 2H, $^3J_{\text{HH}}=6.9\text{Hz}$, CHMe_2), 5.90(s, 5H, C_5H_5), 6.74(t, 1H, $^3J_{\text{HH}}=7.8\text{Hz}$, $p\text{-C}_6\text{H}_3$), 6.83(d, 2H, $^3J_{\text{HH}}=7.6\text{Hz}$, $m\text{-C}_6\text{H}_3$).

^{13}C NMR data (100MHz, C_6D_6 , 298K) : 24.48(q, $^1J_{\text{CH}}=126\text{Hz}$, CHMe_2), 28.39(d, $^1J_{\text{CH}}=130\text{Hz}$, CHMe_2), 116.23(d, $^1J_{\text{CH}}=179\text{Hz}$, C_5H_5), 123.05(d, $^1J_{\text{CH}}=159\text{Hz}$, $m\text{-C}_6\text{H}_3$), 129.30(d, $^1J_{\text{CH}}=160\text{Hz}$, $p\text{-C}_6\text{H}_3$), 150.57(s, $o\text{-C}_6\text{H}_3$), not resolved: *ipso*- C_6H_3 .

6.2.3. Reaction of $\text{CpV}(\text{N}^t\text{Bu})\text{Cl}_2$ with $\text{Zn}(\text{CH}_2\text{Ph})_2$:

Preparation of $[\text{CpV}(\text{N}^t\text{Bu})(\mu\text{-Cl})_2]$ (3).

Cold toluene (-78°C) was added to a mixture of $\text{CpV}(\text{N}^t\text{Bu})\text{Cl}_2$ (0.43g, 1.65 mmol) and $\text{Zn}(\text{CH}_2\text{Ph})_2$ (0.41g, 1.65mmol). The suspension was stirred at -78°C for 30 minutes to afford a purple solution, then allowed to warm to room temperature and stirred for 3 hours. Solvent was removed from the resultant dark red solution under reduced pressure to leave a dark green solid. Extraction and recrystallisation of the solid with pentane afforded a dark red crystalline solid (Yield: 0.41g, 56%).

Elemental analysis for $\text{C}_{18}\text{H}_{28}\text{N}_2\text{Cl}_2\text{V}_2$ (445.21) found (required) : %C = 48.40 (48.56), %H = 6.39 (6.34), %N = 5.89 (6.29).

Infra red data (Nujol, CsI, cm^{-1}) : 1610(w), 1515(w), 1355(s), 1305(w), 1260(m), 1240(vs), 1210(s), 1125(m), 1100(m, sh), 1015(s), 845(m), 815(s), 790(vs), 730(m), 590(w), 560(m), 540(m), 450(w), 395(s), 360(m), 275(m).

Mass spectral data (EI, m/z, ^{35}Cl) : 444 $[\text{M}]^+$.

^1H NMR data (200MHz, C_6D_6 , 298K) : 1.20 (s, CMe_3), 6.24 (broad, C_5H_5).

6.2.4. Reaction of $\text{CpV}(\text{N}^t\text{Bu})\text{Cl}_2$ with PhCH_2MgCl :

Preparation of $[\text{CpV}(\mu\text{-N}^t\text{Bu})(\text{CH}_2\text{Ph})_2]$ (4).

PhCH_2MgCl (1.0M in Et_2O , 5.51ml, 5.51 mmol) was added *via* syringe to a solution of $\text{CpV}(\text{N}^t\text{Bu})\text{Cl}_2$ (0.65g, 2.50 mmol) in diethyl ether (40ml) at -78°C . A purple colouration can be observed immediately. The mixture was allowed to reach room temperature and stirred for 18 hours. The resultant deep red solution was filtered and all volatile components were removed under reduced pressure to leave a red solid. Extraction with acetonitrile followed by cooling at -20°C gave red crystals (Yield: 0.24g, 17%).

Elemental analysis for $\text{C}_{32}\text{H}_{42}\text{N}_2\text{V}_2$ (556.59) found (required) : %C = 68.78 (69.06), %H = 7.35 (7.61), %N = 5.37 (5.03).

Infra red data (Nujol, CsI, cm^{-1}) : 3060(w), 1595(m), 1485(m), 1355(m), 1260(s), 1180(s, sh), 1095(s), 1020(vs), 905(w), 800(vs), 750(m), 695(m), 525(w), 465(w).

Mass spectral data (CI, NH_4^+ , m/z) : 465 $[\text{M}-\text{CH}_2\text{Ph}]^+$.

^1H NMR data (400MHz, C_6D_6 , 298K) : 1.23(d, 2H, $^2J_{\text{HH}}=14.0\text{Hz}$, CH_2Ph), 1.38(s, 18H, CMe_3), 1.47(d, 2H, $^2J_{\text{HH}}=14.0\text{Hz}$, CH_2Ph), 5.66(s, 10H, C_5H_5), 6.88-7.22(m, 10H, *Ph*).

^{13}C NMR data (100MHz, C_6D_6 , 298K) : 34.18(q, $^1J_{\text{CH}}=126\text{Hz}$, CMe_3), 45.49(s, CMe_3), 78.46(t, $^1J_{\text{CH}}=117\text{Hz}$, CH_2Ph), 108.96(d, $^1J_{\text{CH}}=179\text{Hz}$, C_5H_5), 122.26, 126.16, 128.15(*o-*, *m-*, *p-*Ph), 155.20(s, *ipso*-Ph).

6.2.5. Reaction of $\text{CpV}(\text{N-2,6-}^i\text{Pr}_2\text{C}_6\text{H}_3)\text{Cl}_2$ with MeMgBr :

Preparation of $[\text{CpV}(\text{N-2,6-}^i\text{Pr}_2\text{C}_6\text{H}_3)(\mu\text{-Me}_2)]_2(\mu\text{-Mg})$ (5).

Methylmagnesium bromide (3.0M in diethyl ether, 1.00ml, 3.00 mmol) was added *via* syringe to a solution of $\text{CpV}(\text{N-2,6-}^i\text{Pr}_2\text{C}_6\text{H}_3)\text{Cl}_2$ (0.44g, 1.22 mmol) in diethyl ether (40ml) at -78°C . The mixture was allowed to warm up to room temperature then stirred for 12 hours. The resultant dark red solution was filtered from the off-white precipitate and the solvent was removed under reduced pressure to leave an oily red solid. Extraction of the solid with pentane followed by concentration and cooling to -5°C afforded red crystals (Yield: 0.23g, 28%).

Elemental analysis for $\text{C}_{38}\text{H}_{56}\text{N}_2\text{MgV}_2$ (667.08) found (required) : %C = 68.76 (68.42), %H = 8.66 (8.46), %N = 3.86 (4.20).

Infra red data (Nujol, CsI , cm^{-1}) : 3050(w), 1423(m), 1320(w), 1260(vs), 1197(m), 1095(vs, br), 1020(vs, br), 865(m), 800(vs), 755(m; sharp), 600(w), 555(w), 468(w), 400(m).

Mass spectral data (EI, m/z) : 666 $[\text{M}]^+$.

6.2.6. Reaction of $\text{CpV}(\text{N-2,6-}i\text{Pr}_2\text{C}_6\text{H}_3)\text{Cl}_2$ with MeMgCl :

Preparation of $[\text{CpV}(\mu\text{-N-2,6-}i\text{Pr}_2\text{C}_6\text{H}_3)]_2(\mu\text{-Me})$ (6).

Methylmagnesium chloride (3.0M in tetrahydrofuran, 2.34ml, 6.66 mmol) was added *via* syringe to a solution of $\text{CpV}(\text{N-2,6-}i\text{Pr}_2\text{C}_6\text{H}_3)\text{Cl}_2$ (0.80g, 2.22 mmol) in diethyl ether (60ml) at -78°C . The mixture was allowed to warm up to room temperature then stirred for 12 hours. The resultant dark red solution was filtered from the off-white precipitate and the solvent was removed under reduced pressure to leave a red solid. Extraction of the solid with pentane followed by concentration and cooling to -20°C afforded very dark red crystals (Yield: 0.61g, 46%).

Elemental analysis for $\text{C}_{35}\text{H}_{47}\text{N}_2\text{V}_2$ (597.66) found (required) : %C = 70.59 (70.34), %H = 8.22 (7.93), %N = 4.40 (4.69).

Infra red data (Nujol, CsI, cm^{-1}) : 3050(w), 1425(m), 1315(m), 1255(s), 1210(w), 1095(m, sh), 1012(s, sh), 962(w), 930(w), 798(vs), 752(s), 455(w), 415(w), 375(w).

Mass spectral data (EI, m/z) : 597 $[\text{M}]^+$, 582 $[\text{M-CH}_3]^+$.

6.2.7. Reaction of $\text{CpV}(\text{N}^t\text{Bu})\text{Cl}_2$ with Aniline :

Preparation of $\text{CpV}(\text{NPh})\text{Cl}_2$ (7).

Aniline (0.16ml, 1.77 mmol) was added to a solution of $\text{CpV}(\text{N}^t\text{Bu})\text{Cl}_2$ (0.46g, 1.77 mmol) in 1,2-dichloroethane (60ml) at -30°C . After warming to room temperature, the mixture was heated to 60°C and stirred for 2 weeks. All volatile components were then removed from the dark red solution under

reduced pressure to leave a red solid. Recrystallisation of the solid with pentane and subsequent cooling at -5°C afforded red/black crystals (Yield: 0.23g, 47%).

Elemental analysis for $\text{C}_{11}\text{H}_{10}\text{NCl}_2\text{V}$ (278.05) found (required) : %C = 47.46 (47.52), %H = 3.84 (3.63), %N = 4.69 (5.04).

Infra red data (Nujol, CsI, cm^{-1}) : 3070(w), 2730(w), 1600(m, br), 1455(s), 1415(m), 1260(s), 1095(s), 1020(s), 865(m), 800(s), 700(m), 510(w), 465(w).

^1H NMR data (250MHz, CDCl_3 , 298K) : 6.62(s, 5H, C_5H_5), 6.7-7.2(m, 5H, C_6H_5).

6.2.8. Preparation of Supported Catalyst

1,2-dichloroethane (75ml) was added to the copolymer of 9:1 styrene:4-aminostyrene (0.15g, 0.12mmol of 4-aminostyrene)¹² and $\text{CpV}(\text{N}^t\text{Bu})\text{Cl}_2$ (0.03g, 0.12 mmol) and the mixture was stirred for 10 days at 80°C . All volatile components were removed under reduced pressure and the resultant black solid was washed with CH_2Cl_2 (3 x 50ml) and dried *in vacuo* (Yield: 0.15g).

6.3. Experimental Details for Chapter 3

6.3.1. Reaction of CpNbCl_4 with $\text{Me}_3\text{SiNH}(2\text{-}^t\text{BuC}_6\text{H}_4)$:

Preparation of $\text{CpNb}(\text{N-}2^t\text{BuC}_6\text{H}_4)\text{Cl}_2$ (8).

To a stirring suspension of CpNbCl_4 (3.00g, 10.0mmol) in CH_2Cl_2 (70ml) was added a solution of 2,6-lutidine (1.07g, 10.0mmol) in CH_2Cl_2 (20 ml). To this was added dropwise at 0°C a solution of $\text{Me}_3\text{SiNH}(2\text{-}^t\text{BuC}_6\text{H}_4)$ (2.22g, 10.0mmol) in CH_2Cl_2 (40 ml). The mixture was stirred at room temperature for 8 hours to afford a clear red solution. The solvent was removed under reduced pressure to give an orange-yellow solid. Extraction from the solid with hot (70°C) heptane (3 x 100ml) afforded an orange solution which was filtered, concentrated and cooled at -20°C to give orange needle-like crystals (Yield: 2.71g, 72%).

Elemental analysis for $\text{C}_{15}\text{H}_{18}\text{NCl}_2\text{Nb}$ (376.13) found (required) : %C = 47.92 (47.90), %H = 4.93 (4.82), %N = 3.58 (3.72).

Infra red data (Nujol, CsI, cm^{-1}) : 3090(m), 3060(w), 1480(m), 1430(s), 1365(m), 1310(w), 1290(s), 1280(m, sh), 1160(w), 1090(m), 1050(w), 1020(s), 980(s), 930(w), 840(s, sh), 830(w), 820(vs), 815(m), 750(s), 740(s), 600(w), 390(s), 350(m), 340(m).

Mass spectral data (EI, m/z, ^{35}Cl) : 375 [M]⁺.

^1H NMR data (400MHz, C_6D_6 , 298K) : 1.55 (s, 9H, CMe_3), 5.80 (s, 5H, C_5H_5), 6.86 (t, 1H, $^3\text{J}_{\text{HH}}=7.4$ Hz, **H(4)**), 6.95 (d, 1H, $^3\text{J}_{\text{HH}}=8.0$ Hz, **H(6)**), 6.99 (t, 1H, $^3\text{J}_{\text{HH}}=7.3$ Hz, **H(5)**), 7.19 (d, 1H, $^3\text{J}_{\text{HH}}=7.8$ Hz, **H(3)**).

^{13}C NMR data (100MHz, C_6D_6 , 298K) : 30.44 (q, $J_{\text{CH}}=126$ Hz, CMe_3), 35.62 (s, CMe_3), 113.20 (dpent, $J_{\text{CH}}=178$ Hz, $^2J_{\text{CH}}=^3J_{\text{CH}}=6.7$ Hz, C_5H_5), 125.98 (d, $J_{\text{CH}}=156$ Hz, C(3)), 126.50 (d, $J_{\text{CH}}=160$ Hz, C(4)), 126.55 (d, $J_{\text{CH}}=160$ Hz, C(5)), 131.10 (d, $J_{\text{CH}}=160$ Hz, C(6)), 143.17 (s, C(2)), 155.46 (s, C(1)).

6.3.2. Reaction of $\text{CpNb}(\text{N}-2\text{-}^t\text{BuC}_6\text{H}_4)\text{Cl}_2$ with Trimethylphosphine :

Preparation of $\text{CpNb}(\text{N}-2\text{-}^t\text{BuC}_6\text{H}_4)(\text{PMe}_3)\text{Cl}_2$ (9).

PMe_3 (0.73g, 9.60 mmol) was condensed onto a frozen solution of $\text{CpNb}(\text{N}-2\text{-}^t\text{BuC}_6\text{H}_4)\text{Cl}_2$ (3.39g, 9.00 mmol) in toluene (50ml) at -196°C . On warming to room temperature an immediate reaction occurred, resulting in the formation of a yellow precipitate and red solution. After stirring for 2 hours, the supernatant solution was filtered from the yellow solid, which was collected and dried *in vacuo*. Recrystallisation of the solid from toluene at -20°C afforded yellow crystals. (Yield: 3.52g, 86%).

Elemental analysis for $\text{C}_{18}\text{H}_{27}\text{NCl}_2\text{NbP}$ (452.22) found (required) : %C = 48.00 (47.81), %H = 6.09 (6.02), %N = 2.95 (3.10).

Infra red data (Nujol, CsI , cm^{-1}) : 3080(w, br), 1420(s), 1280(s,sh), 1255(vs), 1080(vs,br), 1050(s), 1020(vs, br), 960(vs,sh), 870(w), 840(m), 820(vs), 800(vs), 755(vs), 600(w), 530(w), 450(w, br), 385(m), 355(m), 290(m), 250(m), 220(w).

Mass spectral data (EI, m/z, ^{35}Cl) : 375 $[\text{M}-\text{PMe}_3]^+$.

^1H NMR data (400MHz, CD_2Cl_2 , 298K) : 1.49 (s, 9H, CMe_3), 1.54 (d, 9H, $^2J_{\text{HP}}=9.2$ Hz, PMe_3), 6.42 (s, 5H, C_5H_5), 7.03 (t, 1H, $^3J_{\text{HH}}=7.6$ Hz, H(4)), 7.07 (d,

^1H , $^3\text{J}_{\text{HH}} = 8.0\text{Hz}$, $\text{H}(6)$), 7.17 (t, 1H , $^3\text{J}_{\text{HH}}=7.4\text{Hz}$, $\text{H}(5)$), 7.35 (d, 1H , $^3\text{J}_{\text{HH}}=7.8\text{Hz}$, $\text{H}(3)$).

^{13}C NMR data (100MHz, CD_2Cl_2 , 298K) : 15.14 (qd, $\text{J}_{\text{CH}}=131\text{Hz}$, $\text{J}_{\text{CP}}=25\text{Hz}$, PMe_3), 31.23 (q, $\text{J}_{\text{CH}}=124$, CMe_3), 36.06 (s, CMe_3), 111.31 (d, $\text{J}_{\text{CH}}=180\text{Hz}$, C_5H_5), 126.18 (d, $\text{J}_{\text{CH}}=164\text{Hz}$, $\text{C}(4)$), 126.31 (d, $\text{J}_{\text{CH}}=162\text{Hz}$, $\text{C}(5)$), 126.89 (d, $\text{J}_{\text{CH}}=152\text{Hz}$, $\text{C}(3)$), 129.92 (d, $\text{J}_{\text{CH}}=157\text{Hz}$, $\text{C}(6)$), 142.91 (s, $\text{C}(2)$), 155.60 (s, $\text{C}(1)$).

^{31}P NMR data (161MHz, CD_2Cl_2 , 298K) : 3.74 (s, broad, $\nu_{1/2}=291\text{Hz}$, PMe_3).

6.3.3. Reaction of $\text{CpNb}(\text{N}-2\text{-}^t\text{BuC}_6\text{H}_4)\text{Cl}_2$ with $\text{C}_2\text{H}_5\text{MgCl}$ in the presence of Trimethylphosphine :

Preparation of $\text{CpNb}(\text{N}-2\text{-}^t\text{BuC}_6\text{H}_4)(\eta^2\text{-C}_2\text{H}_4)(\text{PMe}_3)$ (10).

PMe_3 (0.27g, 3.55 mmol) was condensed onto a frozen solution of $\text{CpNb}(\text{N}-2\text{-}^t\text{BuC}_6\text{H}_4)\text{Cl}_2$ (0.267g, 0.71 mmol) in diethyl ether (50ml). An atmosphere of nitrogen was then introduced and a 2M diethyl ether solution of $\text{C}_2\text{H}_5\text{MgCl}$ (0.71 ml, 1.42 mmol) was added *via* syringe. The mixture was allowed to warm to room temperature to afford an orange suspension. After stirring for a further 20 hours, the orange supernatant solution was filtered from the solid residue (MgCl_2) and the volatile components removed under reduced pressure to leave an orange solid. The solid was extracted into pentane and the solution concentrated and cooled to -30°C to yield orange crystals. (Yield: 0.18g, 63%).

Elemental analysis for $\text{C}_{20}\text{H}_{31}\text{NNbP}$ (409.37) found (required) : %C = 58.27 (58.68), %H = 7.70 (7.63), %N = 3.03 (3.42).

Infra red data (Nujol, CsI, cm^{-1}) : 3040(w), 3020(w), 1580(m, sh), 1350(m), 1310(s), 1300(s), 1280(s), 1270(m), 1260(m), 1240(w), 1120(vs), 1085(m), 1040(m), 1010(m), 960(s), 950(s, sh), 870(w), 850(w), 840(w), 790(s, sh), 750(s), 740(vs), 730(w), 710(m), 660(w), 580(w), 500(w), 450(w), 340(w).

Mass spectral data (EI, m/z) : 409 $[\text{M}]^+$, 381 $[\text{M}-\text{C}_2\text{H}_4]^+$.

^1H NMR data (400MHz, C_6D_6 , 298K) : 0.57; 1.19; 1.42; 1.67 (m, 4H, C_2H_4), 0.93 (d, 9H, $^2\text{J}_{\text{PH}}=7.6\text{Hz}$, PMe_3), 1.49 (s, 9H, CMe_3), 5.38 (s, 5H, C_5H_5), 6.85 (t, 1H, $^3\text{J}_{\text{HH}}=7.6\text{Hz}$, $\text{H}(4)$), 6.98 (d, 1H, $^3\text{J}_{\text{HH}} = 7.6\text{Hz}$, $\text{H}(6)$), 7.05 (t, 1H, $^3\text{J}_{\text{HH}}=7.4\text{Hz}$, $\text{H}(5)$), 7.21 (d, 1H, $^3\text{J}_{\text{HH}}=7.6\text{Hz}$, $\text{H}(3)$).

^{13}C NMR data (100MHz, C_6D_6 , 298K) : 17.22 (qd, $\text{J}_{\text{CH}}=129\text{Hz}$, $\text{J}_{\text{CP}}=23\text{Hz}$, PMe_3), 26.43 (t, $\text{J}_{\text{CH}}=150\text{Hz}$, C_2H_4), 29.42 (q, $\text{J}_{\text{CH}}=125$, CMe_3), 30.35 (td, $\text{J}_{\text{CH}}=146\text{Hz}$, $^2\text{J}_{\text{CP}}=13\text{Hz}$, C_2H_4), 35.59 (s, CMe_3), 100.40 (dpent, $\text{J}_{\text{CH}}=172\text{Hz}$, $^2\text{J}_{\text{CH}}=^3\text{J}_{\text{CH}}=7\text{Hz}$, C_5H_5), 121.56 (d, $\text{J}_{\text{CH}}=160\text{Hz}$, $\text{C}(3)$), 125.831 (d, $\text{J}_{\text{CH}}=154\text{Hz}$, $\text{C}(4)$), 126.20 (d, $\text{J}_{\text{CH}}=159\text{Hz}$, $\text{C}(5)$), 132.78 (d, $\text{J}_{\text{CH}}=157\text{Hz}$, $\text{C}(6)$), 140.56 (s, $\text{C}(2)$), 156.58 (s, $\text{C}(1)$).

^{31}P NMR data (162MHz, C_6D_6 , 298K) : 17 (broad, $\nu_{1/2}=1100\text{Hz}$).

6.3.4. Reaction of $\text{CpNb}(\text{N}-2\text{-}^t\text{BuC}_6\text{H}_4)(\text{PMe}_3)\text{Cl}_2$ with $n\text{-C}_3\text{H}_7\text{MgCl}$:

Preparation of $\text{CpNb}(\text{N}-2\text{-}^t\text{BuC}_6\text{H}_4)(\eta^2\text{-C}_3\text{H}_6)(\text{PMe}_3)$ (11).

A 2.0M diethyl ether solution of $n\text{-C}_3\text{H}_7\text{MgCl}$ (1.9 ml, 3.76 mmol) was added *via* syringe to a frozen solution of $\text{CpNb}(\text{N}-2\text{-}^t\text{BuC}_6\text{H}_4)(\text{PMe}_3)\text{Cl}_2$ (0.85g, 1.88 mmol) in diethyl ether (50ml). The mixture was allowed to warm

to room temperature to afford an orange-red solution. After stirring for a further 15 hours, the supernatant solution was filtered from the solid residue and the volatile components removed under reduced pressure to leave a red solid. The solid was extracted into pentane and the solution concentrated and cooled to -20°C to afford large deep red crystals. (Yield: 0.68g, 86%).

Elemental analysis for $\text{C}_{21}\text{H}_{33}\text{NNbP}$ (423.39) found (required) : %C = 59.55 (59.57), %H = 7.94 (7.86), %N = 3.20 (3.31).

Infra red data (Nujol, CsI, cm^{-1}) : 3080(w), 3040(w), 2980(m), 1670(w, br), 1580(m), 1550(w), 1480(m), 1430(vs), 1365(m), 1355(m), 1310(vs), 1300(vs), 1285(vs), 1270(s), 1240(m), 1200(w), 1190(m), 1145(m, sh), 1125(m), 1090(m), 1050(s), 1015(s), 1005(s), 950(vs, sh), 930(s), 895(w), 860(m), 850(m), 830(m), 800(s), 780(vs, sh), 760(vs), 750(vs), 730(s), 670(m), 645(w), 590(m), 530(m), 500(m), 460(w), 325(m, sh).

Mass spectral data (EI, m/z) : 423 $[\text{M}]^+$, 381 $[\text{M}-\text{C}_3\text{H}_6]^+$.

^1H NMR data : (400 MHz, C_6D_6 , 298K) : 4 isomers observed, most abundant=a, least abundant=d.

- (a) 0.33, 1.36 (ddd, coupled to 2 protons and PMe_3 , $\text{CH}_2=\text{CHCH}_3$), 0.92 (d, 9H, $^2\text{J}_{\text{PH}}=7.2\text{Hz}$, PMe_3), 1.50 (s, 9H, CMe_3), 1.94 (d, 3H, $^3\text{J}_{\text{HH}}=6.4\text{Hz}$, $\text{CH}_2=\text{CHCH}_3$), 3.82 (s, broad, 1H, CH_2CHCH_3), 5.41 (d, 5H, $^3\text{J}_{\text{PH}}=1.6\text{Hz}$, C_5H_5), 6.85 (t, 1H, $^3\text{J}_{\text{HH}}=7.5\text{Hz}$, **H(4)**), 6.95 (d, 1H, $^3\text{J}_{\text{HH}}=7.6\text{Hz}$, **H(6)**), 7.05 (t, 1H, $^3\text{J}_{\text{HH}}=7.4\text{Hz}$, **H(5)**), 7.21 (d, 1H, $^3\text{J}_{\text{HH}}=7.8\text{Hz}$, **H(3)**).
- (b) 0.94 (d, 9H, $^2\text{J}_{\text{PH}}=7.2\text{Hz}$, PMe_3), 1.56 (s, 9H, CMe_3), 5.38 (d, 5H, $^3\text{J}_{\text{PH}}=1.6\text{Hz}$, C_5H_5).

- (c) 0.99 (d, 9H, $^2J_{\text{PH}}=7.6\text{Hz}$, PMe_3), 1.46 (s, 9H, CMe_3), 5.43 (d, 5H, $^3J_{\text{PH}}=1.6\text{Hz}$, C_5H_5).
- (d) 1.14 (d, 9H, $^2J_{\text{PH}}=8.0\text{Hz}$, PMe_3), 1.59 (s, 9H, CMe_3), 5.33 (d, 5H, $^3J_{\text{PH}}=1.6\text{Hz}$, C_5H_5).

Not assigned for (b) (c) and (d): $\text{CH}_2=\text{CHCH}_3$; $\text{H}(3)$; $\text{H}(4)$; $\text{H}(5)$; $\text{H}(6)$.

^{13}C NMR data (100MHz, C_6D_6 , 298K): 4 isomers observed, most abundant=a, least abundant=d.

- (a) 17.10 (qd, $J_{\text{CH}}=129\text{Hz}$, $J_{\text{CP}}=23\text{Hz}$, PMe_3), 25.78 (q, $\text{CH}_2=\text{CHCH}_3$), 29.50 (q, $J_{\text{CH}}=125\text{Hz}$, CMe_3), 35.59 (s, CMe_3), 101.19 (dpent, $J_{\text{CH}}=172\text{Hz}$, $^2J_{\text{CH}}=^3J_{\text{CH}}=6.6\text{Hz}$, C_5H_5), 121.52 (d, $J_{\text{CH}}=158\text{Hz}$, $\text{C}(3)$), 125.81 (d, $J_{\text{CH}}=155\text{Hz}$, $\text{C}(4)$), 126.24 (d, $J_{\text{CH}}=159\text{Hz}$, $\text{C}(5)$), 132.72 (d, $J_{\text{CH}}=157\text{Hz}$, $\text{C}(6)$), 140.44 (s, $\text{C}(2)$), 156.63 (s, $\text{C}(1)$), not assigned: $\text{CH}_2=\text{CHCH}_3$.
- (b) 18.02 (q, PMe_3), 24.79 (q, $\text{CH}_2=\text{CHCH}_3$), 29.59 (s, CMe_3), 101.42 (dpent, C_5H_5), 120.98 (d, $\text{C}(3)$), 125.88 (d, $\text{C}(4)$), 126.15 (d, $\text{C}(5)$), 132.12 (d, $\text{C}(6)$), 141.20 (s, $\text{C}(2)$), not assigned: $\text{CH}_2=\text{CHCH}_3$; CMe_3 ; $\text{C}(1)$.
- (c) 17.93 (q, PMe_3), 24.77 (q, $\text{CH}_2=\text{CHCH}_3$), 30.27 (s, CMe_3), 140.86 (s, $\text{C}(2)$), not assigned: $\text{CH}_2=\text{CHCH}_3$; CMe_3 ; C_5H_5 ; $\text{C}(3)$; $\text{C}(4)$; $\text{C}(5)$; $\text{C}(6)$; $\text{C}(1)$.
- No peaks assigned for (d).

^{31}P NMR data (161MHz, C_6D_6 , 298K):

- (a) 17.86 (s, broad, $\nu_{1/2}=971\text{Hz}$, PMe_3).

Not assigned for (b), (c) and (d).

6.3.5. Reduction of CpNb(N-2-^tBuC₆H₄)Cl₂ with Magnesium in the presence of Trimethylphosphine :

Preparation of CpNb(N-2-^tBuC₆H₄)(PMe₃)₂ (12).

PMe₃ (0.67g, 8.76 mmol) was condensed onto a solution of CpNb(N-2-^tBuC₆H₄)Cl₂ (0.82g, 2.19 mmol) and activated magnesium turnings (0.06g, 2.47 mmol) in THF (100 ml) cooled to -196°C. Upon warming to room temperature, a yellow suspension characteristic of the PMe₃ adduct was formed. After stirring for a further 20 hours, a dark green solution was observed. Removal of the volatile components under reduced pressure gave a dark green solid, which was extracted with pentane, concentrated and cooled to -30°C to afford extremely air-sensitive dark green crystals. (Yield: 0.74g, 74%).

Satisfactory elemental analysis has not been obtained for this compound due to its extreme air and moisture sensitivity.

Infra red data (Nujol, CsI, cm⁻¹) : 3070(w), 3030(w), 1885(w), 1580(s), 1550(w), 1460(vs), 1350(w), 1310(vs), 1280(s, sh), 1240(w), 1200(w), 1160(w), 1120(m), 1100(m, sh), 1050(s), 1020(s), 995(s, sharp), 950(vs, sh), 850(m), 820(m), 800(s, sh), 760(vs), 740(s), 710(s), 660(vs), 590(w), 520(m), 450(m, sh), 380(m), 365(m), 340(m).

Mass spectral data (EI, m/z) : 457 [M]⁺, 914 [M₂]⁺.

¹H NMR data (400MHz, C₆D₆, 298K) : 1.09 (d, 18H, ²J_{PH}=6.2Hz, PMe₃), 1.48 (s, 9H, CMe₃), 5.06 (s, 5H, C₅H₅), 6.91 (t, 1H, ³J_{HH}=7.4Hz, H(4)), 7.18 (t, 1H, ³J_{HH}=7.6Hz, H(5)), 7.33 (d, 1H, ³J_{HH}=8.0Hz, H(3)), 7.39 (d, 1H, ³J_{HH}=7.6Hz, H(6)).

^{13}C NMR data (100MHz, C_6D_6 , 298K) : 24.02 (dq, $J_{\text{CP}}=19\text{Hz}$, PMe_3), 29.29 (q, $J_{\text{CH}} = 125\text{Hz}$, CMe_3), 35.97 (s, CMe_3) , 93.85 (dpent, $J_{\text{CH}}=171\text{Hz}$, $^2J_{\text{CH}}=^3J_{\text{CH}}=7\text{Hz}$, C_5H_5), 119.05 (d, $J_{\text{CH}}=157\text{Hz}$, C(3)), 125.91 (d, $J_{\text{CH}}=151\text{Hz}$, C(4)), 126.30 (d, $J_{\text{CH}}=152\text{Hz}$, C(5)), 131.28 (d, $J_{\text{CH}}=152\text{Hz}$, C(6)), 140.27 (s, C(2)), 152.86 (s, C(1)).

^{31}P NMR data (162MHz, C_6D_6 , 298K) : 58 (very broad, $\nu_{1/2}\approx 4500\text{Hz}$).

6.3.6. Reaction of $\text{CpNb}(\text{N}-2\text{-}^t\text{BuC}_6\text{H}_4)(\text{PMe}_3)_2$ with Phenylacetylene:

Preparation of $\text{CpNb}(\text{N}-2\text{-}^t\text{BuC}_6\text{H}_4)(\text{PhC}\equiv\text{CH})(\text{PMe}_3)$ (13).

Pentane (50ml) was added to a mixture of $\text{CpNb}(\text{N}-2\text{-}^t\text{BuC}_6\text{H}_4)(\text{PMe}_3)_2$ (0.210g, 0.46 mmol) and phenylacetylene (0.056g, 0.55mmol) at room temperature and the mixture was stirred for 2 days. The red-brown solution was filtered, concentrated and cooled to -40°C to give a yellow-brown crystalline solid. (Yield: 0.13g, 59%).

Elemental analysis for $\text{C}_{26}\text{H}_{33}\text{NNbP}$ (483.45) found (required) : %C = 64.47 (64.60), %H = 7.27 (6.88), %N = 2.90 (2.90).

Infra red data (Nujol, CsI , cm^{-1}) : 3090(w), 3040(w), 1640(m), 1590(m), 1480(m), 1360(w), 1310(vs), 1285(s, sharp), 1270(m, sh), 1205(w), 1165(w), 1150(w), 1125(m), 1090(m), 1065(m), 1050(m), 1010(m), 1005(m), 965(s), 960(s), 950(s), 940(m), 840(w), 810(m), 790(vs), 760(s), 740(vs), 720(m), 690(s), 665(w), 625(w), 580(w), 520(m, sh), 470(m, sh), 380(w).

Mass spectral data (EI, m/z) : 483 $[\text{M}]^+$.

^1H NMR data (400MHz, C_6D_6 , 298K) : 1.02 (d, 9H, $^2\text{J}_{\text{PH}}=8.0\text{Hz}$, PMe_3), 1.39 (s, 9H, CMe_3), 5.67 (d, 5H, $^3\text{J}_{\text{PH}}=1.6\text{Hz}$, C_5H_5), 6.84 (t, 1H, $^3\text{J}_{\text{HH}}=7.6\text{Hz}$, $\text{H}(4)$), 6.92 (d, 1H, $^3\text{J}_{\text{HH}} = 7.6\text{Hz}$, $\text{H}(6)$), 7.07 (t, 1H, $^3\text{J}_{\text{HH}}=7.2\text{Hz}$, $\text{H}(5)$), 7.21 (t, 1H, $^3\text{J}_{\text{HH}} = 7.4\text{Hz}$, $p\text{-C}_6\text{H}_5$), 7.22 (d, 1H, $^3\text{J}_{\text{HH}}=8.0\text{Hz}$, $\text{H}(3)$), 7.43 (t, 1H, $^3\text{J}_{\text{HH}} = 7.8\text{Hz}$, $m\text{-C}_6\text{H}_5$), 8.03 (d, 1H, $^3\text{J}_{\text{HH}} = 8.0\text{Hz}$, $o\text{-C}_6\text{H}_5$), 8.47 (d, 1H, $^3\text{J}_{\text{PH}} = 12.4\text{Hz}$, $\text{PhC}\equiv\text{CH}$).

^{13}C NMR data (100MHz, C_6D_6 , 298K) : 16.88 (qd, $\text{J}_{\text{CH}}=129\text{Hz}$, $\text{J}_{\text{CP}}=25.1\text{Hz}$, PMe_3), 29.98 (q, $\text{J}_{\text{CH}}=126$, CMe_3), 35.67 (s, CMe_3), 102.19 (dpent, $\text{J}_{\text{CH}}=172\text{Hz}$, $^2\text{J}_{\text{CH}}=^3\text{J}_{\text{CH}}=6.8\text{Hz}$, C_5H_5), 121.88 (d, $\text{J}_{\text{CH}}=158\text{Hz}$, $\text{C}(4)$), 125.87 (d, $\text{J}_{\text{CH}}=156\text{Hz}$, $\text{C}(3)$), 125.94 (d, $\text{J}_{\text{CH}}=156\text{Hz}$, $\text{C}(5)$), 127.24 (d, $\text{J}_{\text{CH}}=156\text{Hz}$, $p\text{-C}_6\text{H}_5$), 128.53 (d, $\text{J}_{\text{CH}}=158\text{Hz}$, $m\text{-C}_6\text{H}_5$), 130.26 (d, $\text{J}_{\text{CH}}=157\text{Hz}$, $\text{C}(6)$), 131.49 (d, $\text{J}_{\text{CH}}=158\text{Hz}$, $o\text{-C}_6\text{H}_5$), 139.05 (s, $ipso\text{-C}_6\text{H}_5$), 141.67 (s, $\text{C}(2)$), 143.53 (dd, $\text{J}_{\text{CH}}=179\text{Hz}$, $^2\text{J}_{\text{CP}}=29.4\text{Hz}$, $\text{PhC}\equiv\text{CH}$), 157.23 (s, $\text{C}(1)$), 166.58 (s, $\text{PhC}\equiv\text{CH}$).

^{31}P NMR data (162MHz, C_6D_6 , 298K) : 14.2 (broad, $\nu_{1/2}=530\text{Hz}$).

6.3.7. Reaction of $\text{CpNb}(\text{N-2-}^t\text{BuC}_6\text{H}_4)(\text{PMe}_3)_2$ with Diphenylacetylene:

Preparation of $\text{CpNb}(\text{N-2-}^t\text{BuC}_6\text{H}_4)(\text{PhC}\equiv\text{CPh})(\text{PMe}_3)$ (14).

Pentane (30ml) was added to $\text{CpNb}(\text{N-2-}^t\text{BuC}_6\text{H}_4)(\text{PMe}_3)_2$ (0.167g, 0.37 mmol) and diphenylacetylene (0.065g, 0.37mmol) at room temperature and the mixture was stirred at 40°C for 4 weeks. The brown solution was filtered, concentrated and cooled to 0°C to yield yellow-brown crystals. (Yield: 0.14g, 68%).

Elemental analysis for $C_{32}H_{37}NNbP$ (559.56) found (required) : %C = 68.34 (68.69), %H = 6.73 (6.67), %N = 2.25 (2.50).

Infra red data (Nujol, CsI, cm^{-1}) : 3070(w), 3040(w), 1695(s, sh), 1595(m, sh), 1440(m), 1360(m), 1310(s), 1290(s), 1265(s, sh), 1120(w), 1090(w), 1070(w), 1050(m), 1010(m, sh), 955(s, sh), 890(w), 840(w), 790(vs), 780(m), 760(m), 750(s), 740(m), 730(m), 700(s, sharp), 695(s, sharp), 580(m), 455(m), 400(w).

Mass spectral data (EI, m/z) : 560 [M]⁺.

1H NMR data (400MHz, C_6D_6 , 298K) : 0.89 (d, 9H, $^2J_{PH}=8.4Hz$, PMe_3), 1.45 (s, 9H, CMe_3), 5.72 (d, 5H, $^3J_{PH}=1.6Hz$, C_5H_5), 6.8-7.3 (m, $H(3)$, $H(4)$, $H(5)$, $H(6)$, *o*- C_6H_5 (*endo*), *m*- C_6H_5 (*endo* & *exo*), *p*- C_6H_5 (*endo* & *exo*)), 7.89 (d, 1H, $^3J_{HH} = 8.4Hz$, *o*- C_6H_5 (*exo*)).

^{13}C NMR data (100MHz, C_6D_6 , 298K) : 16.92 (qd, $J_{CH}=129Hz$, $J_{CP}=23.6Hz$, PMe_3), 30.06 (q, $J_{CH}=125$, CMe_3), 35.65 (s, CMe_3), 102.50 (dpent, $J_{CH}=173Hz$, $^2J_{CH}=^3J_{CH}=7.0Hz$, C_5H_5), 122.58 (d, $J_{CH}=158Hz$, $C(3)$), 123.65 (d, $J_{CH}=158Hz$, *p*- C_6H_5 (*endo*)), 125.00 (d, $J_{CH}=160Hz$, *o*- C_6H_5 (*endo*)), 125.95 (d, $J_{CH}=157Hz$, $C(4)$), 126.04 (d, $J_{CH}=155Hz$, $C(5)$), 126.98 (d, $J_{CH}=159Hz$, *p*- C_6H_5 (*exo*)), 128.43 (d, $J_{CH}=157Hz$, *m*- C_6H_5 (*endo*)), 128.48 (d, $J_{CH}=157Hz$, *m*- C_6H_5 (*exo*)), 130.71 (d, $J_{CH}=157Hz$, $C(6)$), 131.16 (d, $J_{CH}=158Hz$, *o*- C_6H_5 (*exo*)), 138.64 (s, *ipso*- C_6H_5 (*endo*)), 142.33 (s, $C(2)$), 151.82 (s, *ipso*- C_6H_5 (*exo*)), 156.88 (s, $C(1)$), 157.44 (d, $^2J_{CP}=22.1Hz$, $C\equiv C$ (*endo*)), 162.01 (s, $C\equiv C$ (*exo*)).

^{31}P NMR data (162MHz, C_6D_6 , 298K) : 9.8 (broad, $\nu_{1/2}=405Hz$).

6.3.8. Reaction of CpNbCl_4 with $\text{Me}_3\text{SiNH}(2,6\text{-Cl}_2\text{C}_6\text{H}_3)$:

Preparation of $\text{CpNb}(\text{N}-2,6\text{-Cl}_2\text{C}_6\text{H}_3)\text{Cl}_2$ (15).

To a stirring suspension of CpNbCl_4 (3.00g, 10.0mmol) in CH_2Cl_2 (70ml) was added a solution of 2,6-lutidine (1.07g, 10.0mmol) in CH_2Cl_2 (20 ml). A solution of $\text{Me}_3\text{SiNH}(2,6\text{-Cl}_2\text{C}_6\text{H}_3)$ (2.43g, 10.0mmol) in CH_2Cl_2 (40 ml) was added dropwise to this at 0°C . The mixture was stirred at room temperature for 14 hours to afford a clear orange-red solution. The solvent was removed under reduced pressure to give an orange solid. Extraction from this solid with acetonitrile afforded a red solution which was filtered, concentrated and cooled at -20°C to give an orange-red solid (Yield: 2.26g, 58%).

Elemental analysis for $\text{C}_{11}\text{H}_8\text{NCl}_4\text{Nb}$ (388.91) found (required) : %C = 33.75 (33.97), %H = 2.21 (2.07), %N = 3.41 (3.60).

Infra red data (Nujol, CsI, cm^{-1}) : 3100(m), 1920(w), 1850(w), 1770(w), 1540(m), 1440(s, sh), 1360(vs), 1260(m), 1190(s), 1150(w), 1100(m), 1070(m), 1020(m), 1010(m), 980(vs), 965(m), 865(s), 820(vs), 790(vs), 770(vs), 575(s), 550(m), 470(m, sh), 410(s), 380(vs), 365(vs), 340(vs), 305(m, sh).

Mass spectral data (EI, m/z, ^{35}Cl) : 387 $[\text{M}]^+$

(Cl, NH_4^+ , m/z, ^{37}Cl) : 390 $[\text{M}+\text{H}]^+$, 407 $[\text{M}+\text{NH}_4]^+$.

^1H NMR data (400MHz, CDCl_3 , 298K) : 6.65 (s, 5H, C_5H_5), 6.87 (t, 1H, $^3\text{J}_{\text{HH}} = 8.0\text{Hz}$, *p*-2,6- $\text{Cl}_2\text{C}_6\text{H}_3$), 7.25 (d, 2H, $^3\text{J}_{\text{HH}} = 8.4\text{Hz}$, *m*-2,6- $\text{Cl}_2\text{C}_6\text{H}_3$).

^{13}C NMR data (100MHz, CDCl_3 , 298K): 114.68 (dpent, $\text{J}_{\text{CH}} = 179\text{Hz}$, $^2\text{J}_{\text{CH}} = ^3\text{J}_{\text{CH}} = 6.7\text{Hz}$, C_5H_5), 125.81 (d, $\text{J}_{\text{CH}} = 164\text{Hz}$, *p*-2,6- $\text{Cl}_2\text{C}_6\text{H}_3$), 127.78 (d,

$J_{\text{CH}}=167\text{Hz}$, *m*-2,6- $\text{Cl}_2\text{C}_6\text{H}_3$), 131.69 (m, *o*-2,6- $\text{Cl}_2\text{C}_6\text{H}_3$), 148.89 (s, *ipso*-2,6- $\text{Cl}_2\text{C}_6\text{H}_3$).

6.3.9. Reaction of $\text{CpNb}(\text{N-2,6-Cl}_2\text{C}_6\text{H}_3)\text{Cl}_2$ with Trimethylphosphine :

Preparation of $\text{CpNb}(\text{N-2,6-Cl}_2\text{C}_6\text{H}_3)(\text{PMe}_3)\text{Cl}_2$ (16).

PMe_3 (0.294g, 3.86 mmol) was condensed onto a frozen solution of $\text{CpNb}(\text{N-2,6-Cl}_2\text{C}_6\text{H}_3)\text{Cl}_2$ (0.224g, 0.576 mmol) in toluene (50ml) at -196°C . On warming to room temperature an immediate reaction occurred, resulting in the formation of a yellow precipitate and solution. After stirring for 5 hours, the supernatant solution was filtered from the yellow solid, which was collected and dried *in vacuo*. (Yield: 0.22g, 84%).

Elemental analysis for $\text{C}_{14}\text{H}_{17}\text{NCl}_4\text{NbP}$ (464.99) found (required) : %C = 36.23 (36.16), %H = 3.74 (3.69), %N = 2.77 (3.01).

Infra red data (Nujol, CsI , cm^{-1}) : 3120(w), 2980(w), 1540(w), 1450(s), 1360(m), 1310(m), 1290(m), 1260(m), 1195(m), 1150(w), 1090(s, br), 1020(s, br), 960(s, sh), 860(w), 820(s), 805(vs), 790(vs), 770(s), 740(m), 725(s), 670(w), 580(w), 375(w), 320(m, sh), 280(s).

Mass spectral data (EI, m/z , ^{37}Cl) : 389 $[\text{M-PMe}_3]^+$.

^1H NMR data (400MHz, CDCl_3 , 298K) : 1.57 (d, 9H, $^2J_{\text{PH}}=9.6\text{Hz}$, PMe_3), 6.50 (d, 5H, $^3J_{\text{PH}}=2.4\text{Hz}$, C_5H_5), 6.85 (t, 1H, $^3J_{\text{HH}}=8.2\text{Hz}$, *p*-2,6- $\text{Cl}_2\text{C}_6\text{H}_3$), 7.23 (d, 2H, $^3J_{\text{HH}}=8.0\text{Hz}$, *m*-2,6- $\text{Cl}_2\text{C}_6\text{H}_3$).

^{13}C NMR data (100MHz, CDCl_3 , 298K) : 14.91 (qd, $J_{\text{CH}}=131\text{Hz}$, $J_{\text{CP}}=27\text{Hz}$, PMe_3), 112.55 (dpent, $J_{\text{CH}}=178\text{Hz}$, $^2J_{\text{CH}}=^3J_{\text{CH}}=7\text{Hz}$, C_5H_5), 125.72 (d, $J_{\text{CH}}=165\text{Hz}$, *p*-2,6- $\text{Cl}_2\text{C}_6\text{H}_3$), 128.35 (d, $J_{\text{CH}}=166\text{Hz}$, *m*-2,6- $\text{Cl}_2\text{C}_6\text{H}_3$), 131.32 (s, *o*-2,6- $\text{Cl}_2\text{C}_6\text{H}_3$), 148.82 (s, *ipso*-2,6- $\text{Cl}_2\text{C}_6\text{H}_3$).

^{31}P NMR data (162MHz, CDCl_3 , 298K) : 7.81 (s, broad, $\nu_{1/2}=219\text{Hz}$, PMe_3).

6.3.10. Reaction of $\text{CpNb}(\text{N-2,6-Cl}_2\text{C}_6\text{H}_3)\text{Cl}_2$ with $\text{C}_2\text{H}_5\text{MgCl}$ in the presence of Trimethylphosphine :

Preparation of $\text{CpNb}(\text{N-2,6-Cl}_2\text{C}_6\text{H}_3)(\eta^2\text{-C}_2\text{H}_4)(\text{PMe}_3)$ (17).

PMe_3 (0.49g, 6.45 mmol) was condensed onto a frozen solution of $\text{CpNb}(\text{N-2,6-Cl}_2\text{C}_6\text{H}_3)\text{Cl}_2$ (0.500g, 1.29 mmol) in diethyl ether (100ml). An atmosphere of nitrogen was then introduced and a 2M diethyl ether solution of $\text{C}_2\text{H}_5\text{MgCl}$ (1.29 ml, 2.58 mmol) was added *via* syringe. The mixture was allowed to warm to room temperature to afford an orange suspension. After stirring for a further 24 hours, the red supernatant solution was filtered from the solid residue (MgCl_2) and the volatile components removed under reduced pressure to leave a red solid. The solid was extracted into pentane and the solution concentrated and cooled to -30°C to yield small red crystals. (Yield: 0.23g, 43%).

Elemental analysis for $\text{C}_{16}\text{H}_{21}\text{NCl}_2\text{NbP}$ (422.14) found (required) : %C = 45.16 (45.52), %H = 5.03 (5.01), %N = 3.11 (3.32).

Infra red data (Nujol, CsI , cm^{-1}) : 3020(w), 1460(s), 1330(m, sh), 1280(m), 1260(m), 1185(m), 1130(s), 1090(m, br), 1065(m), 1010(m, sh), 960(s), 945(m),

930(m), 875(w), 835(w), 800(s), 785(s), 775(s), 760(s), 720(s), 660(w), 500(w), 450(w), 370(w), 340(w).

Mass spectral data (EI, m/z, ^{35}Cl) : 421 [M]⁺, 393 [M-C₂H₄]⁺.

¹H NMR data (400MHz, C₇D₈, 298K) : 0.98 (d, 9H, $^2J_{\text{PH}}=7\text{Hz}$, PMe₃), 1.78 (broad, C₂H₄), 5.38 (s, 5H, C₅H₅), 6.17 (t, 1H, $^3J_{\text{HH}}=8\text{Hz}$, *p*-2,6-Cl₂C₆H₃), 6.91 (d, 2H, $^3J_{\text{HH}}=8\text{Hz}$, *m*-2,6-Cl₂C₆H₃).

¹³C NMR data (100MHz, C₆D₆, 298K) : 17.27 (qd, $J_{\text{CH}}=129\text{Hz}$, $J_{\text{CP}}=24\text{Hz}$, PMe₃), 29 (broad, $\nu_{1/2}=300\text{Hz}$, C₂H₄), 101.27 (dpent, $J_{\text{CH}}=172\text{Hz}$, $^2J_{\text{CH}}=^3J_{\text{CH}}=7\text{Hz}$, C₅H₅), 120.01 (d, $J_{\text{CH}}=165\text{Hz}$, *p*-2,6-Cl₂C₆H₃), 128.02 (d, $J_{\text{CH}}=164\text{Hz}$, *m*-2,6-Cl₂C₆H₃), 131.50 (s, *o*-2,6-Cl₂C₆H₃), not assigned: *ipso*-2,6-Cl₂C₆H₃.

³¹P NMR data (162MHz, C₆D₆, 298K) : 25 (broad, $\nu_{1/2}=2000\text{Hz}$).

6.4. Experimental Details For Chapter 4

6.4.1. Reaction of Cp*Ta(N^tBu)Cl₂ with Benzylmagnesium chloride:

Preparation of Cp*Ta(N^tBu)(CH₂Ph)₂ (20).

Benzylmagnesium chloride (1.0M in Et₂O, 4.09ml, 4.09 mmol) was added *via* syringe to a stirred solution of Cp*Ta(N^tBu)Cl₂ (0.89g, 1.95 mmol) in diethyl ether (50ml) at -78°C. The mixture was allowed to warm up to room temperature to give a yellow solution and white precipitate. After 11

hours, all volatile components were removed under reduced pressure to leave a yellow solid. Extraction with pentane followed by removal of solvent *in vacuo* afforded a bright yellow solid (Yield: 0.89g, 88%).

Elemental analysis for $C_{28}H_{38}NTa$ (569.57) found (required) : %C = 58.58 (59.05), %H = 6.88 (6.73), %N = 2.52 (2.46).

Infra red data (Nujol, CsI, cm^{-1}) : 3075(w), 3055(w), 3015(m), 2730(w), 1925(w), 1595(s), 1485(s), 1350(s), 1305(w), 1265(vs), 1205(s), 1180(w), 1095(m), 1055(m), 1030(m), 950(w), 890(w), 800(s), 745(vs), 695(vs), 560(w), 535(w), 495(w), 430(w), 405(w).

Mass spectral data (EI, m/z) : 570 [M]⁺.

¹H NMR data (400MHz, C_6D_6 , 298K) : 1.09(s, 9H, CMe_3), 1.38(d, 2H, ²J_{HH}=12.0Hz, CH_2Ph), 1.77(s, 15H, C_5Me_5), 2.07(d, 2H, ²J_{HH}=12.0Hz, CH_2Ph), 6.93(t, 2H, ³J_{HH}=7.2Hz, *p*-Ph), 7.05(d, 4H, ³J_{HH}=7.2Hz, *o*-Ph), 7.20(t, 4H, ³J_{HH}=7.2Hz, *m*-Ph).

¹³C NMR data (100MHz, C_6D_6 , 298K) : 11.36(q, ¹J_{CH}=127Hz, C_5Me_5), 33.20(q, ¹J_{CH}=126Hz, CMe_3), 65.17(s, CMe_3), 71.28(t, ¹J_{CH}=119Hz, CH_2Ph), 115.91(s, C_5Me_5), 122.82(d, ¹J_{CH}=158Hz, *p*-Ph), 128.05(d, ¹J_{CH}=158Hz, *m*-Ph), 128.85(d, ¹J_{CH}=160Hz, *o*-Ph), 149.35(s, *ipso*-Ph).

6.4.2. Reaction of $Cp^*Ta(N^tBu)Cl_2$ with Neophylmagnesium chloride:

Preparation of $Cp^*Ta(N^tBu)(CH_2CMe_2Ph)_2$ (21).

Neophylmagnesium chloride (1.29M in Et_2O , 1.35ml, 1.74 mmol) was added *via* syringe to a solution of $Cp^*Ta(N^tBu)Cl_2$ (0.38g, 0.83 mmol) in

diethyl ether (40ml) at -78°C . The mixture was allowed to warm up to room temperature and stirred for 18 hours to give a dark yellow solution and white precipitate. All volatile components were removed under reduced pressure and extraction with pentane followed by removal of solvent *in vacuo* afforded a brown oily solid. Recrystallisation in acetonitrile at 0°C yielded yellow crystals (Yield: 0.28g, 52%).

Elemental analysis for $\text{C}_{34}\text{H}_{50}\text{NTa}$ (653.72) found (required) : %C = 62.19 (62.47), %H = 7.77 (7.71), %N = 2.49 (2.14).

Infra red data (Nujol, CsI , cm^{-1}) : 3085(m), 3055(m), 3015(m), 2790(w), 2730(w), 2200(w), 1990(s), 1935(w), 1595(m), 1495(s), 1355(s), 1255(vs), 1215(m), 1180(m), 1135(w), 1080(m), 1030(s), 950(w), 900(w), 805(m), 765(vs), 695(vs), 585(m), 565(m), 535(m).

Mass spectral data (EI, m/z) : 654 $[\text{M}]^{+}$.

^1H NMR data (400MHz, C_6D_6 , 298K) : -0.42(d, 2H, $^2\text{J}_{\text{HH}}=13.0\text{Hz}$, CH_2), 1.46(s, 9H, CMe_3), 1.58(d, 2H, $^2\text{J}_{\text{HH}}=13.0\text{Hz}$, CH_2), 1.62(s, 6H, CMe_2Ph), 1.70(s, 15H, C_5Me_5), 1.79(s, 6H, CMe_2Ph), 7.09(t, 2H, $^3\text{J}_{\text{HH}}=7.6\text{Hz}$, *p*-Ph), 7.24(t, 4H, $^3\text{J}_{\text{HH}}=7.6\text{Hz}$, *m*-Ph), 7.43(d, 4H, $^3\text{J}_{\text{HH}}=8.4\text{Hz}$, *o*-Ph).

^{13}C NMR data (100MHz, C_6D_6 , 298K) : 11.58(q, $^1\text{J}_{\text{CH}}=127\text{Hz}$, C_5Me_5), 33.86(q, $^1\text{J}_{\text{CH}}=126\text{Hz}$, CMe_2Ph), 34.12(q, $^1\text{J}_{\text{CH}}=126\text{Hz}$, CMe_3), 35.19(q, $^1\text{J}_{\text{CH}}=126\text{Hz}$, CMe_2Ph), 41.54(s, CMe_2Ph), 65.40(s, CMe_3), 91.52(t, $^1\text{J}_{\text{CH}}=109\text{Hz}$, CH_2), 115.60(s, C_5Me_5), 125.15(d, $^1\text{J}_{\text{CH}}=160\text{Hz}$, *p*-Ph), 125.96(d, $^1\text{J}_{\text{CH}}=157\text{Hz}$, *m*-Ph), 128.17(d, $^1\text{J}_{\text{CH}}=159\text{Hz}$, *o*-Ph), 155.28(s, *ipso*-Ph).

6.4.3. Reaction of Cp*Ta(N^tBu)Cl₂ with Neopentylmagnesium chloride:

Preparation of Cp*Ta(N^tBu)(CH₂CMe₃)₂ (22).

Neopentylmagnesium chloride (0.82M in Et₂O, 4.98ml, 4.09 mmol) was added *via* syringe to a solution of Cp*Ta(N^tBu)Cl₂ (0.85g, 1.86 mmol) in diethyl ether (60ml) at -78°C. The mixture was allowed to warm up to room temperature and stirred for 12 hours. The resultant yellow solution was filtered from the white precipitate and all volatile components were removed under reduced pressure to give a yellow solid. Extraction with pentane followed by recrystallisation in acetonitrile at -20°C yielded yellow crystals (Yield: 0.87g, 88%).

Elemental analysis for C₂₄H₄₆NTa (529.59) found (required) : %C = 54.27 (54.43), %H = 8.89 (8.76), %N = 2.67 (2.64).

Infra red data (Nujol, CsI, cm⁻¹) : 2780(w), 2740(w), 2710(w), 2365(w), 2340(w), 1355(s), 1255(s), 1210(s), 1135(m), 1100(m), 1020(m), 975(m), 805(s), 755(m), 670(w), 535(m), 475(w).

Mass spectral data (CI, NH₄⁺, m/z) : 530 [M+H]⁺.

¹H NMR data (400MHz, C₆D₆, 298K) : -0.61(d, 2H, ²J_{HH}=12.8Hz, CH₂), 1.35(s, 18H, CH₂CMe₃), 1.39(d, 2H, ²J_{HH}=12.8Hz, CH₂), 1.51(s, 9H, NCM₃), 1.79(s, 15H, C₅Me₅).

¹³C NMR data (100MHz, C₆D₆, 298K) : 11.73(q, ¹J_{CH}=127Hz, C₅Me₅), 34.29(q, ¹J_{CH}=126Hz, NCM₃), 34.76(s, CH₂CMe₃), 35.56(q, ¹J_{CH}=124Hz, CH₂CMe₃), 65.28(s, NCM₃), 90.36(t, ¹J_{CH}=106Hz, CH₂), 115.34(s, C₅Me₅).

6.4.4. Generation of $[\text{Cp}^*\text{Ta}(\text{N}^t\text{Bu})(\text{CH}_2\text{Ph})]^+[\text{B}(\text{C}_6\text{F}_5)_4]^-$ (23).

In the treatment of $\text{Cp}^*\text{Ta}(\text{N}^t\text{Bu})(\text{CH}_2\text{Ph})_2$ with one equivalent of $\text{Ph}_3\text{C B}(\text{C}_6\text{F}_5)_4$ or $\text{PhMe}_2\text{NH B}(\text{C}_6\text{F}_5)_4$ in C_6D_6 in an NMR tube, the following resonances have been assigned to $[\text{Cp}^*\text{Ta}(\text{N}^t\text{Bu})(\text{CH}_2\text{Ph})]^+[\text{B}(\text{C}_6\text{F}_5)_4]^-$:

^1H NMR data (400MHz, CD_2Cl_2 , 298K) : 1.26(s, 9H, CMe_3), 2.26(s, 15H, C_5Me_5), 2.96(s, 2H, CH_2Ph), 6.78(d, 2H, *o*-Ph), 6.8–7.6(m, 3H, *m*- and *p*-Ph).

^{13}C NMR data (100MHz, proton decoupled, CD_2Cl_2 , 298K) : 12.02(C_5Me_5), 32.80(CMe_3), 65.60(CH_2Ph), 66.32(CMe_3), 119.96(C_5Me_5), 122–150(Ph).

^{19}F NMR data (376MHz, CD_2Cl_2 , 298K) : -133.08(d, 2F, $^3J_{\text{FF}}=18.6\text{Hz}$, *o*- C_6F_5), -163.35(t, 2F, $^3J_{\text{FF}}=20.3\text{Hz}$, *m*- C_6F_5), -167.32(t, 1F, $^3J_{\text{FF}}=22.4\text{Hz}$, *p*- C_6F_5).

6.4.5. Reaction of $\text{Cp}^*\text{Ta}(\text{N}^t\text{Bu})(\text{CH}_2\text{Ph})_2$ with Pentafluorophenol:

Preparation of $[\text{Cp}^*\text{Ta}(\text{CH}_2\text{Ph})(\text{OC}_6\text{F}_5)(\mu\text{-O})]_2$ (24).

$\text{C}_6\text{F}_5\text{OH}$ (0.32g, 1.74mmol) in cold toluene (20ml at -78°C) was added dropwise to a stirred solution of $\text{Cp}^*\text{Ta}(\text{N}^t\text{Bu})(\text{CH}_2\text{Ph})_2$ (0.50g, 0.87mmol) in cold toluene (40ml) at -78°C . The mixture was allowed to warm up to room temperature over 90 minutes to afford a bright red solution. After stirring for a further 12 hours, the solution was filtered, concentrated and cooled to -30°C to give bright yellow hexagonal crystals (Yield: 0.23g, 22%).

Elemental analysis for $\text{C}_{46}\text{H}_{44}\text{O}_4\text{F}_{10}\text{Ta}_2$ (1212.73) found (required) : %C = 45.37 (45.56), %H = 3.87 (3.66).

Infra red data (Nujol, CsI, cm^{-1}) : 2725(w), 2680(w), 1650(w), 1595(w), 1505(vs), 1315(m), 1260(m), 1190(m), 1165(m), 1095(w), 985(s), 800(m), 755(m), 700(m), 675(m), 480(m), 380(m), 350(w),

^1H NMR data (400MHz, C_6D_6 , 298K) : 1.58(s, 15H, C_5Me_5), 2.80 and 2.97(dd, 2H, $^2\text{J}_{\text{HH}}=13.6\text{Hz}$, CH_2Ph), 7.03(t, 1H, $^3\text{J}_{\text{HH}}=7.4\text{Hz}$, *p*-Ph), 7.16(d, 2H, $^3\text{J}_{\text{HH}}=7.6\text{Hz}$, *o*-Ph), 7.39(t, 2H, $^3\text{J}_{\text{HH}}=7.8\text{Hz}$, *m*-Ph).

^{13}C NMR data (100MHz, proton decoupled, C_6D_6 , 298K) : 10.35(C_5Me_5), 73.10(CH_2Ph), C_5Me_5 not resolved, 123.10, 127.47, 131.22(*o*-, *m*- and *p*-Ph), 132-142(C_6F_5), 143.95(*ipso*-Ph).

^{19}F NMR data (376MHz, C_6D_6 , 298K) : -157.47(d, 2F, $^3\text{J}_{\text{FF}}=25.2\text{Hz}$, *o*- C_6F_5), -166.90(t, 2F, $^3\text{J}_{\text{FF}}=21.4\text{Hz}$, *m*- C_6F_5), -172.52(t, 1F, $^3\text{J}_{\text{FF}}=22.8\text{Hz}$, *p*- C_6F_5).

6.4.6. Reaction of $\text{Cp}^*\text{Ta}(\text{N}^t\text{Bu})(\text{CH}_2\text{CMe}_2\text{Ph})_2$ with Pentafluorophenol:

Preparation of $\text{Cp}^*\text{Ta}(\text{OC}_6\text{F}_5)_4$ (26) and $[\text{Cp}^*\text{Ta}(\text{OC}_6\text{F}_5)_2(\mu\text{-O})]_2$ (27).

$\text{C}_6\text{F}_5\text{OH}$ (0.25g, 1.34mmol) in heptane (30ml) was added dropwise to a solution of $\text{Cp}^*\text{Ta}(\text{N}^t\text{Bu})(\text{CH}_2\text{CMe}_2\text{Ph})_2$ (0.44g, 0.67mmol) in cold heptane (50ml) at -78°C . The mixture was allowed to warm up to room temperature then heated to 60°C . After stirring for 10 days, pale yellow needle crystals of pure 26 formed on the side of the vessel. The filtrate was collected, concentrated and cooled to -20°C to give a second crop of yellow needles consisting of 26 [75%] and 27 [25%]. Repeated recrystallisations in toluene to separate the two products eventually yielded pure 27.

$\text{Cp}^*\text{Ta}(\text{OC}_6\text{F}_5)_4$ (26) : Yield: 0.14g, 20%.

Elemental analysis for $\text{C}_{34}\text{H}_{15}\text{O}_4\text{F}_{20}\text{Ta}$ (1048.40) found (required) : %C = 39.07 (38.95), %H = 1.56 (1.44).

Mass spectral data (EI, m/z) : 864 [M-OC₆F₅]⁺.

¹H NMR data (400MHz, C₆D₆, 298K) : 2.04(s).

¹³C NMR data (100MHz, C₆D₆, 298K) : 10.66(q, ¹J_{CH}=129Hz, C₅Me₅), 109.51(s, C₅Me₅), 134–141(C₆F₅).

¹⁹F NMR data (376MHz, C₆D₆, 298K) : -159.45(d, 2F, ³J_{FF}=18.8Hz, *o*-C₆F₅), -164.59(t, 2F, ³J_{FF}=20.9Hz, *m*-C₆F₅), -166.67(t, 1F, ³J_{FF}=22.8Hz, *p*-C₆F₅).

[Cp*Ta(OC₆F₅)₂(μ-O)]₂ (27) : Yield: 0.11g, 12%.

Elemental analysis for C₄₄H₃₀O₆F₂₀Ta₂ (1396.58) found (required) : %C = 38.17 (37.84), %H = 2.50 (2.17).

¹H NMR data (400MHz, C₆D₆, 298K) : 1.71(s).

¹³C NMR data (100MHz, C₆D₆, 298K) : 10.15(q, ¹J_{CH}=128Hz, C₅Me₅), 134–141(C₆F₅), C₅Me₅ not resolved.

¹⁹F NMR data (376MHz, C₆D₆, 298K) : -157.42(d, 2F, ³J_{FF}=18.4Hz, *o*-C₆F₅), -165.57(t, 2F, ³J_{FF}=20.7Hz, *m*-C₆F₅), -169.67(t, 1F, ³J_{FF}=22.8Hz, *p*-C₆F₅).

Mixture of 26 and 27 :

Infra red data (Nujol, CsI, cm⁻¹) : 2725(w), 2675(w), 1650(w), 1480(s), 1325(m), 1315(s), 1260(m), 1200(m), 1170(vs), 1090(m), 1025(vs), 990(vs), 800(m), 715(m), 690(m), 675(m), 485(m), 390(m), 345(m), 320(w), 295(w).

6.5. Experimental Details for Chapter 5

6.5.1. Reaction of CpTaCl_4 with $\text{LiNH}(2,6\text{-Me}_2\text{C}_6\text{H}_3)$:

Preparation of $\text{CpTa}(\text{N-}2,6\text{-Me}_2\text{C}_6\text{H}_3)\text{Cl}_2$ (28).

A solution of $\text{LiNH}(2,6\text{-Me}_2\text{C}_6\text{H}_3)$ (0.435g, 3.42mmol) in diethyl ether (40ml) was added dropwise to a stirred solution of CpTaCl_4 (0.664g, 1.71mmol) in 60ml of diethyl ether at -78°C . This mixture was slowly allowed to warm up to room temperature and stirred for a further 10 hours. The resultant bright orange solution was filtered from the grey residue (LiCl) and all volatile components were removed under reduced pressure. The resultant red oil was extracted into pentane, concentrated and cooled to -30°C to afford a red crystalline solid (Yield: 0.33g, 44%).

Elemental analysis for $\text{C}_{13}\text{H}_{14}\text{NCl}_2\text{Ta}$ (436.12) found (required) : %C = 36.28 (35.80), %H = 3.34 (3.24), %N = 2.89 (3.21).

Infra red data (Nujol, CsI , cm^{-1}) : 3275(w), 3115(w), 3095(w), 3060(w), 1415(m), 1330(s), 1260(m), 1210(m), 1160(w), 1095(m), 1020(m), 1005(m), 995(m), 915(w), 855(s), 825(s), 765(s), 735(m), 660(w), 580(w), 505(w), 445(w), 350(s, sh).

Mass spectral data (EI, m/z , ^{35}Cl) : 435 $[\text{M}]^+$.

^1H NMR data (250MHz, CDCl_3 , 298K) : 2.46 (s, 6H, $\text{Me}_2\text{C}_6\text{H}_3$), 6.56 (s, 5H, C_5H_5), 6.68 (t, 1H, $^3J_{\text{HH}}=7.5$ Hz, $p\text{-C}_6\text{H}_3$), 7.04 (d, 2H, $^3J_{\text{HH}}=7.5$ Hz, $m\text{-C}_6\text{H}_3$).

^{13}C NMR data (100MHz, proton decoupled, CDCl_3 , 298K) : 18.84 ($\text{Me}_2\text{C}_6\text{H}_3$), 112.61 (C_5H_5), 124.59 (*p*- C_6H_3), 126.89 (*m*- C_6H_3), 135.22 (*o*- C_6H_3), 152.32 (*ipso*- C_6H_3).

6.5.2. Reaction of Cp^*TaCl_4 with $\text{LiNH}(2,6\text{-Me}_2\text{C}_6\text{H}_3)$:

Preparation of $\text{Cp}^*\text{Ta}(\text{N-}2,6\text{-Me}_2\text{C}_6\text{H}_3)\text{Cl}_2$ (29).

A solution of $\text{LiNH}(2,6\text{-Me}_2\text{C}_6\text{H}_3)$ (1.05g, 8.24mmol) in diethyl ether (100ml) was added dropwise to a stirred solution of Cp^*TaCl_4 (1.89g, 4.12mmol) in 150ml of diethyl ether at -20°C . This mixture was slowly allowed to warm up to room temperature and stirred for a further 24 hours. The resultant bright orange solution was filtered from the yellow residue (LiCl), concentrated and cooled to -30°C to afford an orange crystalline solid (Yield: 1.29g, 62%).

Elemental analysis for $\text{C}_{18}\text{H}_{24}\text{NCl}_2\text{Ta}$ (506.25) found (required) : %C = 42.41 (42.71), %H = 5.10 (4.78), %N = 3.01 (2.77).

Infra red data (Nujol, CsI , cm^{-1}) : 3060(w), 1420(m), 1325(s), 1260(m), 1160(w), 1095(m), 1025(m), 990(m), 800(m), 760(s), 740(m), 720(w), 670(w), 575(w), 505(w), 440(w), 400(m), 370(m), 350(s).

Mass spectral data (EI, m/z , ^{35}Cl) : 505 $[\text{M}]^+$.

^1H NMR data (400MHz, C_6D_6 , 298K) : 1.83 (s, 15H, C_5Me_5), 2.45 (s, 6H, $\text{Me}_2\text{C}_6\text{H}_3$), 6.66 (t, 1H, $^3J_{\text{HH}}=7.4$ Hz, *p*- C_6H_3), 6.96 (d, 2H, $^3J_{\text{HH}}=7.6$ Hz, *m*- C_6H_3).

^{13}C NMR data (100MHz, C_6D_6 , 298K) : 11.27 (q, $J_{\text{CH}}=128\text{Hz}$, C_5Me_5), 18.86 (q, $J_{\text{CH}}=127\text{ Hz}$, $\text{Me}_2\text{C}_6\text{H}_3$), 121.33 (s, C_5Me_5), 124.13 (d, $J_{\text{CH}}=158\text{Hz}$, *p*- C_6H_3), 127.31 (d, $J_{\text{CH}}=158\text{Hz}$, *m*- C_6H_3), 135.08 (s, *o*- C_6H_3), 151.11 (s, *ipso*- C_6H_3).

6.5.3. Reaction of Cp^*TaCl_4 with $2\text{LiNH}(2\text{-}^t\text{BuC}_6\text{H}_4)$:

Preparation of $\text{Cp}^*\text{Ta}(\text{N-}2\text{-}^t\text{BuC}_6\text{H}_4)\text{Cl}_2$ (30).

A solution of $\text{LiNH}(2\text{-}^t\text{BuC}_6\text{H}_4)$ (1.42g, 9.12mmol) in diethyl ether (100ml) was added dropwise to a stirred solution of Cp^*TaCl_4 (2.09g, 4.56mmol) in 150ml of diethyl ether at -30°C . This mixture was slowly allowed to warm up to room temperature and stirred for a further 18 hours. The resultant bright orange solution was filtered from the yellow residue (LiCl) and all volatile components were removed *in vacuo* to afford an oily orange solid. Recrystallisation of this solid from diethyl ether/pentane solutions at -30°C gave bright orange crystals (Yield: 1.44g, 59%).

Elemental analysis for $\text{C}_{20}\text{H}_{28}\text{NCl}_2\text{Ta}$ (534.31) found (required) : %C = 45.35 (44.96), %H = 5.41 (5.28), %N = 2.35 (2.62).

Infra red data (Nujol, CsI , cm^{-1}) : 3090(m), 3055(w), 1905(w), 1585(w), 1430(s), 1360(m), 1325(s), 1265(m), 1200(w), 1165(m), 1125(m), 1090(s), 1050(s), 1025(s), 985(s), 865(w), 800(s), 760(s), 750(s), 680(m), 585(m), 525(m), 455(m), 380(s), 355(vs).

Mass spectral data (EI, m/z , ^{35}Cl) : 533 $[\text{M}]^+$.

^1H NMR data (400MHz, C_6D_6 , 298K) : 1.57 (s, 9H, CMe_3), 1.87 (s, 15H, C_5Me_5), 6.80, 7.11 (t's, 2H, $^3J_{\text{HH}}=7.4$ Hz, $\text{H}(4)$ and $\text{H}(5)$), 6.84, 7.34 (d's, 2H, $^3J_{\text{HH}}=7.6$ Hz, $\text{H}(3)$ and $\text{H}(6)$).

^{13}C NMR data (100MHz, C_6D_6 , 298K) : 11.25 (q, $J_{\text{CH}}=128\text{Hz}$, C_5Me_5), 30.16 (q, $J_{\text{CH}}=126$ Hz, CMe_3), 35.32 (s, CMe_3), 121.53 (s, C_5Me_5), 124.85, 125.74, 125.85 (d's, $J_{\text{CH}}=158\text{Hz}$, $\text{C}(3)$, $\text{C}(4)$, $\text{C}(5)$), 132.85 (d, $J_{\text{CH}}=165\text{Hz}$, $\text{C}(6)$), 144.42 (s, $\text{C}(2)$), 153.01 (s, $\text{C}(1)$).

6.5.4. Reaction of Cp^*TaCl_4 with $4\text{LiNH}(2\text{-}^t\text{BuC}_6\text{H}_4)$ in Et_2O :

Preparation of $[\text{Li}(\text{Et}_2\text{O})][\text{Cp}^*\text{Ta}(\text{N-}2\text{-}^t\text{BuC}_6\text{H}_4)_2\text{Cl}]$ (31).

A solution of $\text{LiNH}(2\text{-}^t\text{BuC}_6\text{H}_4)$ (1.717g, 11.07mmol) in diethyl ether (80ml) was added dropwise to a stirred solution of Cp^*TaCl_4 (1.267g, 2.77mmol) in 80ml of diethyl ether at 0°C . This mixture was allowed to warm up to room temperature and stirred for 24 hours. The resultant yellow/brown solution was filtered from the white residue (LiCl), concentrated and cooled to -30°C to yield long yellow crystals (Yield: 1.47g, 73%).

Elemental analysis for $\text{C}_{34}\text{H}_{51}\text{N}_2\text{OCILiTa}$ (727.14) found (required) : %C = 56.17 (56.16), %H = 7.10 (7.07), %N = 3.82 (3.85).

Infra red data (Nujol, CsI , cm^{-1}) : 3085(w), 3050(w), 1580(m), 1555(w), 1420(s), 1330(s), 1295(vs), 1280(s), 1260(s), 1235(m), 1155(w), 1085(m), 1050(m), 945(s), 800(m), 750(m), 585(w), 530(w), 450(w), 390(m), 360(m), 320(m).

Mass spectral data (EI, m/z , ^{35}Cl) : 646 $[\text{M-Li}(\text{Et}_2\text{O})]^+$.

^1H NMR data (400MHz, C_6D_6 , 298K) : 0.57 (t, OCH_2CH_3), 1.62 (s, 18H, CMe_3), 2.08 (s, 15H, C_5Me_5), 2.69 (q, OCH_2CH_3), 6.64 (d, 2H, $^3J_{\text{HH}}=7.6$ Hz, $\text{H}(3)$), 6.70, 7.05 (t's, 4H, $^3J_{\text{HH}}=7.4$ Hz, $\text{H}(4)$ and $\text{H}(5)$), 7.32 (d, 2H, $^3J_{\text{HH}}=7.8$ Hz, $\text{H}(6)$).

^{13}C NMR data (100MHz, C_6D_6 , 298K) : 11.18 (q, $J_{\text{CH}}=127$ Hz, C_5Me_5), 14.36 (q, $J_{\text{CH}}=127$ Hz, OCH_2CH_3), 29.64 (q, $J_{\text{CH}}=125$ Hz, CMe_3), 35.71 (s, CMe_3), 64.61 (t, $J_{\text{CH}}=143$ Hz, OCH_2CH_3), 116.65 (s, C_5Me_5), 118.95, 125.31, 126.29, 126.86 (d's, $J_{\text{CH}}=154\text{--}159$ Hz, $\text{C}(3)$, $\text{C}(4)$, $\text{C}(5)$ and $\text{C}(6)$), 140.49 (s, $\text{C}(2)$), 158.94 (s, $\text{C}(1)$).

6.5.5. Reduction of $\text{Cp}^*\text{Ta}(\text{N-2,6-Me}_2\text{C}_6\text{H}_3)\text{Cl}_2$ with Magnesium in the presence of Trimethylphosphine :

Preparation of $\text{Cp}^*\text{Ta}(\text{N-2,6-Me}_2\text{C}_6\text{H}_3)(\text{PMe}_3)_2$ (32).

PMe_3 (0.38g, 5.05 mmol) was condensed onto a solution of $\text{Cp}^*\text{Ta}(\text{N-2,6-Me}_2\text{C}_6\text{H}_3)\text{Cl}_2$ (0.511g, 1.01 mmol) and activated magnesium turnings (0.03g, 1.23 mmol) in THF (60 ml) cooled to -196°C . This mixture was allowed to warm up to room temperature and then stirred at 40°C for 5 days to yield a dark red solution. Removal of the volatile components under reduced pressure gave a dark red solid, which was extracted with pentane, concentrated and cooled to -30°C to afford an extremely air-sensitive deep red crystalline solid (Yield: 0.08g, 13%).

Satisfactory elemental analysis has not been obtained for this compound due to its extreme air and moisture sensitivity.

Infra red data (Nujol, CsI, cm⁻¹) : 3060(w), 3010(w), 1590(m), 1410(m), 1325(s), 1280(m), 1260(m), 1160(w), 1095(m), 1025(m), 955(s), 840(w), 800(m), 770(m), 760(s), 735(m), 670(m).

¹H NMR data (400MHz, C₆D₆, 298K) : 1.34 (virtual t, 18H, ²J_{PH}=8Hz, PMe₃), 1.96 (s, 15H, C₅Me₅), 2.57 (s, 6H, Me₂C₆H₃), 6.92 (t, 1H, ³J_{HH}=7.6 Hz, *p*-C₆H₃), 7.19 (d, 2H, ³J_{HH}=7.6 Hz, *m*-C₆H₃).

¹³C NMR data (100MHz, proton decoupled, C₆D₆, 298K) : 12.93 (s, C₅Me₅), 20.85 (s, Me₂C₆H₃), 27.32 (virtual t, J_{CP}~20Hz, PMe₃), 103.52 (s, C₅Me₅), 118.80, 128.20, 129.93 (singlets, *o*-, *m*-, *p*-C₆H₃), 157.08 (s, *ipso*-C₆H₃).

³¹P NMR data (162MHz, C₆D₆, 298K) : 1.92 (s).

6.5.6. Reaction of Cp*Ta(N^tBu)Cl₂ with C₂H₅MgCl in the presence of Trimethylphosphine :

Preparation of Cp*Ta(N^tBu)(η²-C₂H₄)(PMe₃) (33).

PMe₃ (0.26g, 3.39 mmol) was condensed onto a frozen solution of Cp*Ta(N^tBu)Cl₂ (0.518g, 1.13 mmol) in diethyl ether (60ml). A white precipitate appeared as the mixture was slowly allowed to warm up to -78°C. An atmosphere of nitrogen was then introduced and a 2M diethyl ether solution of C₂H₅MgCl (1.13 ml, 2.26 mmol) was added *via* syringe. The mixture was allowed to warm to room temperature with regular venting of the vessel to afford a clear yellow solution, which became cloudy during the course of the reaction. After stirring for a further 48 hours, the volatile components were removed under reduced pressure to leave a yellow oily

solid. This solid was extracted into pentane and the resultant solution was concentrated to yield an analytically pure yellow oil (Yield: 0.27g, 49%).

Elemental analysis for $C_{19}H_{37}NPTa$ (491.43) found (required) : %C = 46.95 (46.44), %H = 7.68 (7.59), %N = 2.27 (2.85).

Infra red data (Nujol, CsI, cm^{-1}) : 3011(w), 1420(s), 1350(s), 1300(m), 1265(s), 1210(s), 1125(s), 1090(s), 1025(m), 950(s), 910(m), 840(m), 800(m), 750(m), 715(m), 665(m), 530(m), 425(w).

1H NMR data (400MHz, C_6D_6 , 298K) : -0.45, 0.55, 0.90, 1.34 (m, 4H, C_2H_4), 1.12 (s, 9H, CMe_3), 1.20 (d, 9H, $^2J_{PH}=7.2Hz$, PMe_3), 1.82 (s, 15H, C_5Me_5).

^{13}C NMR data (100MHz, proton decoupled, C_6D_6 , 298K) : 11.92(s, C_5Me_5), 18.93 (d, $J_{CP}=25Hz$, PMe_3), 23.85 (s, C_2H_4), 31.63 (d, $^2J_{CP}=12Hz$, C_2H_4), 33.72 (s, CMe_3), 64.35 (s, CMe_3), 108.04 (s, C_5Me_5).

^{31}P NMR data (162MHz, C_6D_6 , 298K) : 0.14 (s).

6.5.7. Reaction of $Cp^*Ta(N^tBu)Cl_2$ with $n-C_3H_7MgCl$ in the presence of Trimethylphosphine:

Preparation of $Cp^*Ta(N^tBu)(\eta^2-C_3H_6)(PMe_3)$ (34).

PMe_3 (0.30g, 3.99 mmol) was condensed onto a frozen solution of $Cp^*Ta(N^tBu)Cl_2$ (0.609g, 1.33 mmol) in diethyl ether (60ml) at $-196^\circ C$ and the mixture was then slowly allowed to warm up to $-78^\circ C$. An atmosphere of nitrogen was introduced and a 2M diethyl ether solution of $n-C_3H_7MgCl$ (1.77 ml, 2.66 mmol) was added *via* syringe. The mixture was allowed to

warm to room temperature with regular venting of the vessel. After stirring for 38 hours, all volatile components removed under reduced pressure. The resultant yellow solid was extracted into pentane and the solution concentrated and cooled to -20°C to afford a yellow crystalline solid (Yield: 0.41g, 61%).

Elemental analysis for $\text{C}_{20}\text{H}_{39}\text{NPTa}$ (505.46) found (required) : %C = 47.42 (47.52), %H = 8.00 (7.78), %N = 2.89 (2.77).

Infra red data (Nujol, CsI, cm^{-1}) : 1405(m), 1350(m), 1300(m), 1260(vs), 1210(m), 1095(s), 1050(s), 1025(s), 950(s), 870(m), 800(s), 720(m), 665(m), 565(w), 530(m).

^1H NMR data (400 MHz, C_6D_6 , 298K) : 4 isomers observed.

Main isomer : 1.17 (s, 9H, CMe_3), 1.20 (d, 9H, $^2J_{\text{PH}}=7.6\text{Hz}$, PMe_3), 1.86 (s, 15H, C_5Me_5), 2.43 (d, 3H, $^3J_{\text{HH}}=6.0\text{Hz}$, $\text{CH}_2=\text{CHCH}_3$), not assigned: $\text{CH}_2=\text{CHCH}_3$.
 C_5Me_5 resonances for 3 minor isomers: 1.84, 1.91, 1.96.

^{13}C NMR data (100MHz, proton decoupled, C_6D_6 , 298K) : 4 isomers observed.

Main isomer: 11.77 (s, C_5Me_5), 18.99 (d, $J_{\text{CP}}=25\text{Hz}$, PMe_3), 34.14 (s, CMe_3), 64.55 (s, CMe_3), 107.94 (s, C_5Me_5), not assigned: $\text{CH}_2=\text{CHCH}_3$.
 C_5Me_5 resonances for 3 minor isomers: 108.31, 108.94, 109.31.

^{31}P NMR data (161MHz, C_6D_6 , 298K) : -2.75, -3.08, -4.51 (singlets, 3 main isomers).

6.5.8. Reaction of Cp*Ta(N-2,6-Me₂C₆H₃)Cl₂ with C₂H₅MgCl in the presence of Trimethylphosphine :

Preparation of Cp*Ta(N-2,6-Me₂C₆H₃)(η²-C₂H₄)(PMe₃) (35).

PMe₃ (0.27g, 3.60 mmol) was condensed onto a frozen solution of Cp*Ta(N-2,6-Me₂C₆H₃)Cl₂ (0.606g, 1.20 mmol) in diethyl ether (60ml) at -196°C and the mixture was then slowly allowed to warm up to -78°C. An atmosphere of nitrogen was introduced and a 2M diethyl ether solution of C₂H₅MgCl (1.20 ml, 2.40 mmol) was added *via* syringe. The mixture was allowed to warm to room temperature with regular venting of the vessel. After stirring for a further 60 hours, a bright yellow solution and pale precipitate was formed. The supernatant solution was filtered, concentrated and cooled to -20°C to afford a yellow crystalline solid (Yield: 0.43g, 66%).

Elemental analysis for C₂₃H₃₇NPTa (539.48) found (required) : %C = 51.49 (51.21), %H = 6.85 (6.91), %N = 2.45 (2.60).

Infra red data (Nujol, CsI, cm⁻¹) : 3045(w), 3025(w), 1585(m, sharp), 1410(s), 1325(s), 1310(s), 1275(m), 1260(m), 1095(s), 1020(m), 955(s), 915(m), 800(m), 760(s), 725(m), 715(m), 665(m), 525(m), 505(w), 430(w).

Mass spectral data (EI, m/z) : 539 [M]⁺, 511 [M-C₂H₄]⁺.

¹H NMR data (400MHz, C₆D₆, 298K) : -0.19, 1.03, 1.78 (m, 4H, C₂H₄), 1.05 (d, 9H, ²J_{PH}=7.6Hz, PMe₃), 1.77 (s, 15H, C₅Me₅), 2.40 (s, 6H, Me₂C₆H₃), 6.79 (t, 1H, ³J_{HH}=7.5 Hz, *p*-C₆H₃), 7.04 (d, 2H, ³J_{HH}=7.4 Hz, *m*-C₆H₃).

¹³C NMR data (100MHz, proton decoupled, C₆D₆, 298K) : 11.25(s, C₅Me₅), 16.90 (d, J_{CP}=26Hz, PMe₃), 20.51 (s, Me₂C₆H₃), 29.52 (s, C₂H₄), 35.12 (d,

$^2J_{CP}=11\text{Hz}$, C_2H_4), 108.56 (s, C_5Me_5), 119.70 (s, *m*- C_6H_3), not resolved: *o*-, *p*-, *ipso*- C_6H_3 .

^{31}P NMR data (162MHz, C_6D_6 , 298K) : 3.01 (s).

6.5.9. Reaction of $Cp^*Ta(N^tBu)(\eta^2-C_2H_4)(PMe_3)$ with Ethylene:

Observation of $Cp^*Ta(N^tBu)(\sigma-1,4-C_4H_8)$ (36).

Heating a benzene- d_6 solution of $Cp^*Ta(N^tBu)(\eta^2-C_2H_4)(PMe_3)$ with 5 equivalents of ethylene for 7 days at 100°C resulted in 66% conversion to an orange solution with the following 1H NMR resonances (250MHz) : 0.6, 2.2, 2.4 (broad multiplets, C_4H_8); 1.33 (s, 9H, CMe_3), 1.86 (s, 15H, C_5Me_5).

6.5.10. Reaction of $Cp^*Ta(N^tBu)(CH_2=CHMe)(PMe_3)$ with $PhC\equiv CH$:

Observation of $Cp^*Ta(N^tBu)(PhC\equiv CH)(PMe_3)$ (37).

After 3 weeks at 100°C in C_6D_6 , total conversion to a deep red complex was observed by 1H , ^{31}P and ^{13}C NMR spectroscopy :

1H NMR data (250MHz) : 0.96 (d, 9H, $^2J_{PH}=12\text{Hz}$, PMe_3), 1.51 (s, 9H, CMe_3), 1.91 (s, 15H, C_5Me_5), 6.9-7.4 (m, *m*- and *p*-Ph), 7.68 (d, 2H, $^3J_{HH}=7\text{Hz}$, *o*-Ph), 7.87 (d, 1H, $^3J_{PH}=7.5\text{Hz}$, *acetylenic H*).

^{13}C NMR data (63MHz, proton decoupled) : 12.49 (s, C_5Me_5), 18.06 (d, PMe_3), 35.56 (s, CMe_3), 63.81 (s, CMe_3), 111.45 (s, C_5Me_5), 122.96, 126.44, 132.78, 146.7 (singlets, *Ph*), 146.81 (d, $PhC\equiv CH$), 155.73 (s, $PhC\equiv CH$).

^{31}P NMR data (101MHz) : 0.29 (s).

6.5.11. Reaction of $\text{Cp}^*\text{Ta}(\text{N-2,6-Me}_2\text{C}_6\text{H}_3)(\text{CH}_2=\text{CH}_2)(\text{PMe}_3)$ with $\text{PhC}\equiv\text{CPh}$:

Observation of $\text{Cp}^*\text{Ta}(\text{N-2,6-Me}_2\text{C}_6\text{H}_3)(\text{PhC}\equiv\text{CPh})(\text{PMe}_3)$ (38).

The mixture remained bright yellow and an equilibrium was reached after heating the reaction at 100°C for 4 weeks in C_6D_6 . Resonances for new species:

^1H NMR data (250MHz) : 0.91 (d, 9H, $^2J_{\text{PH}}=8.1\text{Hz}$, PMe_3), 1.91 (s, 15H, C_5Me_5), 2.43 (s, 6H, $\text{Me}_2\text{C}_6\text{H}_3$), 6.7-7.3 (m, *m*- and *p*- C_6H_5 and C_6H_3), 7.67 (d, 4H, $^3J_{\text{HH}}=7.5\text{Hz}$, *o*- C_6H_5).

^{31}P NMR data (101MHz) : -8.20 (s).

6.5.12. Reaction of $\text{Cp}^*\text{Ta}(\text{N-2,6-}^i\text{Pr}_2\text{C}_6\text{H}_3)(\text{CH}_2=\text{CH}_2)(\text{PMe}_3)$ with $\text{PhC}\equiv\text{CPh}$:

Observation of $\text{Cp}^*\text{Ta}(\text{N-2,6-}^i\text{Pr}_2\text{C}_6\text{H}_3)(\text{PhC}\equiv\text{CPh})(\text{PMe}_3)$ (39).

A deep red product (39) is observed as the major species by ^1H and ^{31}P NMR spectroscopy after heating a mixture of $\text{Cp}^*\text{Ta}(\text{N-2,6-}^i\text{Pr}_2\text{C}_6\text{H}_3)(\text{CH}_2=\text{CH}_2)(\text{PMe}_3)$ and 2 equivalents of $\text{PhC}\equiv\text{CPh}$ for 3 weeks at 100°C in C_6H_6 :

^1H NMR data (250MHz) : 1.01 (d, 9H, $^2J_{\text{PH}}=8.5\text{Hz}$, PMe_3), 1.16, 1.25 (dd, 12H, $^3J_{\text{HH}}=6.8\text{ Hz}$, CHMe_2), 1.92 (s, 15H, C_5Me_5), 4.12 (sept, 2H, CHMe_2), 6.9-7.8 (m, C_6H_5 and C_6H_3).

^{31}P NMR data (101MHz) : -8.18 (s).

**6.5.13. Reaction of $\text{Cp}^*\text{Ta}(\text{N-2,6-}i\text{Pr}_2\text{C}_6\text{H}_3)(\text{PhC}\equiv\text{CPh})(\text{PMe}_3)$ with $\text{PhC}\equiv\text{CPh}$:
Observation of $\text{Cp}^*\text{Ta}(\text{N-2,6-}i\text{Pr}_2\text{C}_6\text{H}_3)(\text{PhC}\equiv\text{CPh})_2$ (40).**

Continuing from 6.5.12, reaction of $\text{Cp}^*\text{Ta}(\text{N-2,6-}i\text{Pr}_2\text{C}_6\text{H}_3)(\text{PhC}\equiv\text{CPh})(\text{PMe}_3)$ (39) with the excess alkyne slowly continues and after 3 months results in significant conversion to a new product 40 :

$^1\text{H NMR}$ data (250MHz) : 1.52 (d, 12H, $^3J_{\text{HH}}=6.3$ Hz, CHMe_2), 1.86 (s, 15H, C_5Me_5), 5.05 (sept, 2H, CHMe_2), 6.6-7.8 (m, C_6H_5 and C_6H_3).

**6.5.14. Reaction of $\text{Cp}^*\text{Ta}(\text{N-2,6-}i\text{Pr}_2\text{C}_6\text{H}_3)\text{Cl}_2$ with 2^nBuLi in the presence of
Ethylene: Preparation of $\text{Cp}^*\text{Ta}(\text{N-2,6-}i\text{Pr}_2\text{C}_6\text{H}_3)(\sigma\text{-1,4-(2-Et)}\text{C}_4\text{H}_7)$ (41).**

A 1.62M solution of $^n\text{BuLi}$ in hexanes (1.60 ml, 2.60 mmol) was slowly added *via* syringe to a stirred solution of $\text{Cp}^*\text{Ta}(\text{N-2,6-}i\text{Pr}_2\text{C}_6\text{H}_3)\text{Cl}_2$ (0.731g, 1.30 mmol) in diethyl ether (60ml) at -78°C and stirred for 3 hours to afford a clear green solution. This was frozen at -196°C , one atmosphere of C_2H_4 was condensed onto the frozen solution and the mixture was slowly allowed to warm up to room temperature and stirred for 12 hours, after which the vessel was vented and the ethylene atmosphere was replenished. After stirring for a further 12 hours, a bright yellow solution and white precipitate was afforded. The solution was filtered, concentrated and cooled to -78°C to yield a bright orange crystalline solid (Yield: 0.38g, 51%).

Elemental analysis for $\text{C}_{28}\text{H}_{44}\text{NTa}$ (575.61) found (required) : %C = 58.25 (58.43), %H = 7.92 (7.71), %N = 2.68 (2.43).

Infra red data (Nujol, CsI, cm^{-1}) : 3055(w), 1585(w), 1430(s), 1360(s), 1345(s), 1295(m), 1260(m), 1175(w), 1100(m, br), 1025(m, br), 985(w), 935(w), 795(s), 750(s), 595(w), 540(m), 360(m).

Mass spectral data (EI, m/z) : 575 $[\text{M}]^+$, 547 $[\text{M}-\text{C}_2\text{H}_4]^+$, 519 $[\text{M}-\text{C}_4\text{H}_8]^+$.

^1H NMR data (400MHz, C_6D_6 , 298K) : 0.5, 0.8–1.2, 1.8–2.4, 2.8 (m, $\text{C}_4\text{H}_7\text{CH}_2\text{Me}$), 1.35–1.40 (m, 12H, CHMe_2), 1.74 (s, 15H, C_5Me_5), 3.73 (sept, 2H, $^3\text{J}_{\text{HH}}=6.5\text{Hz}$, CHMe_2), 6.99 (t, 1H, $^3\text{J}_{\text{HH}}=7.5\text{Hz}$, $p\text{-C}_6\text{H}_3$), 7.24 (d, 2H, $^3\text{J}_{\text{HH}}=7.5\text{Hz}$, $m\text{-C}_6\text{H}_3$).

^{13}C NMR data (100MHz, C_6D_6 , 298K) : 10.67, 10.68 (q's, $^1\text{J}_{\text{CH}}=127\text{Hz}$, C_5Me_5), 11.11, 11.19 (q's, $^1\text{J}_{\text{CH}}=123\text{Hz}$, $\text{C}_4\text{H}_7\text{CH}_2\text{Me}$), 21.18, 25.53 (t's, $^1\text{J}_{\text{CH}}=125\text{Hz}$, $\text{C}_4\text{H}_7\text{CH}_2\text{Me}$), 24.43, 24.48 (q's, $^1\text{J}_{\text{CH}}=125\text{Hz}$, CHMe_2), 27.56, 31.88 (d's, $^1\text{J}_{\text{CH}}=120\text{Hz}$, $\text{C}(\beta) / \text{CH}_2\text{CHCH}_2\text{Me}$), 28.19, 28.23 (d's, $^1\text{J}_{\text{CH}}=128\text{Hz}$, CHMe_2), 39.29, 39.77 (t's, $^1\text{J}_{\text{CH}}=125\text{Hz}$, $\text{C}(\beta') / \text{CH}_2\text{CH}_2$), 54.11, 57.21, 57.93, 61.83 (t's, $^1\text{J}_{\text{CH}}=125\text{--}128\text{Hz}$, $\text{C}(\alpha) / \text{CH}_2\text{CHCH}_2\text{Me}$ and $\text{C}(\alpha') / \text{CH}_2\text{CH}_2$), 115.82, 115.88 (singlets, C_5Me_5), 122.1–122.2 (d's, $m\text{-}$ and $p\text{-C}_6\text{H}_3$), 143.90, 143.97 (singlets, $o\text{-C}_6\text{H}_3$), 151.9 (singlets, $ipso\text{-C}_6\text{H}_3$).

6.5.15. Reaction of $\text{Cp}^*\text{Ta}(\text{N-2,6-}i\text{Pr}_2\text{C}_6\text{H}_3)(\sigma\text{-1,4-(2-Et)C}_4\text{H}_7)$ with

Carbon Monoxide : Preparation of

$\text{Cp}^*\text{Ta}(\text{N-2,6-}i\text{Pr}_2\text{C}_6\text{H}_3)[\sigma\text{-1,6-C(O)(3-Et)C}_4\text{H}_7\text{C(O)}]$ (42).

One atmosphere of CO was condensed onto a frozen solution of $\text{Cp}^*\text{Ta}(\text{N-2,6-}i\text{Pr}_2\text{C}_6\text{H}_3)(\sigma\text{-1,4-(2-Et)C}_4\text{H}_7)$ (0.450g, 0.78 mmol) in diethyl ether (60ml) at -196°C in an ampoule and an intense red colouration was observed immediately upon removal of the vessel from this temperature. The mixture

continued to slowly warm up to ambient temperatures and was stirred for 2 hours, during which the solution turned deep orange. This solution was filtered, concentrated and cooled to -30°C to yield a yellow/orange crystalline solid (Yield: 0.26g, 53%).

Elemental analysis for $\text{C}_{30}\text{H}_{44}\text{NO}_2\text{Ta}$ (631.64) found (required) : %C = 57.27 (57.05), %H = 6.92 (7.02), %N = 2.56 (2.22).

Infra red data (Nujol, CsI, cm^{-1}) : 3045(w), 3015(w), 1620(w), 1585(w), 1540(w), 1430(vs), 1350(vs), 1290(s), 1260(m), 1210(w), 1090(m), 1055(m), 1025(m), 985(m), 880(w), 795(m), 750(s, sharp), 725(m), 665(w), 610(s), 370(m).

Mass spectral data (EI, m/z) : 631 [M]⁺.

^1H NMR data (400MHz, C_6D_6 , 298K) : 0.56-0.64, 0.90-1.20, 1.35-1.50, 1.80-2.82 (m, $\text{C}_4\text{H}_7\text{CH}_2\text{Me}$), 1.29 (t, 12H, CHMe_2), 1.97 (s, 15H, C_5Me_5), 3.52 (sept, 2H, $^3\text{J}_{\text{HH}}=6.5\text{Hz}$, CHMe_2), 6.84, 6.85 (t's, 1H, $^3\text{J}_{\text{HH}}=7.6\text{ Hz}$, *p*- C_6H_3), 7.10, 7.11 (d's, 2H, $^3\text{J}_{\text{HH}}=7.6\text{ Hz}$, *m*- C_6H_3).

^{13}C NMR data (100MHz, C_6D_6 , 298K) : 10.47 (q, $^1\text{J}_{\text{CH}}=128\text{Hz}$, C_5Me_5), 11.33, 11.67 (q's, $\text{C}_4\text{H}_7\text{CH}_2\text{Me}$), 22.56, 24.10 (t's, $\text{C}_4\text{H}_7\text{CH}_2\text{Me}$), 24.23, 24.47 (q's, $^1\text{J}_{\text{CH}}=125\text{Hz}$, CHMe_2), 27.40, 27.46 (d's, $^1\text{J}_{\text{CH}}=128\text{Hz}$, CHMe_2), 28.18-28.96, 34.52-36.24 (triplets and doublets, $^1\text{J}_{\text{CH}}=125\text{-}130\text{Hz}$, C_4H_7), 118.79, 118.80 (singlets, C_5Me_5), 121.05, 122.08 (d's, $^1\text{J}_{\text{CH}}\sim 157\text{Hz}$, *m*- and *p*- C_6H_3), 132.65, 133.04, 133.77, 134.04 (singlets, CO), 141.08, 141.11 (singlets, *o*- C_6H_3), 150.82, 150.89 (singlets, *ipso*- C_6H_3).

6.5.16. Reaction of $\text{Cp}^*\text{Ta}(\text{N}-2,6\text{-}i\text{Pr}_2\text{C}_6\text{H}_3)\text{Cl}_2$ with 2^nBuLi in the presence of Trimethylphosphine:

Preparation of $\text{Cp}^*\text{Ta}(\text{N}-2,6\text{-}i\text{Pr}_2\text{C}_6\text{H}_3)(\eta^2\text{-C}_4\text{H}_8)(\text{PMe}_3)$ (43).

A 1.62M solution of *n*-BuLi in hexanes (1.36 ml, 2.20 mmol) was slowly added *via* syringe to a stirred solution of $\text{Cp}^*\text{Ta}(\text{N}-2,6\text{-}i\text{Pr}_2\text{C}_6\text{H}_3)\text{Cl}_2$ (0.620g, 1.10 mmol) in diethyl ether (60ml) at -78°C and stirred for 2 hours to afford a clear green solution. This was frozen at -196°C and PMe_3 (0.25g, 3.30 mmol) was condensed onto the frozen solution. The mixture was then slowly allowed to warm up to room temperature with regular venting of the vessel and stirred for a further 24 hours to give an orange/red solution and white precipitate. The solution was filtered and all volatile components were removed under reduced pressure. The resultant yellow solid was extracted into pentane and the solution was concentrated and cooled to -78°C to yield a bright yellow crystalline solid (Yield: 0.40g, 58%).

Elemental analysis for $\text{C}_{29}\text{H}_{49}\text{NPTa}$ (623.64) found (required) : %C = 55.64 (55.85), %H = 8.04 (7.92), %N = 1.85 (2.25).

Infra red data (Nujol, CsI, cm^{-1}) : 3045(w), 1585(m), 1425(s), 1355(m), 1335(s), 1280(s), 1260(m), 1145(m), 1105(m), 1060(m), 1025(m), 955(s), 850(w), 800(m), 755(s), 720(m), 670(m), 450(w).

^1H , ^{13}C and ^{31}P NMR resonances have been assigned for the 3 main isomers:

^1H NMR data (500MHz, C_6D_6 , 298K) : 1.14, 1.15, 1.19 (d's, 9H, $J_{\text{PH}}=7.0\text{Hz}$, PMe_3), 1.24–1.28 (d's, 12H, $^3J_{\text{HH}}=6.5\text{Hz}$, CHMe_2), 1.75, 1.77, 1.80 (singlets, 15H, C_5Me_5), 3.83, 4.02, 4.11 (septets, 2H, $^3J_{\text{HH}}=6.5\text{Hz}$, CHMe_2), 6.94, 6.95,

6.98 (t's, 1H, $^3J_{\text{HH}}=7.5$ Hz, *p*-C₆H₃), 7.06, 7.08, 7.12 (d's, 2H, $^3J_{\text{HH}}=7.5$ Hz, *m*-C₆H₃), not assigned: CH₂=CH*Et*.

¹³C NMR data (100MHz, proton decoupled, C₆D₆, 298K) : 11.12, 11.25, 11.57 (singlets, C₅Me₅), 17.16, 18.60 (d's, J_{CP}=24Hz, P*Me*₃), 23.27, 23.36, 23.55; 34.86, 34.96, 50.05 (singlets, *Et*), 24.89, 25.12, 25.23 (singlets, CH*Me*₂), 25.78, 26.40, 26.44 (singlets, CH*Me*₂), 30.45, 34.14, 36.74 (d's, $^2J_{\text{CP}}=2.3$ Hz, C₂H₃Et), 40.53, 51.32, 54.18 (d's, $^2J_{\text{CP}}=12.6$ Hz, C₂H₃Et), 108.71, 108.89, 109.11 (singlets, C₅Me₅), 120.55, 120.84, 120.89 (singlets, *p*-C₆H₃), 122.57, 122.62, 123.01 (singlets, *m*-C₆H₃), 141.68, 141.70, 142.82 (singlets, *o*-C₆H₃), 152.64, 152.65 (singlets, *ipso*-C₆H₃).

³¹P NMR data (162MHz, C₆D₆, 298K) : -2.40, -2.56, -2.73 (singlets).

6.6. Polymerization Procedure

Ethylene gas was dried by passing through a column of CaCl₂, 4Å molecular sieves and P₂O₅, each separated with glass wool, followed by passing through a silicone oil bubbler (30ml) to which 2ml of DEAC had been added.

In a typical run, the appropriate volume of a toluene solution of DEAC was added *via* syringe to a stirring solution of the catalyst precursor in toluene (ca. 50ml). The mixture was stirred for 10 minutes, after which the solution was purged with a continuous stream of ethylene for the required time period. The ethylene flow was then stopped and the polymerization was terminated by addition of a small amount of methanol. The resultant

polymer was isolated by filtration, washed with acidified methanol and dried *in vacuo* overnight.

For runs using MAO as co-catalyst, a toluene solution of the catalyst precursor was added *via* syringe to the MAO solution.

6.7. References

1. R.B. King, F.G.A. Stone, *Inorg. Synth.*, 1963, 7, 99.
2. W. Wolfsberger, H. Schmidbaur, *Synth. React. Inorg. Metal-Org. Chem.*, 1974, 4, 149.
3. M.J. Bunker, A. De Cian, M.L.H. Green, J.J.E. Green, J.J.E. Moreau, N. Siganoria, *J. Chem. Soc., Dalton Trans.*, 1980, 2155.
4. R.R. Schrock, J.S. Murdzek, G. Bazan, M. Di Mare, M. O'Regan, *J. Am. Chem. Soc.*, 1990, 112, 3875.
5. H.P. Fritz, C.G. Kreiter, *J. Organomet. Chem.*, 1964, 1, 323.
6. C.S. Kraihanzel, M.L. Losee, *J. Am. Chem. Soc.*, 1968, 90, 4701.
7. W. Kaminsky, M. Miri, H. Sinn, R. Woldt, *Makromol. Chem. Rapid. Commun.*, 1983, 4, 417.
8. R.R. Schrock, *J. Organomet. Chem.*, 1976, 122, 209.
9. A.M. Cardoso, R.J.H. Clark, S. Moorhouse, *J. Chem. Soc., Dalton Trans.*, 1980, 1156.
10. J. de la Mata, R. Fandos, M. Gomez, P. Gomez-Sal, S. Martinez-Carrera, P. Royo, *Organometallics*, 1990, 9, 2646.
11. R.R. Schrock, *J. Am. Chem. Soc.*, 1985, 107, 5957.
12. K. Suzuki, K. Yamaguchi, A. Hirao, S. Nakahama, *Macromol.*, 1989, 22, 2607, sample supplied by Dr C.I. Dalby.

Appendices

Appendix A

X-Ray Crystallographic Data

The structural determinations described in this thesis were performed on Rigaku AFC65 and Siemens SMART CCD diffractometers by:

^aProf. J.A.K. Howard, ^bMiss J.M. Cole, ^cJ.-W. Yao, ^dP.S. Ford, ^eDr C.W. Lehmann (University of Durham),

^fProf. W. Clegg, ^gDr M.R.J. Elsegood (University of Newcastle).

Appendix A1: Crystal Data and Selected Bond Lengths (Å) and Angles (°) for CpV(N-2,6-Me₂C₆H₃)Cl₂ (1) ^{a,c}

C ₁₃ H ₁₄ NCl ₂ V:	306.09		
Crystal system:	Monoclinic		
Space group:	P2 ₁ /c		
Cell dimensions:	a = 8.763(2) Å,	α = 90°	
	b = 12.590(3) Å,	β = 103.08(3)°	
	c = 12.611(3) Å,	γ = 90°	
Volume:	1355.2(6) Å ³		
Z:	4		
Density (calc):	1.500 mg/m ³		
Final R indices:	0.0895 (R _w = 0.1886)		
V(1)–N(1)	1.684(9)	V(1)–C(15)	2.262(10)
V(1)–Cl(1)	2.251(3)	V(1)–C(13)	2.346(10)
V(1)–Cl(2)	2.267(3)	V(1)–C(14)	2.366(10)
V(1)–C(11)	2.233(10)	N(1)–C(1)	1.371(12)
V(1)–C(12)	2.260(9)	V(1)–C _p centroid	1.963(3)
N(1)–V(1)–Cl(1)	102.5(3)	N(1)–V(1)–C _p centroid	120.6(5)
N(1)–V(1)–Cl(2)	100.2(3)	Cl(1)–V(1)–C _p centroid	113.0(2)
Cl(1)–V(1)–Cl(2)	105.66(7)	Cl(2)–V(1)–C _p centroid	113.2(2)
C(1)–N(1)–V(1)	166.8(7)		

Appendix A2 : Crystal Data for [CpV(CH₂Ph)(μ-N^tBu)]₂ (4) a,d

C ₃₂ H ₄₂ N ₂ V ₂ :	556.56
Crystal system:	Primitive
Space group:	P2 ₁ /n
Cell dimensions:	a = 8.615(7) Å, α = 90° b = 34.88(2) Å, β = 111.73(6)° c = 10.139(7) Å, γ = 90°
Volume:	2830(3) Å ³
Z:	2
Density (calc):	1.306 mg/m ³
Final R indices:	0.0673 (R _w = 0.1678)

Appendix A3 : Crystal Data for [CpV(NAr)(μ-Me)₂]₂(μ-Mg) (5) a,b

C ₁₉ H ₂₈ NMg _{0.5} V :	1048.41
Crystal system:	Monoclinic
Space group:	P2 ₁ /n
Cell dimensions:	a = 10.220(2) Å, α = 90° b = 9.909(2) Å, β = 104.94(1)° c = 18.658(3) Å, γ = 90°
Volume:	1825.6(6) Å ³
Z:	4
Density (calc):	1.213 mg/m ³
Final R indices:	0.0602 (R _w = 0.0912)

Appendix A4 : Crystal Data for [CpV(μ-NAr)]₂(μ-Me) (6) a,b

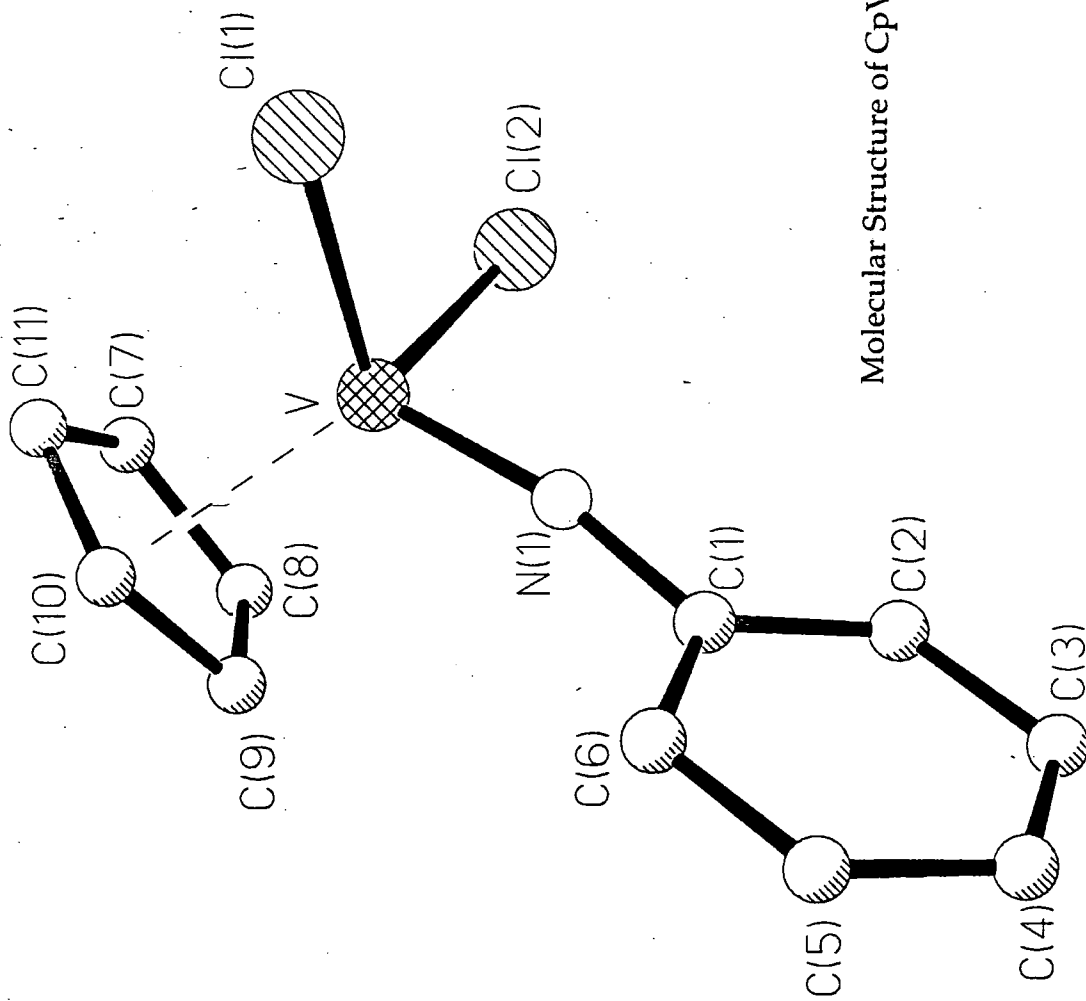
C ₃₅ H ₄₇ N ₂ V ₂ :	597.63
Crystal system:	Monoclinic
Space group:	P2 ₁ /n
Cell dimensions:	a = 9.924(2) Å, α = 90° b = 21.653(4) Å, β = 98.73(3)° c = 16.235(3) Å, γ = 90°
Volume:	3448.2(11) Å ³
Z:	4
Density (calc):	1.151 mg/m ³
Final R indices:	0.0531 (R _w = 0.1476)

**Appendix A5: Crystal Data, Selected Bond Lengths (Å) and Angles (°) and
Molecular Structure for CpV(NC₆H₅)Cl₂ (7) ^{a,b}**

C₁₁H₁₀NCl₂V: 278.04
 Crystal system: Monoclinic
 Space group: P2₁/c
 Cell dimensions: a = 13.641(3) Å, α = 90°
 b = 7.034(1) Å, β = 94.66(3)°
 c = 12.403(2) Å, γ = 90°
 Volume: 1186.1(4) Å³
 Z: 4
 Density (calc): 1.557 mg/m³
 Final R indices: 0.0545 (R_w = 0.0795)

V–N(1)	1.653(4)	V–C(8)	2.263(6)
V–Cl(1)	2.258(2)	V–C(7)	2.351(5)
V–Cl(2)	2.259(2)	V–C(11)	2.354(5)
V–C(9)	2.236(6)	N(1)–C(1)	1.392(5)
V–C(10)	2.246(6)	V–C _p centroid	1.968(6)

N(1)–V–Cl(1)	99.7(1)	N(1)–V–C _p centroid	121.2(4)
N(1)–V–Cl(2)	102.3(1)	Cl(1)–V–C _p centroid	114.1(2)
Cl(1)–V–Cl(2)	103.65(6)	Cl(2)–V–C _p centroid	113.5(2)
C(1)–N(1)–V	169.1(4)		



Molecular Structure of CpV(NC₆H₅)Cl₂ (7).

Appendix A6: Crystal Data for CpNb(N-2-^tBuC₆H₄)Cl₂ (2) ^{a,b}

C₁₅H₁₈NCl₂Nb: 529.57
Crystal system: Orthorhombic
Space group: Pnma
Cell dimensions: a = 11.897(2) Å, α = 90°
b = 9.400(2) Å, β = 90°
c = 14.081(3) Å, γ = 90°
Volume: 1574.7(5) Å³
Z: 4
Density (calc): 1.586 mg/m³
Final R indices: 0.0223 (R_w = 0.0615)

Appendix A7: Crystal Data for CpNb(N-2-^tBuC₆H₄)(PhC≡CPh)(PMe₃) (14) ^{a,e}

C₃₂H₃₇NNbP: 559.91
Crystal system: Monoclinic 2nd
Space group: P2₁/n
Cell dimensions: a = 11.731(6) Å, α = 90°
b = 12.624(3) Å, β = 95.24(3)°
c = 19.282(4) Å, γ = 90°
Volume: 2844(2) Å³
Z: 4
Density (calc): 1.307 mg/m³
Final R indices: 0.0357 (R_w = 0.0800)

Appendix A8: Crystal Data for CpNb(N-2,6-Cl₂C₆H₃)(η²-C₂H₄)(PMe₃) (17) ^{f,g}

C₁₆H₂₁NCl₂NbP: 422.12
Crystal system: Monoclinic
Space group: P2₁/n
Cell dimensions: a = 8.004(1) Å, α = 90°
b = 12.960(2) Å, β = 93.51(2)°
c = 17.615(2) Å, γ = 90°
Volume: 1823.9(4) Å³
Z: 4
Density (calc): 1.537 mg/m³
Final R indices: 0.0260 (R_w = 0.0704)

Appendix A9: Crystal Data for Cp*Ta(N^tBu)(CH₂CMe₃)₂ (22) a,b

C ₂₄ H ₄₆ NTa:	529.57
Crystal system:	Monoclinic
Space group:	P2 ₁ /c
Cell dimensions:	a = 9.083(2) Å, α = 90° b = 16.216(3) Å, β = 99.76(3)° c = 16.872(3) Å, γ = 90°
Volume:	2449.1(8) Å ³
Z:	4
Density (calc):	1.436 mg/m ³
Final R indices:	0.0378 (R _w = 0.0554)

Appendix A10 : Crystal Data for [Cp*Ta(CH₂Ph)(OC₆F₅)(μ-O)]₂ (24) a,b

C ₂₃ H ₂₂ O ₂ F ₅ Ta:	606.36
Crystal system:	Triclinic
Space group:	P-1
Cell dimensions:	a = 9.239(2) Å, α = 117.25(3)° b = 11.647(2) Å, β = 96.37(3)° c = 11.803(2) Å, γ = 106.63(3)°
Volume:	1037.3(3) Å ³
Z:	2
Density (calc):	1.941 mg/m ³
Final R indices:	0.0727 (R _w = 0.1824)

Appendix A11 : Crystal Data for Cp*Ta(OC₆F₅)₄ (26) a,b

C ₃₄ H ₁₅ O ₄ F ₂₀ Ta:	1048.41
Crystal system:	Orthorhombic
Space group:	Pbcm
Cell dimensions:	a = 8.341(2) Å, α = 90° b = 26.389(5) Å, β = 90° c = 15.145(3) Å, γ = 90°
Volume:	3334(1) Å ³
Z:	4
Density (calc):	2.089 mg/m ³
Final R indices:	0.0448 (R _w = 0.0879)

Appendix A12 : Crystal Data for [Cp*Ta(OC₆F₅)₂(μ-O)]₂ (27) a,b

C₄₄H₃₀O₆F₂₀Ta₂•C₇H₈ : 1488.71
Crystal system: Orthorhombic
Space group: P2₁/n
Cell dimensions: a = 12.793(2) Å, α = 90°
b = 15.242(2) Å, β = 100.178(5)°
c = 25.708(3) Å, γ = 90°
Volume: 4939(1) Å³
Z: 4
Density (calc): 2.004 mg/m³
Final R indices: 0.0633 (R_w = 0.0933)

Appendix A13: Crystal Data for [Li(OEt₂)] [Cp*Ta(N-2-^tBuC₆H₄)₂Cl] (31) a,b

C₃₄H₅₁N₂OClLiTa: 727.11
Crystal system: Orthorhombic
Space group: Pbca
Cell dimensions: a = 19.537(1) Å, α = 90°
b = 16.354(1) Å, β = 90°
c = 21.327(1) Å, γ = 90°
Volume: 6814.2(7) Å³
Z: 8
Density (calc): 1.418 mg/m³
Final R indices: 0.0433 (R_w = 0.1246)

Appendix B

Colloquia, Lectures and Seminars Organised by the Department of Chemistry 1992-1995

1992

- October 15 Dr M. Glazer & Dr S. Tarling, Oxford University & Birkbeck College, London
It Pays to be British! - The Chemist's Role as an Expert Witness in Patent Litigation.
- October 20 Dr. H. E. Bryndza, Du Pont Central Research
Synthesis, Reactions and Thermochemistry of Metal (Alkyl) Cyanide Complexes and Their Impact on Olefin Hydrocyanation Catalysis.
- October 22 Prof. A. Davies, University College London
The Ingold-Albert Lecture The Behaviour of Hydrogen as a Pseudometal.
- October 28 Dr. J. K. Cockcroft, University of Durham
Recent Developments in Powder Diffraction.
- October 29 Dr. J. Emsley, Imperial College, London
The Shocking History of Phosphorus.
- November 4^S Dr. T. P. Kee, University of Leeds
Synthesis and Co-ordination Chemistry of Silylated Phosphites.
- November 5^S Dr. C. J. Ludman, University of Durham
Explosions, A Demonstration Lecture.
- November 11 Prof. D. Robins[†], Glasgow University
Pyrrrolizidine Alkaloids : Biological Activity, Biosynthesis and Benefits.
- November 12 Prof. M. R. Truter, University College, London
Luck and Logic in Host - Guest Chemistry.
- November 18 Dr. R. Nix[†], Queen Mary College, London
Characterisation of Heterogeneous Catalysts.
- November 25 Prof. Y. Vallee, University of Caen
Reactive Thiocarbonyl Compounds.
- November 25 Prof. L. D. Quin[†], University of Massachusetts, Amherst
Fragmentation of Phosphorous Heterocycles as a Route to Phosphoryl Species with Uncommon Bonding.
- November 26 Dr. D. Humber, Glaxo, Greenford
AIDS - The Development of a Novel Series of Inhibitors of HIV.
- December 2 Prof. A. F. Hegarty, University College, Dublin
Highly Reactive Enols Stabilised by Steric Protection.
- December 2^S Dr. R. A. Aitken[†], University of St. Andrews
The Versatile Cycloaddition Chemistry of Bu₃P.CS₂.

- December 3 Prof. P. Edwards, Birmingham University
The SCI Lecture - What is Metal?
- December 9 Dr. A. N. Burgess[†], ICI Runcorn
The Structure of Perfluorinated Ionomer Membranes.
- 1993
- January 20 Dr. D. C. Clary[†], University of Cambridge
Energy Flow in Chemical Reactions.
- January 21 Prof. L. Hall, Cambridge
NMR - Window to the Human Body.
- January 27 Dr. W. Kerr, University of Strathclyde
Development of the Pauson-Khand Annulation Reaction : Organocobalt Mediated Synthesis of Natural and Unnatural Products.
- January 28 Prof. J. Mann, University of Reading
Murder, Magic and Medicine.
- February 3 Prof. S. M. Roberts, University of Exeter
Enzymes in Organic Synthesis.
- February 10 Dr. D. Gillies[†], University of Surrey
NMR and Molecular Motion in Solution.
- February 11[§] Prof. S. Knox, Bristol University
The Tilden Lecture: Organic Chemistry at Polynuclear Metal Centres.
- February 17 Dr. R. W. Kemmitt[†], University of Leicester
Oxatrimethylenemethane Metal Complexes.
- February 18 Dr. I. Fraser, ICI Wilton
Reactive Processing of Composite Materials.
- February 22 Prof. D. M. Grant, University of Utah
Single Crystals, Molecular Structure, and Chemical-Shift Anisotropy.
- February 24 Prof. C. J. M. Stirling[†], University of Sheffield
Chemistry on the Flat-Reactivity of Ordered Systems.
- March 10[§] Dr. P. K. Baker, University College of North Wales, Bangor
'Chemistry of Highly Versatile 7-Coordinate Complexes'.
- March 11 Dr. R. A. Y. Jones, University of East Anglia
The Chemistry of Wine Making.
- March 17 Dr. R. J. K. Taylor[†], University of East Anglia
Adventures in Natural Product Synthesis.
- March 24 Prof. I. O. Sutherland[†], University of Liverpool
Chromogenic Reagents for Cations.
- May 13 Prof. J. A. Pople, Carnegie-Mellon University, Pittsburgh, USA
The Boys-Rahman Lecture: Applications of Molecular Orbital Theory

- May 21[§] Prof. L. Weber, University of Bielefeld
Metallo-phospha Alkenes as Synthons in Organometallic Chemistry
- June 1 Prof. J. P. Konopelski, University of California, Santa Cruz
Synthetic Adventures with Enantiomerically Pure Acetals
- June 2 Prof. F. Ciardelli, University of Pisa
Chiral Discrimination in the Stereospecific Polymerisation of Alpha Olefins
- June 7 Prof. R. S. Stein, University of Massachusetts
Scattering Studies of Crystalline and Liquid Crystalline Polymers
- June 16 Prof. A. K. Covington, University of Newcastle
Use of Ion Selective Electrodes as Detectors in Ion Chromatography.
- June 17 Prof. O. F. Nielsen, H. C. Arsted Institute, University of Copenhagen
Low-Frequency IR - and Raman Studies of Hydrogen Bonded Liquids.
- September 13 Prof. Dr. A. D. Schlüter, Freie Universität Berlin, Germany
Synthesis and Characterisation of Molecular Rods and Ribbons.
- September 13 Prof. K. J. Wynne, Office of Naval Research, Washington, U.S.A.
Polymer Surface Design for Minimal Adhesion
- September 14 Prof. J. M. DeSimone, University of North Carolina, Chapel Hill, U.S.A.
Homogeneous and Heterogeneous Polymerisations in Environmentally Responsible Carbon Dioxide.
- September 28 Prof. H. Ila., North Eastern University, India
Synthetic Strategies for Cyclopentanoids via OxoKetene Dithiacetals.
- October 4[§] Prof. F. J. Feher[†], University of California at Irvine
Bridging the Gap between Surfaces and Solution with Sessilquioxanes.
- October 14 Dr. P. Hubberstey, University of Nottingham
Alkali Metals: Alchemist's Nightmare, Biochemist's Puzzle and Technologist's Dream.
- October 20 Dr. P. Qualye[†], University of Manchester
Aspects of Aqueous Romp Chemistry.
- October 23 Prof. R. Adams[†], University of S. Carolina
The Chemistry of Metal Carbonyl Cluster Complexes Containing Platinum and Iron, Ruthenium or Osmium and the Development of a Cluster Based Alkyne Hydrogenating Catalyst.
- October 27 Dr. R. A. L. Jones[†], Cavendish Laboratory
'Perambulating Polymers'.
- November 10 Prof. M. N. R. Ashfold[†], University of Bristol
High-Resolution Photofragment Translational Spectroscopy: A New Way to Watch Photodissociation.
- November 17 Dr. A. Parker[†], Laser Support Facility
Applications of Time Resolved Resonance Raman Spectroscopy to Chemical and

Biochemical Problems.

- November 24^S Dr. P. G. Bruce[†], University of St. Andrews
Synthesis and Applications of Inorganic Materials.
- November 25 Dr. R.P. Wayne, University of Oxford
The Origin and Evolution of the Atmosphere
- December 1 Prof. M. A. McKervey[†], Queens University, Belfast
Functionalised Calixarenes.
- December 8 Prof. O. Meth-Cohen, Sunderland University
Friedel's Folly Revisited.
- December 16 Prof. R. F. Hudson, University of Kent
Close Encounters of the Second Kind.
- 1994
- January 26 Prof. J. Evans[†], University of Southampton
Shining Light on Catalysts.
- February 2 Dr. A. Masters[†], University of Manchester
Modelling Water Without Using Pair Potentials.
- February 9 Prof. D. Young[†], University of Sussex
Chemical and Biological Studies on the Coenzyme Tetrahydrofolic Acid.
- February 16 Prof. K. H. Theopold, University of Delaware, U.S.A
Paramagnetic Chromium Alkyls: Synthesis and Reactivity.
- February 23 Prof. P. M. Maitlis[†], University of Sheffield
Why Rhodium in Homogenous Catalysis.
- March 2 Dr. C. Hunter[†], University of Sheffield
Non Covalent Interactions between Aromatic Molecules.
- March 9 Prof. F. Wilkinson, Loughborough University of Technology
Nanosecond and Picosecond Laser Flash Photolysis.
- March 10 Prof. S.V. Ley, University of Cambridge
New Methods for Organic Synthesis.
- March 25 Dr. J. Dilworth, University of Essex
Technetium and Rhenium Compounds with Applications as Imaging Agents.
- April 28 Prof. R. J. Gillespie, McMaster University, Canada
The Molecular Structure of some Metal Fluorides and OxoFluorides: Apparent Exceptions to the VSEPR Model.
- May 12 Prof. D. A. Humphreys, McMaster University, Canada
Bringing Knowledge to Life
- October 5 Prof. N. L. Owen, Brigham Young University, Utah, USA
Determining Molecular Structure - the INADEQUATE NMR way

- October 19§ Prof. N. Bartlett, University of California
Some Aspects of Ag(II) and Ag(III) Chemistry
- November 2§ Dr P. G. Edwards, University of Wales, Cardiff
The Manipulation of Electronic and Structural Diversity in Metal Complexes - New Ligands
- November 3 Prof. B. F. G. Johnson, Edinburgh University
Arene - Metal Clusters - DUCS Lecture
- November 9 Dr J. P. S. Badyal, University of Durham
Chemistry at Surfaces, A Demonstration Lecture
- November 9§ Dr G. Hogarth, University College, London
New Vistas in Metal Imido Chemistry
- November 10 Dr M. Block, Zeneca Pharmaceuticals, Macclesfield
Large Scale Manufacture of the Thromboxane Antagonist Synthase Inhibitor ZD 1542
- November 16 Prof. M. Page, University of Huddersfield
Four Membered Rings and β -Lactamase
- November 23 Dr J. M. J. Williams, University of Loughborough
New Approaches to Asymmetric Catalysis
- December 7 Prof. D. Briggs, ICI and University of Durham
Surface Mass Spectrometry
- 1995
- January 11 Prof. P. Parsons, University of Reading
Applications of Tandem Reactions in Organic Synthesis
- January 18 Dr G. Rumbles, Imperial College, London
Real or Imaginary 3rd Order non-Linear Optical Materials
- January 25 Dr D. A. Roberts, Zeneca Pharmaceuticals
The Design and Synthesis of Inhibitors of the Renin-Angiotensin System
- February 1 Dr T. Cosgrove, Bristol University
Polymers do it at Interfaces
- February 8§ Dr D. O'Hare, Oxford University
Synthesis and Solid State Properties of Poly-, Oligo- and Multidecker Metallocenes
- February 22 Prof. E. Schaumann, University of Clausthal
Silicon and Sulphur Mediated Ring-opening Reactions of Epoxide
- March 1 Dr M. Rosseinsky, Oxford University
Fullerene Intercalation Chemistry
- March 22§ Dr M. Taylor, University of Auckland, New Zealand
Structural Methods in Main Group Chemistry
- April 26 Dr M. Schroder, University of Edinburgh
Redox Active Macrocyclic Complexes : Rings, Stacks and Liquid Crystals

- May 3 Prof. E. W. Randall, Queen Mary and Westfield College
New Perspectives in NMR Imaging
- May 4 Prof. A. J. Kresge, University of Toronto
The Ingold Lecture - Reactive Intermediates : Carboxylic Acid Enols and Other Unstable Species

§ Attended by the author.

† Invited specially for the graduate training programme.

Appendix C

Conferences attended (§ poster presented)

- April 1994 Sixth Firth Symposium, University of Sheffield.
- July 1994 16th International Conference in Organometallic Chemistry,
University of Sussex.§
- June 1995 North East Graduate Symposium, University of Durham.
- July 1995 ISOM 11, University of Durham.

